

# Contribution of the platelet receptor CLEC-2 and its ligand podoplanin to the pathogenesis of liver disease.

by

Abhishek Chauhan

A thesis submitted to the University of Birmingham for  
the degree of DOCTOR OF PHILOSOPHY

School of Immunology and Immunotherapy,

College of Medicine and Dentistry

University of Birmingham

May 2017

UNIVERSITY OF  
BIRMINGHAM

**University of Birmingham Research Archive**

**e-theses repository**

This unpublished thesis/dissertation is copyright of the author and/or third parties. The intellectual property rights of the author or third parties in respect of this work are as defined by The Copyright Designs and Patents Act 1988 or as modified by any successor legislation.

Any use made of information contained in this thesis/dissertation must be in accordance with that legislation and must be properly acknowledged. Further distribution or reproduction in any format is prohibited without the permission of the copyright holder.

## Abstract

Increasing lines of evidence place platelets as having a central role in liver disease. Platelets are recruited to the liver and, depending upon stage and type of liver injury play varying roles ranging from driving liver fibrosis to aiding regeneration. However the molecular basis and consequences of platelet activation in the liver are less clear. The work presented in this thesis demonstrates for the first time that platelet activation via CLEC-2 is important in the pathogenesis of liver disease. In chronic human diseases (CLD) such as Primary Biliary Cirrhosis, and Alcoholic Liver disease I have demonstrated that the ligand for CLEC-2, podoplanin is upregulated on portal venules and increases proportionately to disease activity. I also note podoplanin staining on macrophage populations in CLD. Furthermore I show that this enhanced podoplanin expression may be a useful predictor of portal venous thrombosis, and correlates with MELD score for some categories of disease.

In acute liver injury, CLEC-2-dependent platelet activation has a profound effect on disease development. Here podoplanin expression occurs upon Kupffer cells in both humans and mice. Using carbon tetrachloride and paracetamol to induce acute liver injury in mice, I show that macrophage-expressed podoplanin activates platelets via CLEC-2. This interaction worsens liver injury, I next show that by blocking this interaction (using either CLEC-2 or podoplanin-deficient mice, or by using a function-blocking podoplanin antibody) liver recovery from toxic liver injury was remarkably enhanced. This was dependent upon enhanced hepatic neutrophil recruitment in a  $\text{TNF}\alpha$  dependent fashion.

This work explains how platelets manipulate the sterile inflammatory response to acute, toxic liver injury and importantly highlights a mechanism that could be targeted therapeutically in human acute liver failure.



## **Work arising from this thesis**

2017 Blocking CLEC-2 dependent platelet activation drives rapid recovery from acetaminophen induced liver damage. **Chauhan A**, Watson SP, Adams DH, Webb GJ, Weston C, Shepherd E, Lax S, Watson S, Patten D, Lalor PL . **Submitted to Nature communications.**

2017 The role of platelets in neutrophil recruitment during toxic liver injury. **Chauhan A**, Adam DH, Watson SP, Shepherd E and Lalor PF. **Poster, EASL, Amsterdam, Netherlands.**

2017 Role of CLEC-2 driven platelet activation in the pathogenesis of toxic liver damage. **Chauhan A**, Adam DH, Watson SP and Lalor PF. **Lancet 2017.**

2017-Platelet activation in the pathogenesis of toxic liver damage. **Chauhan A**, Adams DH, Watson SP and Lalor PF. **Poster, Academy of medical sciences, London.**

2016 Blocking platelet activation enhances recovery from APAP induced liver injury. **Chauhan A**, Adams DH, Watson SP and Lalor PF. **Plenary talk. American association for the study of liver disease (AASLD), Boston, USA 2016.**

2016 Platelet activation via CLEC-2 drives inflammatory liver damage. **Chauhan A**, Adams DH, Watson SP and Lalor PF. **Top Ranked Poster, British association for the study of liver disease, Manchester 2016.**

2016 Platelets: No longer bystanders in liver disease. **Chauhan A**, Adam DH, Watson SP and Lalor PF. **Hepatology**. 2016 Nov;**64(5):1774-1784**. doi: **10.1002/hep.28526**. Epub 2016 Apr 7- I am the lead author on this review and it forms the basis of section 8.3 (part of the introduction).

2016 Platelets: Critical players in immune mediated liver damage. **Chauhan A**, Adams D. **EASL, Plenary oral session. Barcelona 2016**.

2015 Platelet activation via CLEC2 drives liver damage in acute inflammatory hepatitis. **Chauhan A**, Adams D, Watson S and Lalor P. **UK Cell Adhesion Society annual meeting, Birmingham**.

2014 Podoplanin is upregulated on damaged human liver. **Chauhan A**, Adams DH, Watson SP and Lalor P. **FASEB liver biology, Keystone, Colorado**.

## **Dedication**

I would like to dedicate this thesis to my wife Seema, her ability to singlehandedly look after our two gorgeous but feral boys made this thesis possible.





## Acknowledgements

The work in this thesis would not have been achievable without the help and support of several people.

First and foremost, I would like to thank my main supervisor Trish Lalor. From introducing me to the lab and supervision with pilot experiments when I first started, through to the end of my fellowship, her support, advice and guidance have been invaluable. I would also like to thank Professors David Adams and Steve Watson for giving me the opportunity to work in the Birmingham liver labs and with the Birmingham platelet group respectively. Being awarded a Wellcome clinical research training fellowship would not have been possible without their encouragement, support and advice.

I have had great support from excellent colleague both in the liver labs and the platelet group. I would like to thank Sian Lax, Steph Watson and Julie Rayes in the platelet group for their help with mouse breeding, and platelet assays. In the liver labs, I would like to particularly thank Chris Weston, Janine Fear, Emma Shepherd, Gwilym Webb, Debashis Haldar and Sudha Purswani Thakor.

I am very grateful to the Wellcome trust for funding me for this PhD and to the patients in the Queen Elizabeth hospital for tissue donation.

Finally, and most importantly, I would like to thank my parents who have provided unwavering and unconditional support to me and my young family throughout my time in research. This work would simply have been impossible without them.



# Table of contents

<b>Abstract</b> .....	<b>2</b>
<b>Work arising from this thesis</b> .....	<b>5</b>
<b>Dedication</b> .....	<b>7</b>
<b>Acknowledgements</b> .....	<b>9</b>
<b>Table of contents</b> .....	<b>11</b>
<b>List of tables</b> .....	<b>13</b>
<b>List of figures</b> .....	<b>14</b>
<b>1. Introduction</b> .....	<b>1</b>
1.1. The burden of liver disease is increasing .....	1
1.2. Structure of the liver.....	3
1.3. Major classes of liver injury studied .....	7
1.4. Inflammatory cells drive disease pathogenesis in acute and chronic liver disease .....	10
1.5. Is there a role for platelets in liver disease?.....	13
1.6. Platelets and haemostasis .....	14
1.7. ITAM receptors and their ligands .....	19
1.8. Platelets beyond homeostasis.....	30
1.9. Platelets and liver disease: what is already known?.....	33
1.10. Project aims .....	47
<b>2. Materials and methods</b> .....	<b>49</b>
2.1. Human tissue .....	49
2.2. Murine tissue .....	50
2.3. Methods.....	51
2.4. Tissue Preparation .....	56
2.5. Microscopy.....	64
2.6. Quantitative PCR .....	65
2.7. TNF $\alpha$ ELISA.....	66
2.8. Isolation of murine leukocytes .....	68
2.9. Hydroxyproline assay.....	74
2.10. Biochemical liver function assays.....	75
2.11. Statistical analysis.....	75
2.12. Antibodies and isotype controls used .....	77
<b>3. Podoplanin is upregulated in acute and chronic human liver injury</b> .....	<b>79</b>
3.1. Introduction.....	79
3.2. Aims of this chapter .....	85
3.3. Podoplanin is minimally expressed within the liver during normal physiology	86
3.4. Podoplanin expression increases dramatically during acute and chronic human liver disease.....	89
3.5. Clinical correlation between podoplanin and disease severity .....	114
3.6. Summary and discussion .....	122

<b>4. Platelet activation drives liver injury during carbon tetrachloride and paracetamol induced liver injury.....</b>	<b>130</b>
4.1. Models of acute toxic liver damage.....	130
4.2. The sterile inflammatory response of toxic liver injury .....	132
4.3. Aims for this chapter.....	136
4.4. Administration of intraperitoneal CCl <sub>4</sub> or paracetamol results in centrilobular hepatic necroinflammation .....	137
4.5. Podoplanin is upregulated in murine livers after toxic liver injury .....	142
4.6. Platelet and macrophage distribution during acute liver damage .....	147
4.7. Mice with CLEC-2 deficient platelets exhibit enhanced healing after CCl <sub>4</sub> and paracetamol injury.....	152
4.8. Kinetics of immune cell recruitment after toxic liver injury.....	163
4.9. Podoplanin blockade recapitulates the effects seen in CLEC-2 deficient mice .....	176
4.10. The effect of neutrophil depletion on liver injury .....	186
4.11. Macrophage derived TNF- $\alpha$ recruits neutrophils to the injured liver.....	190
4.12. Hepatic CYP2E1 expression is unaffected by CLEC-2 or podoplanin deficiency .....	198
4.13. Discussion .....	200
<b>5. The role of platelet CLEC-2 in chronic murine liver injury .....</b>	<b>210</b>
5.1. Carbon tetrachloride induced chronic liver injury.....	212
5.2. Methionine-choline deficient diet .....	213
5.3. Aims.....	215
5.4. Use of the chronic carbon tetrachloride model.....	216
5.5. Regeneration.....	232
5.6. Methionine choline deficient (MCD) diet.....	239
5.7. Discussion .....	245
<b>6. Conclusion and future directions.....</b>	<b>251</b>
6.1. The macrophage:platelet interaction .....	251
6.2. Hepatic inflammation and liver recovery .....	253
6.3. Model limitations .....	255
6.4. Future clinical implications.....	257
<b>7. Bibliography.....</b>	<b>260</b>
<b>8. Appendix .....</b>	<b>323</b>
8.1. Platelets: no longer bystanders in liver disease.....	323
8.2. Role of CLEC-2 driven platelet activation in the pathogenesis of toxic liver damage.....	329

## List of tables

<i>Table 1.1 Overview of the key receptors expressed in platelets</i>	17
<i>Table 1.2 Summary of the roles platelets play in different liver injuries</i>	35
<i>Table 1.3 Summary of the contribution of key platelet-derived mediators to the pathogenesis of liver injury in different models.</i>	43
<i>Table 2.1 mouse strains used in this project</i>	51
<i>Table 2.2 Materials used for qPCR reaction</i>	66
<i>Table 2.3 T-cell panel and IMCs:</i>	70
<i>Table 2.4 Myeloid Cell panel and IMCs:</i>	71
<i>Table 2.5 Pro-fibrotic and restorative macrophage panel and corresponding IMCs:</i>	71
<i>Table 2.6 : Details of antibodies used for flow cytometry and immunohistochemistry (with corresponding isotype matched controls)</i>	78
<i>Table 3.1 Podoplanin expression and function :</i>	80
<i>Table 3.2 Pattern of podoplanin and CLEC-2 expression in different forms of human liver disease</i>	128
<i>Table 4.1 The effect of genetic disruption and antibody treatment on toxic liver injury</i>	200

## List of figures

Figure 1.1 Structure of the liver acinus: _____	4
Figure 1.2 Metabolic zonation of the liver: _____	6
Figure 1.3 The structure of the CLEC-2 receptor: _____	20
Figure 1.4 Schematic diagram illustrating the structure of Podoplanin: _____	22
Figure 1.5 ITAM signaling: _____	25
Figure 1.6 Platelet-HSEC-lymphocyte interactions during liver injury: _____	38
Figure 1.7 The platelet role in regeneration and fibrosis: _____	46
Figure 2.1 Method of liver lobe isolation: _____	56
Figure 2.2 Procedure for wax embedding of liver tissue _____	57
Figure 2.3 Method to de-wax paraffin sections _____	58
Figure 2.4 Haematoxylin and eosin staining _____	59
Figure 2.5 Method employed for Van Gieson staining _____	61
Figure 2.6 ELISA well set up: _____	67
Summary of how site and timing of podoplanin expression inform podoplanin function (taken from Astarita et al) _____	80
Figure 3.1 Podoplanin expression is minimally expressed in the non-injured human liver: _____	86
Figure 3.2 Minimal colocalisation of platelets and podoplanin in the normal liver: _____	88
Figure 3.3 Podoplanin is upregulated in paracetamol induced acute human liver injury: _____	90
Figure 3.4 Hepatic macrophages upregulate podoplanin after APAP induced liver injury in humans: _____	92
Figure 3.5 Platelets sequester to podoplanin expressing macrophages in APAP injured human liver: _____	94
Figure 3.6 Podoplanin is upregulated in periportal areas in alcoholic liver disease: _____	96
Figure 3.7 Expression of CLEC-2 in alcoholic cirrhosis: _____	98
Figure 3.8 Macrophages in alcoholic liver disease express podoplanin: _____	100
Figure 3.9 Portal veins express podoplanin in alcoholic liver disease: _____	101
Figure 3.10 Podoplanin is upregulated in autoimmune human liver disease: _____	103
Figure 3.11 Podoplanin is upregulated in periportal areas in non-alcoholic fatty liver disease: _____	105
Figure 3.12 CLEC-2 expressing platelets sequester to the injured liver during NASH: _____	106
Figure 3.13 Podoplanin is upregulated in primary biliary cirrhosis (PBC): _____	108
Figure 3.14 Platelets do not sequester to podoplanin expressing areas in PBC: _____	109
Figure 3.15 Podoplanin is upregulated in primary sclerosing cholangitis (PSC): _____	111
Figure 3.16 Vascular endothelial cells and leukocytes express podoplanin in PSC livers: _____	112
Figure 3.17 Macrophages express podoplanin in PSC: _____	113
Figure 3.18 Podoplanin mRNA is upregulated in human chronic liver disease: _____	115
Figure 3.19 Expression of podoplanin mRNA varies with disease type: _____	116
Figure 3.20 Podoplanin is upregulated during acute fulminant liver failure due to paracetamol overdose: _____	117
Figure 3.21 Patient MELD scores correlate hepatic podoplanin mRNA expression at time of transplantation: _____	119
Figure 3.22 In autoimmune liver disease higher MELD scores correspond with lower levels of podoplanin: _____	120
Figure 3.23 Evidence of portal venous thrombosis pre-transplantation is associated with greater podoplanin mRNA expression: _____	121
Figure 4.1 Murine livers develop centrilobular necrosis after IP CCl <sub>4</sub> injection: _____	138
Figure 4.2 Hepatocellular injury peaks at 48 hours post intraperitoneal CCl <sub>4</sub> injection: _____	139
Figure 4.3 Hepatocellular injury peaks at 24 hours post intraperitoneal APAP injection: _____	141
Figure 4.4 Podoplanin expression within uninjured murine liver is restricted to lymphatic vessels: _____	142
Figure 4.5 Podoplanin is upregulated on hepatic macrophages after hepatic injury in mice: _____	144
Figure 4.6 Isolated macrophages upregulate podoplanin expression in vitro on stimulation with lipopolysaccharide: _____	146
Figure 4.7 Macrophages are distributed in a sinusoidal distribution after toxic liver injury: _____	147

Figure 4.8 Platelets are found sequestered within the acutely injured liver:	149
Figure 4.9 Platelets sequester to podoplanin expressing macrophages after acute liver injury:	151
Figure 4.10 Injury at early time points is comparable between WT and CLEC-2 deficient mice after either CCl <sub>4</sub> or APAP induced liver injury:	153
Figure 4.11 CLEC-2 deficient animals develop less hepatic injury after CCl <sub>4</sub> injection:	155
Figure 4.12 CLEC-2 deficient mice exhibit enhanced recovery after APAP injection:	157
Figure 4.13 After toxic injury macrophages sequester to the injured area in CLEC-2 deficient mice:	159
Figure 4.14 After toxic injury larger amounts of platelets sequester to the injured liver in CLEC-2 deficient mice compared to wild type:	160
Figure 4.15 CLEC-2 deficient platelets sequester to wild type macrophages in greater numbers than wild type platelets:	161
Figure 4.16 Wild type and CLEC-2 deficient animals both develop centrilobular damage and leukocyte sequestration after toxic liver damage:	164
Figure 4.17 Liver infiltrating CD45 <sup>+</sup> leukocytes increase and peak at time point of maximal necrotic damage after toxic liver injury:	165
Figure 4.18 Numbers of liver infiltrating CD45 <sup>+</sup> leukocytes are similar at most timepoints after toxic liver injury:	167
Figure 4.19 Lymphocyte gating strategy:	169
Figure 4.20 CD4 and CD8 lymphocytes are present in greater amounts within the livers of CLEC-2 deficient mice after toxic liver injury:	170
Figure 4.21 Myeloid cell gating strategy:	172
Figure 4.22 Hepatic macrophage numbers are similar in WT and CLEC-2 -deficient mice after a toxic liver injury:	173
Figure 4.23 CLEC-2 deficient mice exhibit enhanced hepatic neutrophil numbers at the peak point of liver injury after toxin administration:	175
Figure 4.24 Time line for injury after APAP and CCl <sub>4</sub> injection:	177
Figure 4.25 Podoplanin deficient (Vav1-iCre <sup>+</sup> pdpr <sup>fl/fl</sup> ) mice exhibit less injury after IP CCl <sub>4</sub> injection:	179
Figure 4.26 Podoplanin deficient mice exhibit enhanced neutrophil infiltration after IP CCl <sub>4</sub> administration:	180
Figure 4.27 Podoplanin deficient mice (Vav1-iCre <sup>+</sup> pdpr <sup>fl/fl</sup> ) exhibit reduced injury and enhanced neutrophil infiltration after IP APAP administration:	182
Figure 4.28 Timeline of podoplanin antibody treatment:	183
Figure 4.29 Treating mice with a podoplanin antibody reduces injury after both CCl <sub>4</sub> and APAP mediated injury:	184
Figure 4.30 Mice treated with a podoplanin antibody exhibit enhanced neutrophil infiltration after IP CCl <sub>4</sub> or IP APAP administration:	185
Figure 4.31 Hepatic neutrophil infiltration peaks at time of maximal reduction of ALT in CLEC-2 deficient mice:	186
Figure 4.32 After toxic liver injury more neutrophils sequester to damaged areas within the livers of CLEC-2 deficient mice than WT mice:	187
Figure 4.33 Neutrophil depletion in CLEC-2 deficient mice removes the protective effect of CLEC-2 deficiency in mice undergoing a toxic liver injury:	189
Figure 4.34 CLEC-2 deficient mice have greater amounts of serum TNF- $\alpha$ at early points after toxic liver injury:	191
Figure 4.35 Hepatic macrophages produce TNF- $\alpha$ after stimulation with LPS:	193
Figure 4.36 CLEC-2 deficient platelets enhance hepatic macrophage TNF- $\alpha$ production after stimulation with LPS:	194
Figure 4.37 Podoplanin deficient macrophages produce more TNF- $\alpha$ production after stimulation with LPS:	195
Figure 4.38 Abrogating TNF- $\alpha$ function by pretreating CLEC-2 deficient mice with etanercept removes the protective effect of CLEC-2 deficiency:	197
Figure 4.39 Hepatic CYP2E1 expression is unaffected by CLEC-2 or podoplanin deficiency:	199



<i>Figure 4.40 Blocking the CLEC-2 mediated platelet activation enhances TNF-<math>\alpha</math> production to increase neutrophil recruitment and healing in the injured liver</i>	209
<i>Figure 5.1 Mice exhibit centrizonal fibrosis after chronic CCl<sub>4</sub> administration:</i>	217
<i>Figure 5.2 CLEC-2 deficient mice exhibit greater fibrosis after chronic CCl<sub>4</sub> administration:</i>	218
<i>Figure 5.3 CLEC-2 deficient and WT mice have equivalent levels of fibrosis after chronic CCl<sub>4</sub> administration:</i>	219
<i>Figure 5.4 WT and CLEC-2 deficient mice express podoplanin in portal areas after chronic CCl<sub>4</sub> administration:</i>	220
<i>Figure 5.5 Podoplanin expression increases in fibrotic portal tracts:</i>	222
<i>Figure 5.6 Podoplanin expression does not increase in centrizonal areas after chronic CCl<sub>4</sub> intoxication:</i>	224
<i>Figure 5.7 CLEC-2 deficient mice exhibit less necrotic damage after chronic CCl<sub>4</sub> administration:</i>	226
<i>Figure 5.8 Gating strategy used to define restorative and pro-fibrotic macrophages in our cytometric analysis of liver digests :</i>	228
<i>Figure 5.9 CLEC-2 deficient and WT mice have similar numbers of liver infiltrating leukocytes after chronic CCl<sub>4</sub> administration:</i>	230
<i>Figure 5.10 CLEC-2 deficient mice have lower numbers of both restorative and pro-fibrotic macrophages after chronic CCl<sub>4</sub> administration:</i>	231
<i>Figure 5.11 Timeline used to allow resolution from chronic CCl<sub>4</sub> administration</i>	232
<i>Figure 5.12 CLEC-2 deficient mice and WT do not exhibit resolution of fibrosis three weeks after cessation of IP CCl<sub>4</sub>:</i>	233
<i>Figure 5.13 CLEC-2 deficient mice have a lower serum transaminase level but higher TNF-<math>\alpha</math> levels compared to WT mice after chronic CCl<sub>4</sub> administration:</i>	235
<i>Figure 5.14 Numbers of intrahepatic leukocytes increase during the fibrosis resolution phase within CLEC-2 deficient mice:</i>	236
<i>Figure 5.15 CLEC-2 deficient and WT mice have similar numbers of liver infiltrating leukocytes during the resolution phase after chronic CCl<sub>4</sub> administration:</i>	237
<i>Figure 5.16 CLEC-2 deficient and WT mice have similar numbers of restorative and pro-fibrotic macrophages during the resolution phase from chronic liver injury:</i>	238
<i>Figure 5.17 Time line depicting when mice reached license threshold weight: Table below gives a breakdown of when mice reached threshold weight and whether any hepatic injury was noted (as gauged by serum ALT)</i>	240
<i>Figure 5.18 Podoplanin deficient mice exhibit greater macrophage infiltration whilst wild type mice exhibit greater lymphocyte accumulation after 4 weeks of MCD diet:</i>	242
<i>Figure 5.19 Four weeks of MCD diet induces a small amount of hepatic fibrosis:</i>	243
<i>Figure 5.20 Four weeks of MCD diet causes hepatic necroinflammation:</i>	244
<i>Figure 6.1 Time line for future experiments</i>	259

## List of abbreviations used

ADP (Adenosine diphosphate)

AIH (Autoimmune hepatitis)

Akt [Protein kinase B (PKB)]

APAP (Paracetamol)

CCBE1 (Collagen and calcium-binding EGF domain-containing protein 1)

CCL (C-C motif ligand)

CD (Clusters of differentiation)

COX-1 (Cyclooxygenase 1)

CTL (Cytotoxic T lymphocyte)

CXCL (CXC motif chemokine ligand)

CXCR (CXC receptor)

DAG (diacylglycerol)

DAMP (Damage associated motif pattern)

ERK (extracellular signal-regulated kinases)

ERM (Ezrin, Radixin and Moesin)

GPCR (G protein coupled receptor)

GSH (Glutathione)

GSK (Glycogen synthase kinase 3)

HGF (Hepatocyte growth factor)

HSC (Hepatic stellate cell)

ICAM (Intracellular adhesion molecule-1)

IGF (Insulin like growth factor)

IL (Interleukin)

LAT (Linker for Activation of T cells)

LSEC (Liver sinusoidal endothelial cell)

MEK (Mitogen-activated protein kinase kinase)

MIP (Macrophage inhibitory protein)

NAPQI (N-acetyl-p-benzoquinone mine)

NET (Neutrophil extracellular trap)

NLRP (NACHT, LRR and PYD domains-containing protein)

NOD (nucleotide-binding oligomerization domain)

PBC (Primary biliary cirrhosis)

PCNA (Proliferating cell nuclear antigen)

PDGF (Platelet derived growth factor)

PGE<sub>1</sub> (Prostaglandin E<sub>1</sub>)

PH (partial hepatectomy)

PI3K (Phosphatidylinositol-4,5-bisphosphate 3-kinase)

PIP (Phosphatidylinositol 4,5-bisphosphate)

PKC (protein kinase C)

PSC (Primary sclerosing cholangitis)

PYCARD (Apoptosis-associated speck-like protein containing a CARD)

Rac (Ras-related C3 botulinum toxin substrate)

Rap1b (Ras-related protein Rap-1b)

Src (Proto-oncogene tyrosine-protein kinase)

Syk (Spleen tyrosine kinase)

TGF- $\beta$  (Transforming growth factor- $\beta$ )

TLR (Toll like receptor)

TNF (Tumor necrosis factor)

TP (Thromboxane A2 receptor)

TXA2 (Thromboxane A2)

UDCA (Ursodeoxycholic acid)

VEGF (Vascular endothelial growth factor)

VWF (von Willebrand factor)



# 1. Introduction

## 1.1. The burden of liver disease is increasing

Mortality from liver disease is increasing. The clear majority of the burden of liver disease is due to chronic liver disease (CLD) and deaths due to CLD and its complications have been increasing annually. Between 1980 and 2013 liver disease deaths increased 4-fold (primarily due to alcohol excess)(1), this fact becomes particularly poignant when one compares this to other causes of death which are generally declining(2). Median survival of patients with end stage or decompensated liver disease is poor, approximating only 20 months(3), and the only cure at this stage remains orthotopic liver transplantation.

Acute liver failure (ALF) is at one end of the liver disease spectrum. Although far less common than chronic liver disease, it remains a life threatening illness with little in the way of specific therapy(4). The abrupt loss of immunological and metabolic function that accompanies acute or fulminant liver failure results in encephalopathy, coagulopathy and often multiple organ failure. Fulminant acute liver failure is thus defined as 'a severe but potentially reversible liver injury with the onset hepatic encephalopathy within 8 weeks of the injury, in a patient without antecedent liver disease'. Depending on onset of encephalopathy in relation to when jaundice was first noted ALF is subdivided into hyper-acute, acute and subacute(5). ALF in the developed world has an incidence between 1 and 6 cases per million of the population per year and overall mortality from ALF is about 40%(6). In the west,

paracetamol overdose remains the commonest cause of ALF, whilst viruses account for the vast majority of cases in developing countries(5,7,8).

Improvement in the quality of intensive or supportive care over time has resulted in a reduction in the mortality associated with ALF. However other than for some viral hepatitises, specific therapies are generally lacking. N-acetyl cysteine (NAC) in paracetamol overdose is an example of one of the few specific therapies available and although NAC is efficacious if used early in paracetamol overdose, the effectiveness of this compound decreases markedly in delayed presentations(9).

There is therefore a need for specific therapy for ALF, particularly in certain scenarios such as a delayed paracetamol overdose, where NAC administration is of limited value(10) or other acute liver injuries such as alcoholic hepatitis where a recent study reveals that none of the current treatments extend patient survival(5,11).

Chronic liver disease is the result of iterative bouts of liver damage. Multiple aetiologies can drive this 'repetitive' or persistent damage and these vary geographically; for instance alcohol, fatty liver disease and hepatitis C account for the majority of cases of chronic liver disease in the west(12) whilst hepatitis B is the primary cause in the Asia-Pacific area(12). Other causes include genetic conditions such as Wilsons disease, or autoimmune pathologies such as autoimmune hepatitis, primary sclerosing cholangitis and primary biliary cirrhosis. An important point to note is that despite the varied aetiologies that initiate chronic liver disease there are remarkable pathological and immunological similarities in how liver disease progresses(12,13). The continuum of chronic liver disease thus starts from repetitive

hepatocellular injury (due to a variety of aetiologies) which then causes cellular necrosis and loss; the liver is designed to counteract this cellular loss by regeneration(14), however the iterative nature of the injury in chronic liver disease impairs this process resulting in hepatic fibrosis, progressive loss of liver function and the development of liver cirrhosis which is characterized by the development of severe liver fibrosis with 'regenerative' hepatic nodules(12). Liver cirrhosis is thus 'end stage liver disease' and can be complicated by hepatocellular cancer or 'decompensation' which results in potentially uncontrollable or repetitive bleeding, infections and encephalopathy; the only effective cure at this stage is liver transplantation(13).

I will now briefly discuss the microscopic structure of the liver followed by the different forms of human liver injuries pertinent to this thesis:

## **1.2. Structure of the liver**

The liver is a unique organ as it receives oxygenated blood directly from the heart as well as deoxygenated blood from the gut via the portal vein, blood from these two sources mixes in the liver sinusoids(15). The portal circulation delivers nutrient and antigen rich blood to the liver; the microscopic functional unit of the liver [the liver acinus (fig 1.1)], containing sinusoids lined with specialized endothelium, innate immune cells and bile ducts is key to allowing the liver to serve its metabolic and immunological functions (fig 1.1) (16)



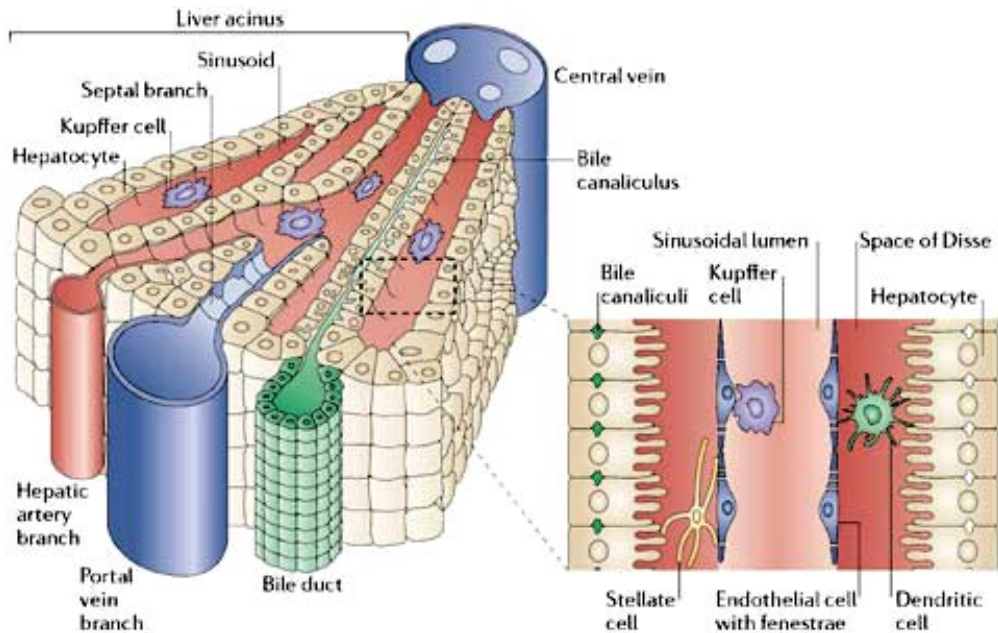


**Figure 1.1 Structure of the liver acinus:**

Deoxygenated blood from the gut rich with nutrients and pathogens drains into the liver via the portal vein whilst oxygen rich blood from the heart enters via the hepatic artery; blood from both these sources mixes within the liver sinusoids. The biliary canaliculi lined by cholangiocytes drain the hepatocyte secreted bile in the opposite direction to the blood flow into small bile ducts which eventually merge to form the larger intra and then extra hepatic biliary system. The hepatic artery, portal vein and associated bile duct are referred together as the portal triad, and are on the portal side of the acinus. Specialized sinusoidal endothelium (lacking a basement membrane and tight junctions) comprised of sinusoidal endothelium cells lines the liver sinusoids. These cells are organized like sieve plates with multiple fenestrations, which aid nutrient extraction from the blood. Liver macrophages or Kupffer cells reside within the sinusoids surveying the blood for pathogenic bacteria whilst simultaneously helping to maintaining immunological tolerance to harmless antigens.

Between the sinusoidal endothelium and hepatocytes is the space of Disse; excess extracellular fluid is believed to drain to the liver lymphatics through this space and it contains liver stellate cells and fibroblasts. Blood exits the sinusoids through the central vein which is on the centrizonal side of the acinus. Multiple central veins merge together to give rise to the hepatic veins which provide venous drainage back to heart. Image taken from Eksteen et al(16)

The hepatocytes that lie along the sinusoids have different metabolic functions starting from the portal to centrilobular end of the acinus; this phenomenon is termed metabolic zonation(17). The hepatocytes closest to the portal triad receive the highest amount of oxygen and form the zone 1 or periportal hepatocytes; they thus have a different set of metabolic functions to the ones nearest the central vein (zone 3 or centrilobular hepatocytes) which receive blood with lower levels of oxygen. The zone 1 hepatocytes carry out oxygen dependent functions such as fatty acid oxidation and sulfation(17), whilst the zone 3 ones have a richer concentration of the cytochrome P450 (CYP) enzymes, and hence are the first ones to be damaged by toxic byproducts of xenobiotics(18).

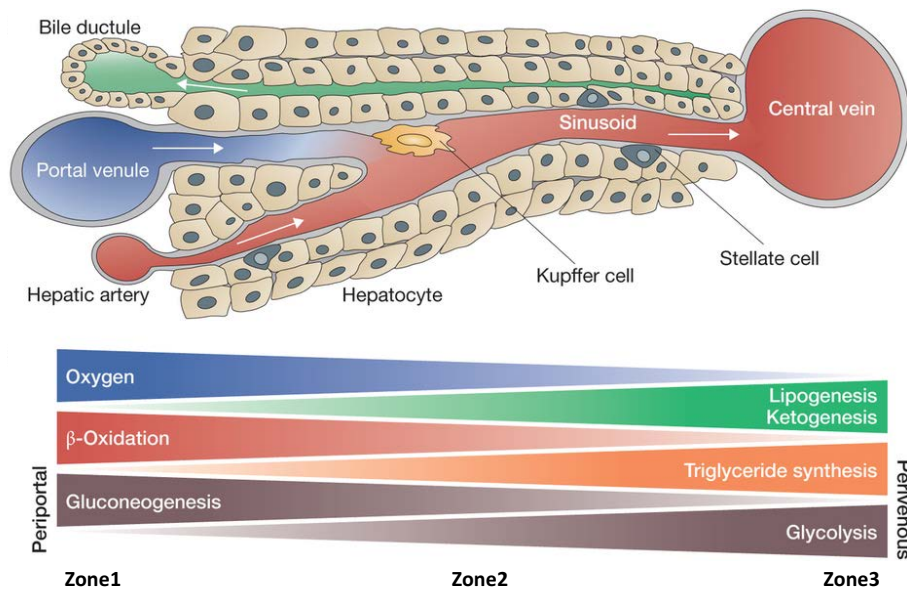


**Figure 1.2 Metabolic zonation of the liver:**

Zone 1 hepatocytes receive the highest oxygen concentration on the periportal side. Zone 3 hepatocytes (in the centrilobal area) contain the highest concentrations of CYP enzymes and also receive the lowest concentration of oxygen and are thus more prone to hypoxic damage(16). Image taken from Birchmeier(19)

### **1.3. Major classes of liver injury studied**

#### **1.3.1. Alcoholic liver disease**

Alcoholic liver disease is the commonest cause of chronic liver disease in the West(20). The spectrum alcoholic liver disease encompasses is wide; starting with simple liver steatosis in its early stages, to alcoholic hepatitis with advancing consumption and eventually alcoholic cirrhosis which is end stage liver disease. Steatosis or fatty liver is an early change seen in the livers of heavy drinkers and begins in the peri-venular or zone 3 hepatocytes, Recent evidence suggests that continued and heavy alcohol exposure, influences the transcription factors that are associated with lipid metabolism. This results in enhanced lipogenesis and lower levels of fatty acid oxidation and thus hepatic steatosis(21). Continued alcohol consumption drives episodes of acute hepatic inflammation (often on a background of steatosis, early fibrosis or even established cirrhosis)(22). These episodes of inflammation are termed alcoholic hepatitis and range from mild to life threatening with the hepatic histology at this point showing ballooning of hepatocytes, neutrophilic infiltration and the characteristic Mallory-Denk inclusion bodies(20). About 30-35 percent of heavy drinkers proceed to develop end stage alcoholic liver disease or alcoholic liver cirrhosis(20).

#### **1.3.2. Non-alcoholic fatty liver disease**

Non-alcoholic fatty liver disease (NAFLD) is the hepatic manifestation of the metabolic syndrome(23). Similar to alcoholic liver disease NAFLD again exists as a histological spectrum starting from steatosis to hepatic necroinflammation [termed

non-alcoholic steatohepatitis or NASH(24)] and eventually to fibrosis and cirrhosis(25). The diagnosis of NAFLD is based on clinico-pathological criteria which require at least the present of steatosis and exclusion of other causes of liver disease(25). NAFLD represents one of the fastest growing causes of liver disease(25,26)

### **1.3.3. Autoimmune liver disease**

Autoimmune hepatitis (AIH), primary biliary cirrhosis (PBC) and primary sclerosing cholangitis (PSC) are the three main forms of immune mediated liver disease, there is variation amongst these according to the initiating autoimmune damaging insult, pattern of histological damage and thus final clinical phenotype(27).

AIH is a classical autoimmune condition, exhibiting many features one would associate with autoimmunity including female preponderance, seropositivity and response to immunosuppressive therapy(27,28). AIH is divided into subtypes (types 1 to 3) on the basis of type of autoantibodies found in the serum. The histopathological findings are fairly uniform amongst the different subtypes; a plasma cell rich lymphocytic infiltrate in the portal and periportal areas leading to interface hepatitis is characteristic(27). In parallel with other forms of liver disease if the damage progresses unchallenged, periportal fibrosis followed by broader fibrotic septa and ultimately cirrhosis with regenerative nodules results(29).

PBC and PSC affect the bile ducts and thus comprise the autoimmune cholangiopathies. PBC characteristically affects the small interlobular bile ducts causing a non-suppurative and destructive cholangitis whereas in PSC the immune

injury affects the medium sized and extra hepatic bile ducts causing obliterative fibrosis and multifocal bile duct stricturing(27). Although both of these conditions exhibit autoimmune features (PSC less so than PBC) such as auto reactive T and B cell responses and the presence of characteristic antibodies (AMA-antimitochondrial antibodies) in PBC or the presence of non-specific antibodies including atypical ANCA and association with other autoimmune diseases such as inflammatory bowel disease in PSC(27), the response to immunosuppressive medication is disappointing.

All three conditions are progressive and if untreated may lead to the need for liver transplantation(27), whilst most cases of AIH respond to immunosuppressive therapy such as corticosteroids and azathioprine(27); the only licensed therapy for PSC and PBC is ursodeoxycholic acid (UDCA). UDCA is a hydrophobic bile acid that has an effect in the cholangiopathies by protecting cholangiocytes (bile duct lining cells) from direct cytotoxicity of hydrophobic bile acids, stimulation of hepatobiliary secretion and reducing bile acid-induced hepatocyte apoptosis(30). Immunosuppressive medication in contrast to its role in AIH has little efficacy (for a variety of reasons) in PBC and PSC and thus is not routinely used(27).

#### **1.3.4. Paracetamol induced fulminant liver failure**

Paracetamol metabolism and the resultant liver injury are both discussed in greater detail in section 4, suffice to say that as paracetamol is metabolized by enzymes of the cytochrome system (present in maximal concentrations in the zone 3 or the centrilobular hepatocytes-fig 1.2), the toxic byproducts of this metabolism in

paracetamol overdose cause a characteristic centrilobular (zone 3) pattern of liver necrosis.

#### **1.4. Inflammatory cells drive disease pathogenesis in acute and chronic liver disease**

In acute liver injury the initial hepatic insult is followed by innate immune system activation(31). Liver resident and infiltrating innate immune cells including macrophages, neutrophils, natural killer cells, cytotoxic T cells and dendritic cells, interact with stromal cells and these collectively survey and monitor the hepatic environment for damage or infection(32,33). The function of this system is to clear dead/dying cells, enable repair and regeneration and guide a return to hepatic homeostasis(34). Most bouts of liver damage result in short lived episodes of liver inflammation or acute hepatitis. These mostly sub-clinical episodes spontaneously remit with little or no long-term sequelae. The hepatic inflammatory response can however on occasion instead of healing the liver, itself cause vast amounts of hepatocellular loss, worsening the initial injury and then potentially acute fulminant liver failure(4). The reasons this happens can sometimes be traced back to the nature or potency of the injurious stimuli (i.e. massive paracetamol overdose or overwhelming viral infection), but similar insults often drive different outcomes in different patients; the reasons for this variability are not completely understood and are likely to be multifactorial. The innate immune response can worsen the initial liver injury by enhancing liver cell death pathways such as necroptosis, necrosis, apoptosis and autophagy(35). Such detrimental innate immune system activation

during acute liver injury often invokes a systemic inflammatory response driving a sepsis like immune paresis(35), The final result of this is multiple organ failure and accelerated hepatocyte loss resulting in the metabolic, immune and coagulopathic collapse characteristic of ALF(5).

On the other hand, repetitive low grade liver insults result in iterative bouts of low grade inflammation and subsequently healing. Iterative patterns of liver damage and resultant inflammation result in the development of a stromal microenvironment comprised of a neomatrix, where interactions particularly between activated fibroblasts and macrophages(13) result in dysregulated cytokine production(36) and contribute to leukocyte positioning, recruitment and persistence, driving the fibrogenesis that results in chronic liver disease(13). Iterative inflammation therefore gradually drives the destruction of the liver macro and micro architecture, development of fibrosis, loss of hepatic function, and end stage liver disease which is characterized by liver cirrhosis and hepatocellular cancer (HCC)(13).

Macrophages in particular have critical roles in both acute and chronic liver disease. The hepatic macrophage population, comprising both resident hepatic (Kupffer cells KCs) and blood derived macrophages (monocyte derived macrophages (MoMf))(37) accounts for the vast majority (almost 80%) of the total number of macrophages in the body(38). In mice, although Kupffer cells have traditionally been thought to perpetuate the initial toxic insult by releasing factors such as  $TNF\alpha$  and CCL2 which initiate the immune response to paracetamol induced liver injury(38), depleting KCs results in a massive aggravation in paracetamol induced liver injury suggesting that



they overall likely play a protective role(39). The protective role of macrophages is also seen in human paracetamol injury where low levels of M-CSF (macrophage chemoattractant) is associated with poor outcomes overall(38). The macrophage role extends beyond acute liver injury; macrophages have divergent roles in chronic liver injury being important in driving both progression and resolution(40). Macrophage heterogeneity within the injured liver is consequent upon distinct pathways of activation which themselves are driven by specific cytokines and cellular interactions, particularly with fibroblasts(13). Large numbers of macrophages accumulate within the livers of patients with chronic liver disease; studies reveal that CD14<sup>high</sup>CD16<sup>+</sup> macrophages are particularly important(38). This particular population is recruited to the liver by CX3CL1 and then undergoes transendothelial migration via VAP-1(41). In humans CD14<sup>high</sup>CD16<sup>+</sup> macrophages secrete pro inflammatory and profibrotic cytokines such as TNF $\alpha$ , IL-8 and IL-1 $\beta$  and activate collagen producing stellate cells(40), thus driving fibrosis. Murine models of fibrosis have arguably been more comprehensively dissected than the human versions, here hepatic macrophage infiltration is driven by chemokine pathways which may drive fibrosis such as CCL2-CCR2(42) and CCL1-CCR8(43) or inhibit it such as CX3CL1-CX3CR1(44). The macrophage role in resolution of fibrosis becomes apparent with the emergence of Ly6C<sup>low</sup> restorative macrophage population on cessation of injury; this population secretes various metalloproteinases (9, 12 and 13) which then aid reduction of fibrosis(45).

Another derivative of the myeloid compartment of cells is the neutrophil. After paracetamol induced liver damage neutrophils accumulate within the livers of both mice and humans(38,46). This is driven by the expression of DAMPs (damaged associated motif patterns) or alarmins, macrophages further enhance neutrophilic recruitment to the liver by sensing the expression of DAMPs by injured hepatocytes and secreting neutrophil recruiting cytokines. This process is part of the 'sterile inflammatory response' to liver injury(47) and is discussed in greater detail in chapter 4. The infiltration of neutrophils is also seen within the livers of patients with chronic liver disease and chronically injured murine livers(38,48), in fact most liver diseases exhibit a degree of neutrophil co-localization. Although their role in acute liver injury and processes such as pathogen clearance and immune cell recruitment are well described and have traditionally been thought of as deleterious to the liver(38,49), recent work highlights a restorative or reparative role for neutrophils after a toxic liver injury(50).

### **1.5. Is there a role for platelets in liver disease?**

Although there is a striking difference between the final clinico-pathological features of acute and chronic liver disease, there are parallels between how they develop, most notably at the level of the initial necroinflammatory and innate immune response to injury. Manipulating the innate immune system may thus help in the treatment of both acute and chronic liver disease. Platelets represent a unique part of the innate immune system with well described functions in haemostasis, and arguably less familiar but equally relevant functions as immune cells(51). Platelets

interact with many of the key cellular protagonists of acute and chronic liver disease including myeloid cells, sinusoidal endothelial cells, lymphocytes and stromal cells(15,52) and unsurprisingly therefore the platelet role in liver pathology has been under much scrutiny over the last decade. Platelets have now been shown to contribute to almost all aspects of liver pathobiology including acute and chronic hepatitis, liver regeneration and the development of fibrosis(53). Although the specific molecular basis of these interactions is yet to be comprehensively be established(32). Manipulating platelet function to modulate the innate immune response during liver inflammation may be valuable in the treatment of both acute and chronic liver disease(52,54). With the growing burden of liver disease and the limited treatments currently available, establishing a definitive role of platelets in the different stages of liver disease, to then potentially use antiplatelet therapy which is already widely available, becomes particularly relevant.

## **1.6. Platelets and haemostasis**

The traditional paradigm of platelet function revolves around how platelets maintain vascular integrity at points of endothelial disruption through haemostasis. Having been extensively studied in cardiovascular science; the archetypal platelet role starting from adhesion to the damaged vessel wall culminating in activation and aggregation in concerto with the clotting cascade has been extensively described(53). The initial interaction with the damaged vessel wall is between platelet (GP) 1b-V-IX with von Willebrand factor (vWF). Formation of a thrombus starting from the initial weak GP1b-vWF interaction requires a rapid upregulation of autocrine

and paracrine signaling to amplify and sustain the platelet response(53,55). Central to this is the GP VI receptor. Platelets flowing at high velocities and under the considerable shear stress found in medium and large arteries thus use GP1b to tether to exposed vWF, this slows them down sufficiently to allow a meaningful collagen GP VI interaction (56,57). When collagen interacts with GP VI an 'inside-out' signal is generated which then institutes a conformational change in platelet integrins. The relevant platelet integrins  $\alpha 2\beta 1$  and GP IIb/IIIa, switch from a resting low affinity state to a high affinity state and bind to collagen resulting in stable platelet adhesion(56). The next stage of platelet activation is dependent on recruitment and activation of more platelets from the circulation. Release of soluble mediators and their interaction with G protein coupled receptors (GPCRs) is the key mechanism here(58).

After a GPVI dependent platelet monolayer develops at the site of vascular injury, local concentrations of potent platelet activating molecules including adenosine diphosphate (ADP), thromboxane A2 (TXA2) and thrombin increases(57). These molecules act on GPCRs, drive positive feedback loops and upregulate their own production resulting in rapid activation and recruitment of platelets to the growing thrombus(58). ADP is stored within the platelet dense granules in high concentrations and is released on platelet activation(58). Thus, released ADP acts on the platelet GPCRs:  $P_2Y_2$  and  $P_2Y_{12}$ , resulting in further platelet activation, characteristic shape change and positive feedback which accentuates platelet responsiveness to other

platelet activators such as TXA<sub>2</sub>(58). The thienopyridine clopidogrel exerts its anti-thrombotic action by irreversibly binding an inhibiting P<sub>2</sub>Y<sub>12</sub>.

Thrombin which is produced by the exposure of tissue factor to plasma coagulation factors on platelet and endothelial cell surfaces is amongst one of the most powerful platelet activators(58). Thrombin receptors are called protease activated receptors (PARs); mouse platelets express PAR 3 and 4, whilst human platelets express PAR 1 and 2 (59).

TXA<sub>2</sub> is produced from arachidonic acid through the action of cyclooxygenase-1 (target of low dose aspirin) (60). TXA<sub>2</sub> activates platelets via its actions on the TXA<sub>2</sub> receptor (TP). This second phase of platelet activation requires a rapid and coordinated response of platelets to soluble mediators, and the versatility and thus responsiveness of the GPCR system is critical to this phase(58).

The major platelet receptors (with their corresponding ligands) are detailed in table 1.1 below [adapted with permission from Moroi et al(57)].

Receptor	Ligand	Receptor type
PAR1 (only in human)	Thrombin, PAR1 peptide (synthetic)	G protein-coupled receptor
PAR4	Thrombin, PAR4 peptide (synthetic)	G protein-coupled receptor
P2Y1	ADP	G protein-coupled receptor
P2Y12	ADP	G protein-coupled receptor
TP	TxA2, U46619 (synthetic)	G protein-coupled receptor
GPVI	Collagen, laminin, CRP (synthetic), convulxin (snake toxin), JAQ1 (antibody)	Immunoglobulin
$\alpha 2\beta 1$	Collagen	Integrin
$\alpha 6\beta 1$	Laminin	Integrin
GPIb-XI-V	vWF, ristocetin (snake toxin)	Leucine-rich
$\alpha IIb\beta 3$	Fibrinogen, vWF	Integrin
P2X1	ATP	Ca <sup>2+</sup> channel
CLEC-2	Podoplanin, rhodocytin (snake toxin)	C type lectin-like

**Table 1.1 Overview of the key receptors expressed in platelets (57).**

Most classes of major platelet receptors have a prominent role in mediating haemostasis (61) and it is pertinent to therefore note that the vast majority are linked to and activate similar downstream pathways, this often begins with phospholipase C (PLC)  $\beta$  (60,62). PLC-  $\beta$  has a variety of roles and induces numerous intracellular responses; critical ones include cytoskeletal rearrangements,  $Ca^{2+}$  dependent Rap1b (Ras-related protein Rap-1b) activation and DAG-dependent protein kinase C (PKC) activation. Rap1 then induces activation of the fibrinogen receptor and  $\alpha_{IIb} \beta_3$  integrin (GPIIb-IIIa) whilst PKC triggers platelet granular secretion(60) (platelet granular secretion is discussed later). GPIIb-IIIa is the main and final receptor for platelet adhesion and aggregation(55)and thus thrombus formation.

## **1.7. ITAM receptors and their ligands**

The focus of this thesis is the role platelet activation via the C-lectin like receptor-2 (CLEC-2) plays in liver disease. CLEC-2 belongs to the ITAM group of receptors; these receptors signal intracellularly through immunoreceptor tyrosine-based activation motif represent a significant mechanism for platelet activation(63). CLEC-2, GPVI and Fc RIIA belong to this class of receptor, Fc RIIA however is present only on human platelets and absent from murine platelets. I will therefore discuss what is already known about the roles of such ITAM receptors in health and disease and why ITAM (and associated signaling pathway) blockade may be of relevance in liver disease.

### **1.7.1. CLEC-2 and Podoplanin**

CLEC-2 (fig 1.3) is encoded by the CLEC 1b gene on chromosome 12; this gene is within the Dectin-1 gene cluster where genes for six other C-type lectin receptors are also present(64). C-type lectin receptors are important pattern recognizing receptors (PRRs) which recognize molecular patterns on pathogens and initiate the intracellular signaling cascades critical to the cellular innate immune response to infection. CLEC-2 was thus originally identified as being present on immune cells and is present albeit in small amounts on a subpopulation of inflammatory dendritic cells (60,64). Using a combination of mass spectrometry and affinity chromatography to the snake venom toxin rhodocytin, Watson et al demonstrated the presence of CLEC-2 on platelets (65) identifying it as the key receptor via which rhodocytin elicited platelet activation.



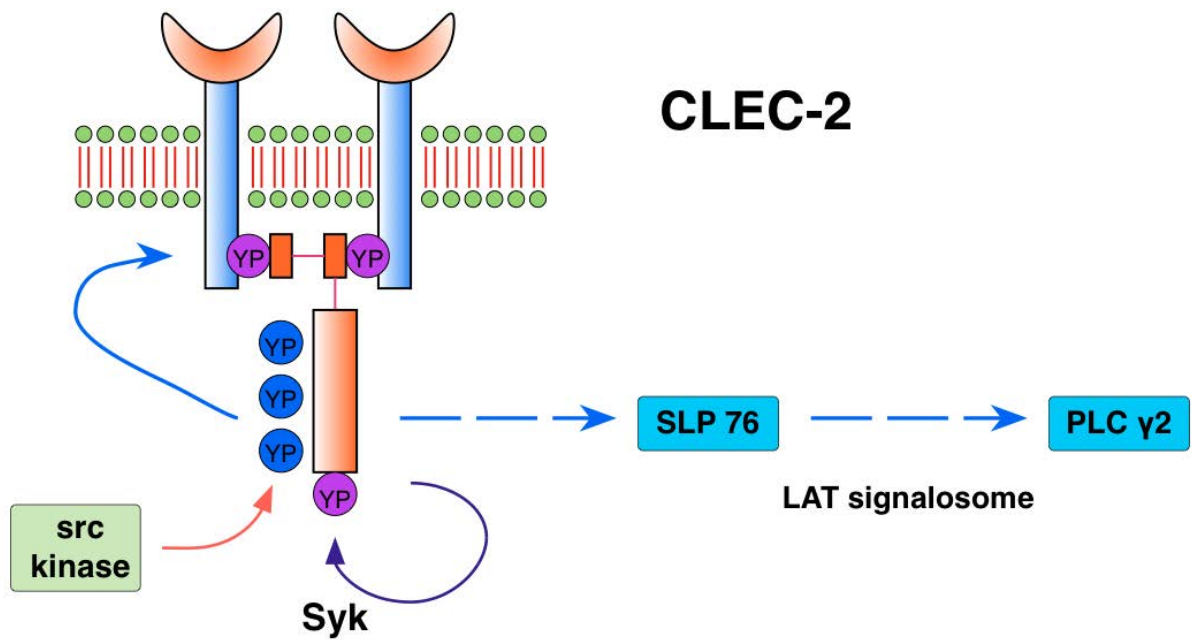


**Figure 1.3 The structure of the CLEC-2 receptor:**

CLEC-2 exists as a homodimer on the surface of the platelet. It dimerizes once it binds its ligand and then signals intracellularly initially via Src (proto-oncogene tyrosine-protein kinase) and Syk (spleen tyrosine kinase) kinases, which then recruit and activate SLP-76 (lymphocyte cytosolic protein 2) and PLC- $\gamma$ 2 via the LAT (linker for activation of T cells) signalosome.

Experiments demonstrating that tumor cells could cause platelet activation (which in turn facilitated cancer expansion) in a manner similar to rhodocytin led to the identification of the only known endogenous ligand for CLEC-2: podoplanin (66). Podoplanin is a 43kDA protein and was initially identified as a key protein in maintaining the glomerular filtration barrier; it was named podoplanin due to its presence on glomerular epithelial foot processes or podocytes (67). Podoplanin expression is rather more ubiquitous in its expression than CLEC-2. It is widely expressed on a variety of mammalian cells and has several names which reflect its discovery in different species including aggrus, T1  $\alpha$  and gp36 in humans, gp38 or OTS-8 in mice, E-11 antigen in rats and gp40 in canine cells(68). Podoplanin is observed on lymphatic endothelium(69) , kidney podocytes (67) and type-1 pneumocytes(68). Podoplanin expression changes during embryonic development, starting at high concentrations in the developing nervous system in the embryo to then being restricted to the choroid plexus in adults(68, 70) thus suggesting that it may have functions both in embryonic development and adult nervous system function.

In addition to activating platelets via CLEC-2, podoplanin itself is linked to the actin cytoskeleton of the cell via the ERM (ezrin, radixin and moesin) proteins(71). Over expression of podoplanin, phosphorylates the ERM proteins thus exposing additional sites for actin and other proteins(69). This pathway may explain some of the effects podoplanin has on cellular motility and why it has been extensively studied in the context of cancer invasiveness and metastases, this is further discussed in chapter 3.

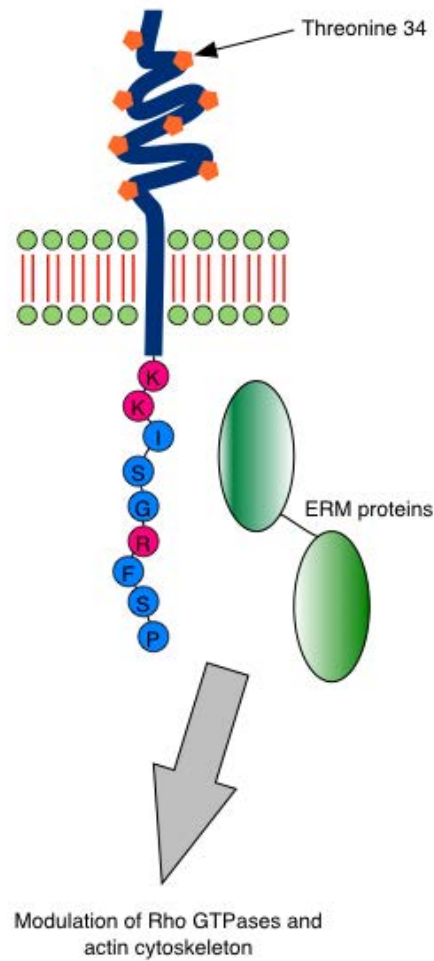


**Figure 1.4 Schematic diagram illustrating the structure of Podoplanin:**

This basic schematic of podoplanin illustrates that podoplanin interacts with the cytosolic ERM proteins via a cytoplasmic amino acid tail (the three key amino acids for this interaction are K, K and R-coloured in pink). This interaction with ERM proteins enables podoplanin to influence cell migration by causing rearrangement of the actin cytoskeleton. Glycosylation of residue threonine 34 in the extracellular domain is necessary to support binding to CLEC-2.(adapted from Astarita et al(69))

### 1.7.2. GPVI and its ligands

The observation that collagen dependent platelet activation is blocked by tyrosine kinase inhibitors led to the discovery of GPVI(72). GPVI is the platelet collagen receptor and belongs to the Ig superfamily of surface receptors with two Ig domains(72). Although GPVI exist in both monomeric and dimeric forms, the monomeric forms inherently low affinity to collagen precludes binding at physiological concentrations(72). Binding of dimeric GPVI to collagen causes cross linking of the two dimers and thus phosphorylation of a conserved ITAM region within the FCR- - chain (72). The gene for GPVI is located on chromosome 19, and in addition to collagen GPVI can also bind to laminin and adiponectin. Although the physiological relevance of these interactions is not immediately clear (66), laminin appears to have a role in facilitation platelet spreading through  $\alpha6\beta1$  (73). Given the central role this receptor plays in the beginning of platelet activation it would seem sensible to assume that a GPVI deficiency would give rise to a substantial bleeding diathesis. Observations in patients with compound heterozygous mutations for the GPVI receptor however reveal that upto a 50% reduction in GPVI levels does not appreciably alter bleeding risk(72). This may be due to the recent observation that platelets have some constitutively active  $\alpha2\beta1$  which can bind to fibrillar collagen without the need for the 'inside-out' signal GPVI provides(74) , or more likely the redundancy in the downstream pathway via which GPVI signals(57).

### 1.7.3. ITAM signaling

Both CLEC-2 and GPVI signal via the ITAM sequence characterized by Yxx(I/L)x(6-12)Yxx(I/L). Upon receptor activation, the ITAM sequence is tyrosine phosphorylated by receptor associated src kinases. Dual ITAMs then serve as a docking site for SH2 containing proteins including Syk tyrosine kinase (60)(75). CLEC-2 is different to the other ITAM receptors as it exists as a homo-dimer on the platelet surface, and dimerizes on meeting its extracellular ligand-podoplanin thus providing the dual ITAM scaffolding required for syk docking (76). Once bound, Syk undergoes both autophosphorylation and further phosphorylation by Src family kinases (57). Activated Syk then starts a signaling cascade involving linker for T cells (LAT) and the SH-2 domain containing leucocyte protein of 76kDa (SLP-76). This results in recruitment and activation of PLC 2 (70), Tec family kinases(57,60) and PI3K-dependent signaling (60)(77) , calcium influx and then platelet activation.

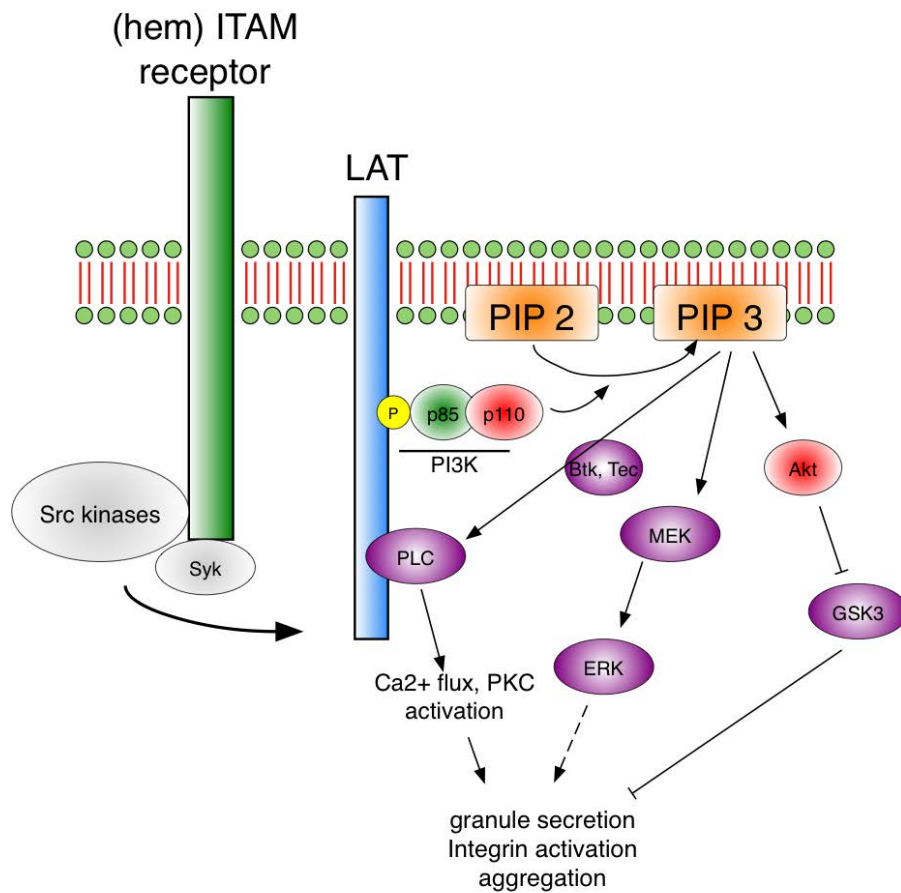


**Figure 1.5 ITAM signaling:**

Once the ITAM receptor GPVI or the hemITAM receptor CLEC-2 are activated, PI3K activation ensues; PI3K converts PIP2 to PIP3 within the platelet plasma membrane. PIP3 then activates Akt, which then phosphorylates GSK3. GSK3 phosphorylation serves to suppress platelet activation in GP VI (thus acting as a negative feedback pathway) but actually enhances platelet activation in CLEC-2. PI3K generated PIP3 also activates MEK and ERK, PLC $\beta$ 2 and recruits Btk and Tec to the plasma membrane to induce calcium elevation and platelet activation (adapted with permission from Moroi et al(57)).

### **1.7.3.1. The coagulopathy of liver disease: could therapeutic blockade of ITAM mediated platelet activation avoid contributing to bleeding risk?**

GPCR signaling as discussed above has a critical role in effective haemostatic plug formation, however individual platelet ITAM receptor removal/blockade appears not to worsen the bleeding risk in a similar fashion to GPCR blockade (60,70,78). Mice with CLEC-2 deficient platelets do not exhibit prolongation of tail bleeding times (57,65). Thus, in keeping with the fact that the CLEC-2 ligand-podoplanin has not been reported as being expressed on structures or cells where it may facilitate thrombus formation such as vascular endothelium, platelets or exposed sub-endothelial matrix (57). This limited role of CLEC-2 in thrombosis and homeostasis has however been debated, as May *et al* demonstrate defective thrombus formation in mice treated with a CLEC-2 depleting antibody (79), this may have been due to the filter blotting assay used by May *et al* to assess clot formation; other groups have found no discernible increase in bleeding times with the same antibody but using non-filter assays (80,81). Similarly, no appreciable bleeding diathesis is noted with a selective GPVI deficiency (82). This aspect of individual ITAM receptor blockade makes blocking one of these receptors a particularly attractive method of abrogating platelet activation in patients where the bleeding risk is substantial, such as in patients with acute liver failure with associated disseminated intravascular coagulation. Although the bleeding risk that accompanies the 'coagulopathy' of chronic liver disease is overstated(83), it would regardless seem sensible to exhibit caution when manipulating platelet function in these patients until a definitive role for platelet function and haemostasis can be established in CLD; again, highlighting a

case for targeting ITAM receptor driven platelet activation. Blocking Syk signaling (downstream of ITAM receptors CLEC-2 and GPVI) using Syk deficient mice or small molecular inhibitors such as PRT060318 again does not prolong tail bleeding times(64) , which is interesting as *in vivo* experiments with mice deficient in both GPVI and CLEC-2 results in profound defects in haemostasis and arterial thrombus formation(57). It thus seems likely that these haemostatic defects in the double deficient mice are thus due to a combination of loss of adhesion plus activation compared to a complete block of the signaling pathway(64).

#### **1.7.3.2. Role of ITAM receptors in maintenance of vascular integrity and inflammation**

Platelets have an important role in the maintenance of vascular endothelium. This is greater than merely mediating healing at points of damage or disruption. Studies in thrombocytopenic rabbits(84) and humans(85) demonstrate endothelial thinning, increased permeability and abnormal capillary fenestrations. The maintenance of endothelial integrity becomes particularly important during situations of increased leukocyte movement such as during inflammatory processes or within lymph nodes for the development of adaptive immunity. Herzog et al recently demonstrated the role of platelets in maintaining high endothelial venue integrity (HEV) in lymph nodes(86). Here platelets (via CLEC-2) interact with podoplanin expressing fibroblastic reticular cells (FRCs), which then causes a localized release of sphingosine-1-phosphate (S1P) from platelets. This platelet derived S1P then maintains vascular integrity by increasing VE-cadherin expression on HEV cells (86).



Similarly, during models of lung inflammation, Boulaftali et al note that inhibiting GPVI or removing CLEC-2 from platelets results in a breakdown of the vascular barrier causing intra-alveolar haemorrhage (78). Interestingly it was noted that blocking GPCR signaling had no effect on the maintenance of vascular integrity in the same model (78). It is pertinent to note that there in order for there to be bleeding or a breakdown in vascular integrity during thrombocytopaenia, a 'second hit' of inflammation after thrombocytopenia is needed (87). George et al imaged the cutaneous Arthus reaction, and demonstrated in real time the breakdown of vascular integrity in thrombocytopaenic mice during inflammation and the increased leukocyte movement this brought(87). It is likely that the increased trafficking of leucocytes that accompanies inflammation essentially 'punches' holes in the endothelium which are then rapidly sealed by platelets in an ITAM dependent fashion, perhaps through a combination of suppressing further inflammation or releasing endothelium healing vasoactive factors (75).

The main leukocytes responsible for the inflammatory bleeding that accompanies thrombocytopaenia are probably neutrophils, as depleting neutrophils or blocking their migrating ability reduces such haemorrhage (88). Whether the vasculoprotective effects of platelets during leukocyte trafficking extend beyond 'healing' the endothelium to actively manipulating leukocyte effector activity, such as by interacting with podoplanin expressing inflammatory macrophages (89,90) is yet to be established.

### **1.7.3.3. Role of CLEC-2 in lymphatic development**

The separation of lymphatic and blood vessels during embryogenesis as well as the maintenance of this separation during adult life is highly dependent on platelets, specifically the ITAM signaling pathway beginning with CLEC-2(70). During embryogenesis, blood within the developing vasculature comes into contact with podoplanin expressing lymphatic endothelium; this interaction initiates platelet ITAM signaling via CLEC-2 resulting in the separation of lymphatic vessels from blood vasculature (75). The role downstream molecules including Syk and SLP-76 play in mediating blood lymphatic separation was established using chimeric mice over 10 years ago(91). Subsequent experiments using mutant mice models with conditional deficiencies of CLEC-2 and Syk within the megakaryocytic cell lineage demonstrate a similar phenotype of abnormal blood-lymph secondary to erroneous lymphatic development(70), the fact that this phenotype was not replicated on inducing a Syk deficiency in any of the other haematopoietic lineages confirms the specific role of platelets in this process(70).

It is interesting to note that CLEC-2 signaling on platelets is not only essential for the initial development of the lymphatic system but also in the maintenance of the 'blood-lymph barrier' in later life(92). This holds particular relevance to the liver as the low shear, non-injured (during health) environment of the liver sinusoids is not dissimilar to the low flow, low shear environment at the lymphovenous junction; additional parallels between both environments is the lack of dependence on integrins for either thrombosis(93) or cellular recruitment(15).

## **1.8. Platelets beyond homeostasis (53)**

It is increasingly being recognized that platelets play a complex role beyond their role as cellular mediators of thrombosis; the platelet ITAM receptors illustrate this point well. Contribution of platelets to diverse processes including atherosclerosis(63), infection(94), lymphangiogenesis(70), acute lung injury(95) has now been described. An emerging theme from recent work is how intricately platelets interact with inflammatory cells and influence the outcome in inflammatory reactions (96). I shall next therefore briefly review what is known about how platelets participate in inflammatory processes in general.

### **1.8.1. The platelet secretome dictates function (53)**

Soluble mediators contained within these cells help account for some of the other observed roles that platelets play in pathophysiological processes; the 'platelet secretome' which is arguably context specific (97) helps shape the outcome of platelet activation. Platelets contain a plethora of biologically active proteins, most of these inflammatory and immune mediators are preformed and stored in the alpha, dense and lysosomal granules within the platelet cytoplasm (63).

The least abundant lysosomal granules contain glycohydrolases and degradative enzymes (63). Dense granule constituents range from the vasoactive peptide serotonin to calcium and pyrophosphate (98), these granules thus contribute to platelet activation, aggregation and modulation of systemic vascular tone (63). The  $\alpha$ -granules are the most abundant granule in platelets; they are synthesized in

megakaryocytes prior to the mature platelets 'budding' off. Proteomic analysis has confirmed the presence of hundreds of proteins within  $\alpha$ -granules (52). The diverse contents include proteins destined to be expressed on the platelet surface and also soluble proteins that are released into the extracellular space (63). Hence  $\alpha$ -granules secrete fibrinogen and von Willebrand factor (vWf), adhesive proteins which mediate platelet-platelet and platelet-endothelial interactions and therefore are critical to primary and secondary haemostasis (99,100). P-selectin, which translocates from  $\alpha$ -granules to the platelet surface following platelet activation is a critical immunomodulatory molecule and participates in platelet interactions with endothelial cells, monocytes, neutrophils, and lymphocytes. Furthermore,  $\alpha$ -granules contain a variety of mediators that induce recruitment, activation, chemokine secretion, and differentiation of other vascular and hematologic cells (99,100).

An interesting but contentious point is whether platelet activation results in a non-specific degranulatory event causing the platelet to release all of its inflammatory payload or whether a more selective profile of cytokine release can be triggered by different activating signals. There is evidence to suggest that depending on the initial stimulus, certain granules are preferentially released. Italiano et al suggest that distinct populations of pro and anti-angiogenic factor containing  $\alpha$ -granules exist, whose secretion is differentially regulated by different stimuli (97). Given the contrasting and varied pathology mediated by platelets, selective granule secretion remains an exciting avenue for further study. Mechanistically this may explain why

platelets behave in different ways mediating seemingly contrasting roles in liver injury(52).

### **1.8.2. Platelet sequestration in tissue contributes to inflammation**

Platelets can bind to the endothelium in the absence of collagen exposure or endothelial denudation(101) , this occurs only if either (or both) the platelet or the endothelium is activated. Indeed bidirectional activation is characteristic of systemic inflammatory states such as hypercholesterolaemia(102). Platelet and endothelial activation is also seen during the sepsis associated systemic inflammatory response and underlies many of the clinically relevant sequelae including microvascular thrombosis and organ dysfunction(103) . A similar consumptive coagulopathy with concomitant small vessel obstruction is seen in the haemolytic uraemic syndrome where the shiga toxin renders both platelets(104) and the endothelium highly thrombogenic(105). Acute lung injury represents an organ specific manifestation of platelet activation aiding inflammatory cell recruitment thus driving endothelial and tissue damage. Projahn et al and Stokes et al [as cited by Boulaftali et al(75,95)] state that these interactions can potentially be mediated by a variety of platelet receptor-ligand pairs including P-selectin-PSGL-1, GPIb  $\alpha$  -Mac1, CD40L-CD40, and  $\alpha$  IIb  $\beta$  3-ICAM1.

### **1.8.3. Platelets are the gatekeepers to innate and adaptive immunity**

The ability of platelets to interact with endothelial and inflammatory cells makes them ideally suited to be part of the 'first response' to invading microbes. Platelets effectively focus haemostatic and immune responses to help prevent pathogen

invasion in situations where physical barriers such as the skin are breached(63). It is unsurprising therefore that platelets secrete and express molecules which are directly microbicidal, such as CXCL4, thymosin- $\beta$ 4, and CCL5 (RANTES)(106), but also modulate and initiate immune responses (both innate and adaptive)(107). Toll like receptors (TLR) which have critical role in antigen capture and initiation of the innate immune response are found on platelets (108) . Of these, platelet based TLR 4 may arguably be the most important by driving TNF $\alpha$  production, LPS induced thrombocytopenia (109) , mediating neutrophil adhesion and NET formation (110). Platelets have the capability to bridge the acute phase response to infection(63) to adaptive immunity by expressing immunostimulatory molecules like CD154(107) and secreting chemokines including CCL3 (MIP 1 $\alpha$ ) and CCL5(111). These molecules are known to help induce antiviral CD 8 T-cell production(112) (central to viral mediated hepatotoxicity) and mediate T-cell activation(113). Platelets additionally regulate and in many cases, are critically important in mediating tissue regeneration(52), angiogenesis, wound healing, cancer and lymphangogenesis. Given the diverse systemic and organ specific roles of platelets-some of which are highlighted above, it is perhaps unsurprising that increasingly evidence suggests that platelets play a profound role in the hepatic environment.

### **1.9. Platelets and liver disease: what is already known?(53)**

The platelet role in inflammation is entirely context dependent and varies according to pathophysiological stage of the reaction, organ involved etc.(89), it is thus important to establish these parameters prior to studying platelets in inflammatory

disease, this holds particular relevance when one examines the contribution of these cells to inflammatory processes within complex organs such as the liver. The platelet role to liver pathology is pleiotropic and sometimes seemingly contradictory especially when comparing liver disease specific platelet contributions(53).

Platelets enter the injured liver and interact with hepatic sinusoidal endothelium influencing effector cell recruitment and activation (15). These cellular interactions can result in the granular release of a range of platelet contained bioactive proteins as discussed above (52). Using these bioactive molecules platelets are able to drive diverse, even seemingly opposite hepatic processes ranging from necro-inflammation and fibrosis to liver repair and regeneration. Such variation is also observed in other organs (89) and is partly explained by the very nature of inflammation, which is a multistep, pleiotropic process with platelets varying in their contribution in a disease and stage specific manner. Strategies to block platelet activation can be platelet specific (low dose aspirin, clopidogrel and platelet depletion) or can also affect other cell types (cilostizol, rho kinase inhibitors and protease activated receptor blockade)(53). The latter must be taken into account when defining a role for platelets in liver disease and crucially these effects may explain discrepancies in the observed platelet effect in models of liver damage(53). Table 1.2 summarizes some of the roles platelets are known to play in liver disease.

<b>Type of model/injury</b>	<b>Species</b>	<b>Intervention</b>	<b>in vivo or in vitro</b>	<b>Effect of intervention on liver</b>
<b>Viral hepatitis</b>	Mouse	Platelet depletion	<i>in vivo</i>	Hepatoprotective
<b>Viral hepatitis</b>	Mouse	Inhibition of platelet activation	<i>in vitro</i> and <i>in vivo</i>	Hepatoprotective
<b>Viral hepatitis</b>	Mouse	Blocking platelet binding to endothelium	<i>in vitro</i> and <i>in vivo</i>	Variable can be either hepatoprotective or hepatotoxic
<b>Isolated HSEC co-culture with platelets</b>	Human	Blocking platelet binding to endothelium	<i>in vitro</i>	Hepatoprotective (reduced effector cell recruitment)
<b>Ischaemia reperfusion</b>	Mouse	Blocking platelet - Kupffer cell interaction	<i>in vivo</i>	Hepatoprotective (reduction in steatosis)
<b>Thermal injury</b>	Mouse	Blocking platelet binding	<i>in vivo</i>	Hepatotoxic (reduced neutrophil mediated repair)
<b>Acute cholestasis</b>	Mouse	Inhibition of platelet activation	<i>in vivo</i>	Hepatoprotective
<b>Chronic cholestasis</b>	Mouse	Platelet depletion/ Inhibition of platelet activation	<i>in vivo</i>	Hepatotoxic (worsens fibrosis)

**Table 1.2 Summary of the roles platelets play in different liver injuries(53)**



### **1.9.1. The interaction between platelets and liver sinusoidal endothelium governs hepatic leukocyte recruitment**

Hepatic sinusoids are lined by unique fenestrated endothelial cells, which are exposed to only minimal shear stress (15) and have scavenger like functions (126). Additionally, the unique phenotype of sinusoidal endothelium characterized by paucity of P-selectin expression (both constitutive and inflammation-induced) and low levels of VWF(15) help set hepatic vasculature apart from the majority of other endothelial beds and render the liver a specialized environment for platelet-endothelial interactions(53). The combinations of signals which govern recruitment of immune cells across the sinusoidal bed are distinct from those reported in other solid organs(15,127) and platelets may compensate for the lack of expression of attachment factors such as selectins to assist in leukocyte recruitment during inflammation. Studies in viral models of murine hepatitis(113,116,128), human liver regeneration and ischaemia-reperfusion injury(129), demonstrate platelet sequestration within hepatic sinusoids. *in vitro* studies with human hepatic sinusoidal endothelial cells (HSEC) demonstrate that platelet adhesion is partly integrin (GPIIb/IIIa and  $\alpha$ V $\beta$ 3) mediated(15) with the precise location of hepatic platelet adhesion varying dependent on the type of injury. For instance, in ischaemia-reperfusion injury platelets are selectively sequestered to the periportal and midzonal sinusoidal endothelium(15). Bound platelets activate isolated HSEC to express CXCL-8 and CCL-2 thereby promoting neutrophil and lymphocyte recruitment (fig 1.3)(15). Studies in rats have revealed that platelet-driven leukocyte recruitment results in hepatic damage during systemic endotoxaemia and that platelet-endothelial

interactions precede and drive leukocyte adherence(130). Furthermore, leukocytes themselves can also recruit platelets to the liver. Models of ischaemia-reperfusion injury in mice reveal the ability of CD4 T-cells to activate endothelial cells thus driving platelet recruitment to the liver sinusoids (Figure 1.3). The end result is a self-perpetuating cycle of microvascular dysfunction and hepatocellular injury(131). A schematic summarizing platelet HSEC and lymphocyte interactions is shown in fig 1.3(53).

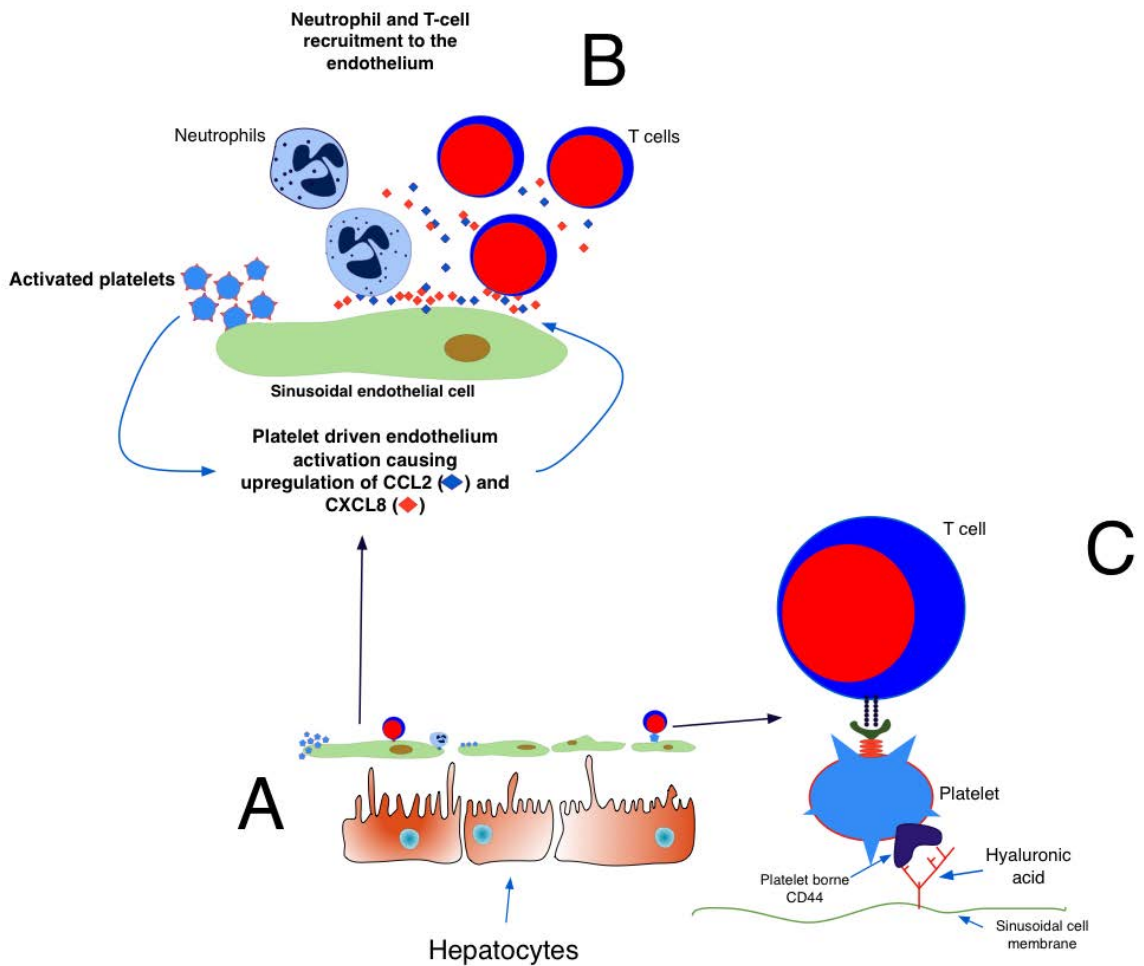


**Figure 1.6 Platelet-HSEC-lymphocyte interactions during liver injury:**

A and B) Activated platelets bind to the endothelium causing the endothelium to upregulate and secrete CXCL 8 and CCL2. These chemokines recruit T cells and neutrophils to the endothelium. C) T cells use the platelets to bind to the endothelium. Platelets use CD44 to bind sinusoidal hyaluronic acid allowing T cells to survey the liver for viral antigen (53).

### 1.9.2. Platelet interactions with myeloid cells

Platelet interaction with myeloid cells, particularly macrophages and neutrophils, has been extensively investigated in the context of cardiovascular disease, thrombosis and atherosclerosis(132–134). As Mantovani et al however point out, the role platelets play in innate immunity and inflammation via interaction with myeloid cells is frequently overlooked(135). These inflammatory and immune interactions are highly relevant to liver disease because (as already mentioned above) neutrophils and macrophages play central roles in liver injury, fibrogenesis and regeneration(40,136,137). Although the accepted paradigm is that regardless of initial insult, neutrophils recruited to the site of liver damage exacerbate liver damage, recent evidence suggests that they may also have anti-inflammatory and restorative properties(138); For example, platelets have recently been shown to physically 'pave the way' for neutrophils to enter the liver during sterile liver injury to aid repair(50)(Table 1.2). The macrophages role in liver disease has been touched upon above. Platelets have an important role in regulating macrophage differentiation and recruitment; platelet derived CXCL4 and microparticles induce patterns of macrophage activation consistent with tissue repair(139) and matrilysis(140), respectively. *in vitro* studies using human cells demonstrated the ability of platelet derived CXCL4 to induce differentiation of blood monocytes to tissue macrophages(141). These macrophages then switch to a pro-inflammatory phenotype on interacting with activated platelets at sites of tissue inflammation(142). In the liver, Kupffer cell-platelet interactions are important determinants of the outcome in liver ischaemia-reperfusion injury. During the early period of an ischaemic

insult, platelets sequester in the liver with most adhering to Kupffer cells(117) most likely through the interactions between platelet CLEC-2 and macrophage podoplanin which is up-regulated under inflammatory conditions. The interaction between platelets and Kupffer cells provides bidirectional signals which together drive tissue injury; reducing platelet-Kupffer cell binding ameliorates hepatic inflammation in steatotic livers of rodents (90,143). During ischaemia-reperfusion injury platelet-Kupffer cell interaction precedes and initiates leukocyte accumulation, sinusoidal dysfunction and the iterative inflammation which eventually results in liver failure (32).

### **1.9.3. The roles of platelets in specific liver diseases (53)**

#### **1.9.3.1. *Viral Hepatitis: are platelets a primary mediator of viral hepatitis (53)***

The generation of virus specific T cells is an important determinant of the outcome of viral hepatitis. Lang et al described how platelets aggravate viral hepatitis in mice through the secretion of serotonin that results in hepatic sinusoid microcirculation failure, delayed viral clearance and enhanced cytotoxic T-cell (CTL) mediated liver damage (128). Several other murine studies also demonstrate that depleting platelets attenuates CTL mediated liver damage (114); platelet reconstitution is able to restore intrahepatic T cell accumulation and cytotoxicity. The need for platelet activation is shown by studies in which reconstituting platelet-depleted mice with platelets rendered resistant to activation by treatment with prostaglandin E1 (PGE1) did not restore T cell mediated liver damage(116) (Table 1.3). Blocking GPIIb/IIIa and  $\alpha$ V $\beta$ 3 reduces platelet-sinusoidal binding *in vitro* by about 50%(15), suggesting that other

molecules and mechanisms promote platelet binding to hepatic sinusoids including platelet based CD44 binding to sinusoidal hyaluronan(32). (Figure 1.6)(53).

### **1.9.3.2. *Contribution of platelets to non-alcoholic fatty liver disease***

The hepatic manifestation of the 'metabolic syndrome' is non-alcoholic fatty liver disease (NAFLD)(23). Platelets already have well described roles in the vascular complications of the metabolic syndrome and atherosclerosis; a role for platelets in NAFLD is also beginning to emerge. Mean platelet volume (MPV), a surrogate marker of platelet turnover is consistently higher in patients with NAFLD(144) and there is a direct correlation between MPV and histological severity of hepatic inflammation and fibrosis(145). *in vivo* murine studies support a role for platelets in fatty liver disease(146). These studies however need to be interpreted with caution as the antiplatelet drug (cilostizol) demonstrated to have the most marked effect on reducing hepatic steatosis, inflammation and fibrosis in mice on high fat/high calorie or choline-deficient diets(146), has numerous 'non-platelet' effects. Data regarding antiplatelet therapy and liver disease in humans is generally lacking but a large recent cross-sectional analysis suggests that regular aspirin use may be associated with a lower prevalence of NAFLD(53,147).

### **1.9.3.3. *Dual roles for platelets in cholestatic liver injury***

Depletion of platelets protects against cholestasis-induced hepatic inflammation and injury suggesting that platelet interactions within the micro-vasculature may be important in cholestasis induced liver damage(121). A variety of strategies designed to block platelet function have similar effects in acute murine cholestatic injury. Rho-

kinase inhibitors reduce liver damage in bile duct ligation models of cholestasis(122) whilst platelet depletion reduces hepatic necro-inflammation in response to alpha-naphthylisothiocyanate (ANIT)-mediated cholestatic liver injury(123) However, as with other injury models, the role of platelets in cholestatic liver injury evolves with the development of chronicity. Although perpetuating acute inflammation early on, in the late stages of cholestasis, platelet activation is hepatoprotective. Thus, inducing thrombocytopaenia in mice during the latter stages of chronic cholestasis worsens liver function by causing hepatic fibrosis(148)(Table 1.3). Studies in PAR-4 (protease activated receptor) deficient mice suggest that it is probably platelet activation resulting in platelet MMP secretion and fibrolysis that underlies their observed hepatoprotective effect in chronic cholestasis(124,125) (Table 1.3).

Context (type/stage of liver injury)	Platelet derived cytokine (if any) involved	Cell(s)/structure(s) involved	Effect on cell/structure	Overall effect on liver
<b>Resection</b>	HGF, VEGF, IGF1	Hepatocyte	akt and ERK1/2 phosphorylation	Liver regeneration
<b>Resection</b>	Sphingosine-1-phosphate	Sinusoidal endothelium cells (LSEC)	LSECs start to produce IL6 and VEGF	Liver regeneration
<b>Resection</b>	Direct KC adherence	Kupffer Cell	KCs produce TNF $\alpha$ and IL6	Liver regeneration
<b>Hepatectomy</b>	Serotonin	Hepatocyte	Hepatocyte proliferation	Liver regeneration
<b>CCl<sub>4</sub> induced murine fibrosis</b>	HGF	Hepatocytes, HSCs	Hepatocyte apoptosis inhibited, HSC trans-differentiation to myofibroblast blocked	Fibrolysis, liver regeneration
<b>Hepatitis C fibrosis</b>	PDGF- $\beta$	HSCs	HSC trans-differentiation to myofibroblast	Liver fibrosis
<b>CCl<sub>4</sub> and TAA induced murine fibrosis</b>	CXCL-4	HSC	HSC chemotaxis, chemokine expression and immune cell recruitment	Liver fibrosis
<b>Viral Hepatitis</b>	Serotonin	Sinusoidal circulation	Delayed viral clearance, enhanced T cell toxicity	Liver inflammation, fibrosis and cancer

**Table 1.3 Summary of the contribution of key platelet-derived mediators to the pathogenesis of liver injury in different models.**



#### **1.9.4. Liver regeneration and fibrosis: two sides of the same platelet?**

##### **1.9.4.1. *Platelets drive liver regeneration and inhibit fibrosis***

Platelets are critical regulators of liver regeneration. After hepatic resection, platelets sequester at the resection margins and orchestrate complex processes necessary for functional hepatic architecture(149). The first suggestion that platelets may have a role in liver regeneration came from studies in rats, where thrombocytosis was observed to aid liver regeneration via hepatocyte derived growth factor (HGF)(150). Subsequently, it has been shown that platelets are potent mediators of liver regeneration; thrombopoietin induced thrombocytosis experiments have demonstrated improved survival in rodent models of partial hepatectomy (PH) ordinarily lethal (eg 90% hepatectomy)(149) or situations where regeneration has been traditionally been thought of as undermined such as cirrhosis(151). Additionally, thrombocytopenia inhibits liver regeneration in partially hepatectomized mice(129). Platelet-mediated hepatic regeneration is dependent on their ability to bind to sinusoidal endothelium, interact with Kupffer cells and traverse the space of Disse to interact with the hepatocytes as described below(152) and shown schematically in fig 1.7. *in vitro* studies with cultured HSEC reveal that platelets promote endothelial production of IL6 and vascular endothelial growth factor (VEGF) via sphingosine 1-phosphate. These two proteins simultaneously inhibit apoptosis and stimulate hepatocyte proliferation (fig 1.7)(153,154) thus providing important cues in the regenerating liver.

#### 1.9.4.2. *But platelets can also drive fibrosis*

Liver repair and regeneration requires both pro- and anti-proliferative signals to coordinate tissue repair. Platelets play a dual role: in addition to their ability to suppress fibrogenesis and drive hepatic mitogenesis, under certain conditions platelets have the potential to diminish hepatocyte regeneration and exacerbate fibrosis(140,155).

Rodent studies reveal that platelets lysates have the potential to drive the release of profibrotic factors by hepatic stellate (HSC) *in vitro* (156). A platelet-derived cytokine implicated in liver fibrosis is CXCL4. Hepatic CXCL4 levels increase proportionately to fibrotic burden and CXCL4<sup>-/-</sup> mice display markedly less hepatic fibrosis in response to injurious stimuli than their WT counterparts(157). Similar findings have been reported in human chronic liver disease; patients with advanced fibrosis have high intrahepatic and serum concentrations of CXCL4(157). A schematic summarizing the platelet role in liver regeneration and fibrosis is shown in figure 1.7(53).

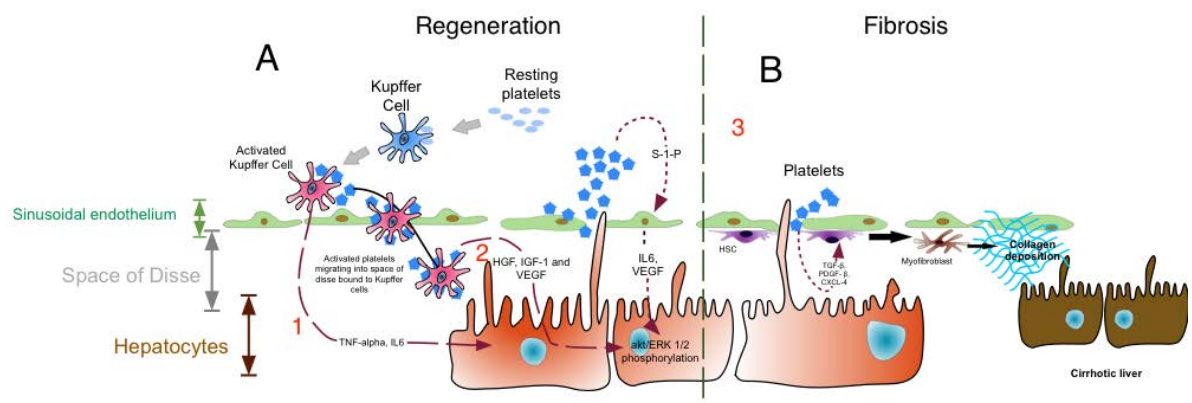


**Figure 1.7 The platelet role in regeneration and fibrosis:**

A) Regeneration; Platelets stimulate liver regeneration by three simultaneous interactions 1) Kupffer cells: on binding platelets, Kupffer cells become activated and produce TNF $\alpha$  and IL6. 2) Hepatocytes: Platelets directly stimulate hepatocyte growth and proliferation via HGF, IGF-1 and VEGF. 3) Sinusoidal endothelial cells: activated platelets produce S-1-P, which promotes liver regeneration via akt and ERK1/2 phosphorylation. B) Fibrosis; Platelets produce TGF- $\beta$ , PDGF- $\beta$  and CXCL4 to aid conversion of hepatic stellate cells into collagen producing myofibroblasts(53).

### 1.9.5. Therapeutic implications of platelets in liver disease

Platelets have diverse roles in liver patho-biology. Defining the stage and disease specific molecular contributions will help us to devise sensible treatment strategies using antiplatelet drugs. The ultimate goal of studying platelets in liver disease thus is the potential of this work to yield new therapies of the treatment of acute and chronic liver disease. With the large amount of anti-platelet drugs already in use, evidence for how antiplatelet therapy may impact liver disease is beginning to emerge. Recent work for instance suggests that aspirin reduces the risk of liver fibrosis in patients who have been transplanted for hepatitis C(158) Mechanistically, aspirin and clopidogrel inhibit dense granule release, blocking serotonin among other small

molecules. These drugs also inhibit the expression of  $\alpha$ -granule-stored proteins that are involved in heterotypic interactions between platelets/ leukocytes and the endothelium including P-selectin and CD40L(159) Reducing platelet activation alters how immune-mediated chronic hepatitis progresses, impacting even cancer development(159).

### **1.10. Project aims**

The overarching hypothesis behind this project was that 'platelet activation via CLEC-2 has a role in driving liver damage'. Establishing the role of platelets role in liver disease is critical to designing sensible and rational platelet targeting therapy in the management of such patients. I chose the ITAM receptor CLEC-2 specifically in this regard as abrogating individual ITAM receptors does not appreciably increase bleeding risk in mice (64) and human patients with advanced acute or chronic liver disease often exhibit marked coagulopathy. Although as mentioned above this risk particularly in association with chronic liver disease is often overstated(83).

Therefore in order to address this hypothesis, this project had the following specific aims:

*1) To assess whether chronically and acutely injured human livers express the requisite ligand for CLEC-2 mediated platelet activation: podoplanin.* Here I also aimed to document whether platelets sequester to the liver during human liver diseases and whether such co-localization varies with disease type and stage, and importantly whether platelets are able to sequester to podoplanin expressing areas. I

also established whether podoplanin expression varies between type and extent of hepatic injury seen. Lastly as podoplanin is known to mediate inflammatory hepatic thromboses(94) I assessed whether they may be a link between podoplanin expression and portal venous thrombosis.

*2) to ascertain the functional relevance of the CLEC-2:podoplanin axis in mediating or perpetuating acute inflammatory liver damage such as that seen with toxic agents including carbon tetrachloride and paracetamol.* Here I blocked this axis using a combination of mutant mice and function-blocking antibodies.

*3) to establish if there is any role for the CLEC-2 podoplanin axis in chronic liver injury specifically the development or regression of fibrosis and the development of fatty liver disease.* Here I used the chronic carbon tetrachloride model to induce fibrosis and study regression of fibrosis. I also used the methionine choline-deficient diet in mice to induce fatty liver disease and determined to consequences of CLEC-2-deficiency on disease development.

## 2. Materials and methods

### 2.1. Human tissue

All tissue used for this thesis was collected at the Queen Elizabeth Hospital Hepatobiliary Unit in Birmingham, obtained with prior written, informed patient consent and approved by our local research ethics committee. Normal liver tissue was from hepatic resection margins and donor tissue that was surplus to requirement for transplantation. Diseased liver tissue from explanted livers with drug induced liver injury (DILI), primary sclerosing cholangitis (PSC), primary biliary cirrhosis (PBC), alcoholic liver disease (ALD) and autoimmune hepatitis (AIH) was obtained from patients in the Birmingham liver transplant programme. Limited patient details for each of the liver samples obtained were available to clinical staff in the Centre for Liver Research. These included Model for End stage Liver Disease (MELD) scores which were calculated from patient blood taken immediately pre-transplant using the following equation.

$$MELD = 3.78 * \ln[serumbilirubin(mg/dl)] + 11.2 * \ln[INR] + 9.57 * \ln[serumcreatinine(mg/dL)] + 6.43$$

### **2.1.1. Liver tissue section preparation**

Fresh liver when obtained from liver explant specimens was as per lab protocols cut into 1cm<sup>3</sup> cubes, and immediately placed into liquid nitrogen for snap freezing. The cubes were then stored at - 80° C until needed. OCT TissueTek mount was used to embed the liver cubes and 7µm section were cut using a cryostat (Bright OTF). The freshly cut sections were then mounted on 0.01 % Poly-L-Lysine (Sigma, UK) coated microscopy glass slides (Leica, UK). The slides were then fixed in acetone (NHS supplies) and stored at -20° C until needed.

### **2.1.2. PCR**

Tissue for quantitative polymerase chain reaction (qPCR) was obtained from frozen cubes of diseased or normal livers as detailed above. The process is described below.

## **2.2. Murine tissue**

Eight to twelve week old wild type (WT) C57BL/6J mice were purchase from HO Harlan OLAC Ltd. (Bicester, U.K.). Multiple genetically modified mice were used in this study and the mutant mice strains are detailed in table 2.1. All genetically modified mice were bred from in-house colonies at the University of Birmingham Biomedical Services Unit (BMSU), these colonies were maintained by the Birmingham Platelet Group. All animals were housed at the BMSU in conditions free from specific- pathogens. All experiments were performed in accordance with UK

Home Office regulations, under the remit of an appropriate HO project license and were ethically approved by the local research ethics committee.

Mouse strain	Phenotype	Source
Platelet factor 4.cre. <i>CLEC1b</i> <sup>fl/fl</sup> C57Bl/6 background	Absence of CLEC-2 on cells of the megakaryocytic lineage including platelets. Generated by Cre-mediated recombination of the CLEC-2 allele through the cre/loxP system.	Professor Steve Watson (University of Birmingham)
Vav1-iCre. <i>PDPN</i> <sup>fl/fl</sup> C57Bl/6 background	Absence of podoplanin on vav1 expressing cells (haematopoietic cells). Generated by Cre-mediated recombination of the podoplanin allele through the cre/loxP system.	Professor Steve Watson (University of Birmingham)

**Table 2.1 mouse strains used in this project**

## 2.3. Methods

### 2.3.1. Induction of murine liver injury

#### 2.3.1.1. Carbon tetrachloride

##### **Acute**

Carbon tetrachloride (CCl<sub>4</sub>) (Sigma, UK) was administered intraperitoneally to induce hepatic necroinflammation. For the acute models, CCl<sub>4</sub> was administered dosed by weight at 1ml/Kg. CCl<sub>4</sub> was dissolved in mineral oil (Sigma, UK) in a 1:4 ratio (1 part CCl<sub>4</sub> to 4 parts solution or 1 part CCl<sub>4</sub> to 3 parts mineral oil). The mixture was made up in glass containers due to the ability of CCl<sub>4</sub> to act as a solvent and dissolve plastic. Control group animals received IP mineral oil only. Owing to the viscosity of



the mineral oil/CCl<sub>4</sub> mixture and thus the pressures required to administer the mixture, only luer lock syringes were used for the procedure. For the acute CCl<sub>4</sub> intoxication models the dose was only administered once. Mice were harvested at the end point of the experiment via cardiac puncture (schedule 1 procedure) under deep sedation. Whole blood was obtained via cardiac puncture and livers were harvested in their entirety as described below.

### **Chronic**

For the chronic models, as per our previously used lab protocol I initially used the same dose as for the acute models i.e. 1ml/kg. This resulted in some animals losing too much weight and thus needing to be culled before adequate hepatic fibrosis could be established. So I repeated the experiment using a lower dose of CCl<sub>4</sub> (0.6 ml/Kg) again made up by dissolving in mineral oil (again 1:4), this dose has been described in the literature(160). Control mice were given only mineral oil. Mice were injected with mineral oil or CCl<sub>4</sub> twice a week, for 7 weeks to induce fibrosis. To minimize concomitant hepatic necroinflammation mice were taken at 72 hours after the last injection of CCl<sub>4</sub>.

To study the resolution phase and allow for reversal of fibrosis; after 7 weeks of biweekly CCl<sub>4</sub> injections the treatment was stopped. Mice were then left with no further treatment for three weeks prior to culling them. Mice were harvested at the end point of the experiment via cardiac puncture (schedule 1 procedure) under deep sedation. Whole blood was obtained via cardiac puncture and livers were harvested in their entirety as described below.

### **2.3.1.2. Paracetamol induced liver injury**

Paracetamol (Sigma, UK) was dissolved in PBS. This necessitated heating the solution to 60°C, with continued stirring. The solution was cooled to 37°C prior to injecting intraperitoneally into the mice. The final dose used 350mg/kg and a maximum of 350ul of solution was injected per animal. Mice were monitored closely after injection and we found that they exhibited an antalgic gait, reduced feeding and reduced movement at around 6-8 hours' post injection. This was transient and by 24 hours all mice spontaneously improved. Mice were harvested at the end point of the experiment via cardiac puncture (schedule 1 procedure) under deep sedation. Whole blood was obtained via cardiac puncture and livers were harvested in their entirety as described below.

### **2.3.1.3. Methionine Choline deficient diet**

To study the development of steatohepatitis and fibrosis mice were administered the methionine choline deficient (MCD) diet(161). This lipogenic was obtained from Harlan-teklad laboratories, and was used to completely replace the chow the mice were normally fed. Mice had free access to chow and were weighed and monitored daily. They all exhibited greasy coats and a degree of overgrooming at the start of the diet but within two weeks this reverted to normal behaviour in most of the animals placed on the diet. The end point for this experiment was 6 weeks on the diet, 35% weight loss on the diet or excessive grooming leading to wounds. Mice were harvested at the end point of the experiment via cardiac puncture (schedule 1

procedure) under deep sedation. Whole blood was obtained via cardiac puncture and livers were harvested in their entirety as described below.

#### **2.3.1.4. Therapeutic interventions used in the murine models**

##### **Etanercept**

Etanercept antibody was obtained from Amgen and injected intravenously where indicated at a dose of 10mg/Kg, diluted in sterile PBS. Control animals received PBS alone.

##### **Neutrophil depletion**

Neutrophil depletion was achieved using a specific alpha Ly6G antibody (1A8). The use of a selective alpha Ly-6G antibody for the purposes of neutrophil depletion has been described previously (162,163). The antibody was obtained from Bioxcell, West Lebanon, NH, USA. Where indicated mice were pretreated (24 hours prior to either APAP or CCl<sub>4</sub> injection) with 200 µg of 1A8 in phosphate buffered saline (PBS) intravenously. Control animals were given PBS alone.

##### **Anti-podoplanin antibody**

We used a function blocking anti-podoplanin antibody to abrogate CLEC-2 dependent platelet activation in our murine experiments. An IgG anti mouse monoclonal, specific podoplanin IgG targeting antibody (8.1.1) was raised in Golden Syrian hamsters (made in house by Margaret Goodall). This was injected at a dose of 5µg/gm intravenously (diluted again in PBS). Control animals received isotype

matched control antibody (Purified IgG, golden Syrian hamster-again made in house) diluted in PBS.

#### **2.3.1.5. Experimental end point**

Mice were sacrificed under deep anaesthesia using isoflurane. Up to 1 ml of whole blood was obtained from each animal via cardiac puncture using a 25g x 5/8" gauge needle which was directly inserted into the heart. Blood was transferred to eppendorf tubes and allowed to clot at room temperature for 1 hour. The clotted blood was centrifuged at 15000 RPM for 15 minutes, the supernatant was removed and centrifuged again at 15000 RPM for 15 mins (Sorvall Legend Micro 17 Centrifuge). The supernatant harvested at this point was either sent for measurement of serum alanine transaminase (ALT) levels or immediately frozen down to -80°C for storage.

Where blood platelet isolation was required (see macrophage isolation assays below section 2.8.3) syringes were pre-coated/prefilled with acid-citrate dextrose (ACD) as an anticoagulant (100µl of ACD per 900µl of whole blood). This anticoagulated blood was kept at room temperature prior to being used for platelet isolation (see section 2.8.4). Where whole blood counts of cells were required anticoagulated mouse blood was analyzed using ABX pentra 60 blood counter (Horiba medical, France).

## 2.4. Tissue Preparation

### 2.4.1. Liver harvesting

After being bled via cardiac puncture, mice were next subjected to a schedule 1 procedure (cervical dislocation). The liver was then dissected out and care was then to harvest in its entirety (fig 2.1). The liver was then divided into 3 sections labelled as lobes A-C below (fig 2.1).

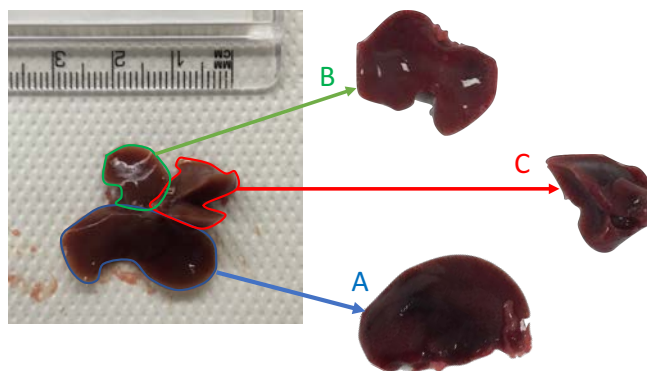


**Figure 2.1 Method of liver lobe isolation:**

Once dissected out lobe A was placed in 4% formaldehyde (for paraffin embedding and sectioning-see below). Lobe B was immediately snap frozen by being placed in liquid nitrogen after extraction, the lobe was then stored at  $-80^{\circ}\text{C}$  until required. This lobe was used either for preparing frozen sections for confocal immunofluorescent microscopy or for providing tissue for PCR or for hydroxyproline assays (all described below). Lobe C was placed into ice cold RPMI supplemented with glutamine (Sigma-Aldrich, UK), this entire lobe was used for isolating and staining intrahepatic leukocytes for flow cytometric analysis.

### 2.4.2. Histology

Lobe A of the liver which was initially suspended in formalin, was next trimmed to remove fibrous/tough parts of the liver capsule, and then resuspended in fresh 4% formaldehyde after being placed in a plastic cassette (Wheaton, UK). These were then embedded in paraffin according to the following protocol:

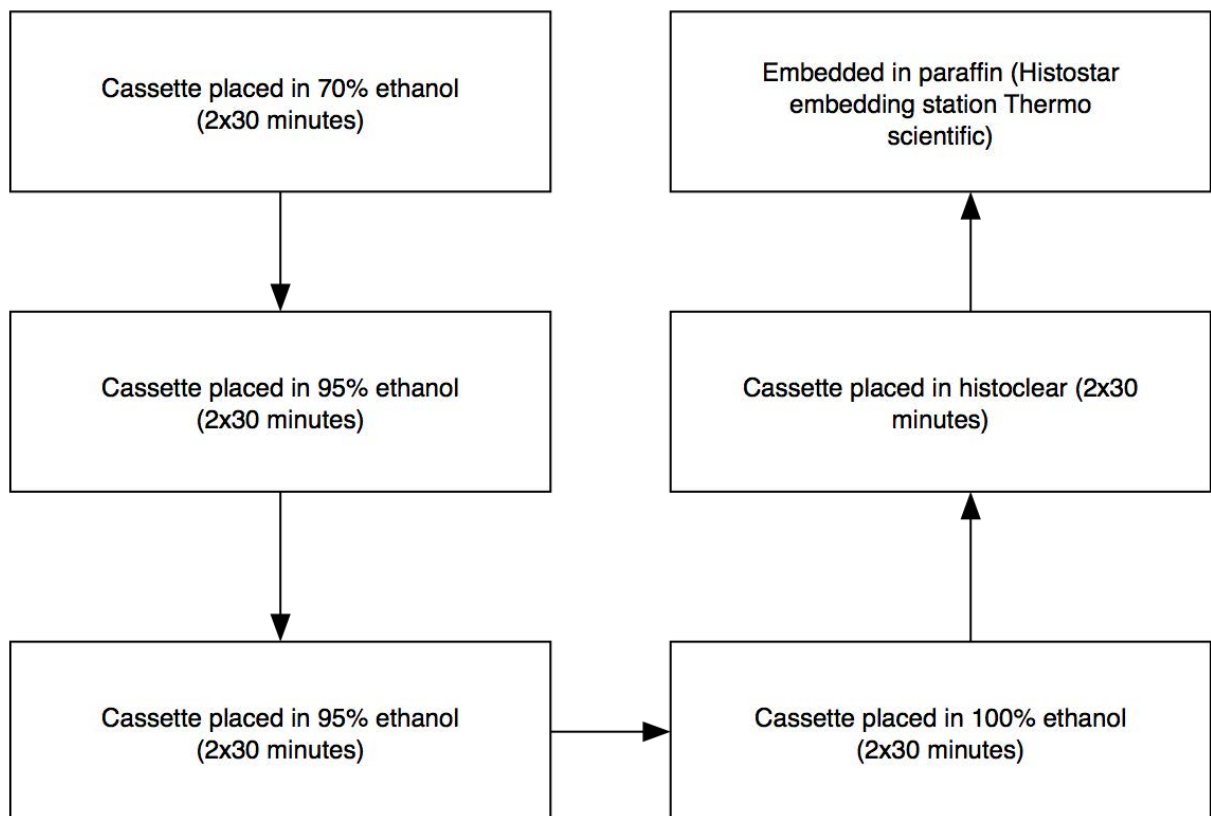


**Figure 2.2 Procedure for wax embedding of liver tissue**

5  $\mu$ m sections were cut from paraffin embedded tissue and then fixed onto microscope slides (X-tra Adhesive, Leica).

### 2.4.3. Haematoxylin and Eosin staining

Paraffin embedded liver sections (mouse) (made as described above) were 'de-waxed' as detailed in figure 2.3. All reagents were purchased from Leica microsystems, Peterborough, UK.

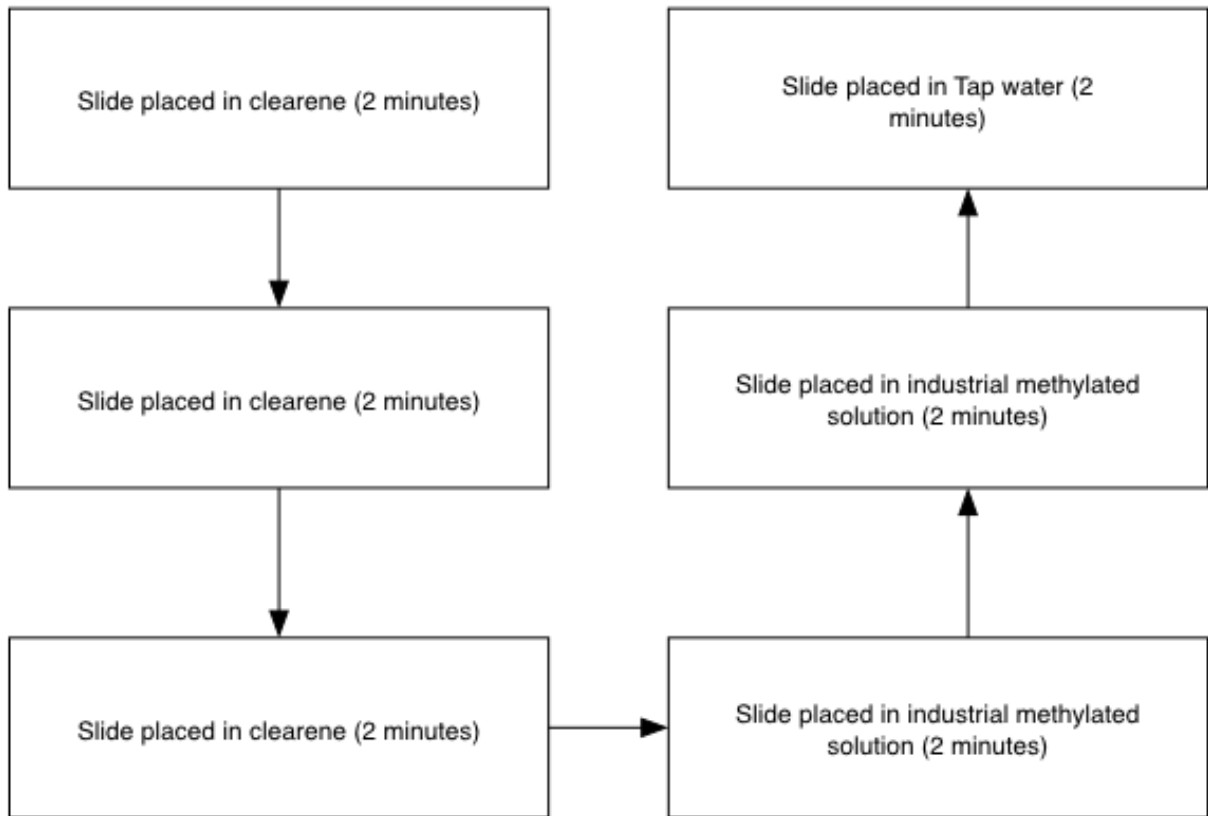


**Figure 2.3 Method to de-wax paraffin sections**

'Dewaxed' mouse sections as described in fig 2.3, or frozen human liver sections (that had been stored at -20°C) were thawed and stained with haematoxylin and eosin as described in fig 2.4.

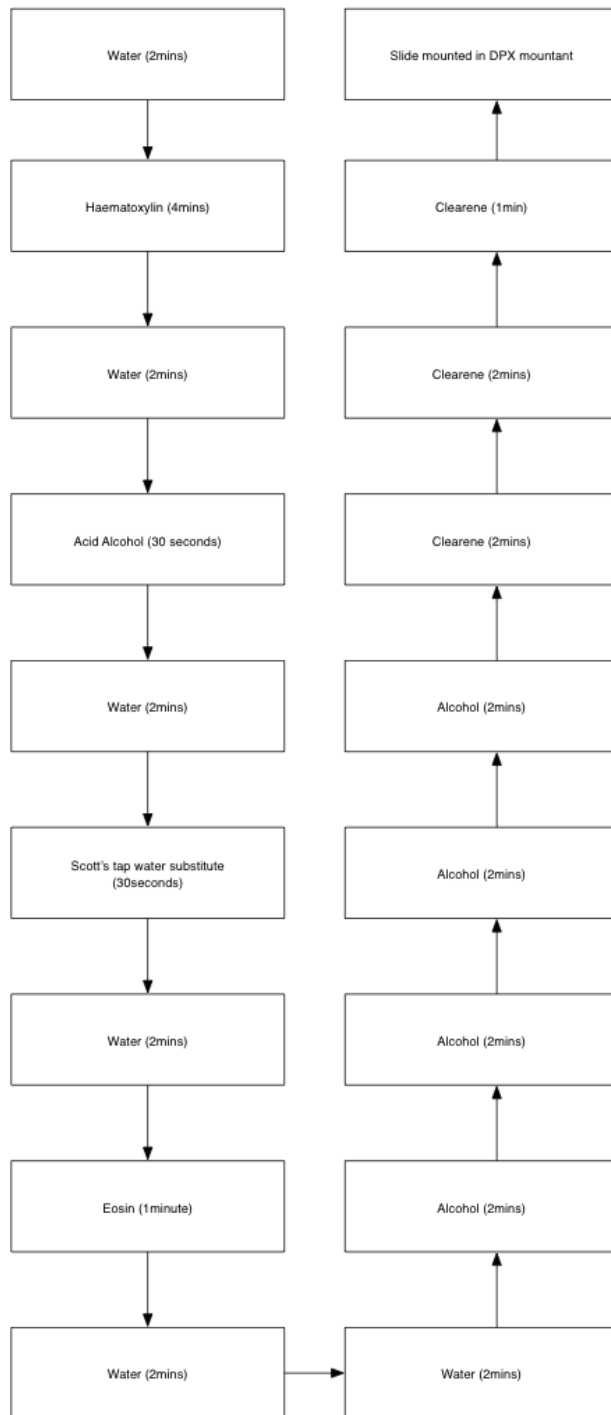


**Figure 2.4 Haematoxylin and eosin staining**



#### **2.4.4. Picrosirius red staining**

Paraffin sections were de-waxed and hydrated as detailed above in figure 2.3. The slides were next laid out in a humidified chamber and wax squares drawn around the sections. 5% phosphomolybdic acid solution (PMA-Sigma, UK) was used to cover the tissue sections. The slides were placed on the rocker for 5 minutes, following which the PMA was tapped off and the slides placed into a pre-made picrosirius-red dye (0.1%, Sigma UK) bath. The bath was placed on a rocker for 30 minutes, at which point slides were removed and excess picrosirius red tapped off. The slides were now dipped sequentially in 0.1M HCl and then dH<sub>2</sub>O (1-2 seconds each), and then 3 batches of fresh ethanol (for 2 minutes each). Slides were then left in clearane (Leica, UK) for 5 minutes and mounted in DPX (Sigma, UK).

#### **2.4.5. Van Gieson stain**

Mouse paraffin sections were dewaxed as described in fig 2.3 stained with Van Gieson stain (fig 2.5) to visualize excess collagen deposition in murine models of liver fibrosis.

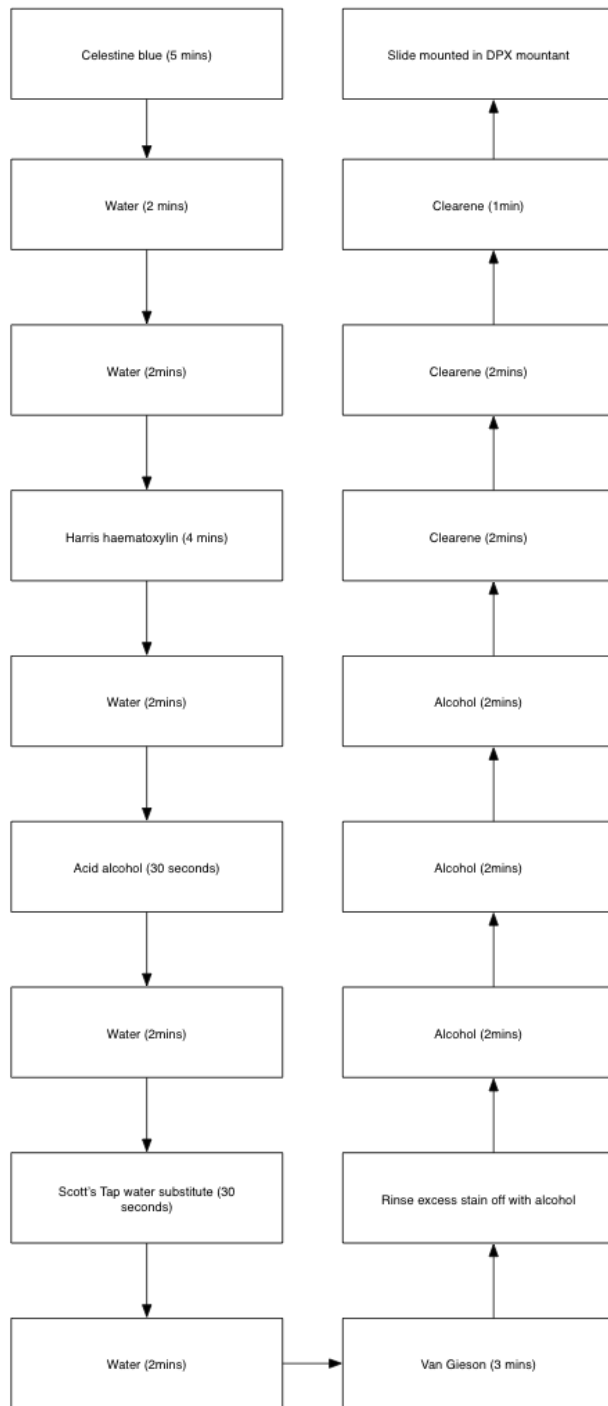


**Figure 2.5 Method employed for Van Gieson staining**

#### **2.4.6. Immunohistochemistry**

Both mouse and human sections were stained using immunohistochemistry (IHC) to visualize protein expression or infiltrating leucocyte patterns. For fluorescent IHC, only frozen sections were used (both mouse and human). These frozen sections were removed from -20°C storage and allowed to thaw before staining. For certain antibodies, paraffin sections were recommended for optimum visualization. All paraffin sections were obtained from mice, and had to undergo an antigen retrieval procedure prior to staining.

##### **2.4.6.1. Antigen retrieval**

The sections were de-waxed as described in section 2.3. They were then placed in a plastic bucket containing 990ml of distilled H<sub>2</sub>O and 10 ml of high pH antigen retrieval solution (Vector, UK), and placed in a microwave (Sanyo, Japan) and heated at high power for 10 minutes. The solution containing the slides was then allowed to rest at room temperature for 10 minutes following which cold water was added to bring the temperature of the solution down to room temperature. The slides were then placed in TBS (tris buffered saline, Ph 7.6, Sigma, UK) for 5 minutes.

Once the antigen retrieval procedure was completed (in the case of paraffin sections) or the frozen sections had thawed, a common IHC staining pathway as described below was used for both.

#### 2.4.6.2. Staining protocol

The slides were initially placed in a blocking solution for 20 minutes to block endogenous tissue peroxidase (Dako, UK). The slides were next washed twice in TBS for 5 minutes each. A wax pen was then used to draw a well around the tissue section. 100  $\mu$ l of 20% casein solution and 1 drop of horse serum (both Vector, UK) were then placed within the wax well-ensuring complete coverage of the section, and the slides were placed in a humid chamber on slow rocking for 30 minutes. The casein solution was then tapped off, and 75  $\mu$ l of solution containing the primary antibody (made up to the appropriate concentration using TBS) was placed within the wax well, the slides were incubated with the primary antibody for 60 minutes (with slow rocking). The primary antibody was then washed off, by washing the slides in TBS and 0.05% tween (Sigma-aldrich, UK). All secondary antibodies used had already been commercially adsorbed and were again made up to the appropriate concentrations using TBS. 75  $\mu$ l of secondary antibody solution was placed on the sections for a 45 minute incubation (with slow rocking) and then washed off as described above. The primary and secondary antibodies used, species, clones and concentrations are detailed in table 2.6.

If the desired secondary antibody to be used was linked to horse-radish peroxidase (HRP), the slides were then developed using a peroxidase substrate (Vector, UK). The substrate was 3, 3'-diaminobenzidine tetrahydrochloride (DAB SK-4100) (Vector) and made up as per the manufacturer's instructions. Briefly 2 drops of buffer stock solution, 4 drops of DAB stock solution and 2 drops of hydrogen peroxide solution

were added to 5 mls of dH<sub>2</sub>O. 150  $\mu$ l of the resulting solution was added to the section containing the HRP linked antibody and the slide developed to the required intensity usually (60 seconds to 2 minutes). The slides were then washed as described above, and counterstained with filtered Mayer's haematoxylin for 20 seconds. The slides were then sequentially washed in cold and then warm water (2.5 mins each), following which they were dehydrated in alcohol and clearane, then mounted in DPX (Sigma).

## **2.5. Microscopy**

### **2.5.1. Brightfield**

Photographs of stained tissue were taken using a Zeiss Axioscope microscope using brightfield illumination and then analyzed using Axiovision software (Carl Zeiss, UK).

### **2.5.2. Confocal**

Confocal microscopy was used to define the nature of the cellular infiltration that occurred in acute and chronic human and murine liver damage. Sections cut using a cryotome and stored at -20°C were thawed at room temperature. The tissue sections were drawn around with a wax pen, following which the tissue was covered with blocking solution (100  $\mu$ l of 20% casein solution, and a drop of horse serum (both vector)). The sections were then gently rocked in a moisture chamber (covered with foil to block exposure of the fluorescent antibodies to light thus minimising potential bleaching). The blocking solution was then tapped off and the primary antibody made up to the appropriate concentration (in TBS) was added to the section, the slide was

then placed back into the moisture chamber and allowed to rock for 60 minutes. The slides were then washed twice in TBS with 0.05% tween as described above and incubated in the rocking chamber with the fluorescent secondaries (if indicated) at the appropriate concentrations for 30 minutes. The slides were then washed again, a hoechst 33258 stain was next used to stain the nuclei (2 minutes) and then the stained section was mounted using Prolong Diamond Anti-fade Reagent (Invitrogen, Paisley, UK). A LSM510 microscope (Zeiss) was used to acquire the pictures, the software used for acquisition was Zeiss LSM software.

#### **2.5.2.1. Isotype controls**

To set the fluorescence detection levels of the LSM510 appropriately (specifically the amount of fluorescence detected by each channel), we always prepared a section control within which the primary antibody was omitted, conjugated secondary antibodies were added as with the other sections. The laser emission strength of the microscope was then set to a level where only minimal fluorescence was detected on the isotype control. This ensured that non-specific background fluorescence was minimized. I have included an isotype control sample in chapter 3, figure 3.2 to illustrate this. Isotype control images obtained on the confocal microscope have not been repeated throughout.

## **2.6. Quantitative PCR**

RNA was extracted from human livers using a RNEasy kit (Qiagen, UK) and cDNA was generated using a High capacity cDNA reverse transcription kit (ThermoFisher,

UK) according to manufacturer's instructions. Quantitative analysis of Podoplanin mRNA expression was performed using Taqman Fluorogenic 5' nuclease assays using gene-specific 5' FAM labelled probes (PDPN gene; aliases A-GGRUS, gp36, gp40, gp38, HT1A-1, OTS8, PA2.26, T1A, T1A-2, T1A2, TI1A: Hs00366766\_m1, Applied biosystems UK) run on a ABI Prism 7900 sequencer with 18s;SFRS4 used as internal control. Differential expression levels were calculated according to the  $2^{-\Delta\Delta C_t}$  method.

Component	Concentration at which used
Taqman 2x master mix (Applied Biosystems)	1x
20x Assay mix (Applied Biosystems)	0.5x
RNAse free water	Up to 10 $\mu$ l
cDNA	100 $\mu$ g/ml

**Table 2.2 Materials used for qPCR reaction**

## 2.7. TNF $\alpha$ ELISA

Serum from mice or supernatant from cell cultures/assays (section 2.8.3) was used for ELISA. The TNF- $\alpha$  ELISA was conducted using the manufacturers instructions (Thermo Fisher Scientific, 88-7324). An ELISA plate (Corning Costar 9018), was

incubated overnight with 100 $\mu$ l/well of capture antibody. The wells were washed with wash 250 $\mu$ l of wash buffer three times, and then 200 $\mu$ l of ELISPOT diluent was added to each well. The plate was set to rest at room temperature for 1 hour. Next the standards were made up to the appropriate concentrations and placed in order of increasing dilution (2 fold) in the plate, along with the standards (100 $\mu$ l of sample per well-each sample placed in triplicate) and incubated for 2 hours (fig 2.6)

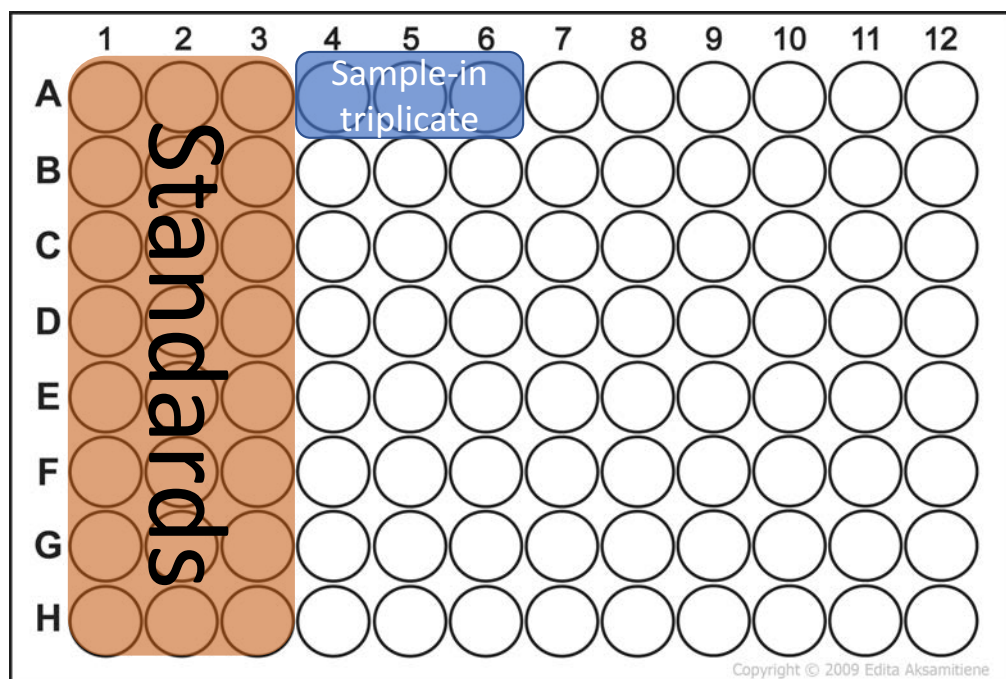


**Figure 2.6 ELISA well set up:**

The standards were placed in order of increasing dilution from A through to H, H had no detectable standard (diluent control only). The remaining wells were used for samples, each was added in triplicate.



The wells were then aspirated/washed as previously described and the plate incubated with detection antibody for 1 hour. After another aspiration/wash cycle, avidin-HRP was added to each well and the plate incubated at room temperature for 30 minutes. The plate was then aspirated, washed and then the tetramethylbenzidine (TMB) substrate solution was added to each well, the plate was covered and incubated at room temperature for 15 minutes, next 50 $\mu$ l of stop solution was added to each well. The plate was read at 450nm on a versamax plate reader and analyzed using Softmax pro software. The standard curve was plotted using PRISM 7.0 software.

## **2.8. Isolation of murine leukocytes**

### **2.8.1. Preparation of leukocyte suspension from murine liver**

Lobe C prepared as described in figure 2.1, was immediately placed into 3 mls of ice cold RPMI. The lobe was then weighed and dissociated (GentleMACS dissociator) in a gentleMACS C tube (Miltenyi Biotec). The programme used was spleen\_04\_01. The homogenate from the tube was then filtered using a 70 $\mu$ m cell strainer (Falcon) into a 20ml Falcon tube. The filtrate was made up to 10mls using cold RPMI and then centrifuged at 2000 rpm for 5 minutes, the pellet was then resuspended in 10 mls of RPMI and the process repeated. After two washes, the pellet was resuspended in 10ml of RPMI. The cell suspension was then divided into two volumes of 5 mls each.

For each sample 7 mls of optiprep solution (at room temperature) was used. 160 mls of optiprep solution (enough for 10 animals) was prepared as follows [42.6 mls of Optiprep (Sigma) + 117.4 mls PBS].

5ml of the cell suspension was layered upon 7 mls of the prepared optiprep solution in a 15ml corning tube. Thus for each sample, two layered cell suspensions were created. These were then centrifuged at 1000 rpm for 25 mins with no brake. The cells at the interface of both tubes were extracted and combined; the cells were then washed twice and then resuspended in RPMI. This solution was now the leukocyte suspension.

## **2.8.2. Flow cytometry**

### **2.8.2.1. Live dead stain**

The leukocyte suspension obtained above was washed in and then re-suspended in 1ml of PBS. A live-dead stain (Zombie NIR-Biolegend) was made up in DMSO as per the manufacturer's instructions and 1 $\mu$ l of dye was added per ml of cell suspension. The cells were incubated at room temperature protected from light for 30 mins. The cell suspension was then washed twice in MACS buffer and then resuspended in 1ml MACS buffer (PBS+1mM EDTA+2%FCS).

### **2.8.2.2. Flow cytometric staining**

The live-dead stained cell suspension was aliquoted into round bottomed polypropylene FACS tubes (corning) as detailed below:

100 $\mu$ l for cells alone

100µl for isotype matched controls

200µl for combination tubes

Compensation beads (AbD serotec) were used for single colour controls. A single drop of the bead solution was suspended in 100µl of PBS to which the fluorophore containing antibody was added. The volumes of each antibody for single colour control used are detailed in tables 2.3-2.5.

The volumes of fluorescent antibodies and isotype matched controls added per tube is detailed below.

T-cell combination:	5µl anti-CD3-PB 5µl anti-CD4-PE 5µl anti-CD45-PerCPCy5.5 5µl anti-CD8a-APC
T-cell IMCs:	5µl hamster IgG2-PB 5µl rat IgG2a-PE 5µl rat IgG2b-PerCP-Cy5.5 5µl rat IgG2a-APC

**Table 2.3 T-cell panel and IMCs:**

Volumes of antibody and isotype matched controls used per sample for flow cytometric staining.

<b>Myeloid combination:</b>	5 $\mu$ l anti-CD3-PB 2 $\mu$ l anti-F480-FITC 10 $\mu$ l anti-CD11b-PE 5 $\mu$ l anti-CD45-PerCPCy5.5 5 $\mu$ l anti-Gr-1-APC
<b>Myeloid IMCs:</b>	5 $\mu$ l hamster IgG2-PB 2 $\mu$ l rat IgG2a-FITC 10 $\mu$ l rat IgG2b-PE 5 $\mu$ l rat IgG2b-PerCP-Cy5.5 5 $\mu$ l rat IgG2b-APC

**Table 2.4 Myeloid Cell panel and IMCs:**

Volumes of antibody and isotype matched controls used per sample for flow cytometric staining.

<b>Fibrotic/restorative macrophage panel</b>	5 $\mu$ l CD3-PB 5 $\mu$ l DX5-V450 5 $\mu$ l B220 (CD45R)-PB 5 $\mu$ l Ly6G-BV510 2 $\mu$ l F4/80-FITC 10 $\mu$ l CD11b-PE 5 $\mu$ l CD45-PerCPCy5.5 5 $\mu$ l Ly6C-APC
<b>Fibrotic/restorative macrophage IMCs</b>	5 $\mu$ l Hamster IgG2-PB 5 $\mu$ l IgM V450 5 $\mu$ l IgG2a-PB 5 $\mu$ l Rat IgG2a-BV510 2 $\mu$ l Rat IgG2a-FITC 10 $\mu$ l Rat IgG2b-PE 5 $\mu$ l Rat IgG2b-PerCPCy5.5 5 $\mu$ l Rat IgG2c-APC

**Table 2.5 Pro-fibrotic and restorative macrophage panel and corresponding IMCs:**

Volumes of antibody and isotype matched controls used per sample for flow cytometric staining.

The stained samples were next incubated at 4°C under foil for 30 mins. The stained cells were then washed again and resuspended in 400µl of macs buffer. 50µl of AccuCheck counting beads (Invitrogen, UK) were added per tube. The samples were vortexed to ensure homogenous distribution of cells and beads, and then acquired using the CyAn FACS Analyser (Dako, Denmark) using Summit v4.3 software. Data were analysed using FlowJo software [Version 8.7(TreeStar)]. The gating strategies are shown in the relevant sections.

Cells per gram was worked out using the following formula:

$$\text{cells/gm} = (\text{counted cells on flow scatter plot} \times \text{total counting beads in } 50\mu\text{l of accucheck solution}) / (\text{counted beads on flow scatter plot} \times \text{weight of liver lobe})$$

### **2.8.3. Hepatic macrophage isolation**

To isolate macrophages for *in vitro* studies we used Blomhoff's principle of selective plastic adherence(164). Once the leukocyte suspension was obtained as detailed above in section 2.8.1, it was washed again and this time made up to 6 mls using Dulbecco's modified eagle medium (DMEM-Gibco) supplemented with fetal bovine serum (FBS, Gibco, UK) and penicillin/streptomycin/glutamine (PSG, Gibco, UK). The solution gently vortexed to ensure uniform distribution of leukocytes throughout the solution, and then 1ml of solution was added per well in a 6 well plate (Corning). The plate was incubated for 2 hours at 37°C in a 5% CO<sub>2</sub> atmosphere. Non-adherent cells were then gently washed off with PBS. To confirm that the remaining cells were

macrophages a fluorescent F4/80 (FITC conjugated, ebioscience) antibody was used (fig 4.6).

Once adequate a number of cells had seeded in each well (gauged using phase contrast microscopy), 1ml of DMEM (with or without lipopolysaccharide-LPS 100ng/ml, Sigma) supplemented with FBS (Gibco) and PSG (Gibco) was added to each well. In experiments where platelets (isolation described in section 2.8.4) were added, these were layered on 6 hours after the macrophages had been incubated at 37°C in a 5% CO<sub>2</sub> atmosphere.

Macrophages were either isolated from wild type mice or when podoplanin deficient macrophages were required, these were isolated from *Vav1-iCre<sup>+</sup>pdpn<sup>fl/fl</sup>* mice.

#### **2.8.4. Isolation of platelets from murine whole blood**

Blood was obtained from an anaesthetized mouse as described above, via cardiac puncture using a 25-gauge needle with a 1 ml syringe containing 100µl of acid citrate dextrose (ACD, Sigma). The whole blood was transferred to an eppendorf tube and centrifuged for about 7 mins at 1000rpm using a Sorvall centrifuge. The top phase (platelet rich plasma-PRP) was removed and 200µl of modified Tyrode's buffer (ph 6.6) was added to the remaining blood in the eppendorf tube. The eppendorf was then centrifuged again, this time for 5 mins at 1000rpm- and the upper phase was removed again. The process was repeated until the upper phase became clear (and thus had no or very little platelets).

5 $\mu$ l of platelet rich plasma was removed for gauging platelet counts [ABX pentra 60 blood counter (Horiba medical)]. 1  $\mu$ g/ml of prostacyclin was then added per ml of PRP (to prevent platelet aggregation prior to use), the PRP was then immediately centrifuged for 5 minutes at 2750 rpm, the supernatant was now discarded and the pellet resuspended in Tyrode's buffer (pH 7.3). Platelets from multiple mice (of the same strain) were pooled together to achieve the final requisite concentration; 300 $\mu$ l of  $1 \times 10^8$  platelets/ml was added per well of 6 well plate (where platelets were indicated).

Platelets were isolated from WT mice; where CLEC-2 deficient platelets were required, these were isolated from PF4Cre*CLEC1b*<sup>fl/fl</sup> mice.

## 2.9. Hydroxyproline assay

Between 50 and 100mg of murine hepatic tissue was cut from murine liver blocks stored at -80°C (preparation of these blocks is described above in fig 2.1). The exact weight of the sample was noted prior to addition on 0.5ml of dH<sub>2</sub>O, and the sample homogenized with a hand held homogenizer (Polytron MR 2100). The homogenate was topped up to 1ml with distilled dH<sub>2</sub>O. Next 125 $\mu$ l of 50% trichloroacetic acid was added and the solution incubated on ice for 30 minutes. The solution was next centrifuged to precipitate out protein (the supernatant was discarded); following which the protein precipitate was placed in sealed borosilicate tubes containing 500  $\mu$ l of 6N hydrochloric acid (HCL), overnight at a temperature of 120°C. The next day the lids were taken off the tubes to allow the HCL to evaporate. The following day the

remaining precipitate was resuspended in 250 $\mu$ l of double distilled H<sub>2</sub>O, and then filtered using a 0.45  $\mu$ m nylon containing polypropylene costar centrifuge tube (Corning, Fisher scientific). 50 $\mu$ l of the filtered solution was transferred to glass tubes; and the hydroxyproline standards were prepared. 950 $\mu$ l of ddH<sub>2</sub>O was added to the filtered solution to make up a total volume of 1ml. Next 500 $\mu$ l of Chloramine-T was added and the resultant solution incubated at room temperature (RT) for 20 min. Following this incubation 500 $\mu$ l of dimethylaminobenzaldehyde-perchloric acid solution was added and the solution vortexed and then incubated in the fume cupboard at 65°C for 15 min. Finally 200 $\mu$ l of solution was pipetted into ELISA plate wells in triplicates and read at 561nm. The hydroxyproline was expressed as  $\mu$ g hydroxyproline per gram liver.

## **2.10. Biochemical liver function assays**

Whole mouse blood collected at cardiac puncture was centrifuged at 15,000 rpm for 15 minutes twice as described above to isolate serum. 100 $\mu$ l of serum from the final supernatant was removed and placed in a 13mm false-bottomed sample tube (Sarstedt) the remainder as discussed above was frozen down for long term storage at -80°C. Serum was assayed for alanine transaminase (ALT) levels by the clinical biochemistry team at Birmingham Women's Hospital using clinical analysers.

## **2.11. Statistical analysis**

Where possible (if there were greater than 5 variables in each group) normality for each group was tested using the Kolmogorov-Smirnov test (with the Dallas-



Wilkinson-Lillie for corrected P value) or D'Agostino-Pearson omnibus test. If the two groups exhibited a gaussian distribution a parametric unpaired t test was conducted to compare the two groups. If the groups did not exhibit a gaussian distribution (this was the case for the majority of our samples) the difference between the medians of the two groups was assessed using the two-tailed Mann-Whitney non-parametric sum of ranks test.

Where the relationship between a scalar dependent variable and an explanatory variable was modelled (for instance MELD score vs intrahepatic podoplanin concentration), linear regression analysis with a line of best fit was used.

The statistics programme GraphPad Prism version 7.0 was used to calculate P values. These are detailed in each figure according to the following criteria for significance \*P < 0.05, \*\*P < 0.01, \*\*\*P < 0.001.

## 2.12. Antibodies and isotype controls used

Antibody/IMC	Fluorophore	Final concentration	Intended use	Supplier
CD3	Pacific blue	0.2 mg/ml	FC	BD Biosciences
Hamster IgG2, K (anti-KLH)	Pacific Blue	0.2 mg/ml	FC	BD Biosciences
CD4	PE	0.2 mg/ml	FC	BD Biosciences
Rat IgG2a	PE	0.2 mg/ml	FC	BD Biosciences
CD8	APC	0.2 mg/ml	FC	BD Biosciences
Rat IgG2a, I (anti-KLH)	APC	0.2 mg/ml	FC	BD Biosciences
CD11b	PE	0.2 mg/ml	FC	BD Biosciences
Rat IgG2b	PE	0.2 mg/ml	FC	BD Biosciences
Gr-1	APC	0.2 mg/ml	FC	BD Biosciences
Rat IgG2b	APC	0.2 mg/ml	FC	BD Biosciences
CD45	PerCP-Cy5.5	0.2 mg/ml	FC	BD Biosciences
Rat IgG2b	PerCP-Cy5.5	0.2 mg/ml	FC	BD Biosciences
F4/80	FITC	0.5 mg/ml	FC	Biolegend
Rat IgG2a	FITC	0.5 mg/ml	FC	Biolegend
Ly6G	BV510	0.2 mg/ml	FC	Biolegend
Rat IgG2a	BV510	0.2 mg/ml	FC	Biolegend
Ly6C	APC	0.2 mg/ml	FC	Biolegend
Rat IgG2c	APC	0.2 mg/ml	FC	Biolegend
DX5	V450	0.2 mg/ml	FC	BD Biosciences
Rat IgM	V450	0.2 mg/ml	FC	BD Biosciences
B220	PB	0.2 mg/ml	FC	BD

				Biosciences BD Biosciences
Rat IgG2a	PB	0.2 mg/ml	FC	
CD61 (human)	Alexa Fluor® 647	1µg/ml	IHC	Biologend
CD41 (mouse)	BV605	1µg/ml	IHC	Biologend
Podoplanin (mouse 8.1.1) Unconjugated	-	0.5 µg/ml	IHC	ebioscience
Syrian Hamster IgG	-	0.5 µg/ml	IHC	ebioscience
HRP conjugated rabbit Anti- Syrian Hamster IgG H&L	N/A	1µg/ml	IHC	Abcam
Podoplanin (human 8.1.1) Unconjugated	-	0.5 µg/ml	IHC	ebioscience
Goat Anti-mouse IgG H&L	Cy3	1µg/ml	IHC	abcam
CLEC-2 (human) Unconjugated	-	1µg/ml	IHC	Biorbyt
HRP-conjugated anti rabbit Ig	N/A	Pre-diluted	IHC	Vector
HRP-conjugated anti rat Ig	N/A	Pre-diluted	IHC	Vector
HRP-conjugated anti mouse Ig	N/A	Pre-diluted	IHC	Vector
CD68 (human)	FITC	1µg/ml	IHC	Biologend
CD45 (human)	Alexafluor 647	2µg/ml	IHC	Biologend
CD31 (human)	FITC	2µg/ml	IHC	Biologend
F4/80 (mouse)	FITC	1µg/ml	IHC	Biologend
F4/80 (mouse, unconjugated)	-	1µg/ml	IHC	Biologend
Rat IgG2a, κ	-	1µg/ml	IHC	Biologend
Anti-neutrophil elastase antibody (mouse, unconjugated)	N/A	0.5µg/ml	IHC	Abcam
Rabbit IgG, polyclonal	N/A	1µg/ml	IHC	Abcam

**Table 2.6 : Details of antibodies used for flow cytometry and immunohistochemistry (with corresponding isotype matched controls)**

## **3. Podoplanin is upregulated in acute and chronic human liver injury**

### **3.1. Introduction**

Podoplanin (PDPN) is a 36- to 43-kDa sialomucin-like transmembrane glycoprotein and the only known endogenous ligand for CLEC-2 (70). Podoplanin has homologues in humans, mice, rats, dogs, and hamsters(68). Under normal physiological conditions spatial and cellular localization of podoplanin precludes access to platelet CLEC-2 and it thus cannot activate platelets, however during specific phases of embryological development and certain pathological conditions, a variety of cells up regulate podoplanin and allow platelet activation(69,165).

Podoplanin is ubiquitously expressed on multiple cell types, and this expression is driven by a variety of transcriptional pathways including ones pertinent to normal development such as Prox-1 and others which are pathological including pro-inflammatory and pro-tumorigenic mechanisms(69). Table 3.1 (69) summarizes podoplanin function and patterns of organ specific expression.

Organ	Time and site of expression	PDPN function
Central nervous system	Beginning day E9, becomes restricted to choroid plexus in adult mouse	No specific function reported during development; high PDPN expression in brain tumors
Heart	Starts E9, expression continues in adults	Required for normal heart development, specifically for EMT in epicardium-derived cells
Lungs	Appears in foregut on day E9 before lung buds; subsequently restricted to alveolar type I epithelial cells	Required for lung development; specifically the effective maturation of alveolar type I epithelial cells
Intestine	Expressed on day E9 in foregut; continued expression in lamina propria	No specific function determined
Lymphoid organs	Present in spleen 4 days postnatally; in adult, expression by FRCs, LECs, and FDCs in lymph node and spleen, and thymic medullary epithelial cells	Required for proper formation and organization of lymph nodes and spleen; necessary for efficient DC migration to and within lymph nodes; highly expressed by stroma and some T cells in ectopic lymphoid tissue

**Table 3.1 Podoplanin expression and function(69) :**

**Summary of how site and timing of podoplanin expression inform podoplanin function (taken from Astarita et al)**

Podoplanin is expressed on lymphatic endothelium (in both mice and humans) and is used as an immunohistochemical marker for lymphatic vessels in both species(68). Since intact platelets normally do not enter the lymphatic vasculature, lymphatic podoplanin (during normal adult physiology) does not activate platelets (92). An exception is at lymphovenous junction in the thoracic duct where lymphatic fluid from the body is returned to the vascular system, here the lymphovenous valve prevents back flow from the thoracic duct to the lymphatic vessels. As blood platelets come into direct contact with lymphatic podoplanin at the lymphovenous junction, platelet aggregation occurs and these aggregates are critical to the maintenance of barrier integrity between lymphatic and blood vessels integrity in neonatal but adult mice (92). Podoplanin first appears on PROX-1 positive lymphatic cells at embryonic day 11.5(75), and mice that are deficient in podoplanin, in keeping with their CLEC-2 deficient counterparts exhibit anomalous lymphatic development and blood lymph mixing(166). Podoplanin is also required to maintain the lymph-blood barrier and lymph node integrity in adult mice(167).The role the CLEC-2/podoplanin axis plays lymphatic development has already been discussed in greater detail above (chapter 1).

Podoplanin has important roles in the development of multiple other organ systems. As mentioned in the table above the embryonic heart starts expressing podoplanin around day 9 and lack of podoplanin expression is associated with a multitude of cardiac developmental abnormalities including septal hypoplasia and underdevelopment of the pulmonary vein(168). Podoplanin is also important within

neonatal lungs, and supports lung inflation after birth(69) . Lymphatic vessels are crucial to lung inflation in the neonate, as mice with genetic deletions for the lymphangiogenic factor CCBE1 or VEGFR3 function, fail to develop lymphatic vessels and die shortly after birth due reduced lung compliance and thus post-natal lung inflation(169); as podoplanin is critical to the development of the lymphatic vasculature this may in part explain which podoplanin/CLEC-2 deficient mice exhibit high rates of perinatal mortality (70,170). In addition podoplanin knockout (*podpn*<sup>-/-</sup>) mice may not be able to inflate lungs after birth because podoplanin is required for the development of type 1 alveolar cells, these cells cover the majority of the lung surface and are crucial for the development of alveoli(171). Podoplanin also begins to be expressed within the central nervous system specifically on the neuro-epithelium around day 9-10 (69). Interactions between this neurally expressed podoplanin and platelet CLEC-2 promotes aggregation and adhesion of platelets, which then guides the development or 'patterning' of cerebral vasculature thus preventing haemorrhage during cerebral development(172).

In addition to its role in developmental of various organ systems as detailed above, podoplanin expression varies with a variety of pathological processes/injuries and the CLEC-2/podoplanin axis here has roles can facilitate healing or in certain situation perpetuate further damage.

The podoplanin-CLEC 2 axis has an important role in facilitating wound healing. Podoplanin is expressed by keratinocytes at the edge of wounds. Asai et al found that keratinocyte expressed podoplanin interacted with platelet CLEC-2 after skin

injury in mice resulting in reduced migration of normal human epidermal keratinocytes (NHEKs) via podoplanin mediated inhibition of keratinocyte migration (due to loss of E-cadherin). This influenced wound healing in a RhoA dependent mechanism, thus highlighting the role for this axis in wound healing (173).

The platelet role in propagating cancer by facilitating metastatic spread has been extensively studied (174). Podoplanin itself has been extensively studied in the context of cancer, especially as it is expressed by lymphatic vessels and increased lymphangiogenesis is associated with poor outcomes after malignancy(69).

Podoplanin is unregulated by a number of cancers including head and neck squamous cell carcinomas, malignant mesotheliomas and various central nervous system tumours (69,175). Podoplanin co-localizes with the ezrin, radixin and moesin (ERM) family proteins; ERM proteins link membrane proteins to the actin cytoskeleton thus having the ability to translate signals from the cell surface into conformational changes in the cellular cytoskeleton influencing cellular processes including adhesion and migration(176). Studies in epithelial cells reveal that an over expression of podoplanin results in increased ERM phosphorylation, which gives these cells a more mesenchymal appearance, with increased filopodia and decreased stress fibres. Thus unsurprisingly studies demonstrate that expression of podoplanin correlates with increased cellular motility(68,69). Such increased cellular motility may explain why podoplanin expression in several cancers (177,178) correlates with a more aggressive and thus invasive phenotype. However others have found that in other contexts including lung squamous and uterine cancer the



opposite appears to be true; higher podoplanin expression in primary tumours correlates with lack of lymphatic invasion and better patient survival(179,180). With the findings above in mind, it is unsurprising therefore that functional *in vivo* studies report conflicting roles of the CLEC-2 podoplanin axis in facilitating tumor spread; an anti-podoplanin antibody has been demonstrated to reduce the number of metastatic lung nodules in murine models of metastatic cancer(181) but similar findings were not replicated in CLEC-2 deficient chimeric mice(165).

Recent evidence identifies podoplanin as a crucial player in various aspects of immune system functioning (90,182). Kerrigan et al reported that during inflammatory states macrophages up regulate podoplanin(90). In fact a recent study identified a number of other cells within the injured liver including distinct stromal populations that may thus also provide ligand for CLEC-2 dependent platelet activation(183).

Podoplanin also has a critical role in adaptive immunity, beyond its role in maintenance of high endothelial vein integrity during lymphocyte trafficking (86).

Acton et al describe the importance of podoplanin expression by stromal scaffolds (lymphatic endothelial and fibroblastic reticular cells) in activating dendritic cells (DCs) via CLEC-2, thus allowing enhanced DC motility across stromal surfaces and facilitating the adaptive immune response (182). Lastly the CLEC-2/podoplanin axis also plays an important role in driving thrombosis during inflammation as an eloquent study by Hitchcock *et al* details; here they find that CLEC-2 and podoplanin play an important role in facilitating inflammatory thrombosis in the liver during salmonella infection(94).

### **3.2. Aims of this chapter**

As we hypothesized that platelet activation via CLEC-2 plays a role in liver damage, we sought to examine whether the ligand for CLEC-2, podoplanin was expressed in the liver. It is important to establish whether expression increases after, or during liver injury and indeed whether the type of liver disease influences podoplanin expression. In order for platelet activation to occur, podoplanin must be accessible to CLEC-2 expressing platelets thus we next sought to define the patterns of platelet sequestration in the damaged liver and critically whether this sequestration was associated with podoplanin expressing cells. Lastly, we wished to examine whether podoplanin expression within the inflamed liver provided a stimulus for hepatic thrombosis and if expression varied with severity of liver disease. Thus the specific aims for this chapter were as follows:

1. To establish the pattern of podoplanin expression in the non-injured and injured human liver.
2. To examine whether platelets sequestered to podoplanin expressing cells during human liver disease.
3. To correlate podoplanin expression with clinical markers of human liver disease including severity as gauged by MELD scores and occurrence of clinically relevant thrombosis (specifically portal venous thrombosis).

### 3.3. Podoplanin is minimally expressed within the liver during normal physiology

Podoplanin expression was fairly limited within normal non-injured human liver. Most of this expression in non-injured liver was confined to the portal tracts on lymphatic vessels (fig 3.1)

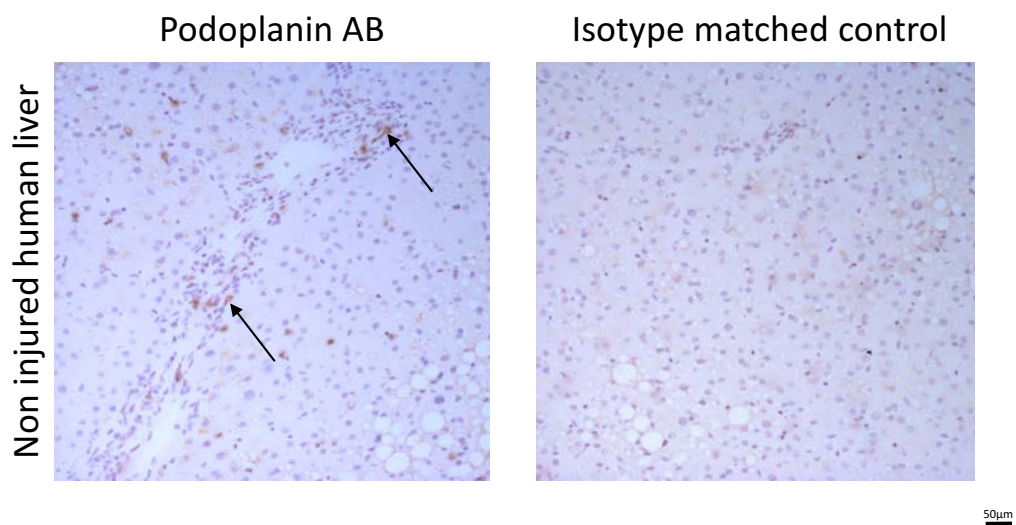
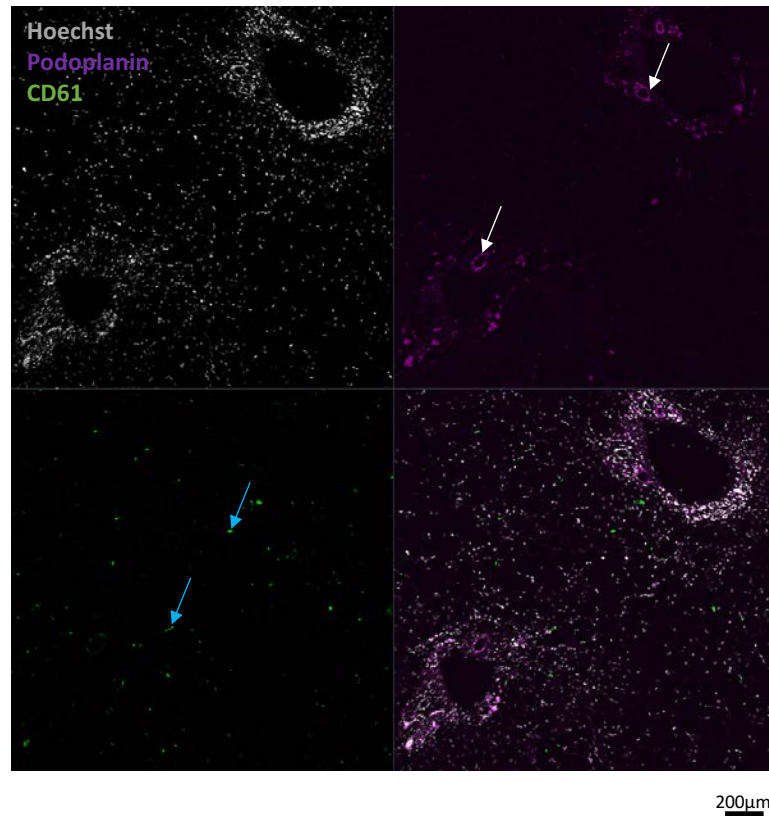


**Figure 3.1 Podoplanin expression is minimally expressed in the non-injured human liver:**

Podoplanin was visualized using indirect immunohistochemical staining with DAB substrate (arrows, brown) on frozen human liver sections. Representative image of non-injured donor tissue is shown with podoplanin antibody (left panel) or Isotype matched control (right panel) original magnification 20x . Arrows indicate positive staining on lymphatic vessels in portal area.

We next used confocal microscopy to determine whether podoplanin expression in a non-injured liver was associated with platelets. We found that platelets (using CD61 as a marker) were found to reside within hepatic sinusoids but did not associate with podoplanin expressing cells or structures in uninjured normal liver (representative images in fig 3.2). Podoplanin expression was in keeping with our DAB stain restricted to portal tracts, on vessels morphologically consistent with lymphatics (fig 3.2).

### Non-injured human liver



### Isotype control



#### **Figure 3.2 Minimal colocalisation of platelets and podoplanin in the normal liver:**

An explanted frozen non-injured human liver section is shown. The nuclei are stained with hoechst-grey, CD61<sup>+</sup> platelets are green and podoplanin is purple. Image representative of at least 5 different livers. 10x magnification. Isotype control was negative (bottom image).

Platelets highlighted by blue arrows and lymphatics by white arrows.

### **3.4. Podoplanin expression increases dramatically during acute and chronic human liver disease**

Once we had established the basal expression of podoplanin in uninjured human liver samples, we then examined tissues from diseased patients to assess the patterns of expression in acute and chronic liver injury.

#### **3.4.1. Podoplanin expression in acute liver injury**

The livers we studied for acute human liver injury sample studied were from explanted livers from patients with acute fulminant liver failure due to paracetamol overdose. An upregulation of podoplanin was noted in these acute drug induced liver injuries. Again the staining was observed in a predominantly periportal distribution but in far greater amounts than what was noted in non-injured livers. The distribution of this upregulated podoplanin was concentrated within periportal areas (blue arrows fig 3.3) with very minimal expression by hepatocytes or other parenchymal cells. The morphology of positively stained structures was indicative of the thickened endothelial lining of lymphatic vessels (see higher magnification image examples in fig 3.3). In addition we noted that podoplanin was also expressed upon cells of the inflammatory infiltrate(see black arrows in fig 3.3).

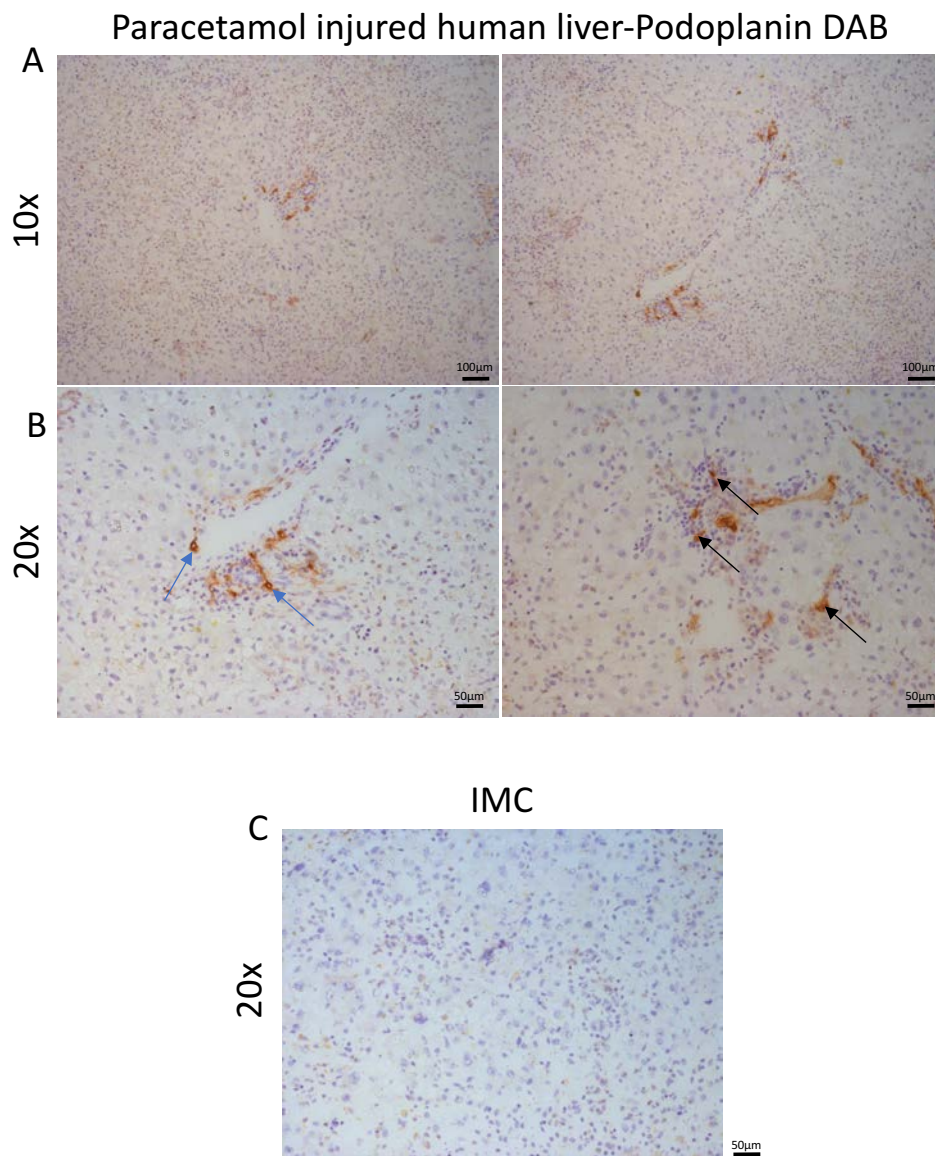


**Figure 3.3 Podoplanin is upregulated in paracetamol induced acute human liver injury:**

Representative images from frozen human liver sections stained with podoplanin specific antibody(brown staining) in a standard indirect immunochemical protocol. Images are from representative cases of paracetamol toxicity and are shown at A) 10x, or B) 20x original magnification. Isotype control staining (IMC) is shown in panel C. Positive staining on lymphatic vessels (blue arrows) and infiltrating mononuclear cells (black arrows) is present. Bar indicates 50 or 100  $\mu\text{m}$ .

To identify the immune cells that stained positively for podoplanin in acutely injured livers I performed confocal microscopy on sections stained with fluorescent antibodies. Figure 3.4 shows representative examples of this staining and illustrates that CD68<sup>+</sup> macrophages in the parenchyma (green staining) also express podoplanin (blue stain, dual stain-sea blue indicated by arrowheads on Figure 3.4).



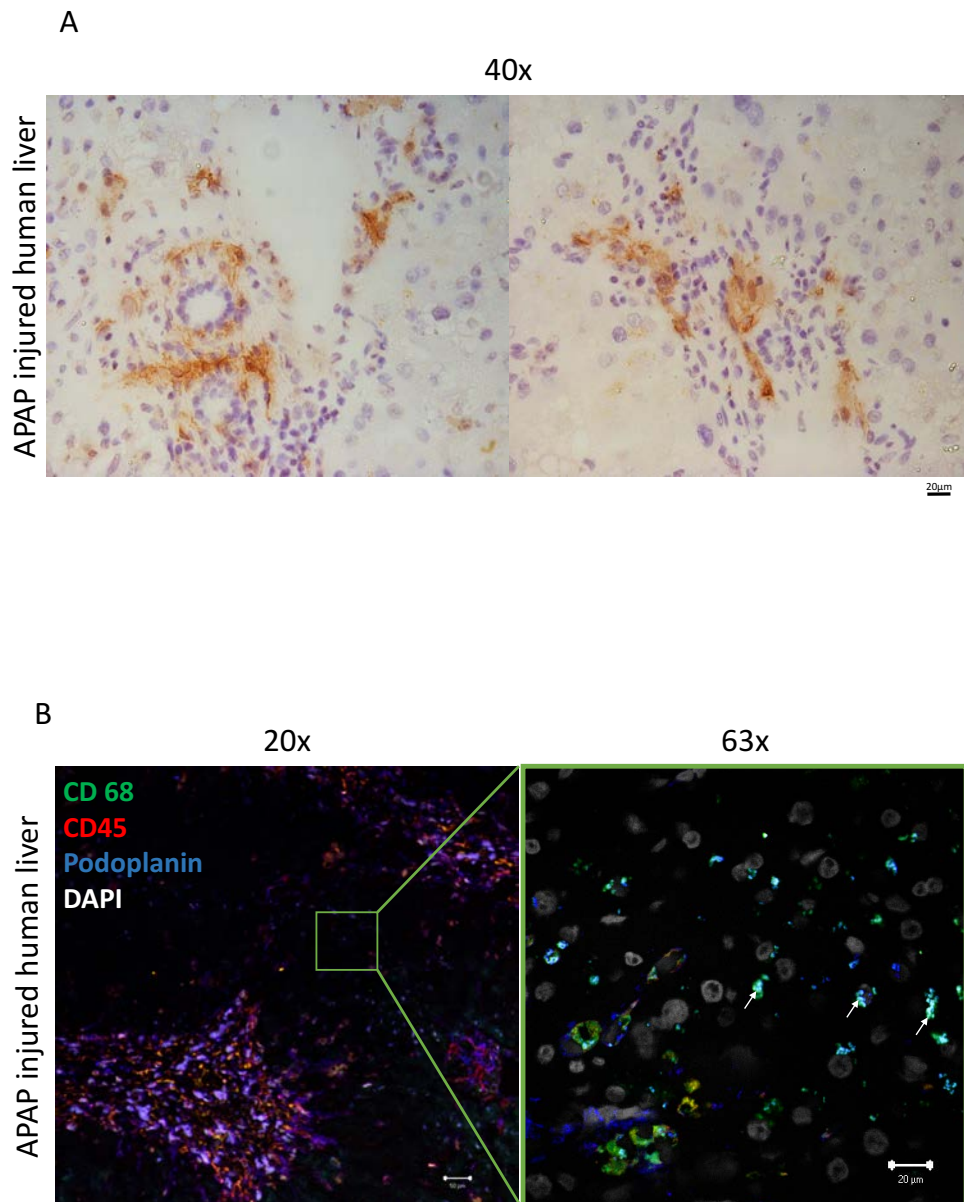


**Figure 3.4 Hepatic macrophages upregulate podoplanin after APAP induced liver injury in humans:**

A) Representative images from frozen human liver sections stained with podoplanin specific antibody (brown staining) in a standard indirect immunohistochemical protocol. Images are from representative cases of paracetamol toxicity and are shown at 40x, or B) Representative confocal images from the same human liver section presented at either 20x or 63x magnification. Podoplanin (blue) expression on hepatic macrophages—arrows (CD68-macrophages—green) (CD45-leukocytes—red, DAPI—white). Podoplanin expressing macrophages are sea blue (arrows—bottom right picture).

#### **3.4.1.1. Platelets sequester to podoplanin expressing macrophages during paracetamol-induced acute liver injury.**

To ascertain whether podoplanin expression in the acutely injured liver could potentially provide ligand for and thus activate platelets we next undertook confocal microscopy to study platelet distribution after paracetamol overdose. We found that platelets sequestered to podoplanin expressing macrophages here (fig 3.5) within portal areas and also sinusoids. Podoplanin (green) expressing macrophages (red) clearly exhibit platelet (CD61-blue) sequestration. Figure 3.5 is representative of all samples of paracetamol overdose we studied.

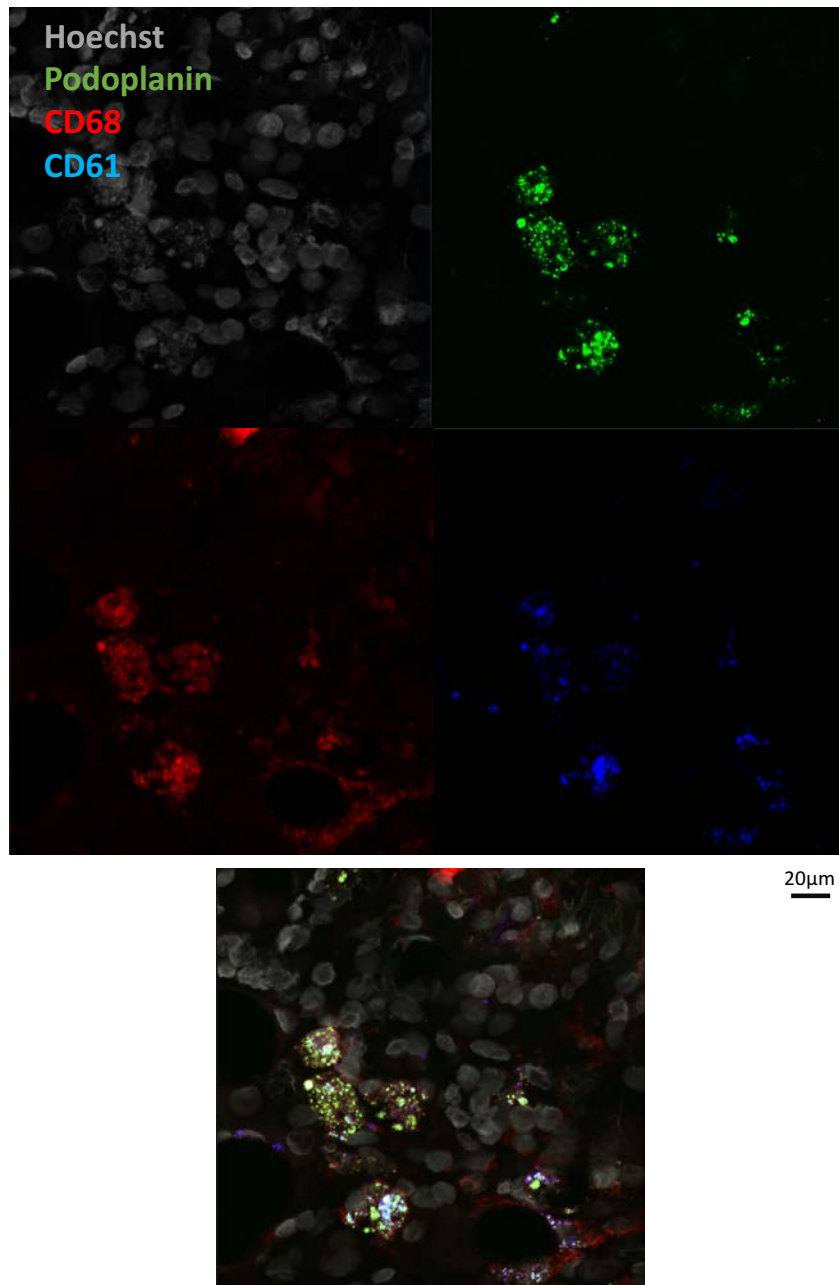


**Figure 3.5 Platelets sequester to podoplanin expressing macrophages in APAP injured human liver:**

A frozen section from an explanted APAP injured human liver is shown. The nuclei are stained with hoechst-grey, CD41 (platelet) is blue, podoplanin is in green and CD68 (macrophages) is red. Image is representative of at least 4 different livers. 63x magnification. Composite image bottom shows macrophages (CD68) expressing podoplanin to which are attached platelets (CD61) (white).

### **3.4.2. Podoplanin expression in chronic liver injury**

Chronic liver disease (CLD) as discussed in the section 1.3, is the result of iterative insults to the liver. Although there are similarities in the initial immunological processes that drive both acute and chronic liver disease, the final outcomes vary considerably. Having established the expression of podoplanin in the acutely injured liver we next proceeded to examine if this was different in chronically injured human livers.

#### **3.4.2.1. Alcoholic liver disease**

Livers from patients with alcoholic cirrhosis (ALD) demonstrated a significant upregulation of podoplanin within periportal areas compared to the picture in normal or acutely injured livers. Here podoplanin was expressed on both vessels in the portal areas and upon cells of the inflammatory infiltrate (see higher magnification images in fig 3.6). The staining on vessels appeared more intense (darker) than acutely injured samples and was accompanied by a lower intensity stain with a more 'stromal' appearance around portal vessels and biliary structures and areas of ductular reaction (arrows panel D figure 3.6). No staining was seen with isotype-matched control antibodies (Panel F, fig 3.6)

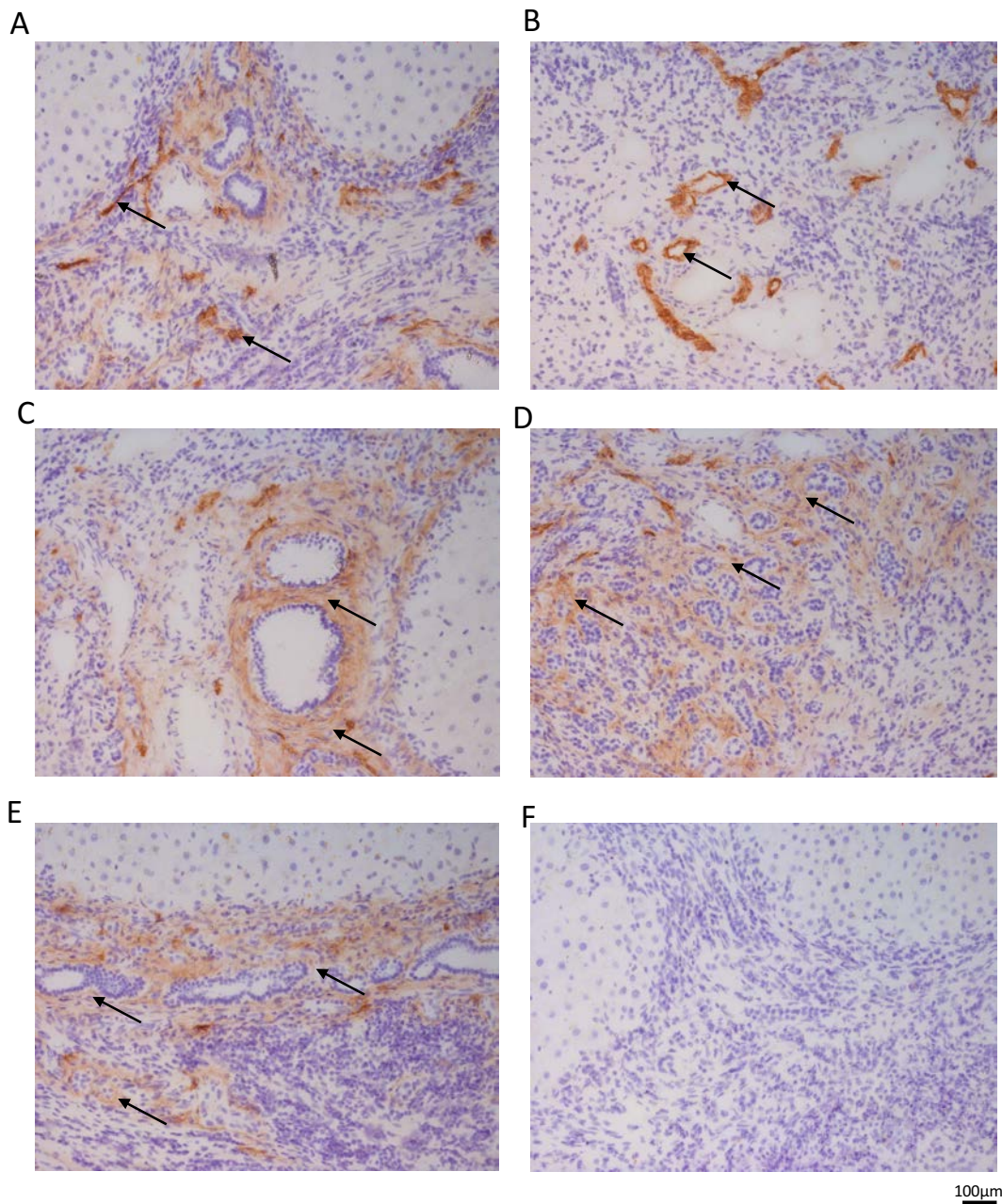


**Figure 3.6 Podoplanin is upregulated in periportal areas in alcoholic liver disease:**

Representative images from frozen human liver sections stained with podoplanin specific antibody (brown staining) in a standard indirect immunohistochemical protocol. Images are from representative cases of ALD and are shown at 10x magnification. A-B) Demonstrate podoplanin expression in periportal areas, on vessels (arrows). C, E) podoplanin expression is seen around bile ducts (arrows). D) Podoplanin expression is seen in areas of ductular reaction (arrows). F) Isotype matched control was negative. Images are representative of at least 6 different livers.

We next used a CLEC-2 -specific antibody to establish whether there was any CLEC-2 expression in alcoholic liver disease. Interestingly we observed that CLEC-2 -expressing platelets or structures appeared to sequester to cells within the inflammatory infiltrate (panel C fig 3.7). We also noted enhanced CLEC-2 staining of both mature biliary ductules and neoducts formed are part of the ductular reaction (fig 3.7)

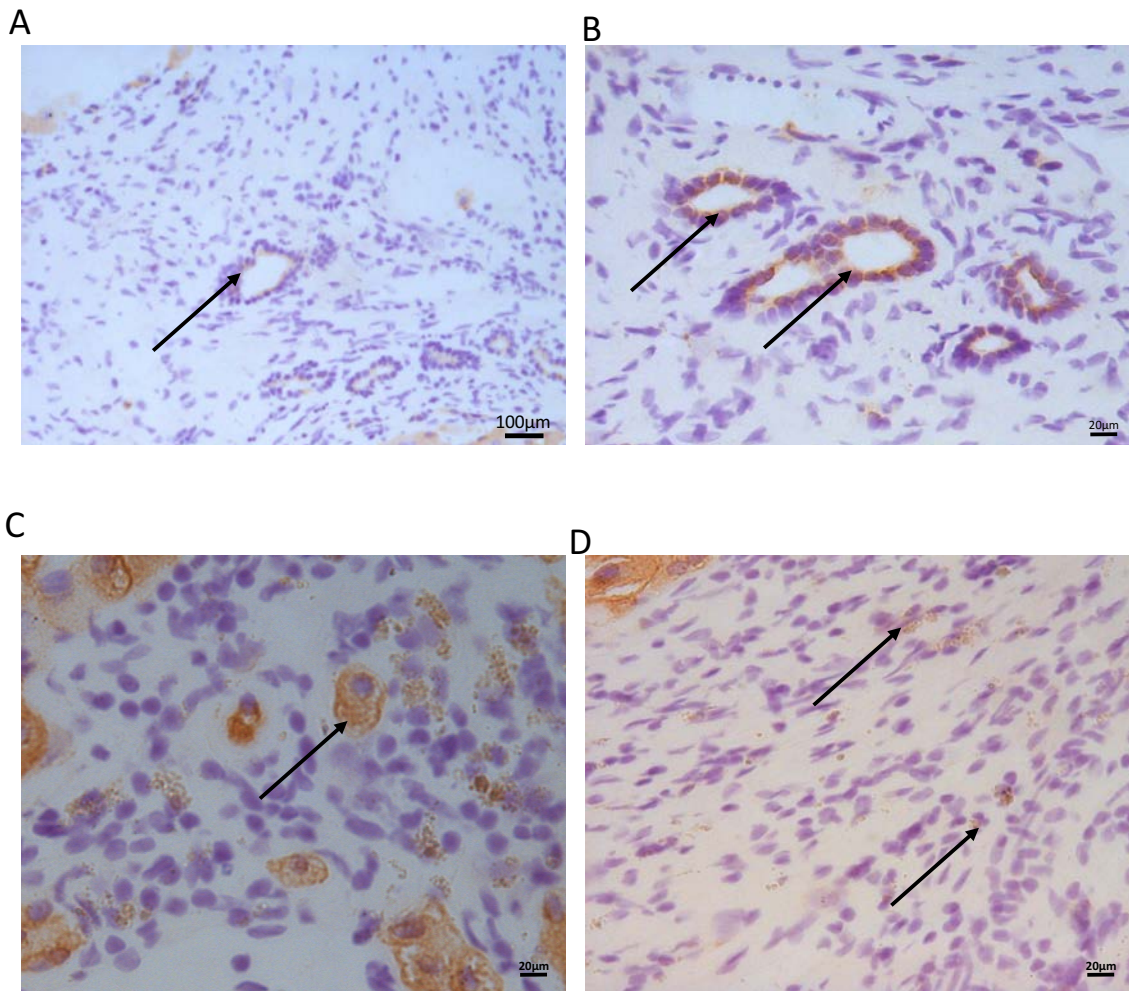


**Figure 3.7 Expression of CLEC-2 in alcoholic cirrhosis:**

Frozen sections of explanted livers from patients with end stage liver disease (cirrhosis) due to alcohol were stained using a CLEC-2 primary antibody and DAB (brown, arrows) secondary stain. Sections were counterstained with hameotoxylin (nuclei-purple), 20X or 40X magnification. A-B) Demonstrate increased CLEC-2 expression within biliary structures. C-D) CLEC-2 expression is seen on platelets sequestering to inflammatory infiltrate within an injured liver.

Confocal microscopic analysis with fluorescent antibodies was also performed. In alcoholic liver disease, similar to our findings in acute liver injury we found that podoplanin was upregulated upon macrophages (fig 3.8) but also upon periportal vessels (fig 3.9). The morphology of these vessels seemed distinct to lymphatic vessels so I dual stained these sections with podoplanin and CD31 (marker of vascular endothelium) (fig 3.9). We demonstrate that in chronic human liver disease due to alcohol podoplanin is upregulated upon vascular endothelium (fig 3.9). The morphology and location of these vessels was consistent with portal venules. Notably the enhanced stromal DAB stain we observed (fig 3.6) earlier was replicated in our confocal images (fig 3.9).



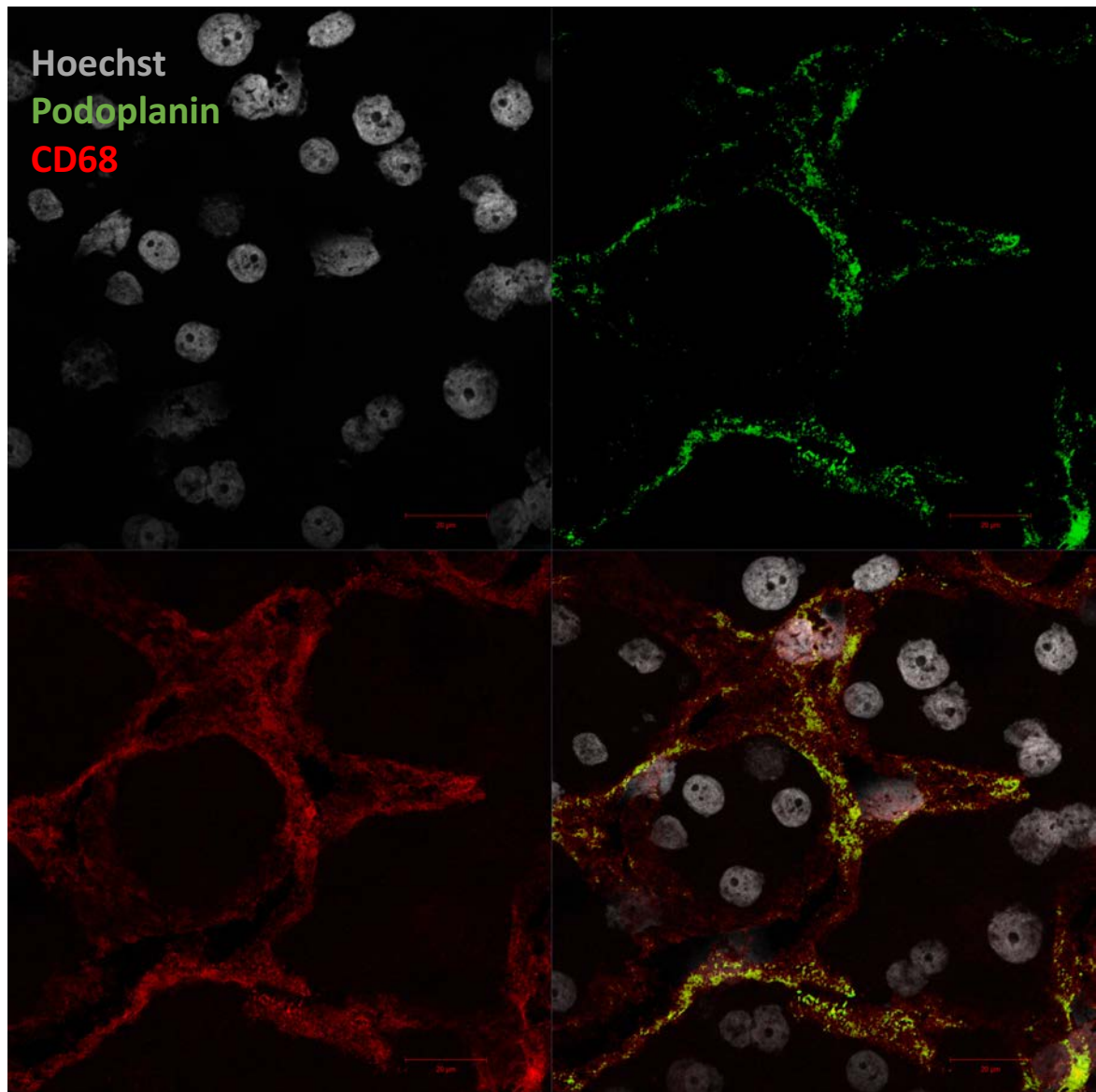
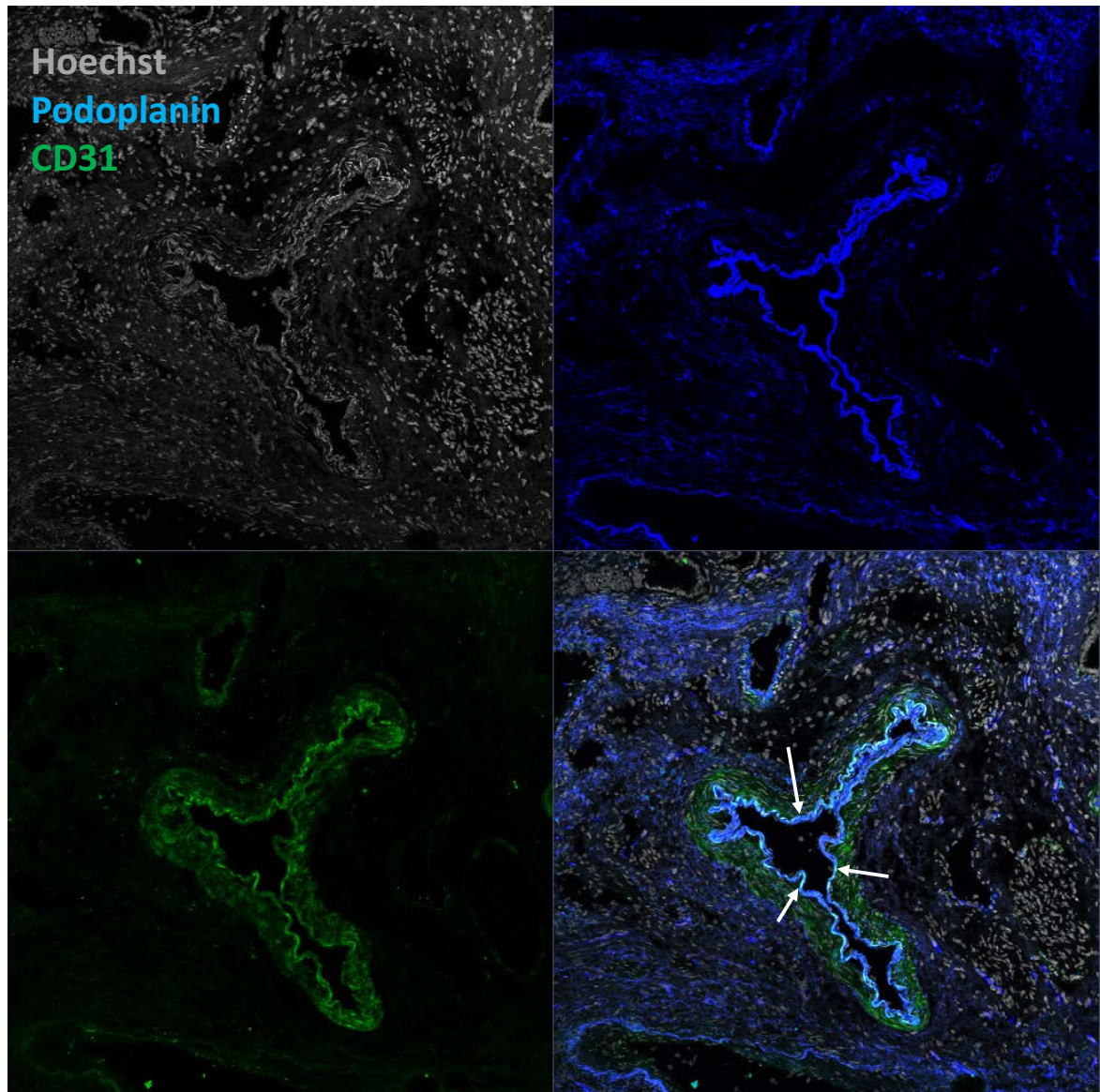


**Figure 3.8 Macrophages in alcoholic liver disease express podoplanin:**

A frozen liver section from a patient with alcoholic cirrhosis section is shown. The nuclei are stained with hoechst-grey, podoplanin is in green and CD68 (macrophages) is red. Image is representative of at least 4 different livers. 100x magnification. Composite image bottom right shows macrophages (CD68) expressing podoplanin (yellow).



50µm

**Figure 3.9 Portal veins express podoplanin in alcoholic liver disease:**

A frozen liver section from a patient with alcoholic cirrhosis section is shown. The nuclei are stained with hoechst-grey, podoplanin is in blue and CD31 (vascular endothelium) is in green. Image is representative of at least 4 different livers. 20x magnification. Composite image bottom right shows portal venule endothelium expressing podoplanin (see blue-arrows).

#### **3.4.2.2. The expression of podoplanin in autoimmune liver disease**

The pattern of podoplanin expression detected immunochemically in autoimmune liver disease (AIH) was similar to that seen in alcoholic cirrhosis. Thus we saw podoplanin expression around portal vessels with high intensity (blue arrows) and a lower intensity 'stromal' stain (fig 3.10, panel A-C). No staining was seen with isotype-matched control antibodies (Panel D, fig 3.10). However a notable difference was a lack of podoplanin upregulation around biliary vessels (fig 3.10).

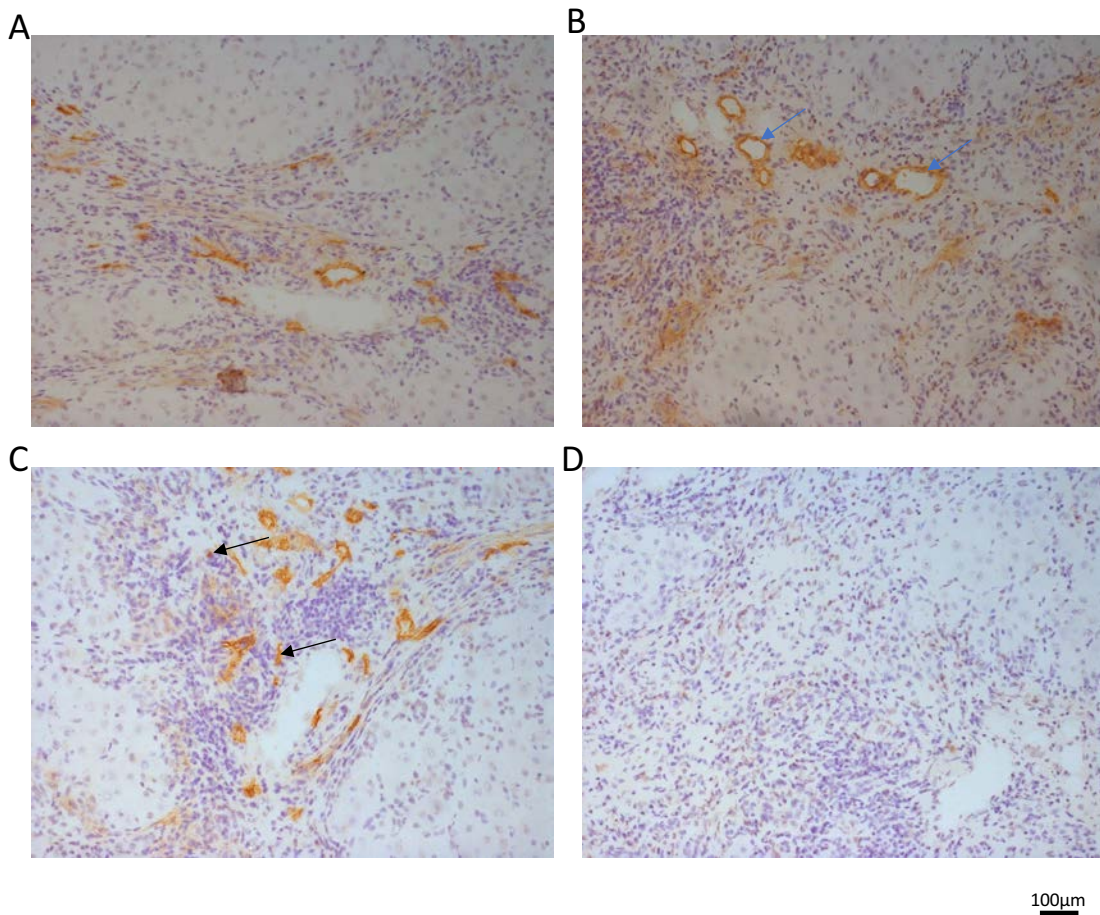
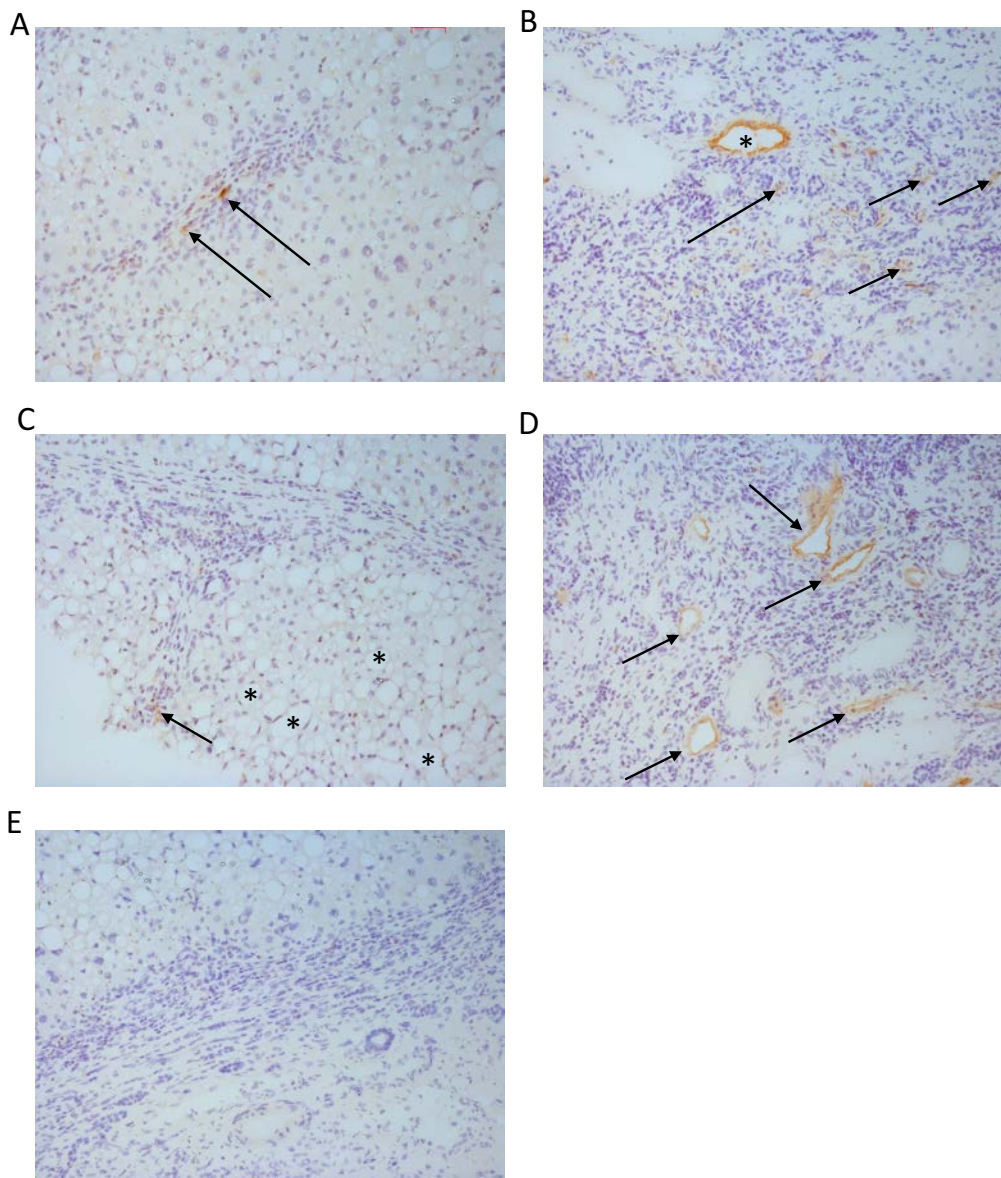


**Figure 3.10 Podoplanin is upregulated in autoimmune human liver disease:**

Representative images from frozen human liver sections stained with podoplanin specific antibody (brown staining) in a standard indirect immunohistochemical protocol. Images are from representative cases of AIH and are shown at 20x magnification. Sections were counterstained with hematoxylin (nuclei-purple), A-C) Demonstrate increased podoplanin expression (brown) in periportal areas, on vessels (blue arrows) and inflammatory cells (black arrows). D) Isotype matched control was negative. Image is representative of at least 4 different livers

### **3.4.2.3. Non-alcoholic steatohepatitis**

Compared to alcoholic liver disease less overall podoplanin expression was seen in human non-alcoholic steatohepatitis (NASH). Expression was seen periportally, on infiltrating mononuclear cells and periportal vessels. On the whole a lower intensity of podoplanin stain uptake particularly in the stromal areas was seen compared to what we observed in ALD and PSC. Podoplanin was seen on periportal vessels (fig 3.11, panel A arrows, panel B asterisk, panel C arrow and panel D arrows) and cells of the inflammatory infiltrate (fig 3.11, panel B arrows). Minimal expression on steatotic hepatocytes was seen (fig 3.11, panel C asterisks).



100µm

**Figure 3.11 Podoplanin is upregulated in periportal areas in non-alcoholic fatty liver disease:**

Representative images from frozen human liver sections stained with podoplanin specific antibody (brown staining) in a standard indirect immunochemical protocol. Sections were counterstained with hameotoxylin (nuclei-purple), 20X magnification. A) podoplanin expression in periportal areas on cells of the inflammatory infiltrate (arrows) B) A single enhancing portal vessel is seen (asterisk), multiple areas of podoplanin expression are seen within the inflammatory infiltrate (arrows). C) Wider angle views reveal steatotic hepatocytes (asterisks) do not express podoplanin, podoplanin expression is seen periportally (arrow) D) Numerous periportal vessels expressing podoplanin are seen (arrows). E) Isotype matched control was negative. Image is representative of at least 4 different livers.

CLEC-2 expression was also harder to discern in NASH, however broadly followed the same pattern as what has been seen previously with ALD. Hence CLEC-2 expression was again seen in neo biliary structures and on platelets sequestering to areas of inflammatory infiltrate (fig 3.12).

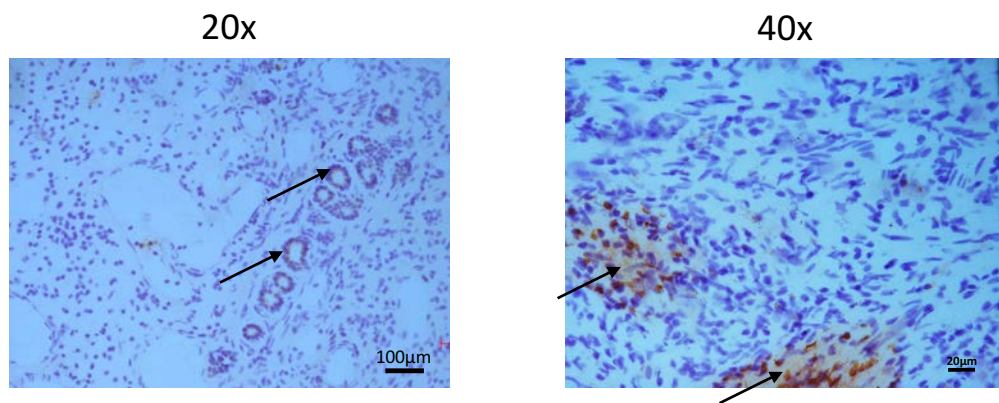


**Figure 3.12 CLEC-2 expressing platelets sequester to the injured liver during NASH:**

Representative images from frozen NASH human liver sections stained with CLEC-2 specific antibody (brown staining) in a standard indirect immunohistochemical protocol. Sections were counterstained with hematoxylin (nuclei-purple), A) CLEC-2 expression within biliary structures is seen-arrows (20x). B) CLEC-2 expression on platelets sequestering to inflammatory infiltrate within injured liver (arrows) (40x). Images are representative of at least 4 different livers.

#### **3.4.2.4. Primary biliary cirrhosis**

The immunochemical staining pattern for podoplanin expression in PBC was much different than we observed with other chronic diseases. A much greater quantity of cells expressing podoplanin was seen (fig 3.13 panels A-E). Thus we saw high intensity dark staining of portal vessels (fig 3.13), a very intense stromal stain (particularly around biliary structures 3.13, A-B) and enhanced vascular staining within areas of inflammatory cell accumulation along fibrous septa (fig 3.13, panel D). Confocal microscopy also revealed that we saw an increased accumulation of platelets within PBC livers (blue staining fig 3.14). However it was interesting to note that this staining did not localize in proximity to green-stained podoplanin positive structures (fig 3.14)



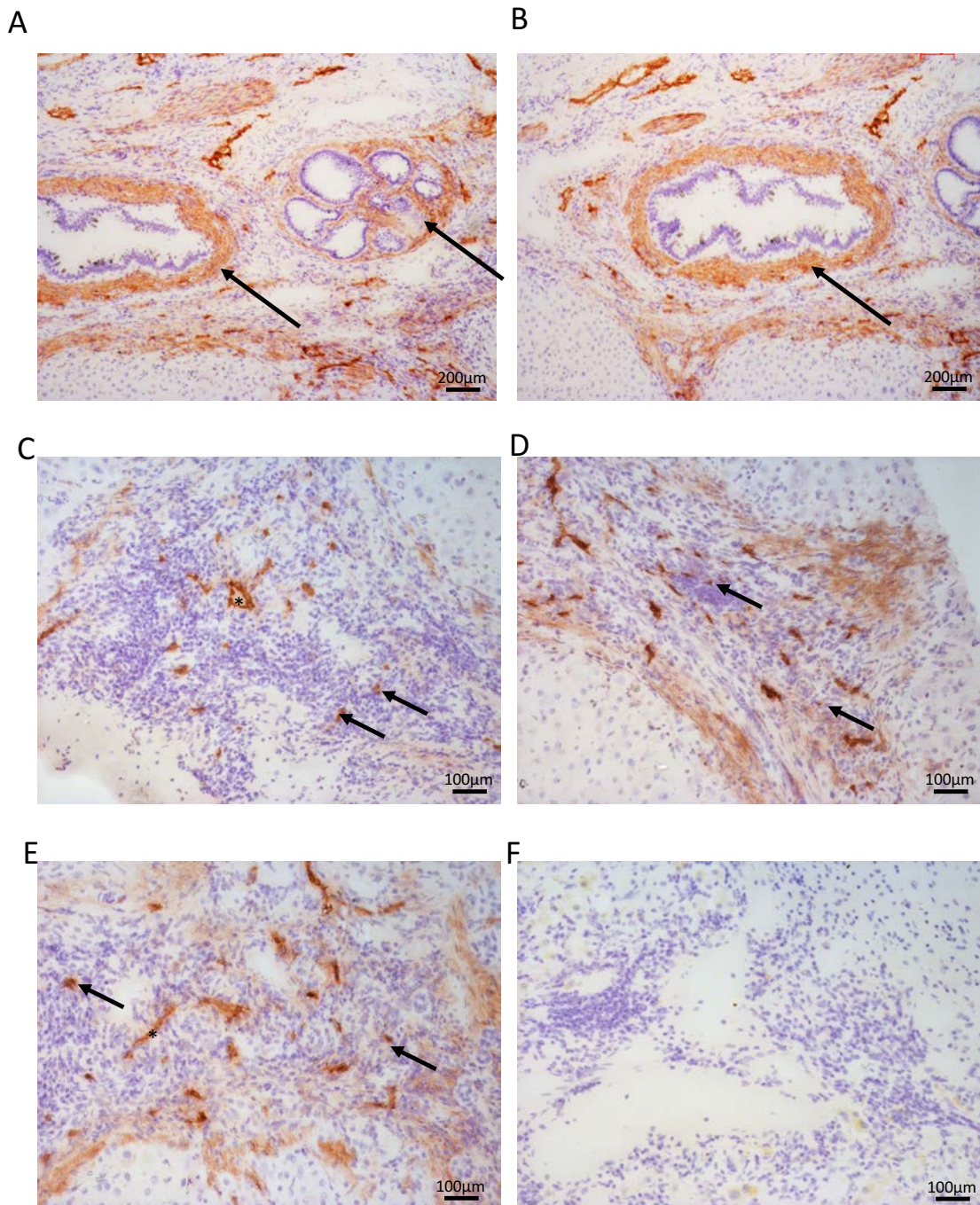
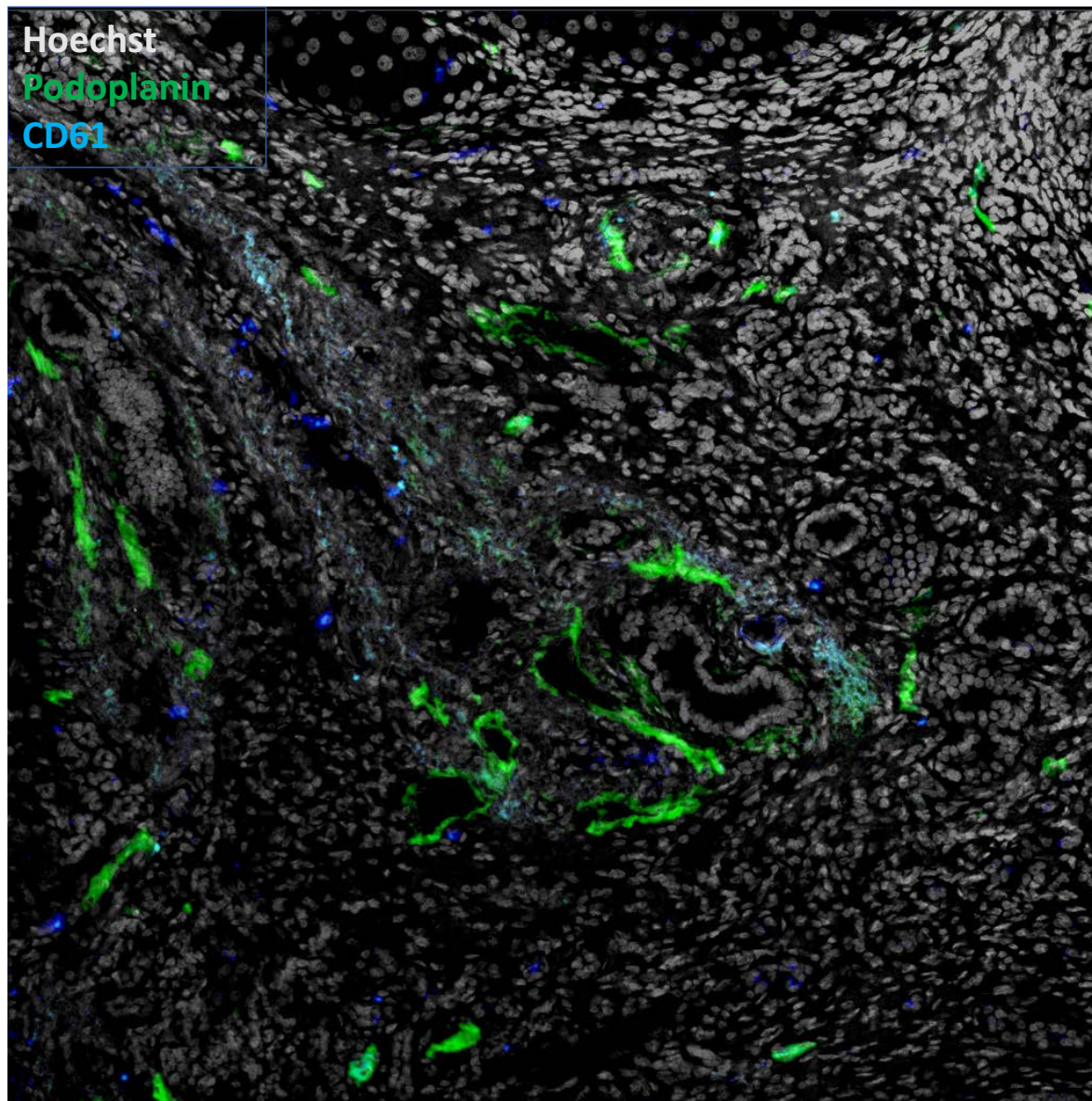


**Figure 3.13 Podoplanin is upregulated in primary biliary cirrhosis (PBC):**

Representative images from frozen PBC human liver sections stained with a podoplanin specific antibody (brown staining) in a standard indirect immunochemical protocol. Sections were counterstained with hameotoxylin (nuclei-purple), 10X or 20X magnification. A-B) Peri-biliary podoplanin expression areas (arrows-brown). C,D,E) Periportal vessel (asterisk) and the portal infiltrate podoplanin expression (arrows) F) Isotype matched control was negative. Image is representative of at least 5 different livers.



100μm

**Figure 3.14 Platelets do not sequester to podoplanin expressing areas in PBC:**

Frozen sections of explanted livers from patients with PBC were stained using a podoplanin antibody (green), hoechst nuclear stain (grey) and CD41 platelet stain (blue). Image representative of at least 4 livers. 10x magnification.

#### **3.4.2.5. Primary sclerosing cholangitis**

Podoplanin expression in explanted livers from patients with primary sclerosing cholangitis (PSC) again followed a similar pattern to other liver diseases with most of the podoplanin being expressed within the portal tracts, with no expression on the hepatocytes themselves. The staining was the most pronounced amongst all the diseases we studied. Notably the stromal stain intensity was greatest in PSC (fig 3.15, panel A and B, asterisks). A significant amount of podoplanin expression was noted on periportal vessels (fig 3.15, panel A-D, black arrows). High magnification images confirm that the podoplanin was upon the endothelial vessel lining and not just the vessel wall (fig 3.15, panel E arrows). Another difference in pattern of expression to other liver pathologies studies was the presence of podoplanin on larger periportal vessels, with little or no peri-biliary podoplanin expression. Podoplanin was again found on cells of the portal infiltrate (fig 3.15, panel C-D, blue arrows)

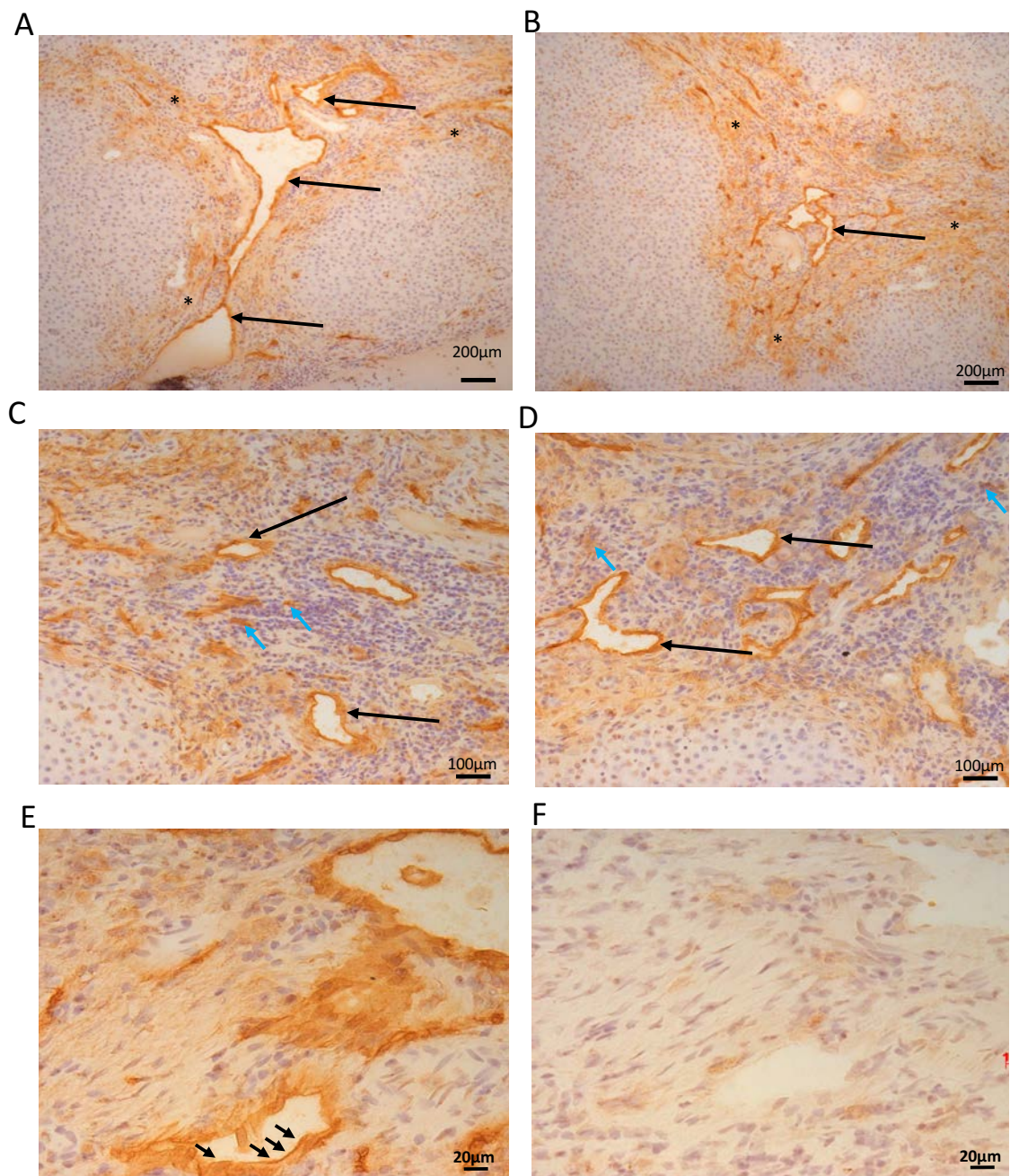


**Figure 3.15 Podoplanin is upregulated in primary sclerosing cholangitis (PSC):**

Representative images from frozen PSC human liver sections stained with a podoplanin specific antibody (brown staining) in a standard indirect immunochemical protocol. Sections were counterstained with hameotoxylin (nuclei-purple), 10X, 20X or 40X magnification. A-B) podoplanin expression in a portal vessels (black arrows) (10x). C,D) Podoplanin expression is seen on periportal vessels ( black arrows) and the portal infiltrate (blue arrows) (20X). E) High magnification (40X) picture a vessel confirms endothelial podoplanin expression (arrows). F) Isotype matched control staining was negative (same structure as seen in E).Image is representative of at least 6 different livers.

In PSC we again noted podoplanin expression upon vascular endothelium (CD31<sup>+</sup>vessels) (fig 3.16, blue arrows) and upon leukocytes (as characterized by CD45<sup>+</sup> cells) (fig 3.16, white arrows)

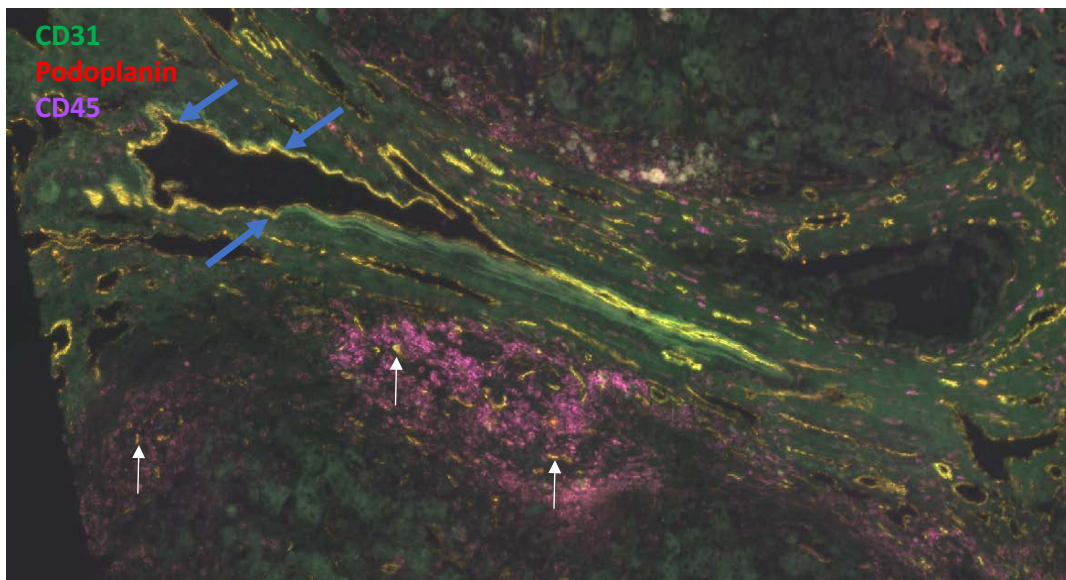


**Figure 3.16 Vascular endothelial cells and leukocytes express podoplanin in PSC livers:**

Frozen sections of explanted livers from patients with PSC were stained using a podoplanin antibody (red), CD31 (vascular endothelium) (green) and a CD45 (pan leukocyte marker) stain (magenta). Vascular endothelium that expressed podoplanin appears yellow in composite figure (blue arrows), leukocytes expressing podoplanin are highlighted with black arrows. Image representative of at least 6 livers. 10x magnification.

To confirm what leukocytes may be up regulating podoplanin we stained for macrophages using a CD68 marker and found that similar to acute liver injury macrophages upregulated podoplanin (fig 3.17).

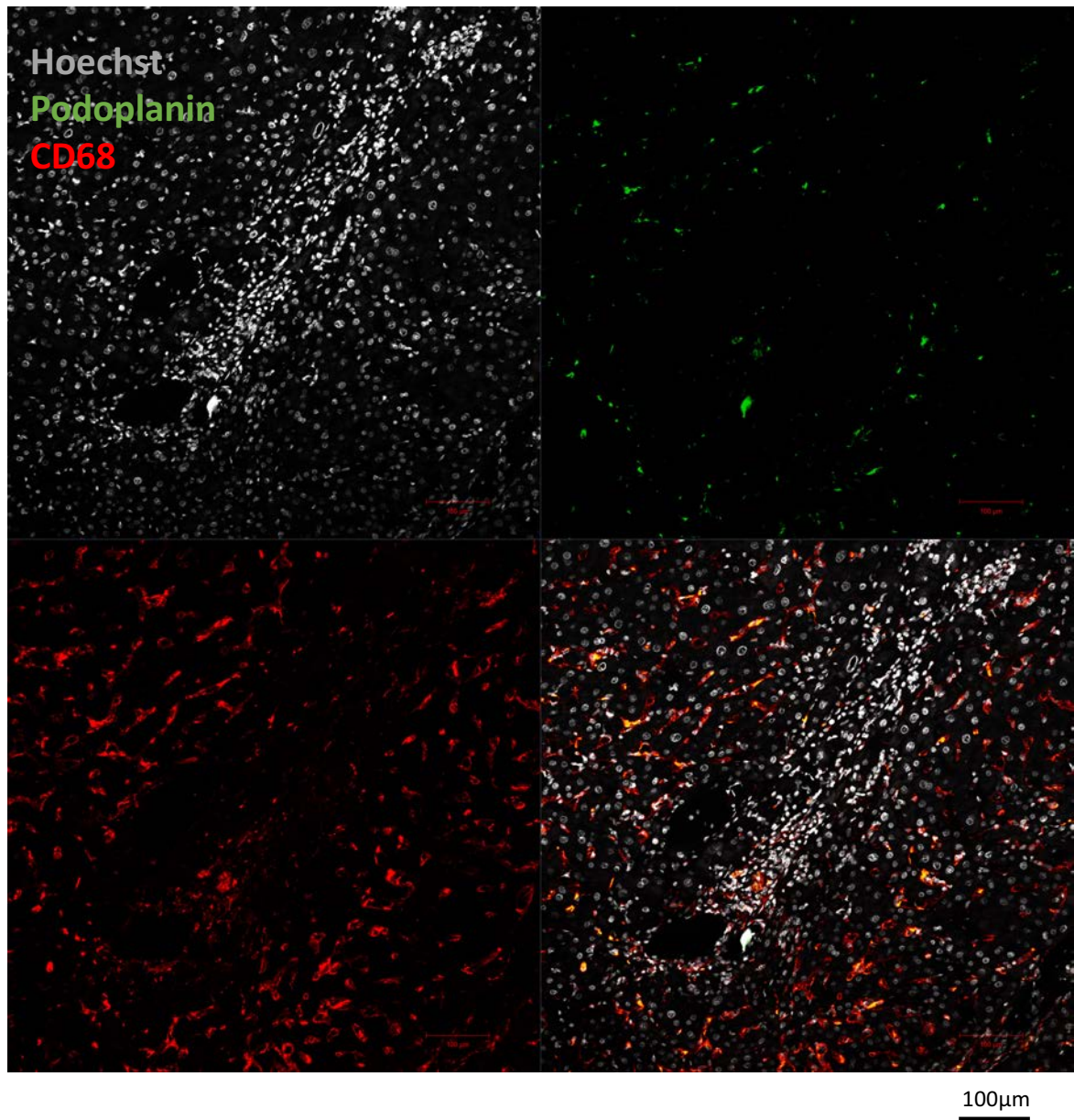


**Figure 3.17 Macrophages express podoplanin in PSC:**

Frozen sections of explanted livers from patients with PSC were stained using a podoplanin antibody (green), hoechst nuclear stain (grey) and CD68 macrophage stain (red). Macrophages expressing podoplanin appear yellow in composite figure. Image representative of at least 6 livers. 10x magnification.

### **3.5. Clinical correlation between podoplanin and disease severity**

The data above confirm that podoplanin is upregulated during both chronic and acute liver disease. In very acute injuries such as fulminant liver failure secondary to drugs (paracetamol overdose) podoplanin upregulation was primarily seen upon macrophages. In chronic variants of human liver disease however, podoplanin appears in peri-portal areas on both periportal vessels and inflammatory cells. Where there was evidence of macrophage podoplanin, I observed that platelets sequestered to these podoplanin expressing macrophages, thus potentially providing an avenue for CLEC-2-dependent platelet activation. I will explore the functional consequences of this interaction in the subsequent chapters, whilst the role of podoplanin in chronic human liver disease is considered in the sections below.

#### **3.5.1. Podoplanin mRNA is increased in damaged livers**

To support my immunohistochemical findings I quantified the amount of podoplanin mRNA in injured human livers by qPCR. Figure 3.18 below confirms that compared to non-injured control livers, chronically injured livers expressed significantly greater amounts of podoplanin mRNA, although there was considerable variation between donors.

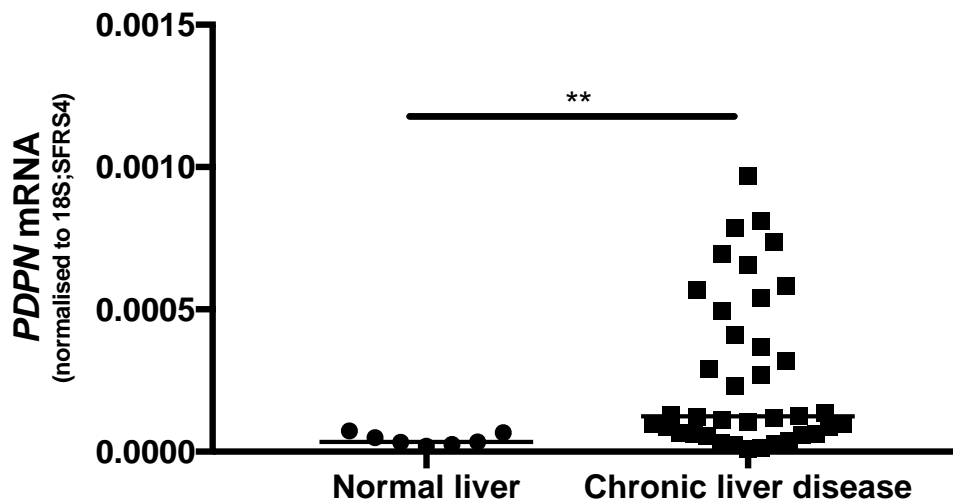


**Figure 3.18 Podoplanin mRNA is upregulated in human chronic liver disease:**

RNA was extracted from normal or chronically diseased (ALD, PSC, PBC, AIH or NASH) human livers using a RNEasykit (Qiagen, UK) and cDNA was generated using a High capacity cDNA reverse transcription kit (ThermoFisher, UK) according to manufacturer's instructions. Quantitative analysis of Podoplanin mRNA expression was performed using TaqmanFluorogenic5' nuclease assays using gene-specific 5' FAM labelled probes (Applied Biosystems) run on a ABI Prism 7900 sequencer with 18S;SRFS4 used as internal control. Differential expression levels were calculated according to the  $2^{-\Delta\Delta C_t}$  method. Mann-whitney test confirmed that expression was significantly different in diseased groups compared to control livers \* $P < 0.05$ , \*\* $P < 0.01$ , \*\*\* $P < 0.001$ . each dot indicates an individual patient sample and bar is median expression within the indicated cohort.

We next sought to investigate whether the amount of podoplanin expressed by diseased liver tissue varied with type of disease studied. We found that the autoimmune cholangiopathies (PSC and PBC) and end stage liver disease arising from chronic alcohol exposure (ALD) had the highest expression of podoplanin, whilst the other disease types were not significantly elevated compared to non-diseased tissue (fig 3.19).



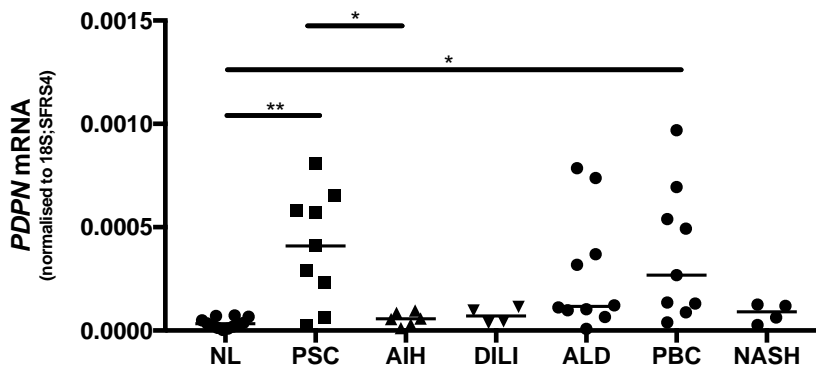


**Figure 3.19 Expression of podoplanin mRNA varies with disease type:**

qPCR was performed on mRNA extracted from explanted normal or diseased livers (PSC, AIH, DILI, ALD, PBC, NASH cirrhosis) as described in Figure X. ANOVA test confirmed that expression was significantly different in diseased groups compared to control livers \* $P < 0.05$ , \*\* $P < 0.01$ , \*\*\* $P < 0.001$ . Each dot indicates an individual patient sample and bar is median expression within the indicated cohort.

Our histological analyses broadly suggested that whilst podoplanin expression was also elevated in acutely injured livers (eg paracetamol induced fulminant liver failure) this was (in contrast to chronically damaged livers) primarily upon hepatic macrophages. Figure 3.20 confirms that at least at the level of mRNA there is an increase in podoplanin expression in DILI. All of the values for the DILI livers were above the mean mRNA level seen in normal controls but the change was not significant with our small sample size.

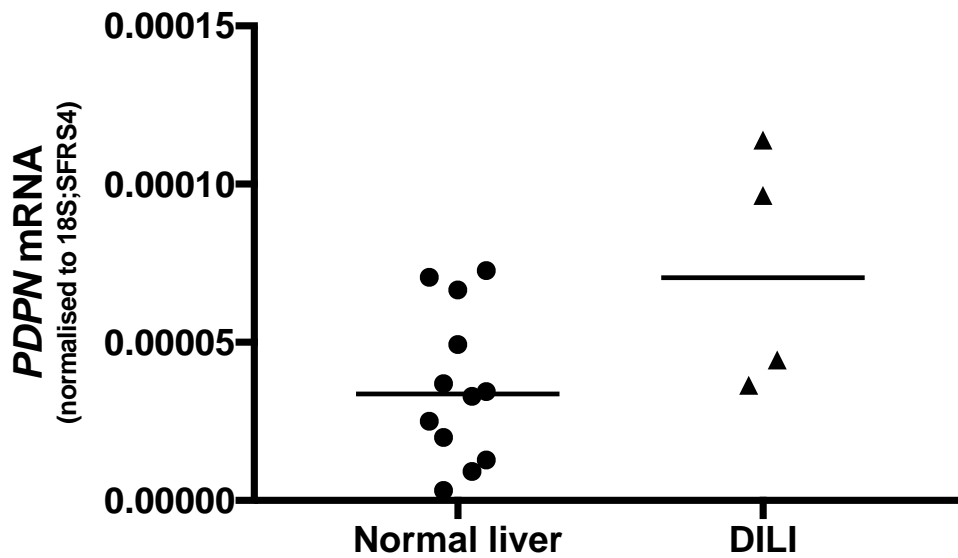


**Figure 3.20 Podoplanin is upregulated during acute fulminant liver failure due to paracetamol overdose:**

qPCR was performed on mRNA extracted from explanted normal or diseased livers (DILI) as described in Figure X. Mann-Whitney test confirmed that expression was significantly different in diseased groups compared to control livers. Each dot indicates an individual patient sample and bar is median expression within the indicated cohort.

### **3.5.2. Hepatic podoplanin expression increases with severity of liver disease**

The MELD score is a commonly used clinical score to predict survival in patients with chronic liver disease. This score is used to assess urgency for transplantation and generally correlates with the severity of liver disease(184). As we noted elevated podoplanin expression within explanted livers with end stage liver disease, we next wished to see whether severity of liver disease correlated with podoplanin expression. Hence, I calculated the MELD scores of patients at time of transplantation and correlated it with the amount of hepatic podoplanin mRNA within the explanted liver sample. Figure 3.21 shows that although there was significant variability in values from the grouped cohorts of damaged liver samples, there was a correlation between podoplanin expression and MELD scores. The relationship was particularly evident in samples with the highest MELD scores.

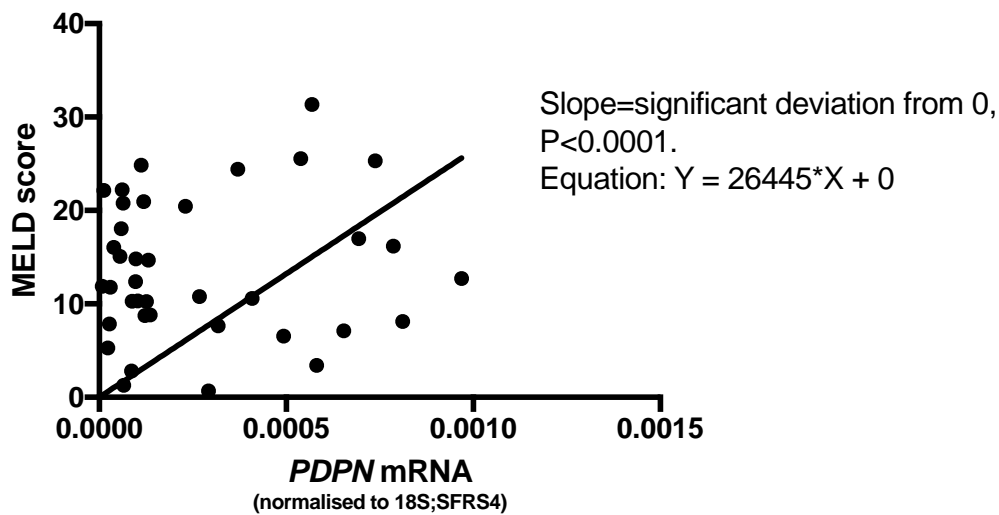


**Figure 3.21 Patient MELD scores correlate hepatic podoplanin mRNA expression at time of transplantation:**

MELD scores corresponding to each diseased or normal liver were calculated. Podoplanin mRNA levels were measured by qPCR as described previously. Samples shown are pooled (PSC, AIH, DILI, ALD, PBC, NASH cirrhosis- state types) and each point represents an individual patient. The line of best fit is shown.

It is important to note however that an increase in podoplanin commensurate with MELD score was not always observed for every individual disease category. Notably figure 3.22 shows that in autoimmune liver disease we found that higher MELD scores were associated with lower podoplanin expression.

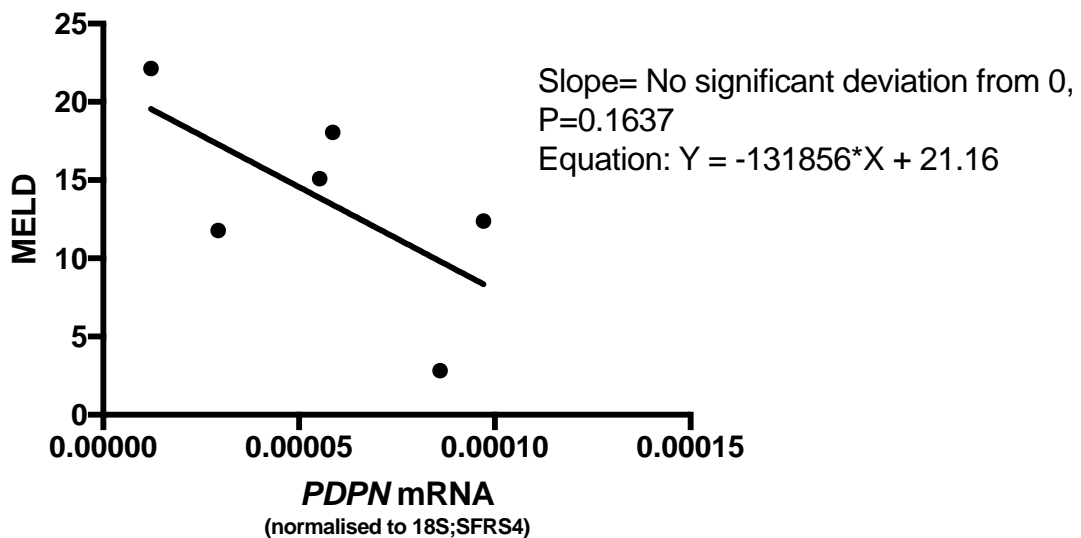


**Figure 3.22 In autoimmune liver disease higher MELD scores correspond with lower levels of podoplanin:**

MELD scores corresponding to each diseased or normal liver were calculated. Podoplanin mRNA levels were measured by qPCR as described previously. Samples shown are pooled (AIH) and each point represents an individual patient. The line of best fit is shown.

### 3.5.3. Venous thrombosis

The data in fig 3.9 suggested that at least some of the increase in podoplanin expression seen in chronic liver disease occurred upon vascular endothelium (CD31<sup>+</sup>), see representative images in section 3.9). Previous studies in Birmingham have shown that perivascular expression of podoplanin in murine sepsis is associated with intravascular thrombosis(94). Portal vein thrombosis is a common and feared complication of cirrhosis, and so it is possible that this may be explained by vascular podoplanin expression in chronic disease. Thus I sought to determine

whether there was a link between the occurrence of portal venous thrombosis and the amount of podoplanin expressed within livers in my cohort. Figure 3.23 shows that approximately 30% of our patients had evidence of portal venous thrombosis developments, and that more podoplanin mRNA expression was evident in these livers. However the data were highly variable between individuals.

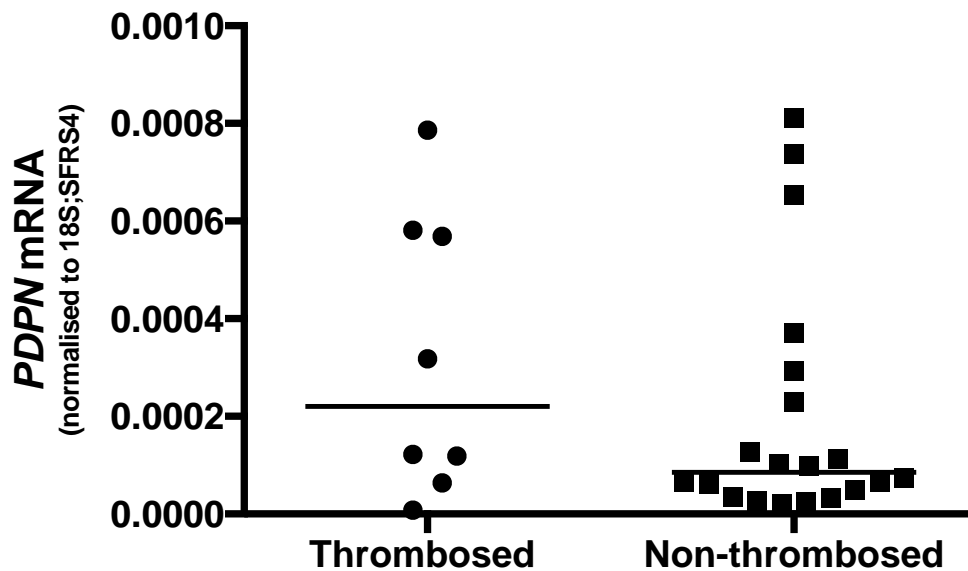


**Figure 3.23 Evidence of portal venous thrombosis pre-transplantation is associated with greater podoplanin mRNA expression:**

Podoplanin mRNA was quantified by qPCR as described previously in explanted normal or diseased human livers. Presence of portal venous thrombosis prior to transplant was assessed by interrogation of the corresponding patient notes. Samples are divided into two groups based on whether a portal venous thrombosis was present or not and points represent data from an individual patient. Each dot is an individual patient, median shown.

## **3.6. Summary and discussion**

### **3.6.1. Role of podoplanin in the liver**

Our data suggests that hepatic podoplanin levels are upregulated in both chronic and acute human liver disease. In a non-injured liver platelets do not interact with podoplanin, as most of the podoplanin is present within lymphatic vessels and we found very little expression upon leukocytes (fig 3.1), thus platelet activation via CLEC-2 is unlikely to be necessary to normal liver function. In acutely injured livers (explanted paracetamol overdose) we noted that podoplanin was upregulated upon portal and sinusoidal leukocytes (fig 3.4, 3.4). We confirmed that at least some of these cells were macrophages (fig 3.5). Although podoplanin expression on inflammatory macrophages has been previously noted(90), we provide the first demonstration of hepatic macrophages expressing the only known ligand for CLEC-2 and thus potentially a role for CLEC-2 dependent platelet activation in acute liver injury. This is an important finding as the platelet interaction with macrophages has relevance in acute inflammation particularly in the context of the liver. For example, the Kupffer cell-platelet interaction aids pathogen clearance, platelets interact with Kupffer cells in the early period following ischaemia-reperfusion injury(117,185) and these interactions dictate injury severity in steatotic livers(186). Furthermore as platelets sequester to podoplanin expressing macrophages in drug induced acute liver injury it may be that this interaction has a role in the pathogenesis of DILI (we investigate this further in the next chapter). The role this axis has in thrombosis

during acute liver inflammation has also been described as podoplanin expression on inflammatory monocytes and Kupffer cells (in mice) within the liver during salmonella infection drives post-infection inflammatory thrombosis(94).

### **3.6.2. Vascular expression**

In chronic human liver disease we noted that most of the podoplanin upregulation was found localized to periportal areas of the liver. Here it appeared to be expressed on both inflammatory cells and on vessels. The lymphatic vessel expression is perhaps unsurprising as podoplanin has been used as a marker for lymphatic endothelium and thus lymphatic vessels(166) in cirrhotic and normal livers. Little is known about the lymphatic venous system in the liver, perturbation in lymphatic function is however thought to be contributory to the development of ascites(187) . Thus enhanced expression in the context of cirrhotic end stage diseased livers may reflect expansion of lymphangiogenesis in an attempt to improve lymphatic drainage. Certainly lymphatic expansion is observed in portal areas during cirrhosis, the role of such lymphangiogenesis is not clear(188); but this fits with lymphatic expansion as a compensatory mechanism designed to offset the increased lymphatic flow(188) that occurs in liver cirrhosis; alternatively the enhanced lymphatic vasculature may itself be contributing to the increased portal pressures, by physically compressing the portal blood outflow.

We also noted that some of the vessels that expressed podoplanin (fig 3.9) did not morphologically resemble lymphatic vessels, the fact that these portal vessels were lined with CD31<sup>+</sup> cells suggested that they contained vascular endothelium and were



probably portal venules (fig 3.9). We thus provide the first ex vivo demonstration of vascular endothelium anywhere in the body expressing podoplanin. However we also noted that there also appeared to be degree of sub endothelial stromal staining (fig 3.13, 3.14), this fits with recent work that has revealed that podoplanin is expressed by stromal cells in injured murine livers(183), work to elucidate whether similar stromal progenitor cells express podoplanin in the injured human liver is currently underway. As the endothelium that lines in the liver vasculature is fundamentally different to that found elsewhere(15), with there being multiple similarities between lymphatic endothelium and sinusoidal endothelium it is not inconceivable therefore that the response to liver damage an upregulation of podoplanin is observed. Furthermore subsequent *in vitro* experiments from our lab have confirmed that isolated liver endothelial cells express podoplanin(189).

### **3.6.3. Venous thrombosis**

The relevance of the expression of a platelet activating ligand within the vascular space is however less clear. Authors have shown that platelets come into contact with podoplanin at the point where lymph returns to the circulation, and this interaction causes thrombosis maintaining the integrity of the lympho-venular valve(92). An upregulation of vascular podoplanin in chronic liver disease may provide a mechanism for explaining the occurrence of portal venous thrombosis in cirrhotic patients. In support of this I showed that higher levels of podoplanin within cirrhotic livers is linked to greater occurrence of portal venous thrombosis. This data is not statistically significant based on the small numbers of samples and mixed

etiologies of liver disease analyzed. One of the key issues with extensive portal venous thrombosis is that it can render patients untransplantable. Thus we may have missed a key cohort of patients from our analysis, as patients with the most extensive portal venous thrombosis would never undergo transplantation and thus donate their explanted liver for our studies. Obtaining liver biopsies from patients with cirrhosis with or without portal venous thrombosis is a potential solution to this problem. Nonetheless given our current lack of understanding about how portal venous thrombosis occurs(190) and the its potentially devastating complications including worsening portal hypertension, liver failure (acute portal venous thrombosis) and the consequence of portal venous thrombosis on transplantability; podoplanin driven inflammatory venous thrombosis in the cirrhotic liver merits further analysis. A particularly exciting aspect of this work is the fact that blocking CLEC-2/podoplanin does not worsen bleeding risk(94), therefore in patients with oesophageo-gastric varices and portal venous thrombosis, therapy to block CLEC-2 driven platelet activation could block further propagation of the thrombus whilst theoretically not worsening the risk of a variceal bleed.

#### **3.6.4. Regeneration**

We noted an upregulation of podoplanin amongst and around areas of ductular reaction in the cirrhotic livers we studied. This was more pronounced in alcoholic liver disease, PBC and PSC. These were also the diseases that the highest levels of podoplanin mRNA was observed (fig 3.19). The significance of the ductular reaction has not been comprehensively evaluated, but the prevailing concept appears to be

one of driving parenchymal regeneration early on in liver injury, and persistent activation being linked with increasing amounts of hepatocyte senescence in chronic fibrotic disease(191) . Podoplanin may have a role in driving these ductular reactions as it has recently been described as being present on a distinct subset of progenitor stromal cells within chronically damaged murine livers(183). Furthermore recent work reveals that platelet CLEC-2 is important in driving liver regeneration in murine models of hemi-hepatectomy(192).

#### **3.6.5. Correlation with disease activity**

Although the overall score for all livers with chronic liver disease revealed that there was an overall positive correlation between MELD score and podoplanin expression we noted that this was not that case when we did a sub-group analysis with livers only from the autoimmune hepatitis group. These patients had a significantly high MELD score (thus were placed on the transplant list) and we noted that the podoplanin levels seemed to dip with higher MELDs (fig 3.21). This may be due to the fact that the patients with the autoimmune hepatitis were the only cohort of patients on immune modulating drugs (azathioprine and prednisolone), and the immunosuppressive medication may have had a role in suppressing hepatic podoplanin production. This is particularly the case with prednisolone which is known to suppress macrophage function(193), one of the key cells that we found to upregulate podoplanin. The fact that all the livers we analyzed were end stage cirrhotic livers makes drawing meaningful conclusions about how podoplanin levels

vary with severity of disease, particularly early on in the disease and what effect immunosuppressant medication may have difficult, further studies are warranted.

Since podoplanin levels go up with severity of liver disease, it is interesting to speculate whether podoplanin has diagnostic utility as a biomarker of severity of fibrosis, or even as a predictor of tendency to develop portal venous thrombosis. Our work focused on intrahepatic podoplanin expression but researchers have also found soluble versions of this molecule detectable in human serum in the context of certain cancers(194) correlating this with the development of portal venous thrombosis, extent of hepatic fibrosis and MELD scores will be the focus of our future studies.

Type of disease	Pattern of CLEC-2 expression	Pattern of podoplanin expression/upregulation
Normal non-diseased human liver	Not expressed	Only in portal areas on lymphatic vessels
Paracetamol induced liver failure	NA	On Kupffer cells
Primary biliary cholangitis	NA	Periportal expression on portal venules, marked upregulation in areas of a peri-biliary areas particularly in areas of biliary reaction.
Primary sclerosing cholangitis	CLEC-2 expressing platelets within bile ducts	Periportal upregulation on macrophages, portal venules and stroma.
Alcoholic liver disease	Within regenerating bile ductules	On portal venules, macrophages and on stroma in areas of ductular reaction.
Non-alcoholic fatty liver disease	CLEC-2 expressing platelets within regenerating bile ductules and attached to cells in the inflammatory infiltrate.	Periportal expression on lymphatics and portal venules.
Autoimmune hepatitis	NA	Portal podoplanin expression on portal veins and stroma.

**Table 3.2 Pattern of podoplanin and CLEC-2 expression in different forms of human liver disease**



## **4. Platelet activation drives liver injury during carbon tetrachloride and paracetamol induced liver injury**

### **4.1. Models of acute toxic liver damage**

Carbon tetrachloride (CCl<sub>4</sub>) induced hepatic necroinflammation represents a widely used and easily reproducible model of murine liver injury. This organic has been used as a grain fumigant, solvent for oils, in the manufacture of chlorofluorocarbons and as a dry-cleaning agent in the past. Owing however to its profound toxicity, its use became prohibited in the US in the 1970s(195,196) .

To induce hepatic damage CCl<sub>4</sub> is normally administered intraperitoneally dissolved in mineral oil(160) . Within the liver CCl<sub>4</sub> is metabolized by the cytochrome P450 isozymes of the endoplasmic reticulum (ER) system to trichloromethyl free radicals. These then react with molecular oxygen to form highly toxic trichloromethyl peroxy radicals(195). The specific isoform responsible for majority of CCl<sub>4</sub> metabolism is CYP2E1; mice deficient in this enzyme are therefore resistant to the hepatotoxic effects of CCl<sub>4</sub> (195) . After being produced these highly reactive radicals react with the polyunsaturated fatty acids(196) comprising the phospholipids present within cell and cell organelle membranes. The resultant effect on the permeability of the cell plasma membrane, ER membrane and mitochondrial membrane causes a marked dysregulation of cellular calcium homeostasis and eventually cell death(197) . CCl<sub>4</sub>

also causes hypomethylation of cellular components including RNA and phospholipids thereby resulting in impairment of protein synthesis and lipoprotein production respectively and this is thought to also be contributory to CCl<sub>4</sub> mediated cellular injury(197). CCl<sub>4</sub> bioactivation thus sets in place an essentially self-propagating cycle of lipid peroxidation, which eventually results in massive amounts of necrotic hepatocyte death(198) . The need for bioactivation of CCl<sub>4</sub> to generate its reactive metabolites dictates the histological pattern of injury induced by CCl<sub>4</sub>. The majority of liver injury is centrilobular as the zone 3 (centrilobular) hepatocytes have the most abundant CYP450 expression.

Paracetamol overdose is also used to model acute hepatitis in rodent models. This has the added advantage of being pathophysiologically very similar to human paracetamol-induced liver damage, and has thus already yielded clinically relevant treatments such as N-acetylcysteine (NAC)(18) . The majority of paracetamol (almost 90%) is metabolized in the liver by glucuronidation and sulfation and then excreted in the urine(199), this pathway results in safe metabolism and clearance of paracetamol and therefore no liver damage. The remaining 10% is metabolized within hepatocytes by isozymes of the cytochrome P450 system-mainly CYP2E1 (hence paralleling CCl<sub>4</sub> metabolism), to N-acetyl-p-benzoquinone imine (NAPQI)(200). Liver glutathione (GSH) reduces NAPQI into a harmless form, which is then excreted in the bile(199). In situations of excessive paracetamol consumption, the reductive capacity of GSH is overwhelmed and toxic NAPQI starts to build up. Excess NAPQI binds to the sulfhydryl groups within proteins resulting in the formation of toxic protein



adducts(18). The formation of these adducts within mitochondrial proteins is thought to be critical to APAP hepatotoxicity(201). Mitochondrial NAPQI-protein adducts disrupt mitochondrial electron transport triggering peroxynitrite formation within the mitochondria(18). The resultant oxidant stress results in the membrane permeability transition (MPT) pore opening and ultimately the collapse of mitochondrial membrane potential(18). As the mitochondria swell, collapse and eventually disintegrate they release inter-membrane proteins including endonuclease G and apoptosis inducing factor (AIF)(201). Both of these molecules translocate to nucleus causing rapid and extensive nuclear fragmentation(202). It is this combination of nuclear fragmentation and mitochondrial collapse that results in the massive pericentral hepatocellular necrosis that is characteristic of paracetamol overdose.

#### **4.2. The sterile inflammatory response of toxic liver injury**

After both APAP and CCl<sub>4</sub> induced liver damage a striking increase in the amount of infiltrating hepatic leukocytes indicating a pronounced inflammatory response is observed(160,203). The type of inflammation that both paracetamol and CCl<sub>4</sub> elicit is known as sterile liver inflammation. Sterile inflammation (SI) occurs in the absence of pathogens in response to a wide variety of stimuli including toxic agents such as CCl<sub>4</sub>, acetaminophen (APAP) and thioacetamide (TAA) or other tissue stress inducing injuries such as ischaemia-reperfusion and crush injuries(47,204). Liver SI is a key component of human liver injuries including non-alcoholic steatohepatitis (NASH), alcoholic steatohepatitis and drug induced liver injury(47). The unifying molecular characteristic of SI is the expression of endogenous damage associated

motif patterns (DAMPs) on tissue damage(33), over 20 DAMPs have thus far been identified(47). DAMPs are molecules that are released from dying cells and serve as ligands for toll-like receptors (TLRs) on macrophages and other cell types. After APAP or CCl<sub>4</sub> induced necrotic hepatocyte damage, Kupffer cells (KCs), dendritic cells and possibly circulating monocyte derived macrophages recognize DAMPs expressed by the damaged liver tissue(33). This recognition is via pattern recognizing receptors (PRRs) such as toll like receptors (TLRs) expressed on these cells and represents a crucial step, linking toxic necrotic cell death to immune system activation and recruitment; the beginning of the sterile inflammatory response(200). DAMP recognizing cells thus become activated and produce the cytokine milieu that is characteristic of acute liver injury.

Liver resident macrophages are activated within 1-2 hours of an APAP overdose in mice(34). Initially numbers of these cells seems to go down probably due to a direct cytotoxic effect of CCl<sub>4</sub>, but then overall macrophage numbers within the liver actually increase due to CCL2 driven recruitment from the blood(33). On recognizing DAMPs expressed by necrotic hepatocytes, KCs and infiltrating macrophages start producing inflammatory cytokines including TNF $\alpha$ , IL-1 $\beta$  and IL6(33). It is clear that both TNF $\alpha$  and hepatic macrophages are important in dictating the outcome from toxic liver damage(205), but a comprehensive role for either is yet to be defined. Depleting Kupffer cells preferentially using gadolinium chloride or all populations that contribute to hepatic macrophages including monocyte derived macrophages and circulating monocytes using clodronate result in varying phenotypes after APAP challenge, with

the former ameliorating liver injury and the latter aggravating it(33). As already mentioned in the introduction, platelets influence the macrophage contribution to liver injury or sterile inflammation at multiple levels linked to monocyte recruitment from the blood(15) and phenotypic modulation(53).

Another critical cell that helps dictate the outcome from acute liver damage is the neutrophil(48). Inflammation including both infective and sterile results in trafficking of neutrophils to the damaged areas within the liver(47). The central role of these granulocytic cells in combating fungal and bacterial infections is underlined by the profound susceptibility neutropaenic patients have to invasive infections(206) . Neutrophils accumulate within the liver vasculature in response to a number of cytokines produced by cells within the inflamed liver including but not exclusively  $TNF-\alpha$ ,  $IL-1\beta$ , platelet activating factor (PAF) and a number of CXC chemokines(207). Sequestration of neutrophils within the liver vasculature is not enough for the cells to function as effectors; extravasation to the hepatic parenchyma is a prerequisite(207). Once through the endothelium, danger signals guide granulocytic infiltration to the area of maximal liver damage via inflammasome activation as detailed above and a combination of CXCL chemokine gradients and adhesion (ICAM-1 and VCAM-1) molecule upregulation(208). Multiple models of human and rodent live injury demonstrate neutrophil accumulation within the liver parenchyma, unsurprisingly neutrophil cytotoxicity has thus been extensively studied in the context of liver damage and blocking hepatic neutrophil homing, sequestration and extravasation have all been identified as potential therapeutic strategies(206).

Recent evidence however suggests that neutrophils may not always be deleterious during liver injury and in fact have been shown to (as already mentioned in the introduction) have restorative roles particularly as part of the sterile inflammatory response(50).

An increasing body of recent literature recognizes that platelets play a central but paradoxical role in liver injury, being able to both drive damage and aid resolution(53). Platelets interact with the key protagonists of the sterile inflammatory response including neutrophils and macrophages(52) and can enhance hepatic leucocyte recruitment into the liver across the sinusoidal endothelium(15). However, little is known about the molecular basis of platelet activation during acute liver failure and specifically whether manipulating platelet function could influence the sterile inflammatory response to toxic liver injury. As already discussed platelet activation occurs through multiple pathways including ligation of platelet-expressed CLEC-2 by its ligand podoplanin(70) . Because inflammatory macrophages upregulate podoplanin(90) and have an important role in driving the sterile inflammatory response to toxic liver injury(33), we wanted to investigate whether CLEC-2 driven platelet activation by inflammatory macrophages had a role in acute toxic liver injury. The outcome from toxic hepatic insults such as CCl<sub>4</sub> intoxication is dictated by the SI response, which may contribute to and worsen the liver damage, or be reparative and drive resolution(47). Manipulating the sterile inflammatory response to a toxic liver insult such as paracetamol overdose induced liver injury in humans may allow

for the development of treatments in human drug induced acute liver failure (ALF); platelets may provide exactly such as an avenue.

### **4.3. Aims for this chapter**

The focus of this chapter is to elucidate how platelets may interact with the cells of the innate immune system that are of key importance in sterile inflammation, and to investigate whether blocking platelet activation may influence recruitment of these effector cells to the damaged liver. Importantly I also wanted to, ascertain whether this may influence the outcome from a toxic liver injury. My ultimate goal was to replicate a clinically relevant problem, such a paracetamol-induced acute liver failure and investigate the therapeutic potential of blocking platelet activation in such a context .

Thus the specific aims for this chapter were:

- 1) To assess the nature of the sterile inflammatory response and amount of liver damage intraperitoneally administered CCl<sub>4</sub> or APAP elicit in C57Bl6 wild type mice.
- 2) To abrogate CLEC-2 mediated platelet activation during CCl<sub>4</sub> and APAP -induced liver damage, and assess whether platelet activation influences the outcome from these injuries.
- 3) To ascertain how platelet function influences the nature of the sterile inflammatory response after toxic liver injury and whether this abrogates or worsens liver damage.

#### **4.4. Administration of intraperitoneal CCl<sub>4</sub> or paracetamol results in centrizonal hepatic necroinflammation**

Wild type C57Bl6 Mice were injected with a single dose of intraperitoneal CCl<sub>4</sub> as described above, and then sacrificed at serial time points. We detected liver damage as measured by histological necrosis and mononuclear cell infiltration as early as 24 hours after a single dose of CCl<sub>4</sub> (figure 4.1). This was accompanied by raised serum transaminases (fig 4.1), which continued to increase until 48 hours after administration, but started to reduce thereafter. The pattern of damage observed was dominantly centrizonal, or around the central vein (panel A, fig 4.1). Importantly mice administered the mineral oil carrier alone did not demonstrate injury (panel B, fig 4.1)

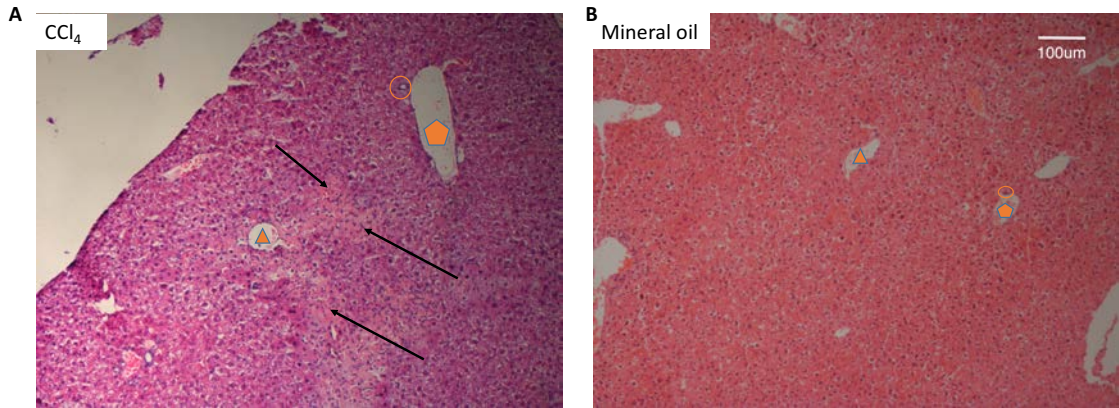


**Figure 4.1 Murine livers develop centrilobular necrosis after IP CCl<sub>4</sub> injection:**

WT mice were injected with CCl<sub>4</sub> (dose) or mineral oil alone as indicated, and sacrificed after 24 hours. The livers were removed and paraffin embedded and representative images from stained with H/E are presented above. A) Original magnification 10x, n>10 animals per group. Centrilobular (around the central vein) necrosis is highlighted with arrows, portal vein-pentagon, bile duct circle.

The peak serum ALT values at 48 hours after CCl<sub>4</sub> injection, this correlates with the amount of hepatocellular necrosis observed histologically (figure 4.2). After 48 hours, resolution of injury began and this correlated with histological improvement of the necrotic injury, reduction in the visible amount of infiltrating mononuclear cells (arrows, fig 4.2) and reduction in serum ALT(fig 4.2).

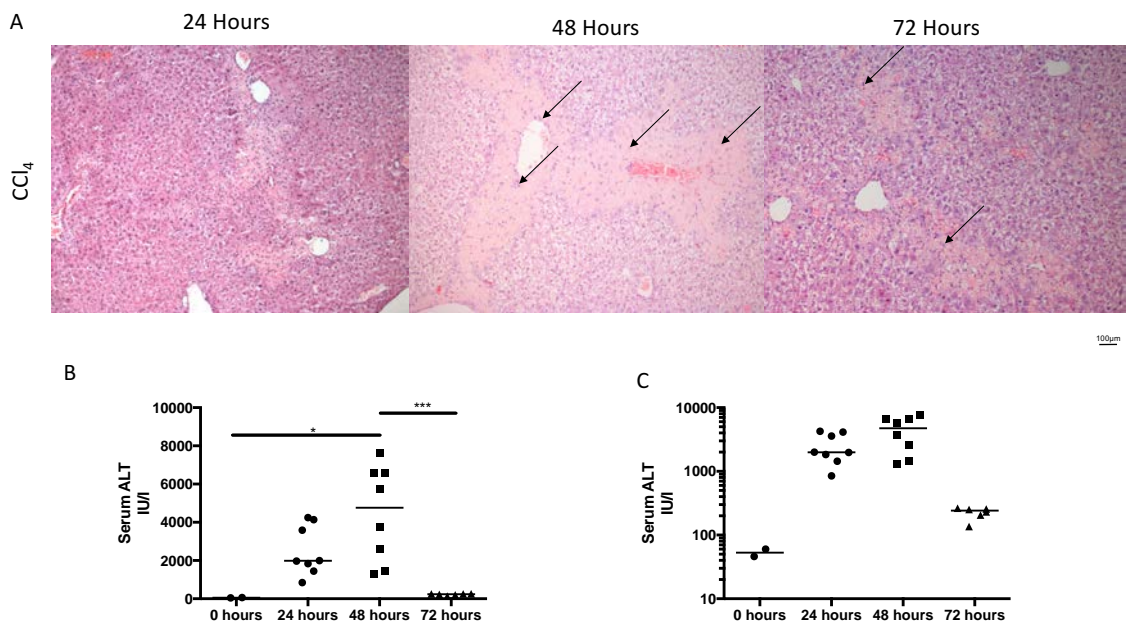


**Figure 4.2 Hepatocellular injury peaks at 48 hours post intraperitoneal CCl<sub>4</sub> injection:**

WT mice were injected with CCl<sub>4</sub> and sacrificed at 24, 48 or 72 hours. Representative images from H/E stained sections are shown for each timepoint (10x original magnification, A). Serum was harvested via cardiac puncture for ALT analysis (B) and each dot represents one animal. C) same data as B, X-axis changed to log<sub>10</sub> to illustrate the difference between serum ALT levels at 0 hrs. and 72 hrs. Each dot is an individual mouse, median shown. (ANOVA test indicated differences between groups, \*P < 0.05, \*\*P < 0.01, \*\*\*P < 0.001)



IP administration of paracetamol elicited more extensive liver damage and this occurred at earlier time points compared to CCl<sub>4</sub> (fig 4.3). Serum evidence of hepatic necroinflammation as gauged by a rise in ALT was detected as early as 6 hours (panel A, B fig 4.3) after the paracetamol was administered and this correlated with clinical parameters, including the mice exhibiting an antalgic gait, reduced grooming and reduced feeding. This clinical deterioration was however transient and mice began to show signs of clinical improvement at 24 hours. In a similar pattern to CCl<sub>4</sub>, this sub-lethal dose of paracetamol resulted in a peak of necrosis as indicated by H/E staining at 24 hours and then resolution of injury thereafter (fig 4.3).

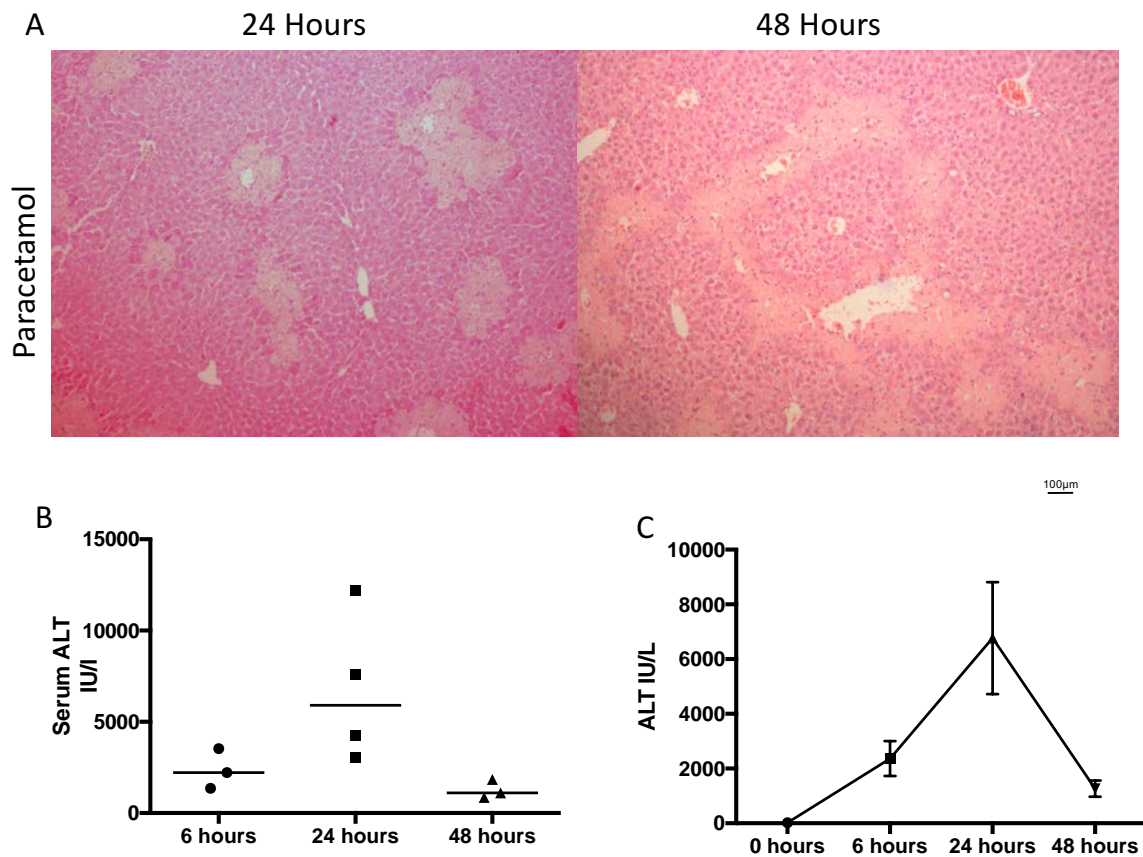


**Figure 4.3 Hepatocellular injury peaks at 24 hours post intraperitoneal APAP injection:**

WT mice were injected with APAP and sacrificed at 6, 24 or 48 hours. Serum was harvested via cardiac puncture for ALT analysis and representative sections stained with H/E are presented above. A) 10x magnification representative pictures for each time point are shown. H/E stain, paraffin section. B) Serum ALT values from WT mice taken at each point are shown, each dot represents one animal. C) Timeline for paracetamol induced liver injury and recovery.

H/E stain, paraffin section. B) Serum ALT values from WT mice taken at each point are shown, each dot represents one animal. C) Timeline for paracetamol induced liver injury and recovery.

## 4.5. Podoplanin is upregulated in murine livers after toxic liver injury

We had already established that in acute and chronic human disease podoplanin expression is upregulated and that platelets sequester to this podoplanin thus providing a potential mechanism for platelet activation via CLEC-2 in liver disease (Chapter 3). We next sought to determine if this also occurred in murine liver injury. We found that in uninjured or non-inflamed livers, podoplanin expression in mouse livers was similar to human liver disease i.e. fairly limited. In non-injured wild type murine livers podoplanin expression was limited to small periportal vessels that were morphologically and anatomically consistent with lymphatic vessels(166)(figure 4.4).

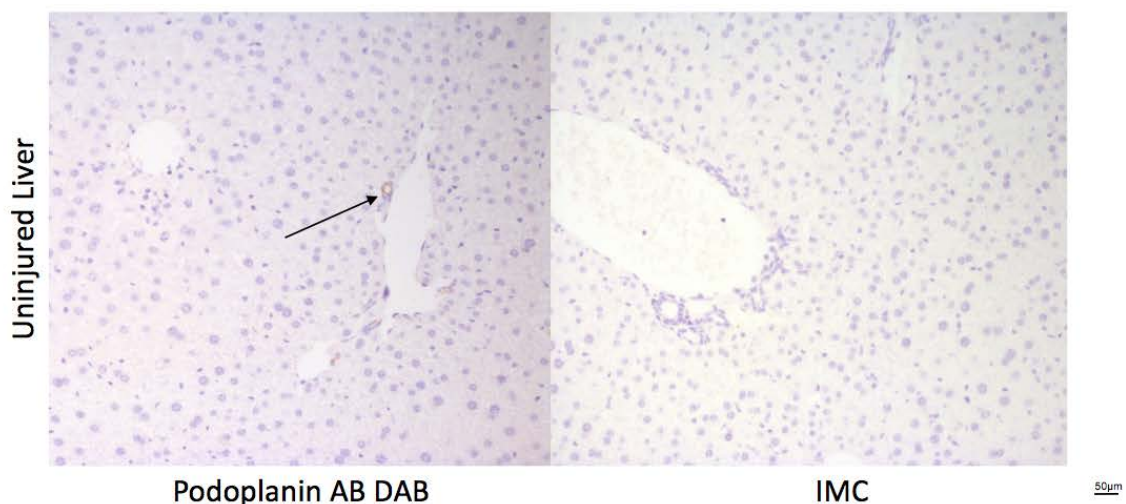


**Figure 4.4 Podoplanin expression within uninjured murine liver is restricted to lymphatic vessels:**

Representative images from uninjured WT mice were stained with podoplanin antibody and visualized using DAB stain (brown). Representative samples shown at 20x original magnification. Arrow

highlights lymphatic vessel, IMC stain was negative (right). Samples are representative of at least 4 livers

After both APAP and CCl<sub>4</sub> induced hepatic injury, we noted an increase in the amount of podoplanin expressed within murine livers (figure 4.5). This upregulation was not seen in control mice that were treated with mineral oil or PBS (figure 4.5). Microscopic analysis suggested that podoplanin was upregulated on a sub-population of mononuclear cells within the hepatic infiltrate and also upon vessels (figure 4.5). Further immunohistochemical analyses confirmed that podoplanin expression co-localized with the F4/80 expressing cells (fig 4.5, blue arrows). Such upregulation of podoplanin was not observed in uninjured control mice.

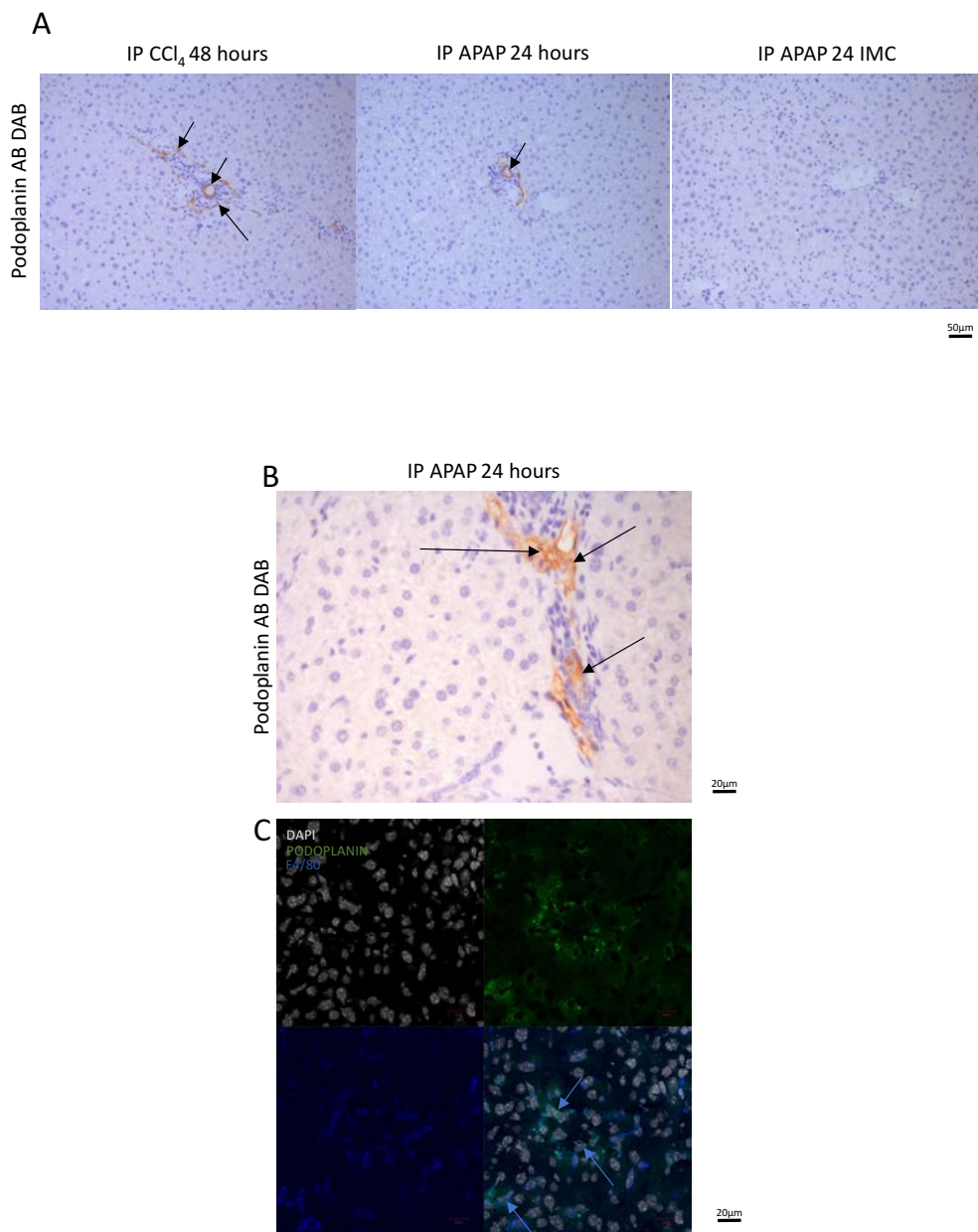


**Figure 4.5 Podoplanin is upregulated on hepatic macrophages after hepatic injury in mice:**

Representative images from acutely injured murine livers taken at time point of peak hepatic injury i.e. 24 hours after APAP injection or 48 hours after CCl<sub>4</sub> injection are shown A) WT Murine liver sections stained with podoplanin DAB, and at 20X original magnification demonstrating podoplanin upregulation (brown, arrows) on cells and vessels (IMC was negative). B) Higher magnification 40x image from a representative APAP sample demonstrating staining of cells within the hepatic inflammatory infiltrate (brown, arrows) C) Confocal microscopy (40x original magnification) demonstrating colocalisation of macrophages (F4/80-green) and podoplanin (blue). Macrophages co-expressing podoplanin are sea-blue (arrows). Isotype stains negative (not shown). Images representative of at least 4 mice.

To confirm that it was the macrophages that specifically upregulated podoplanin during hepatic injury we used Blomhoff's method of selective adherence (164) to isolate a pure population of hepatic macrophages from non-injured wild type livers (figure 4.6). Macrophages could be distinguished amongst cellular debris by F4/80 expression (figure 4.6, panel A, B). These cells were confirmed as being macrophages by F4/80 expression (figure 4.6). Paralleling our *in vivo* findings, very little basal expression of podoplanin was found on these cells in the unstimulated state. However, on stimulating these isolated macrophages with lipopolysaccharide (LPS) (100ng/ml in DMEM) we observed a change in morphology of the macrophages and an upregulation of podoplanin expression.

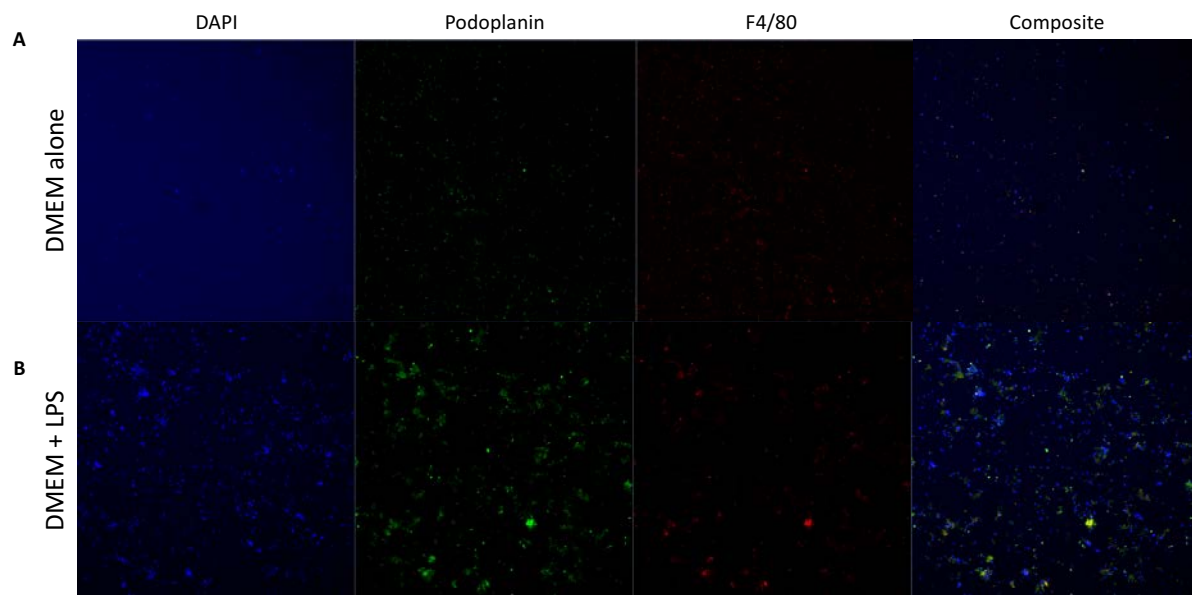


**Figure 4.6 Isolated macrophages upregulate podoplanin expression *in vitro* on stimulation with lipopolysaccharide:**

Macrophages were isolated from WT mouse livers and cultured in DMEM alone or DMEM containing 100ng/ml LPS for 6 hours. Confocal microscopy images showing F4/80<sup>+</sup> cells (red), and podoplanin (green) on isolated macrophages under basal (A) or LPS-stimulated (B) conditions. DAPI was used as a nuclear counterstain (Blue). Both A and B from the same mouse.

#### 4.6. Platelet and macrophage distribution during acute liver damage

After noting enhanced podoplanin expression on macrophages within the injured liver we next sought to define the distribution and numbers of hepatic macrophages after liver injury. Histochemical analysis, in WT mice suggested that the number of macrophages appeared to increase after liver injury and that these cells had a predominantly sinusoidal distribution(fig 4.7).

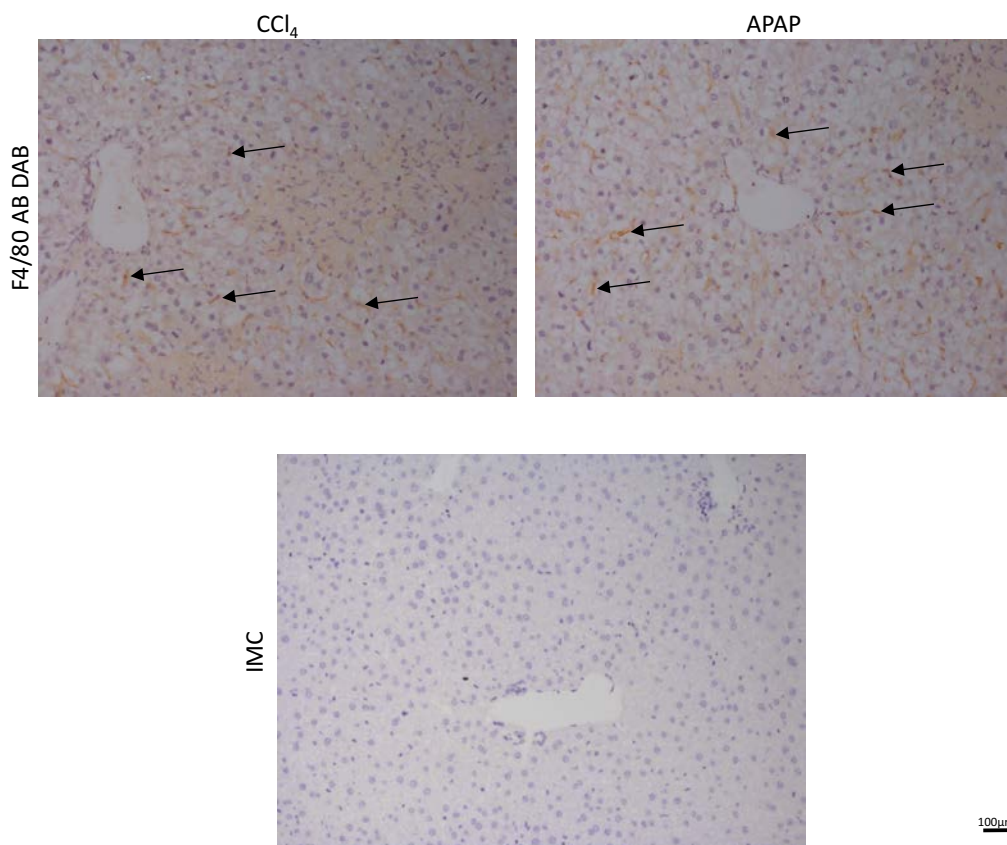


**Figure 4.7 Macrophages are distributed in a sinusoidal distribution after toxic liver injury:**

Representative images from acutely injured murine livers taken at time point of peak hepatic injury i.e. 24 hours after APAP injection or 48 hours after CCl<sub>4</sub> injection are shown. WT Murine liver sections stained with F4/80 DAB, and at 20X original magnification demonstrating podoplanin upregulation (brown, arrows) on cells and vessels (IMC was negative).



We next investigated whether platelets sequestered to the injured liver. Figure 4.8 reveals that after both APAP and CCl<sub>4</sub> injury CD41<sup>+</sup> platelets accumulated within the hepatic sinusoids and within the hepatic inflammatory cell infiltrate. Higher magnification pictures (fig 4.8) revealed that platelets actually sequestered to mononuclear cells rather than being localized amongst the liver parenchymal cells or upon sinusoidal endothelium. We next assessed whether these inflammatory cells were macrophages. Confocal microscopy confirmed that platelets (CD41<sup>+</sup>) colocalised with podoplanin expressing macrophages (F4/80<sup>+</sup>) during acute toxic liver injury (fig 4.8).

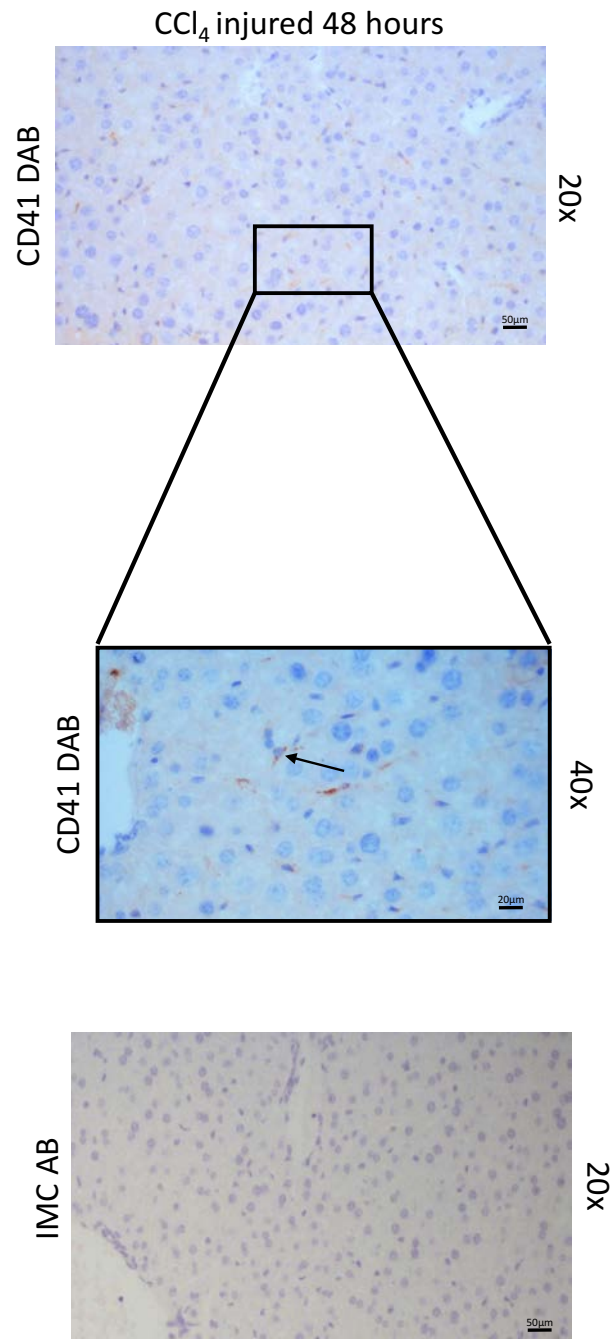


**Figure 4.8 Platelets are found sequestered within the acutely injured liver:**

WT mice were injected with CCl<sub>4</sub> and sacrificed at 48 hours. Liver paraffin sections stained with a platelet (CD41) DAB stain (brown, arrows), with a haematoxylin nuclear counterstain. Top picture at 20x magnification demonstrates platelet sequestration within hepatic sinusoids. Higher magnification (40x) reveals that platelet sequestration is also to mononuclear cells distinct to hepatocytes or sinusoidal endothelium (arrow). Isotype matched control (bottom) were negative.

We have already established that macrophages upregulate podoplanin during acute liver injury (fig 4.5, 4.6). As platelets appeared to sequester to mononuclear inflammatory cells within the damaged liver; we next assessed whether these inflammatory cells were macrophages. Confocal microscopy confirmed that platelets (CD41<sup>+</sup>) sequester to podoplanin expressing macrophages (F4/80) during acute toxic liver injury (fig 4.9-arrows)

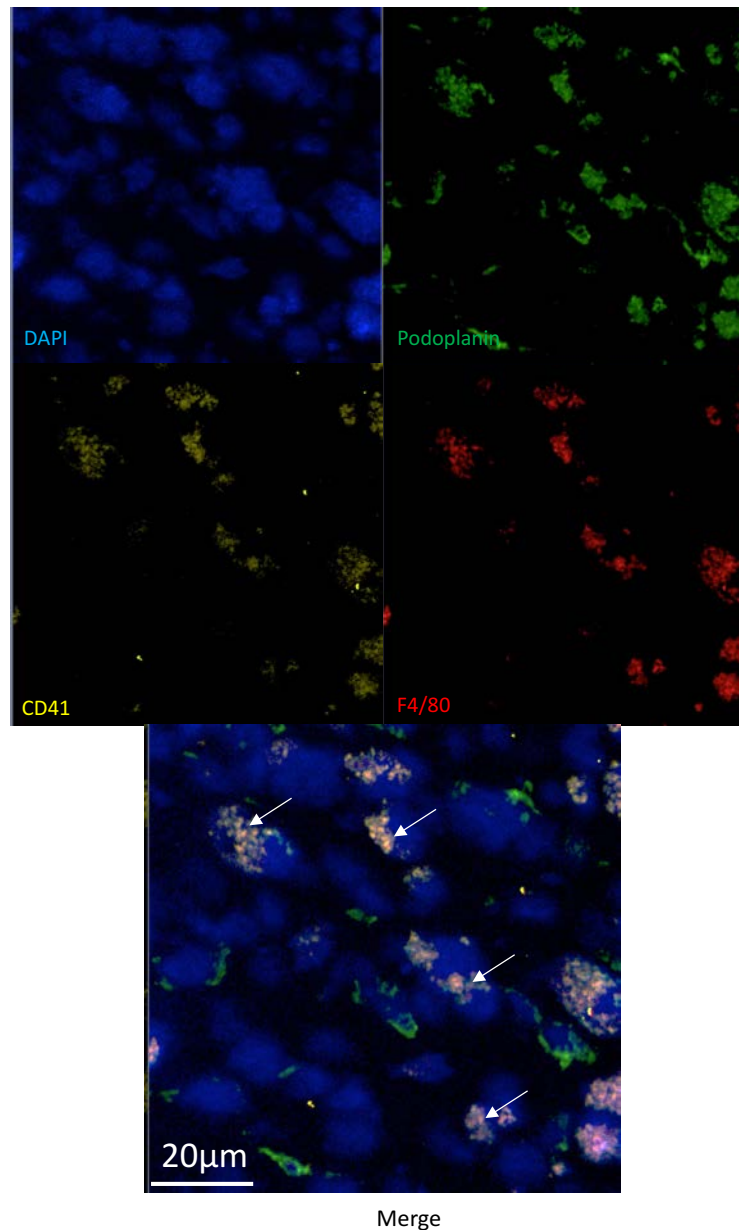


**Figure 4.9 Platelets sequester to podoplanin expressing macrophages after acute liver injury:**

APAP injured mouse liver, frozen section(taken at peak time of injury-24 hours after injection) demonstrating platelet (CD41-yellow) sequestration to podoplanin (green) expressing macrophages (F4/80-red).(63x frozen sections) (arrows). Image representative of at least 5 mice.

#### **4.7. Mice with CLEC-2 deficient platelets exhibit enhanced healing after CCl<sub>4</sub> and paracetamol injury**

After establishing the nature and time course of the hepatic necroinflammatory response to both IP CCl<sub>4</sub> and APAP in WT animals, and critically that platelets sequestered to podoplanin expressing macrophages in the injured liver areas in both models, we next sought to investigate whether CLEC-2 dependent platelet activation had a role to play in driving this injury. We thus used mice that bore a conditional deletion of the CLEC1b gene in cells expressing PF4 (PF4Cre*CLEC1b*<sup>fl/fl</sup>) i.e. the megakaryocytic lineage in our CCl<sub>4</sub> and paracetamol-induced injury models. At the earliest time points studied, after both APAP (6 hours) and CCl<sub>4</sub> (24 hours) no difference in liver damage as gauged by serum ALT rise and liver histology was evident (fig 4.10). Hence all mice showed elevation of ALT and classic pericentral necrosis.

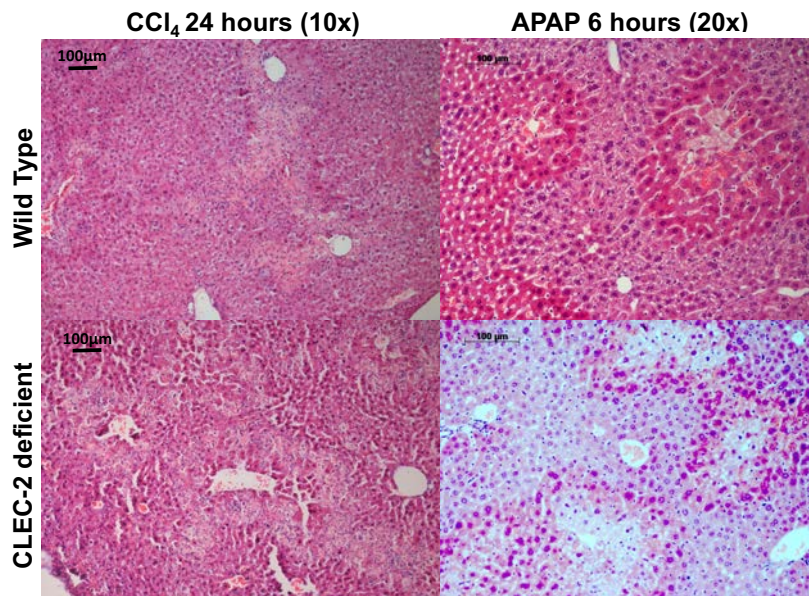
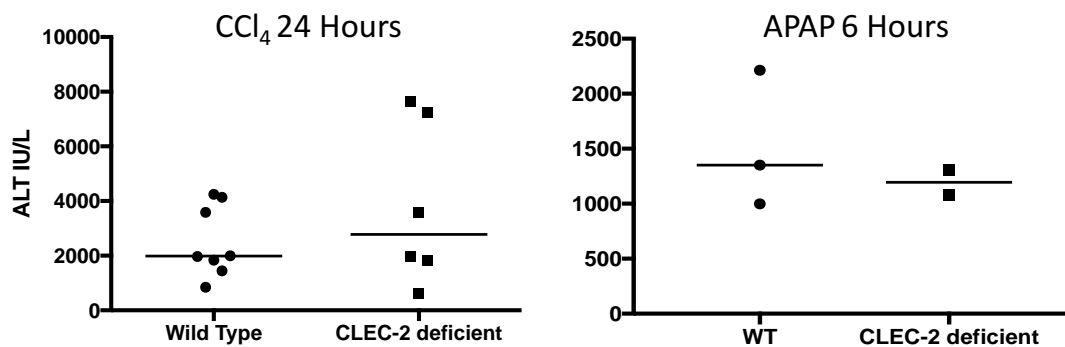


**Figure 4.10 Injury at early time points is comparable between WT and CLEC-2 deficient mice after either CCl<sub>4</sub> or APAP induced liver injury:**

WT or CLEC-2 deficient mice were injected with CCl<sub>4</sub> and sacrificed at 24 hours or APAP and sacrificed at 6 hrs. Serum was harvested and sent for ALT analysis, livers were removed, embedded in paraffin and sections prepared. Serum ALT from both groups is presented in the top graphs (CCl<sub>4</sub>-left, APAP-right). Each dot is an individual mouse, median shown. H/E stained paraffin sections are shown below. H/E stain 10x or 20x. (Mann-Whitney test to gauge significance- \*P < 0.05, \*\*P < 0.01, \*\*\*P < 0.001).

However when we compared WT murine livers with livers from CLEC-2 -deficient mice 48 and 72 hours after IP CCl<sub>4</sub> administration we noted far less hepatic injury in the livers from the PF4Cre*CLEC1b*<sup>f/f</sup> mice compared to WT (figure 4.11). The CLEC-2 deficient mice had much smaller areas of hepatic necrosis and lower serum ALT levels at both 48 and 72 hours compared to age and litter matched WT control mice (figure 4.11).

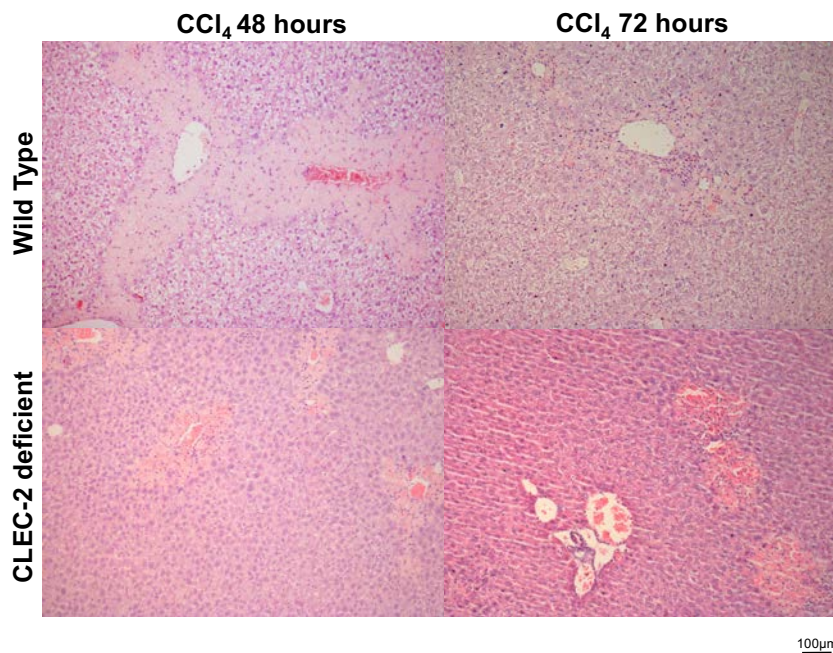
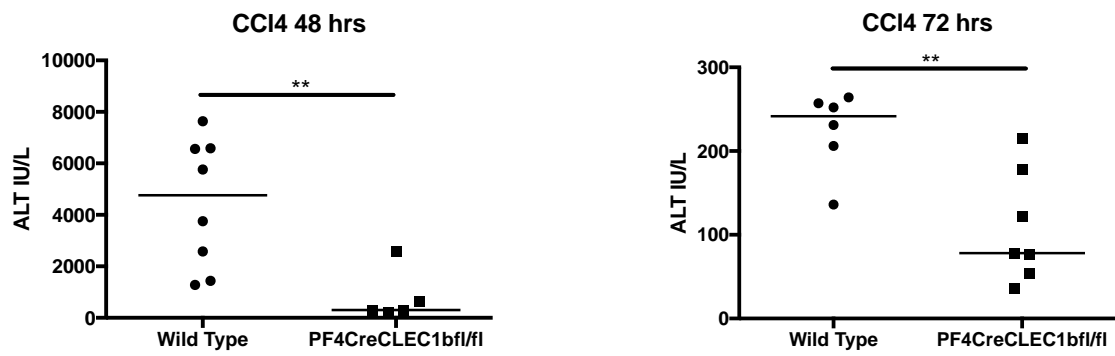


**Figure 4.11 CLEC-2 deficient animals develop less hepatic injury after CCl<sub>4</sub> injection:**

WT or CLEC-2 deficient mice were injected with CCl<sub>4</sub> and sacrificed at 48 or 72 hours. Serum ALT level (top of figure) and hepatic necrosis observed (bottom of figure. H and E stain, paraffin sections, 10x magnification). Each dot represents an individual mouse, median shown. (Mann Whitney test to gauge significance \*P < 0.05, \*\*P < 0.01, \*\*\*P < 0.001).



This phenotype was reproduced when we used paracetamol injury. When we analyzed the CLEC-2-deficient mice at 24 and 48 hours after treatment, we noted far less damage in the PF4Cre*CLEC1b<sup>fl/fl</sup>* mice when compared to age and litter matched controls (figure 4.12). Thus a similar pattern of liver injury and healing was noted after both APAP and CCl<sub>4</sub> injection, with the CLEC-2 deficient animals exhibiting enhanced healing after both toxic insults (figures 4.11). The magnitude and temporal pattern of liver damage was however different when comparing the two injury models, as liver injury occurred sooner after APAP injection and the severity of injury (as gauged by ALT) was greater in both WT and PF4Cre*CLEC1b<sup>fl/fl</sup>* mice after APAP compared to CCl<sub>4</sub>. Another notable difference was that no observable clinical deterioration in the physical health of the mice (both WT and PF4Cre*CLEC1b<sup>fl/fl</sup>* mice) aside from a mild and transient antalgic gait was noted after CCl<sub>4</sub> administration. Mice treated with IP APAP (both WT and PF4Cre*CLEC1b<sup>fl/fl</sup>*) in contrast exhibited more significant behavioral signs manifest as reduced feeding, reduced grooming, the development of a greasy coat and an antalgic gait as soon as 4 hours after the injection. This observed clinical deterioration was transient with the mice improving spontaneously by 24 hours.

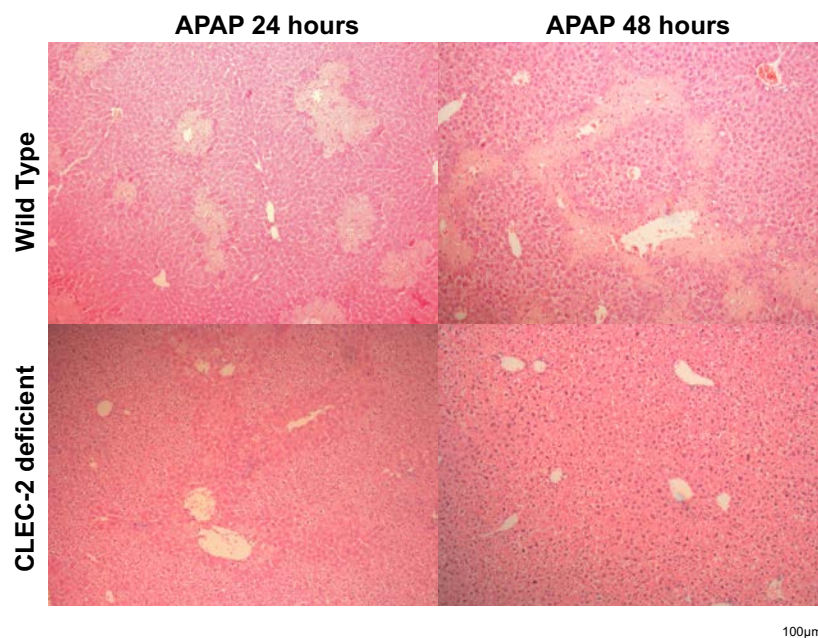
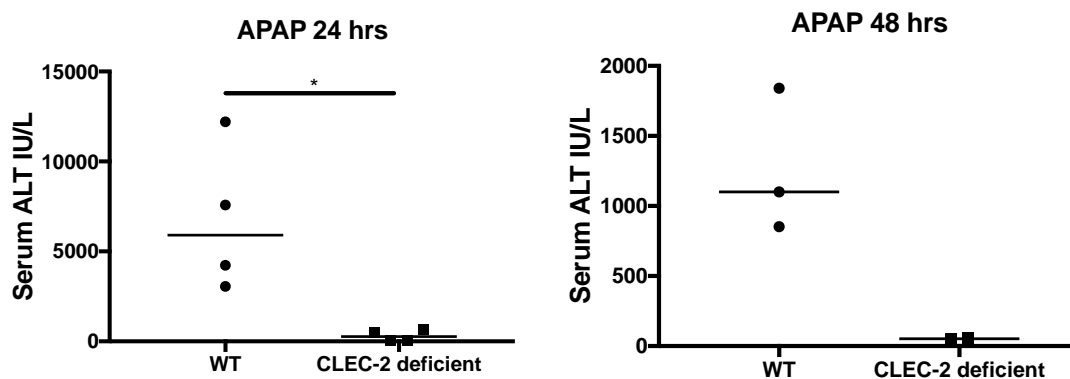


**Figure 4.12 CLEC-2 deficient mice exhibit enhanced recovery after APAP injection:**

WT or CLEC-2 deficient mice were injected with APAP and sacrificed at 24 or 48 hours. Serum ALT level (top of figure) and representative histology (bottom of figure. H and E stain, paraffin sections, 10x magnification). Each dot represents one animal. Median shown. (Mann Whitney test to gauge significance \* $P < 0.05$ , \*\* $P < 0.01$ , \*\*\* $P < 0.001$ ).

As macrophages were a source of podoplanin in the injured liver and thus were potentially providing an activation stimulus for CLEC-2 in the injured liver, we next examined livers from both WT and CLEC-2 deficient (PF4Cre*CLEC1b*<sup>fl/fl</sup>) mice to see if there was a difference in pattern of macrophage distribution after injury, which could help potentially explain the enhanced liver healing observed in the CLEC-2 deficient mice.

We noted that after a toxic injury there were an overall greater number of macrophages in both WT and CLEC-2 deficient animals compared to uninjured controls (fig 4.13) (on initial histological analysis alone). In the WT mice the macrophages were present primarily within the sinusoids (Fig 4.13), in the CLEC-2 deficient mice however a large number of greater macrophages were (in addition to the sinusoids) present around the central vein (centrizonal distribution-this is where both APAP and CCl<sub>4</sub> caused maximum necrotic damage, fig 4.13).

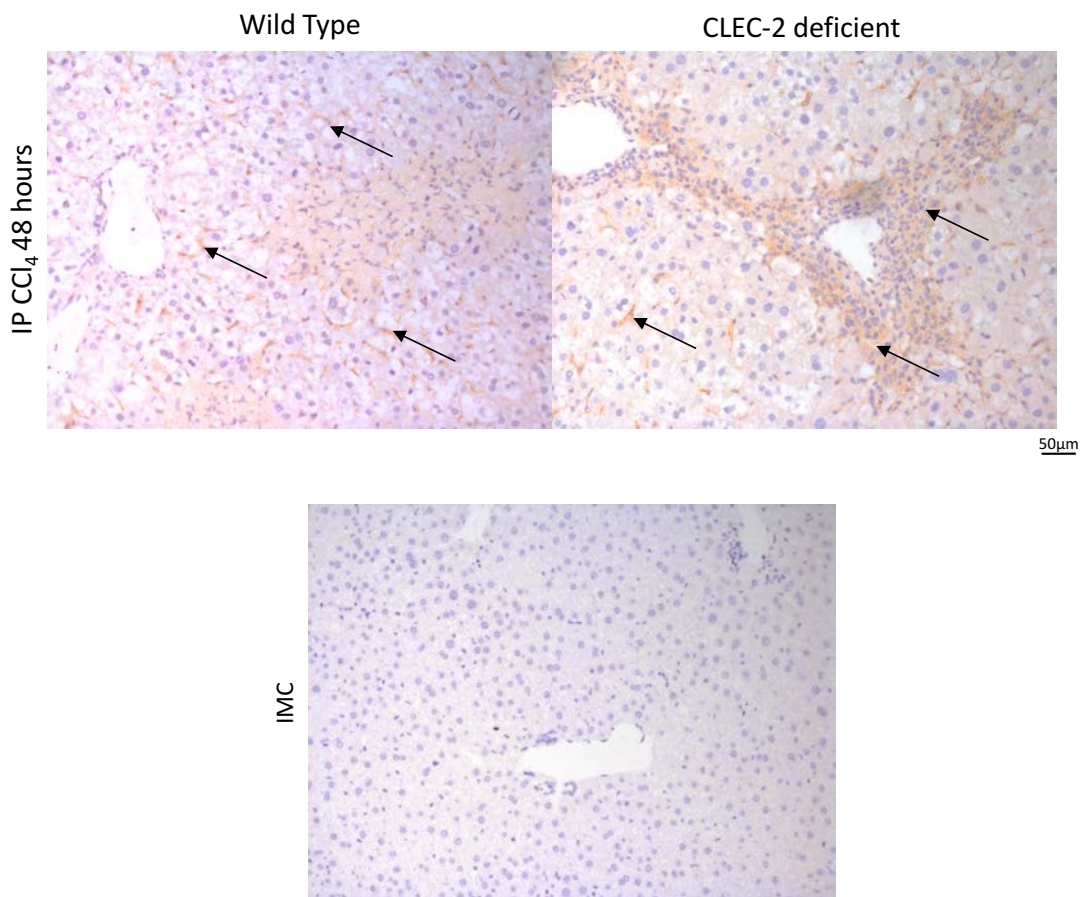


**Figure 4.13 After toxic injury macrophages sequester to the injured area in CLEC-2 deficient mice:**

WT or CLEC-2 deficient mice were injected with CCl<sub>4</sub> and sacrificed at 48 hours. Representative paraffin sections stained with a macrophage (F4/80) DAB stain (arrows), and visualized at 20X magnification with a haematoxylin counterstain. IMC staining was negative.

Next, when we studied platelet sequestration within the same injured livers we noted that there was remarkably more intrahepatic platelet sequestration within the livers of CLEC-2 deficient mice (PF4Cre*CLEC1b*<sup>fl/fl</sup>) compared to WT mice after toxic liver

injury (figure 4.14). The CLEC-2 deficient animals had greater platelet sequestration (arrows) along the hepatic sinusoids and also within the centrilobular inflammatory infiltrate (fig 4.14). This spatially correlated with the macrophage (F4/80) distribution in the CLEC-2 deficient mice at the same time points.

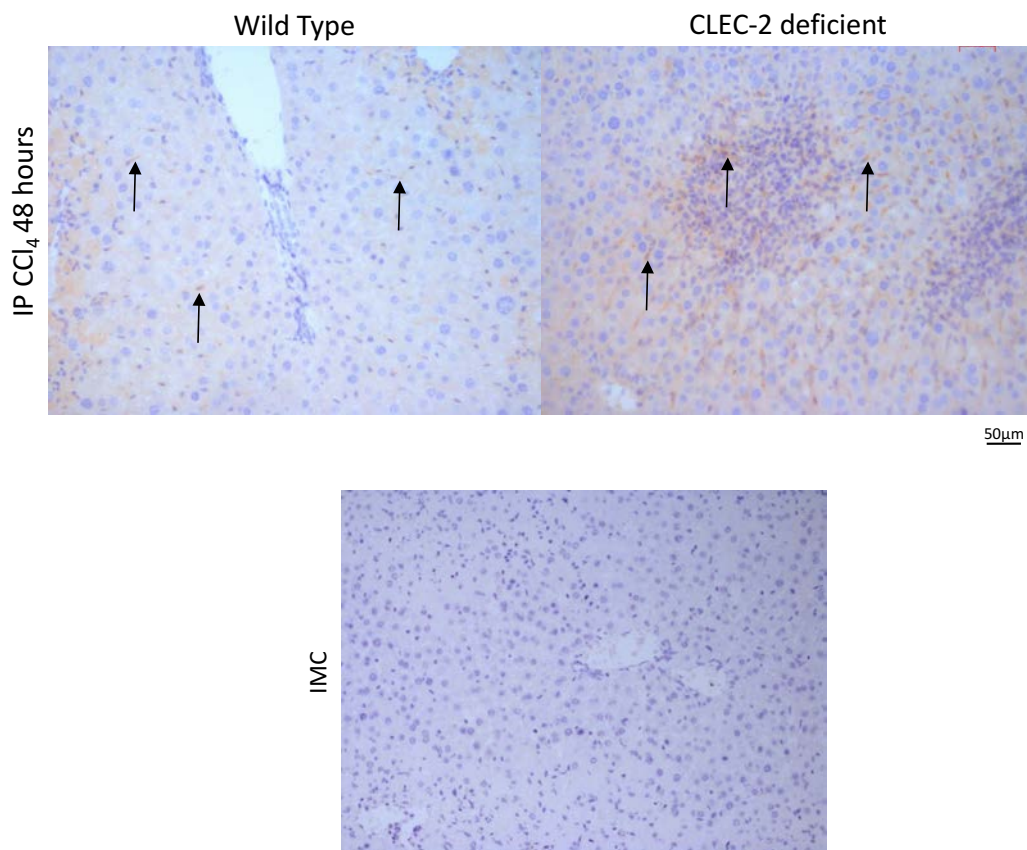


**Figure 4.14 After toxic injury larger amounts of platelets sequester to the injured liver in CLEC-2 deficient mice compared to wild type:**

WT or CLEC-2 deficient mice were injected with CCl<sub>4</sub> and sacrificed at 48 hours. Liver paraffin sections stained with a platelet (CD41) DAB stain (arrows), and visualized at 20X magnification with a haematoxylin counterstain. IMC staining was negative.

This suggested that platelets could associate with greater avidity to podoplanin<sup>hi</sup> macrophages if they were CLEC-2 deficient. To confirm this we again isolated liver macrophages (as described in chapter 2) and after stimulating them with LPS co-cultured the macrophages with either WT or CLEC-2 deficient platelets (isolated from WT or PF4Cre*CLEC1b*<sup>fl/fl</sup> mice respectively). More CLEC-2 deficient platelets attached to LPS stimulated hepatic macrophages than WT platelets (figure 4.15). However, it was not clear from our experiments whether the macrophages were actively phagocytosing platelets or the platelets were merely binding to the surface of the macrophages (fig 4.15).

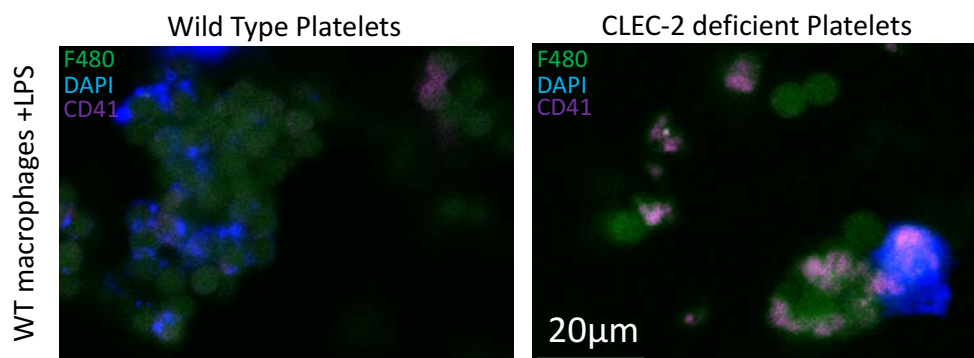


**Figure 4.15 CLEC-2 deficient platelets sequester to wild type macrophages in greater numbers than wild type platelets:**

Macrophages isolated from a single WT mouse liver were divided and plated in a 6 well plate. DMEM containing LPS was added to all the wells. To these macrophages were added WT or CLEC-2 deficient platelets, after a 1 hour incubation the wells were washed with sterile PBS and cells fixed. Images representative of confocal microscopic analysis of 6 wells are shown. Platelets CD41<sup>+</sup> are in purple, nuclear stain DAPI is blue and the macrophage marker F4/80 is green. 63X original magnification.

After we had established that mice with CLEC-2 deficient platelets exhibited enhanced liver healing after toxic insults and that both macrophages and platelets in CLEC-2 deficient mice sequestered to the injured liver (specifically to areas of centrilobular necrosis) with greater avidity than in WT mice we next sought to investigate the functional consequences of this enhanced sequestration and interaction.

Hepatic macrophages (specifically Kupffer cells) are known to be key cells in monitoring the liver environment for signs of damage and upon sensing damage (DAMP expression) (33) initiate the sterile inflammatory response characterized by further immune cell recruitment (47). This immune response can then, depending upon context and nature of injury heal the liver or worsen damage(204). We thus wondered whether there was indeed an enhanced macrophage presence in the livers of CLEC-2 deficient mice (as per our initial histological investigations) and whether the macrophage interaction with CLEC-2 deficient platelets influenced the sterile inflammatory response to drive enhanced liver recovery in the PF4Cre*CLEC1b*<sup>fl/fl</sup> mice.

Thus, we next assessed the damaged livers to establish the kinetics of immune cell particularly macrophage recruitment to see whether this was different between WT and CLEC-2 deficient animals and critically whether this correlated with the enhanced healing observed in the CLEC-2 deficient mice.

## **4.8. Kinetics of immune cell recruitment after toxic liver injury**

### **4.8.1. CD45<sup>+</sup> recruitment**

Our data demonstrates that both the maximum amount of liver damage and leukocyte sequestration occurred in centrilobular areas of the liver after a single dose of both APAP and CCl<sub>4</sub>, at 48 hrs. in the case of CCl<sub>4</sub> and 24 hrs. in the case of APAP. This pattern was seen in both WT and CLEC-2 deficient animals (fig 4.16). Initial histological analysis suggested there may be greater amounts of inflammatory leukocytes present within the livers of CLEC-2 deficient mice after injury (see arrows on figure 4.16).



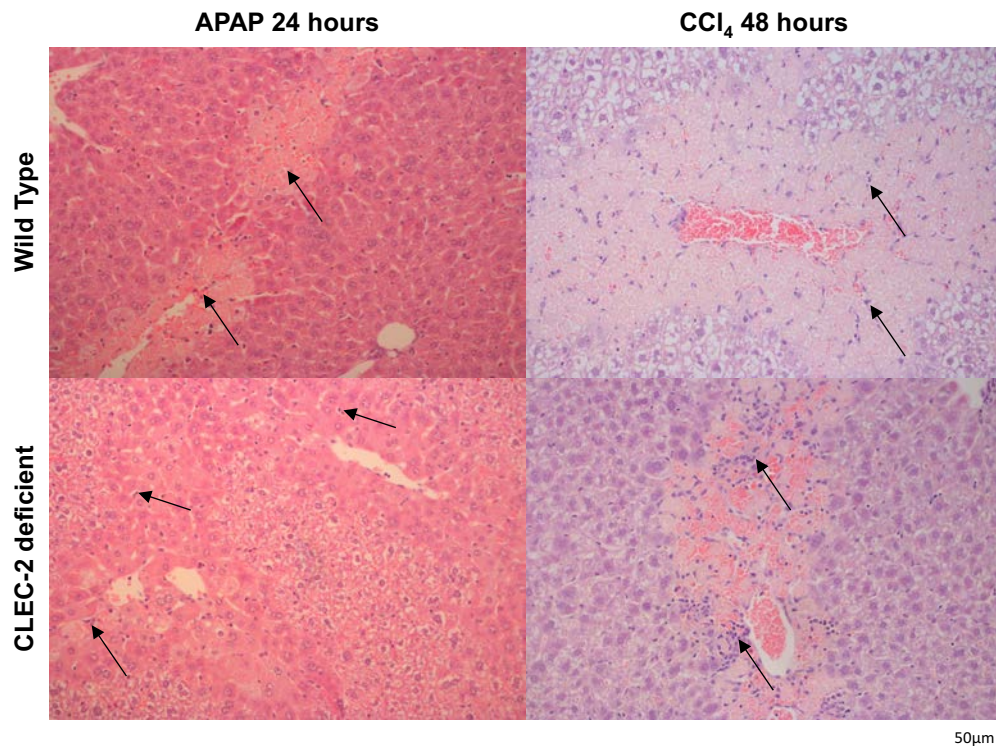


**Figure 4.16 Wild type and CLEC-2 deficient animals both develop centrilobular damage and leukocyte sequestration after toxic liver damage:**

WT or CLEC-2 deficient mice were injected with a single dose of IP CCl<sub>4</sub> or IP APAP. Mice were sacrificed at point of peak injury (i.e. 48 hrs. after IP CCl<sub>4</sub> or 24 hours after IP APAP). Centrilobular injury with intralesional leukocyte sequestration (arrows). 20X magnification, Paraffin sections, H/E stain.

To quantify and phenotype the inflammatory infiltrate we digested murine livers as detailed above (chapter 2) and then used flow cytometric analysis to quantify the numbers of infiltrating leukocytes per gram of liver tissue. We used CD45 as a pan leukocyte marker (see gating strategy in fig 4.18) and found that in WT mice after a toxic liver injury such as CCl<sub>4</sub>, the numbers of infiltrating CD45<sup>+</sup> cells increased (Fig 4.17, top right panel), peaking at time of maximum injury indicated by serum ALT quantitation (48 hours, fig 4.17 bottom panel).

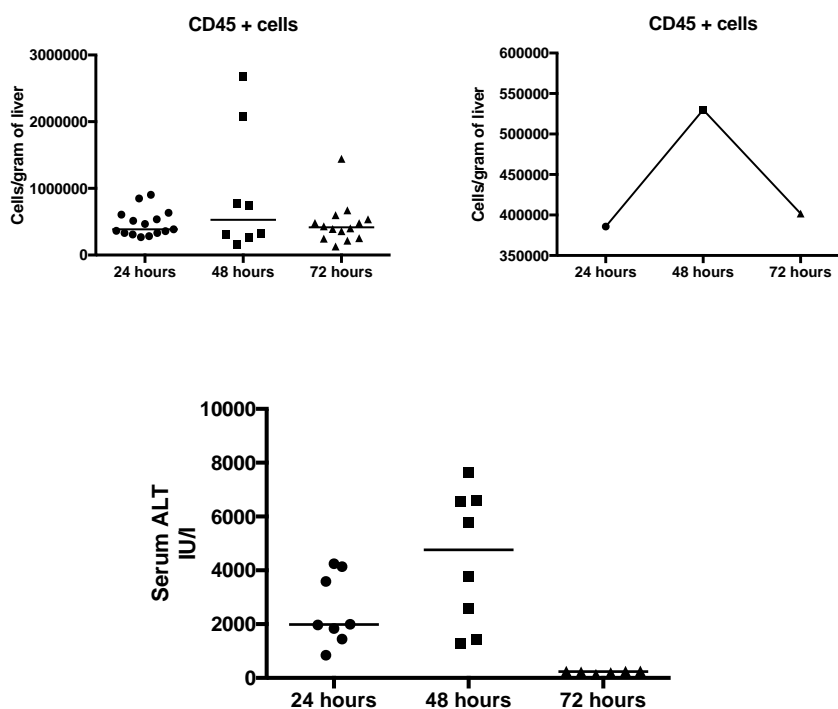


**Figure 4.17 Liver infiltrating CD45<sup>+</sup> leukocytes increase and peak at time point of maximal necrotic damage after toxic liver injury:**

WT mice were injected with a single dose of IP CCl<sub>4</sub>. Mice were sacrificed at 24, 48 or 72 hours after injection. Serum was analyzed for ALT level and the liver was digested to isolate leukocytes, which are expressed as numbers of CD45<sup>+</sup> cells per gram of liver. Top graphs demonstrate the same data as a scatter plot (left) or connected mean (right). Graph below shows ALT at the time points after CCl<sub>4</sub> administration. Each dot represents an individual mouse, median shown.

When I compared CD45<sup>+</sup> immune cell number in injured WT and CLEC-2 deficient mice (PF4Cre*CLEC1b*<sup>fl/fl</sup>) I noted that despite initial histochemical analyses suggesting greater leukocyte infiltration within the livers of CLEC-2 deficient animals, absolute numbers of liver infiltrating CD45<sup>+</sup> cells were not significantly different. There were only marginally greater numbers of CD45<sup>+</sup> cells in CLEC-2 deficient mice at 24 hours in the IP CCl<sub>4</sub> group, and this difference was not statistically significant. At all other time points (particularly at points of maximum histological and biochemical damage, i.e. 48 hrs. after IP CCl<sub>4</sub> and 24 hours after IP APAP) there was no difference in amount of leukocytes per gram of liver tissue when comparing the CLEC-2 deficient to WT mice, with either injury (fig 4.18).

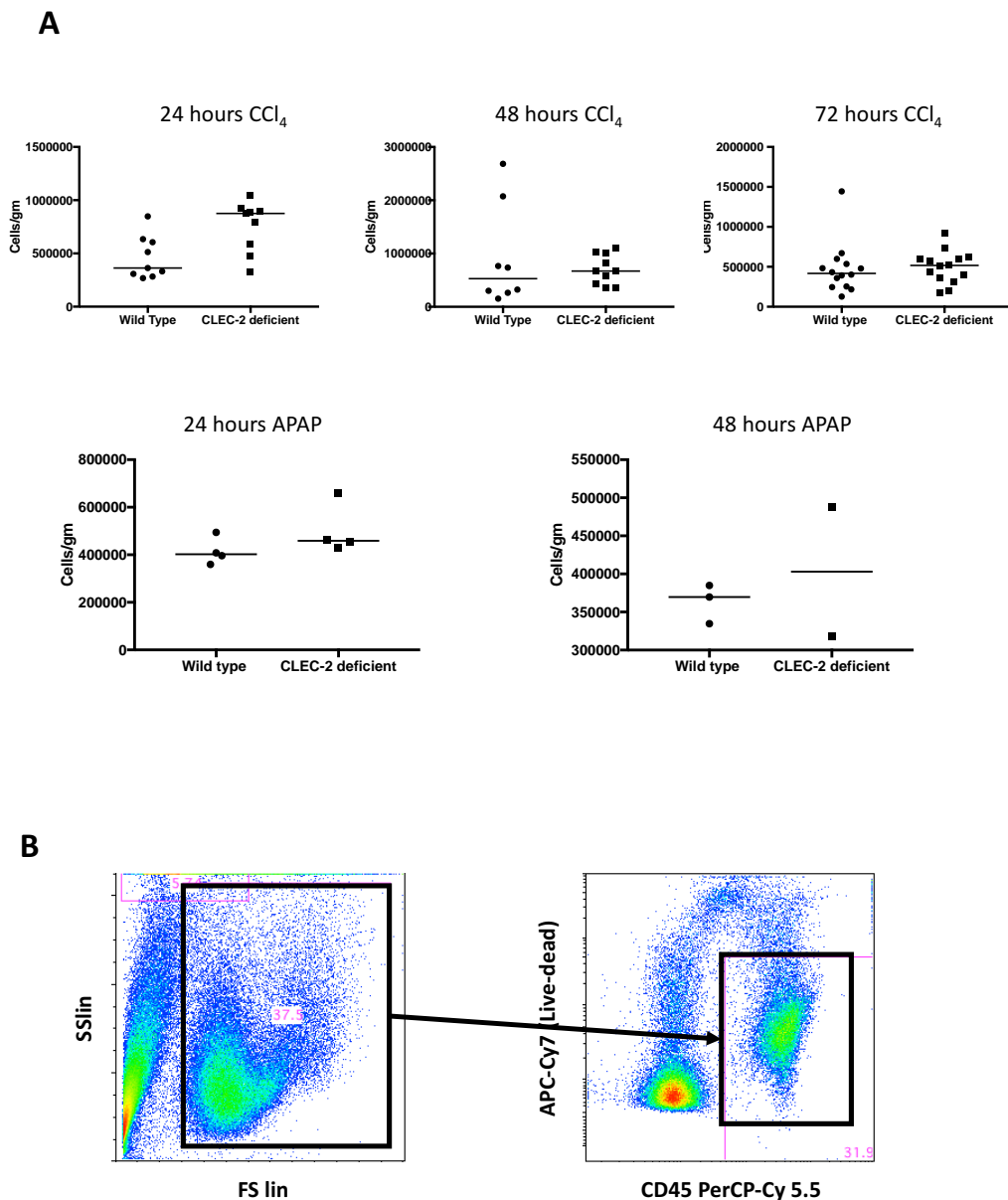


**Figure 4.18 Numbers of liver infiltrating CD45<sup>+</sup> leukocytes are similar at most timepoints after toxic liver injury:**

A) WT or CLEC-2 deficient mice ( mice were injected with a single dose of IP CCl<sub>4</sub> or IP APAP. Mice were sacrificed at 24, 48 or 72 hours after injection. The liver was digested to isolate leukocytes, which were expressed as numbers of cells per gram of liver tissue. B) CD45<sup>+</sup> cells were gated as shown in the strategy . The figure on the left is a side scatter vs forward scatter plot, with the leukocyte population being gated out. The image in the right, gates out the dead cells and CD45<sup>-</sup> cells. The plot is a live dead stain (APC-Cy7) Vs CD45(PerCP-Cy5.5), the gated population is thus live (APC-cy7-) and CD45<sup>+</sup>. At no point was a statistically significant difference seen when comparing WT and CLEC-2 deficient mice undergoing a toxic insult. (Each dot represents an individual mouse, median shown.

We next immunophenotyped the CD45<sup>+</sup> positive cells into lymphocytes and myeloid cells as detailed below.

#### **4.8.2. Lymphocyte recruitment**

To identify the lymphocyte compartment from the infiltrating CD45<sup>+</sup> cells, we first gated the CD3<sup>+</sup> and CD3<sup>-</sup> populations and then subsequently applied a gating strategy to define CD4<sup>+</sup> and CD8<sup>+</sup> T cells (see strategy in Fig 4.19). In both WT and CLEC-2 deficient animals an increase in the number of lymphocytes was observed post injury. We noted that at 48 hours after CCl<sub>4</sub> injection statistically greater amounts of CD4 and CD8 T cells were seen within the CLEC-2 deficient mice and at 24 hrs. after APAP injection a statistically greater amount of CD4 T cells was observed within CLEC-2 deficient murine livers (Fig 4.20). At the remaining time points the numbers were comparable between CLEC-2 deficient and WT mice.

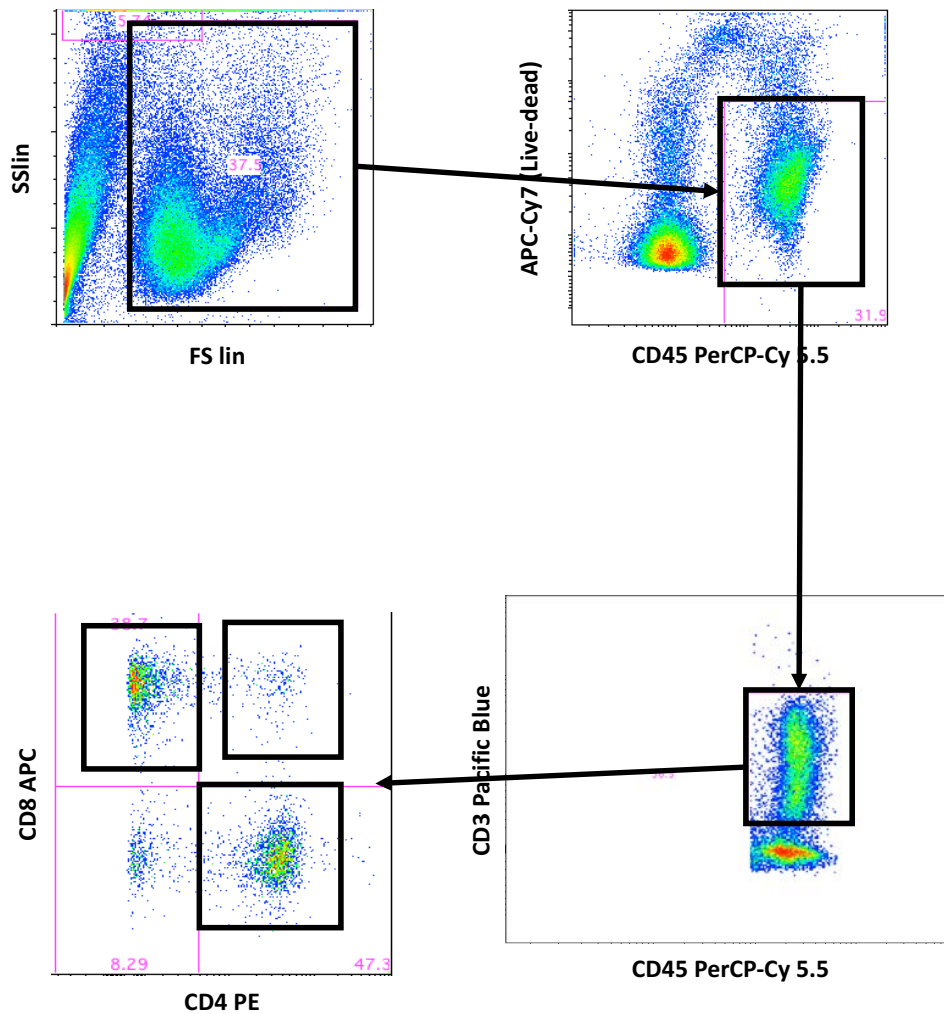


**Figure 4.19 Lymphocyte gating strategy:**

Mice were injected with a single dose of IP CCl<sub>4</sub> or IP APAP. Mice were sacrificed at 24, 48 or 72 hours after injection. The liver was digested to isolate leukocytes. After the live CD45<sup>+</sup> population was gated out (top right), gates were applied to separate out the CD3<sup>-</sup> population (bottom right figure). The CD3<sup>+</sup> population was then further gated into CD8 T-cells (thus CD45<sup>+</sup>CD3<sup>+</sup>CD8<sup>+</sup>CD4<sup>-</sup>), CD4 T-cells (CD45<sup>+</sup>CD3<sup>+</sup>CD8<sup>-</sup>CD4<sup>+</sup>) and CD3 T-cells (CD45<sup>+</sup>CD3<sup>+</sup>CD8<sup>-</sup>CD4<sup>-</sup>) (bottom left figure).

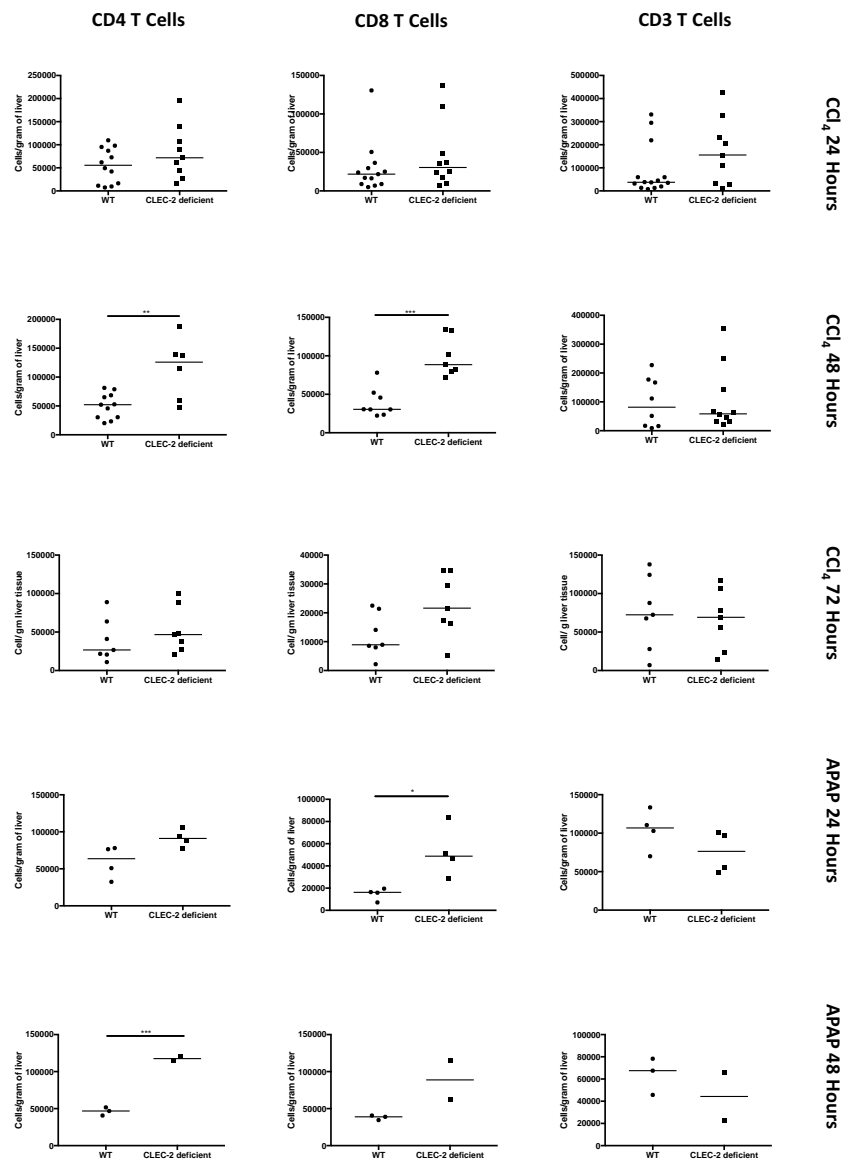


**Figure 4.20 CD4 and CD8 lymphocytes are present in greater amounts within the livers of CLEC-2 deficient mice after toxic liver injury:**

WT or CLEC-2 deficient mice were injected with a single dose of IP CCl<sub>4</sub> or IP APAP. Mice were sacrificed at 24, 48 or 72 hours after injection. The liver was digested to isolate leukocytes. CD4<sup>+</sup>, CD8<sup>+</sup> and CD3<sup>+</sup> leukocytes were analyzed using previously described flow cytometric methods and gated using the previously defined strategy and expressed as number of cells per gram of liver tissue. Absolute CD4<sup>+</sup>, CD8<sup>+</sup> and CD3<sup>+</sup> numbers are shown for individual animals at each time point after either CCl<sub>4</sub> or APAP was administered. Each dot represents an individual animal. The bar represents median values of each group and Mann Whitney test used \*P < 0.05, \*\*P < 0.01, \*\*\*P < 0.001.

### **4.8.3. Myeloid cell recruitment**

We next undertook further phenotyping of the hepatic infiltrate after liver injury to specifically see if there was a difference between WT and CLEC-2 deficient animals when quantifying absolute numbers of macrophages and neutrophils (see gating strategy in Fig 4.21). Despite histological evidence suggesting enhanced platelet-macrophage cell interaction in CLEC-2 deficient animals, and greater macrophage accumulation within the livers of CLEC-2 deficient mice, cytometric analysis showed that absolute numbers of macrophages (CD3<sup>-</sup>CD11b<sup>+</sup>F4/80<sup>+</sup>) were similar between WT and CLEC-2 deficient animals at all time points studied (Fig 4.22) after either APAP or CCl<sub>4</sub>.



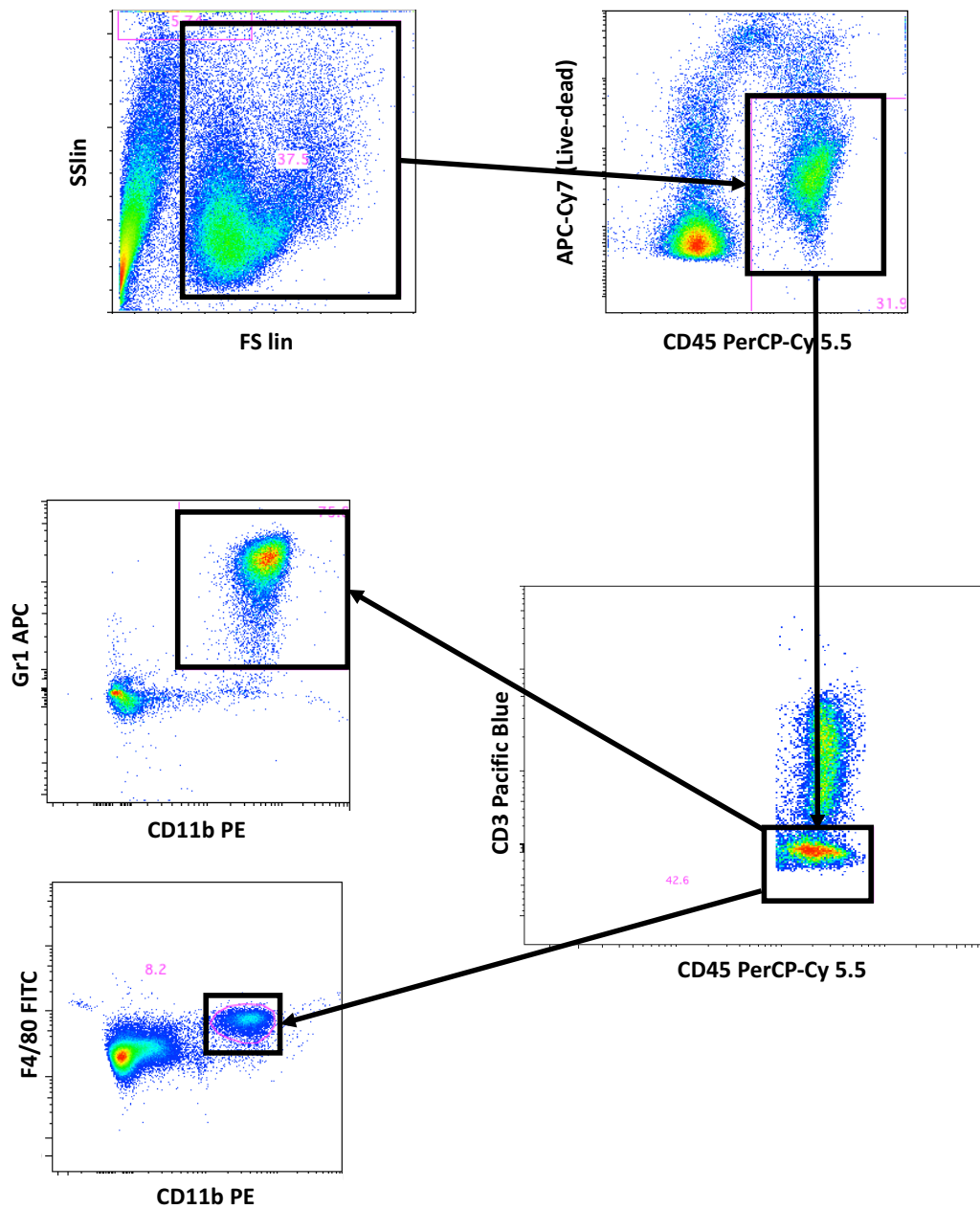


**Figure 4.21 Myeloid cell gating strategy:**

Mice were injected with a single dose of IP CCl<sub>4</sub> or IP APAP. Mice were sacrificed at 24, 48 or 72 hours after injection. The liver was digested to isolate leukocytes. After the live CD45<sup>+</sup> population was gated out (top right), gates were applied to separate out the CD3<sup>+</sup> population (bottom right figure). The CD3<sup>-</sup> population was then further gated into macrophages (CD45<sup>+</sup>CD3<sup>-</sup>CD11b<sup>+</sup>F4/80<sup>+</sup>) (bottom left) and neutrophils (CD45<sup>+</sup>CD3<sup>-</sup>CD11b<sup>+</sup>GR1<sup>hi</sup>) (figure in the middle, left hand side). numbers are shown for individual animals at each time point after either CCl<sub>4</sub> or APAP was administered.

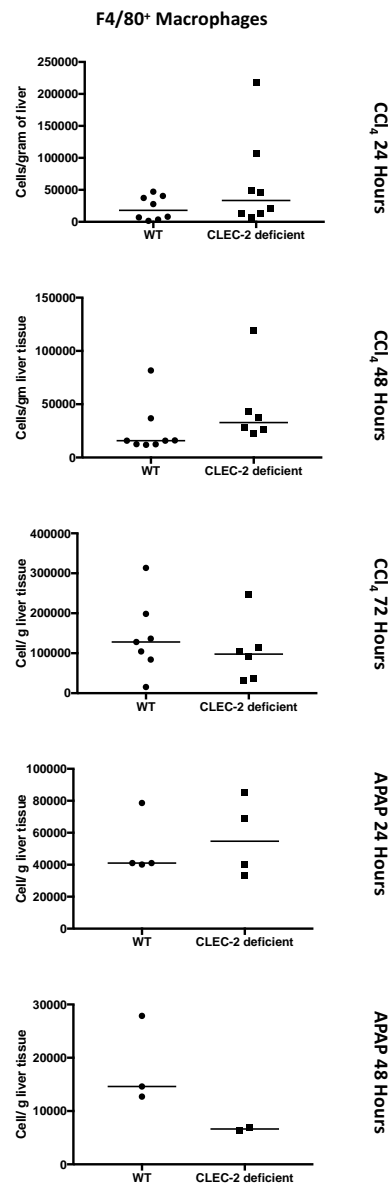


**Figure 4.22 Hepatic macrophage numbers are similar in WT and CLEC-2 -deficient mice after a toxic liver injury:**

WT or CLEC-2 -deficient mice were injected with a single dose of IP CCl<sub>4</sub> or IP APAP. Mice were sacrificed at 24, 48 or 72 hours after injection. The liver was digested to isolate leukocytes. Leukocytes were analyzed using flow cytometric methods. Macrophages were gated using the previously defined strategy and expressed as number of cells per gram of liver tissue. Absolute macrophage numbers are compared in WT and CLEC-2 deficient mice at each time point after either CCl<sub>4</sub> or APAP was administered. Each dot represents an individual mouse. The bar represents median values of each group and Mann Whitney test used to gauge significance \*P < 0.05, \*\*P < 0.01, \*\*\*P < 0.001.

However when we examined neutrophil infiltration (Cd3<sup>+</sup>Cd11b<sup>+</sup>Gr1<sup>hi</sup>), we noted that in response to a toxic injury (both APAP and CCl<sub>4</sub>) CLEC-2 deficient mice exhibited significantly greater numbers of infiltrating neutrophils per gram of liver tissue compared to control WT animals (fig 4.23) at most time points studied (the exceptions being the late time points studied: 48 hours after APAP and 72 hours after CCl<sub>4</sub>).

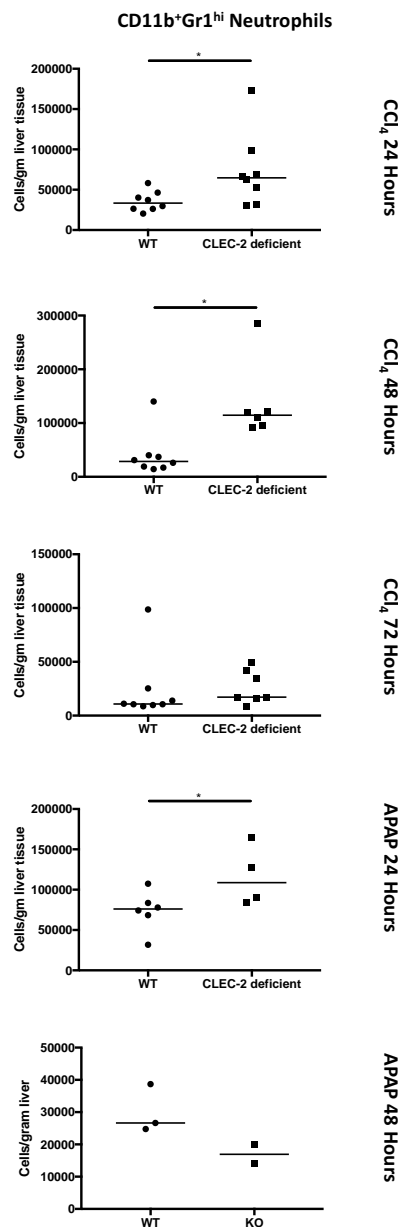


**Figure 4.23 CLEC-2 deficient mice exhibit enhanced hepatic neutrophil numbers at the peak point of liver injury after toxin administration:**

WT or CLEC-2 deficient mice were injected with a single dose of IP CCl<sub>4</sub> or IP APAP. Mice were sacrificed at 24, 48 or 72 hours after injection. The liver was digested to isolate leukocytes. Leukocytes were analyzed using flow cytometric methods. Neutrophils gated using the previously defined strategy and expressed as number of cells per gram of liver tissue. Absolute neutrophil numbers are compared in WT and CLEC-2 deficient mice at each time point after either CCl<sub>4</sub> or APAP was administered. Each dot represents an individual mouse. The bar represents median values of each group and Mann Whitney test used to gauge significance \*P < 0.05, \*\*P < 0.01, \*\*\*P < 0.001.

#### **4.9. Podoplanin blockade recapitulates the effects seen in CLEC-2 deficient mice**

After having established that the cognate ligand for CLEC-2, podoplanin was upregulated within the livers of mice undergoing a toxic acute liver injury and that mice with CLEC-2 deficient platelets exhibited enhanced healing after toxic liver injury, we next sought to establish whether it was indeed podoplanin upregulation within injured livers that provided the signal for platelet activation, thus worsening injury after a toxic hepatic insult. Therefore we next interrogated the role of this pathway from the other side by removing podoplanin and assessed whether removing this platelet activation stimulus would result in reduced injury after APAP or CCl<sub>4</sub> mediated liver injury.

The most pronounced difference in terms of hepatic damage was noted at 48hrs after CCl<sub>4</sub> administration and 24 hrs. after APAP administration when comparing CLEC-2 deficient mice to WT mice. At these time points whilst the WT mice continued to develop worsening liver damage with a rising serum ALT and increasing hepatic necrosis, the CLEC-2 deficient mice had much lower serum level of ALT (fig 4.24, blue boxes) and exhibited restoration of the hepatic architecture as well. For our subsequent experiments examining podoplanin blockade we thus focused on these time points.

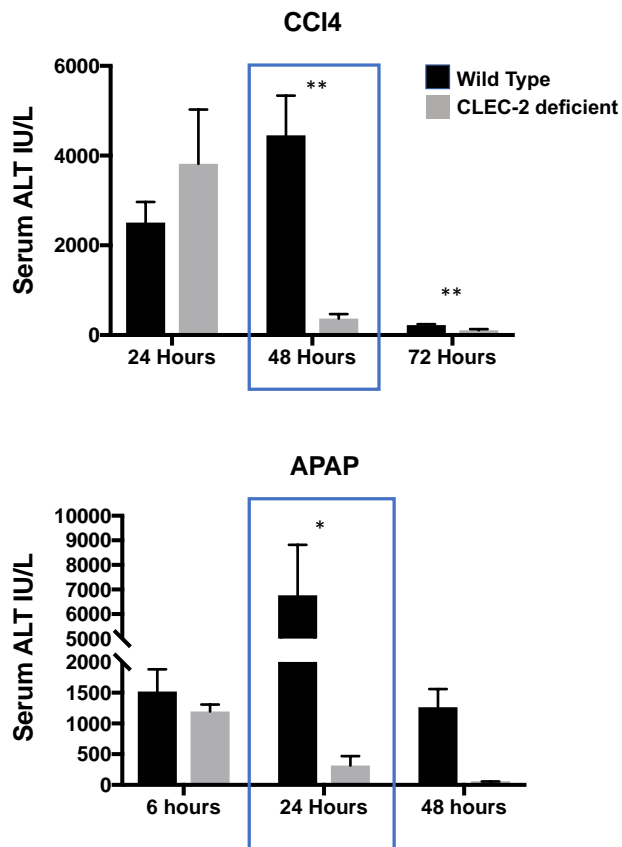


**Figure 4.24 Time line for injury after APAP and CCl<sub>4</sub> injection:**

WT and CLEC-2 deficient mice were injected with CCl<sub>4</sub> and sacrificed at 24, 48 or 72 hours; or WT and CLEC-2 deficient mice were injected with APAP and sacrificed either 6, 24 or 48 hours. Mice were sacrificed using cardiac puncture and serum harvested for ALT analysis. Time points of peak injury in WT mice are highlighted. (n=5-11). S.E.M shown and Mann Whitney test used \*P < 0.05, \*\*P < 0.01, \*\*\*P < 0.001.

#### 4.9.1. Genetic podoplanin deletion

To remove podoplanin we used a genetic mutant mouse with a conditional deletion for podoplanin (*Vav1-iCre<sup>+</sup>pdpr<sup>fl/fl</sup>*) (209). The mice were subjected to either a single dose of IP CCl<sub>4</sub> or APAP as described above, and sacrificed at points of maximal

liver injury as determined in our previous experiments, this was [24 hours in the case of APAP and 48 hours in the case of CCl<sub>4</sub> (fig 4.25)]

#### 4.9.1.1. CCl<sub>4</sub>

After a single injection of IP CCl<sub>4</sub>, podoplanin deficient mice (*Vav1-iCre<sup>+</sup>pdpn<sup>fl/fl</sup>*) or WT (cre negative) control animals were sacrificed at 48 hours. The podoplanin mice had less injury as gauged by reduced serum ALT levels and histological analysis compared to their cre-negative counterparts.

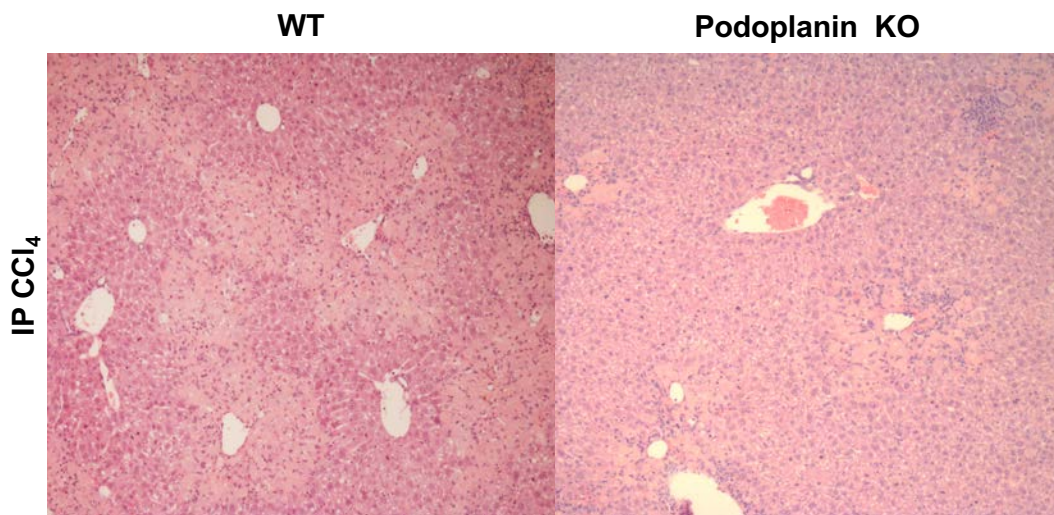
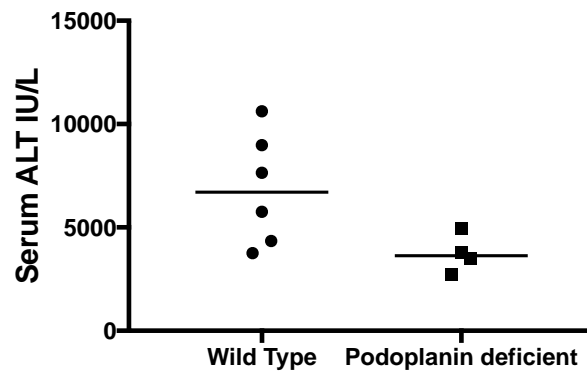


**Figure 4.25 Podoplanin deficient ( $Vav1-iCre^+pdpn^{fl/fl}$ ) mice exhibit less injury after IP  $CCl_4$  injection:**

Podoplanin deficient mice or WT mice were injected with IP  $CCl_4$  and sacrificed at 48 hours. Serum ALT level (top graph) comparing WT and podoplanin deficient mice is shown. Images below are paraffin sections and are representative of at least 5 mice (10x, H/E stain). Each dot represents an individual mouse. The bars represent median values of each group.



Analysis of the hepatic inflammatory infiltrate again revealed that although overall numbers of infiltrating cells were similar between the two groups (this extended to most subtypes-all data not shown); there again appeared to be a tendency to greater neutrophil accumulation after CCl<sub>4</sub> was administered (fig 4.26).

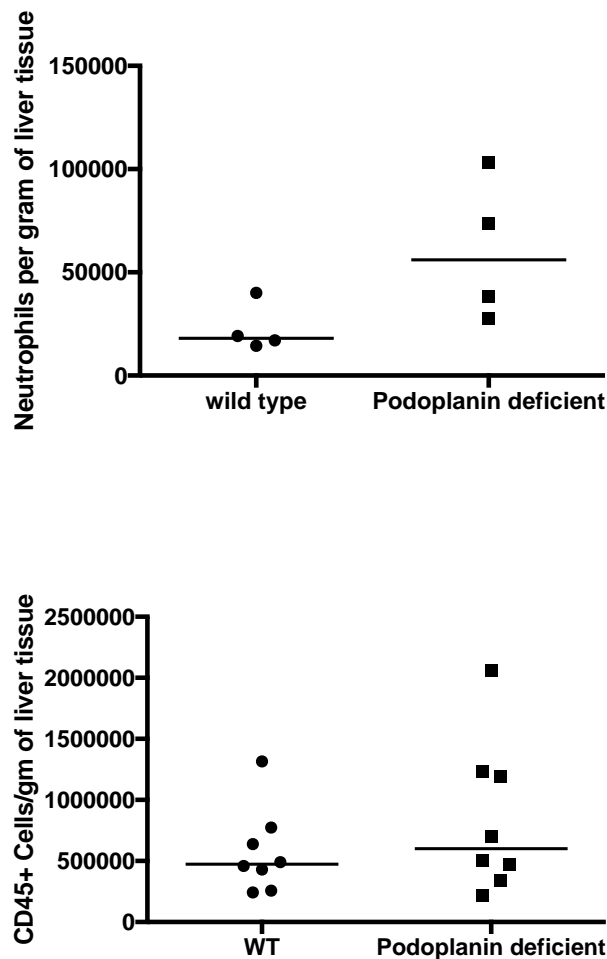


**Figure 4.26 Podoplanin deficient mice exhibit enhanced neutrophil infiltration after IP CCl<sub>4</sub> administration:**

Podoplanin deficient mice (*Vav1-iCre<sup>+</sup>pdpn<sup>fl/fl</sup>*) or WT mice were injected with a single dose of IP CCl<sub>4</sub>. Mice were sacrificed at 48 after injection. The liver was digested to isolate leukocytes, these were analyzed using flow cytometric techniques and then were expressed as numbers of cells per gram of liver tissue. The bars represent median values of each group.

#### 4.9.1.2. APAP

We next used podoplanin deficient mice ( $Vav1-iCre^+pdpn^{fl/fl}$ ) in APAP models of liver damage. Mice were taken at 24 hours after IP APAP injection. We found that the podoplanin deficient mice again had less injury than their cre negative counterparts, and again this correlated with enhanced neutrophil recruitment to the injured liver. The remainder of leukocyte recruitment studied was similar between the two groups ( $CD45^+$  shown in fig 4.27, remaining subtypes not shown)

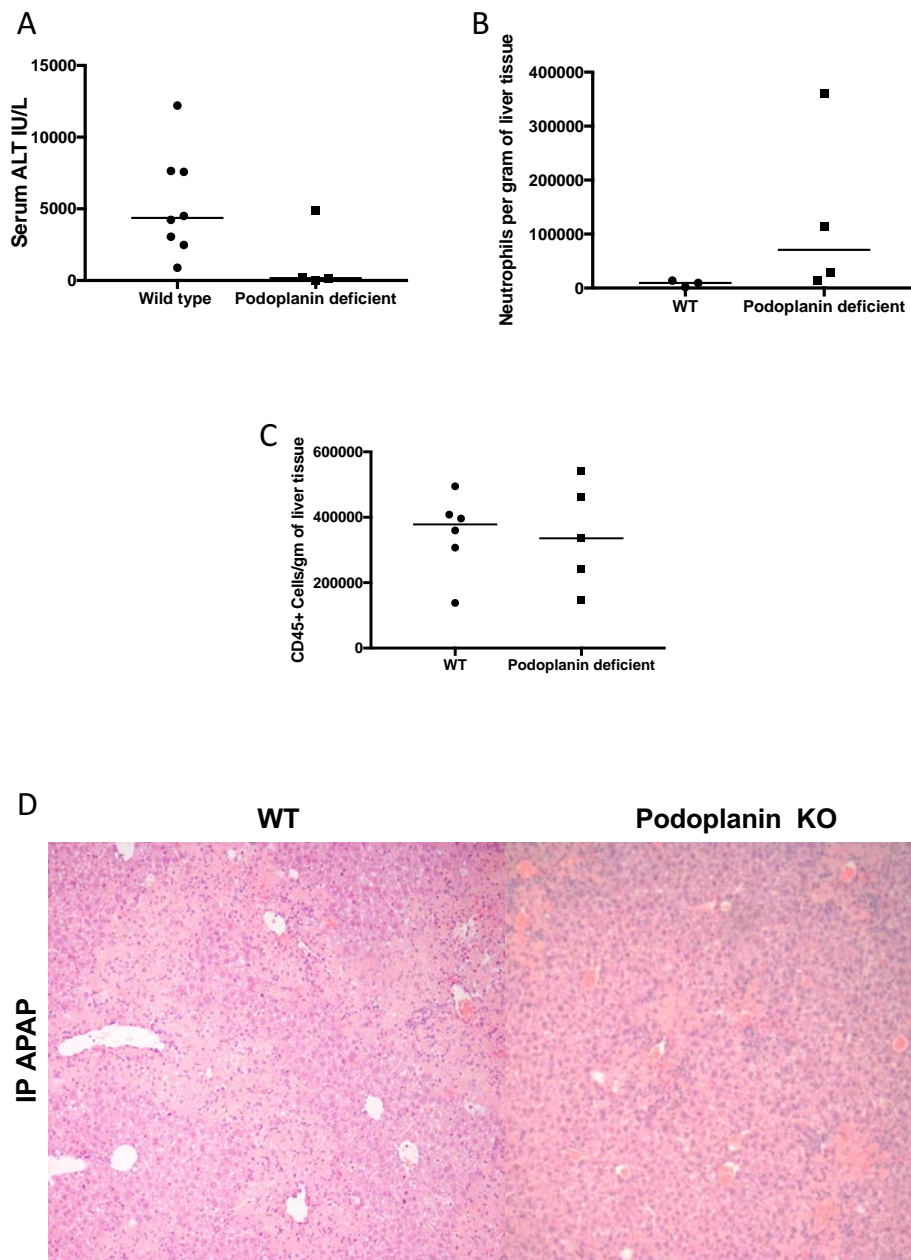


**Figure 4.27 Podoplanin deficient mice ( $Vav1-iCre^+pdpn^{fl/fl}$ ) exhibit reduced injury and enhanced neutrophil infiltration after IP APAP administration:**

Podoplanin deficient mice ( $Vav1-iCre^+pdpn^{fl/fl}$ ) or WT mice were injected with a single dose of IP APAP. Mice were sacrificed at 24 hrs. after injection. The liver was digested to isolate leukocytes, which were expressed as numbers of cells per gram of liver tissue and serum ALT was measured in extracted blood. A) serum ALT is shown, B and C) neutrophils and CD45<sup>+</sup> leukocytes per gram of liver tissue are shown. D) representative histology from 5 animals per group is shown (H/E, 10x, Paraffin). Each dot in the scatter plots represents a single mouse.

#### 4.9.2. Use of function blocking antibody

Our ultimate goal was to see if we could therapeutically treat toxic liver injury and thus we next used a specific podoplanin function-blocking antibody to see whether we could enhance liver healing after toxic liver injury, in a manner similar to what we observed in the genetic models of CLEC-2 or podoplanin deficiency. We thus pre-treated wild type mice with a function blocking antibody, prior to injecting them with the injurious stimulus (i.e. APAP or CCl<sub>4</sub>, see treatment schedule in fig 4.28). We found that mice that had been pretreated with the anti-podoplanin function blocking antibody exhibited reduced hepatic injury after both APAP and CCl<sub>4</sub> at peak point(s) of liver injury (i.e. 48 hrs. after CCl<sub>4</sub> and 24 hrs. after APAP).

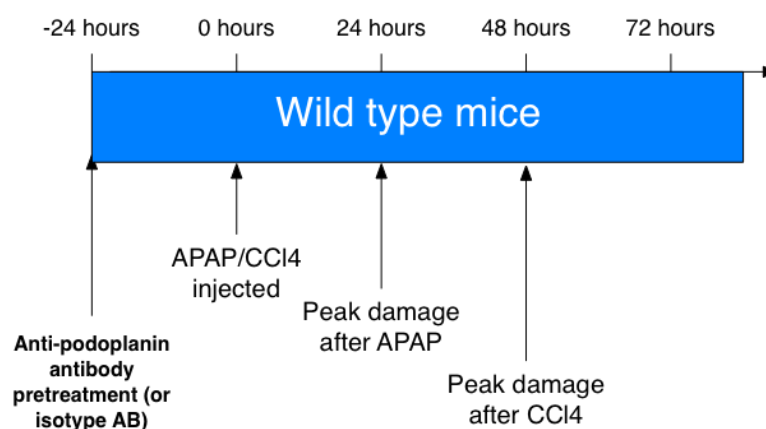


**Figure 4.28 Timeline of podoplanin antibody treatment:**

WT mice were pretreated with a podoplanin function blocking antibody (or the corresponding isotype matched control). The mice were then administered either IP CCl<sub>4</sub> or IP APAP 24 hours later. The mice that had been administered CCl<sub>4</sub> were taken 48 hours after the toxin was administered; mice that had been given APAP were culled at 24 hours after toxin administration.

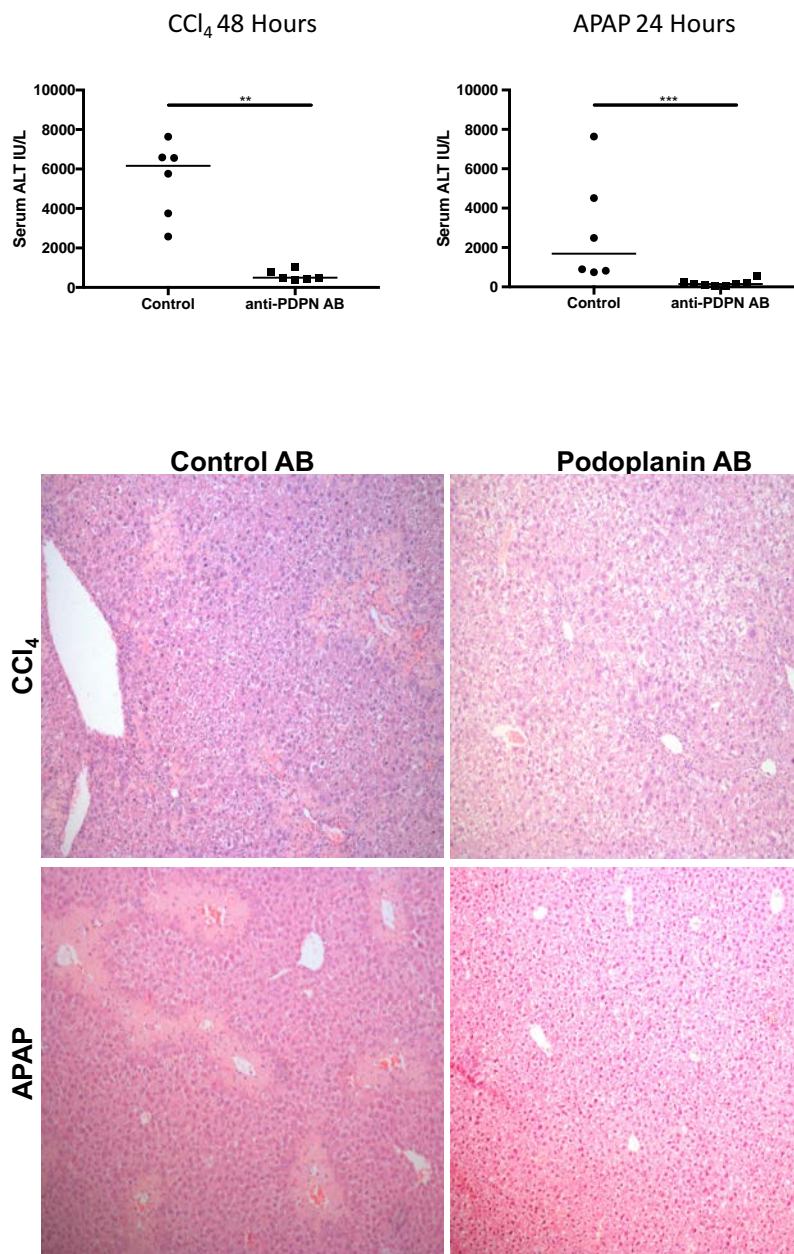


**Figure 4.29 Treating mice with a podoplanin antibody reduces injury after both CCl<sub>4</sub> and APAP mediated injury:**

Mice were treated with a podoplanin function blocking (5  $\mu\text{g}$  /gm) or isotype matched control AB and then treated with either APAP or CCl<sub>4</sub>. Blood was harvested via cardiac puncture and serum ALT measured at time points shown. The graphs at the top compare serum ALT after APAP and CCl<sub>4</sub> injection in podoplanin AB treated and control AB groups. Representative histology from 4 mice in each group is shown at the bottom (H/E, 10x, Paraffin). Each dot in the scatter plots represents a single mouse, the bars represents median values of each group and the Mann Whitney test was used to gauge significance \*P < 0.05, \*\*P < 0.01, \*\*\*P < 0.001.

We next analyzed the livers from these mice for absolute leukocyte numbers, and found that again there was a greater amount of neutrophils within the livers of the mice that had been given the podoplanin blocking antibody compared to the isotype treated controls (IMC fig 4.30). Total number of leukocytes (CD45<sup>+</sup>) and remaining subtypes (data not shown) were similar in both AB and IMC groups (in both APAP and CCl<sub>4</sub> arms).

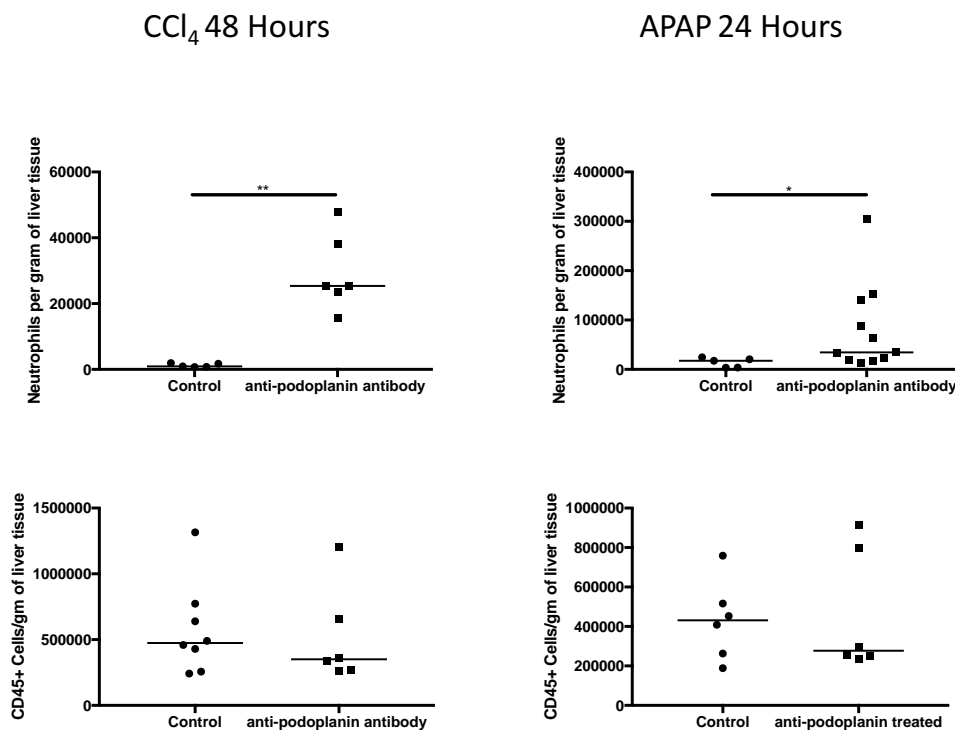


**Figure 4.30 Mice treated with a podoplanin antibody exhibit enhanced neutrophil infiltration after IP CCl<sub>4</sub> or IP APAP administration:**

Mice were treated with a podoplanin function blocking or isotype matched control AB and then injected with a single dose of IP CCl<sub>4</sub> or APAP. Mice were sacrificed at time points shown. The liver was digested to isolate leukocytes, which were expressed as numbers of cells per gram of liver tissue. Each dot in the scatter plots represents a single mouse, the bars represents median values of each group and the Mann Whitney test was used to gauge significance \*P < 0.05, \*\*P < 0.01, \*\*\*P < 0.001.

#### 4.10. The effect of neutrophil depletion on liver injury

The cell type that was consistently the most numerous within the livers of mice that had either a CLEC-2 deficiency or podoplanin blockade (both genetic and AB mediated) after an acute toxic liver insult was the neutrophil. In our models' neutrophil infiltration (assessed cytometrically) clearly correlated temporally with a reduction in liver injury (blue box, fig 4.31). Furthermore, histochemical analyses (using a neutrophil elastase antibody) confirmed that neutrophils were present within areas of resolving injury in the CLEC-2 deficient and podoplanin blocked mice, and in greater numbers than their WT counterparts (fig 4.32).

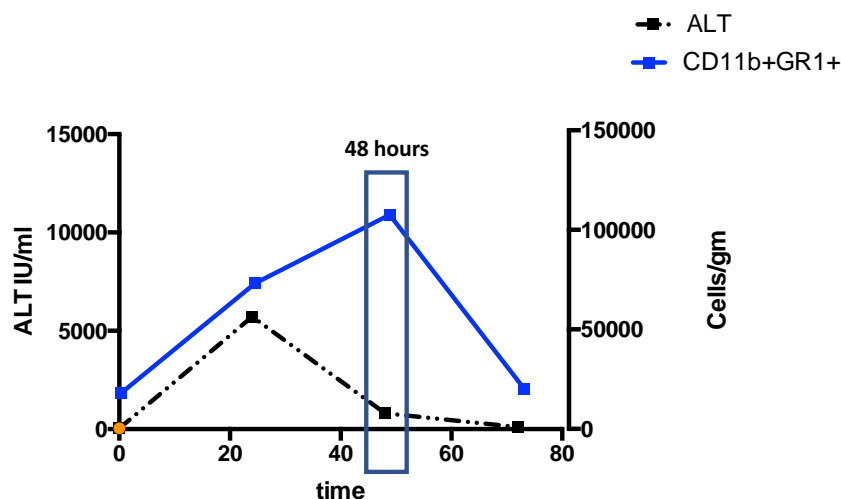


**Figure 4.31 Hepatic neutrophil infiltration peaks at time of maximal reduction of ALT in CLEC-2 deficient mice:**

CLEC-2 deficient mice were injected with CCl<sub>4</sub> and sacrifice at either 24, 48 or 72 hours. Blood was harvested via cardiac puncture and serum ALT measured at time points shown. The liver was collected and digested. Neutrophils (CD11b<sup>+</sup>Gr1<sup>+</sup>) were isolated using a gradient centrifugation method, stained and expressed as cells per gram of liver tissue. Highlighted area (at 48 hours' post CCl<sub>4</sub> dose) reveals time point of peak neutrophil infiltration and maximum reduction in serum ALT.

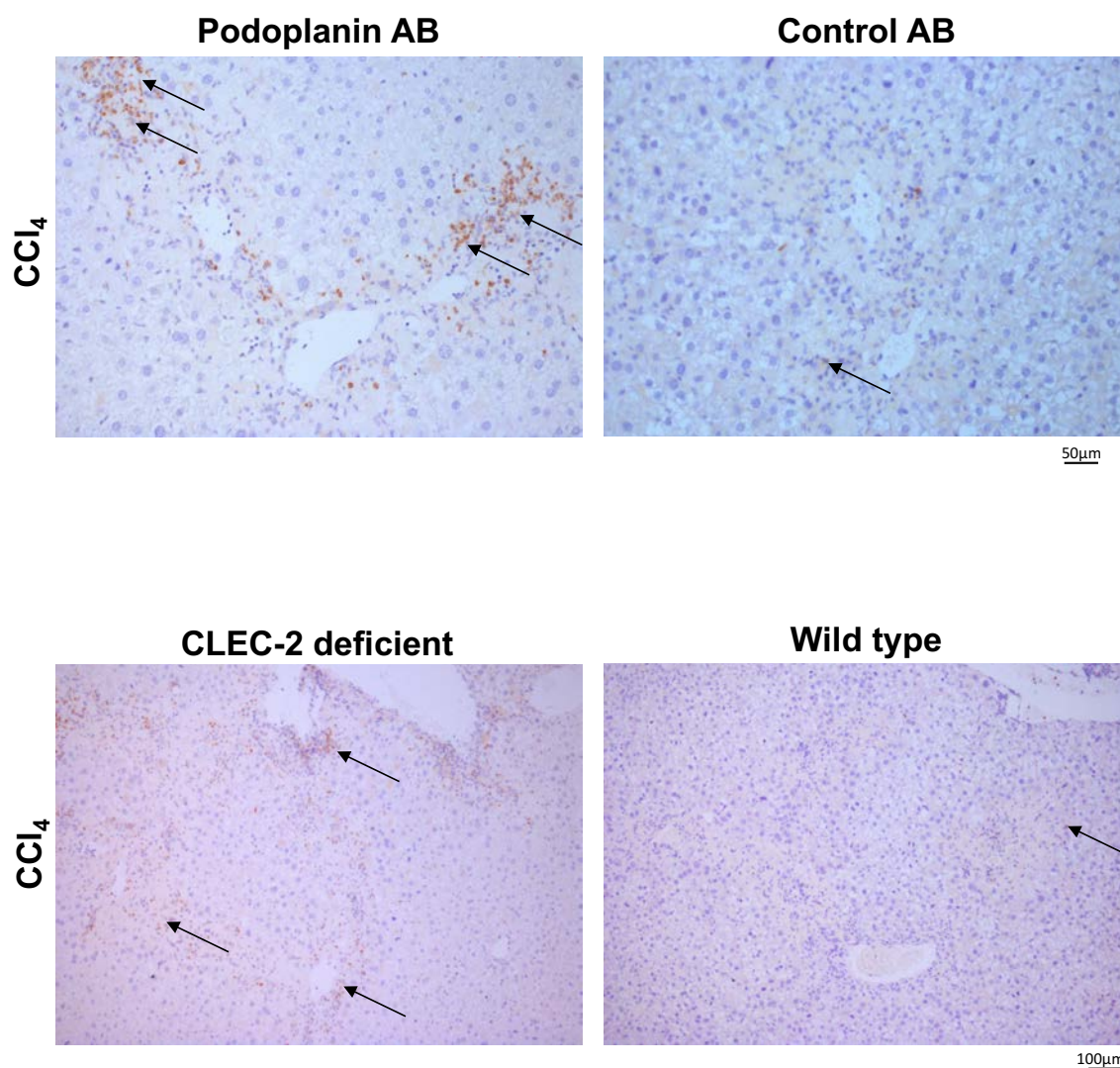


**Figure 4.32 After toxic liver injury more neutrophils sequester to damaged areas within the livers of CLEC-2 deficient mice than WT mice:**

WT or CLEC-2 deficient mice were injected with CCl<sub>4</sub> and sacrificed at 48 hours. Liver paraffin sections stained with a neutrophil elastase primary AB with DAB (brown) secondary stain (arrows), and visualized at 20X (top images) or 10X magnification (bottom images) with a haematoxylin counterstain. Images representative of at least 5 animals per groups.



After confirming the temporal and spatial relationship between neutrophil infiltration and liver healing we next sought to functionally confirm that it was indeed this enhanced neutrophil infiltration that was driving liver healing in the CLEC-2 deficient mice. We thus pre-treated CLEC-2 deficient mice with either a neutrophil depleting antibody or control AB, prior to administering CCl<sub>4</sub> (see timeline in fig 4.33). We found that CLEC-2 deficient mice that had been administered a selective neutrophil depleting antibody (anti-Ly6G) prior to CCl<sub>4</sub> treatment had lower levels of peripheral circulating neutrophils and had reduced hepatic neutrophil infiltration (fig 4.33). The lower hepatic neutrophil infiltration in the antibody treated group correlated with worse injury as gauged by serum ALT levels compared to the CLEC-2 deficient mice that had the control AB prior to CCl<sub>4</sub> administration. (Fig 4.33).

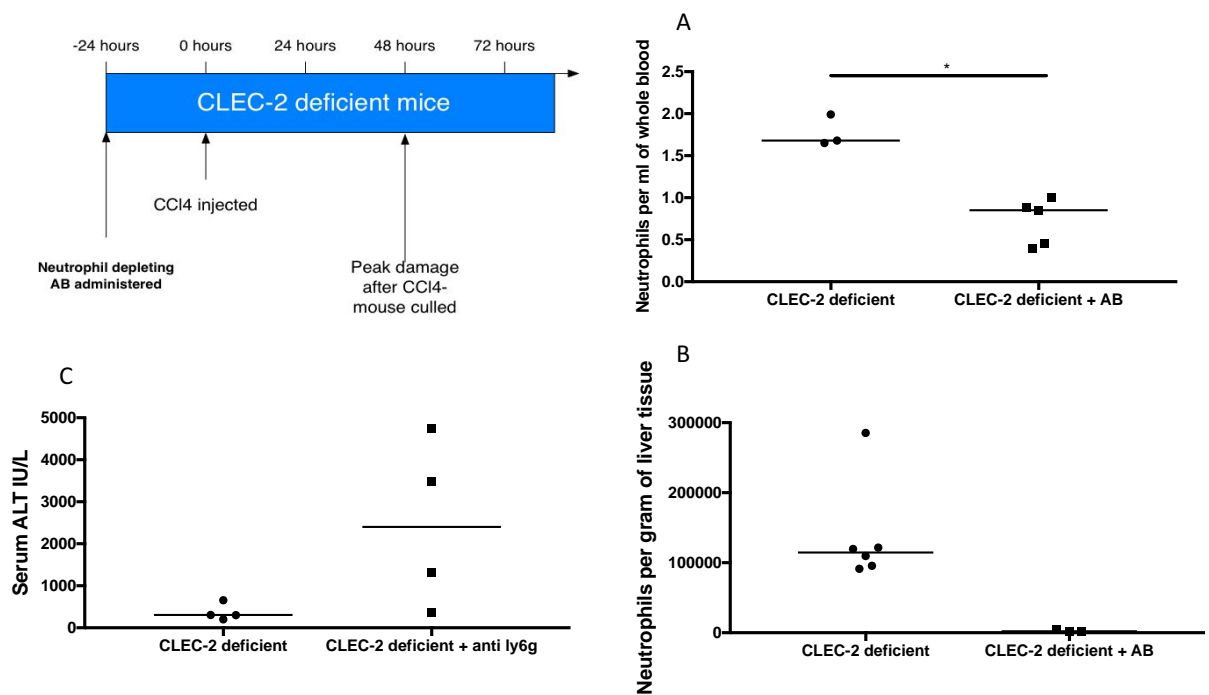


**Figure 4.33 Neutrophil depletion in CLEC-2 deficient mice removes the protective effect of CLEC-2 deficiency in mice undergoing a toxic liver injury:**

CLEC-2 deficient mice were pre-treated with either saline or a neutrophil depleting antibody. All mice were then administered IP CCl<sub>4</sub> and sacrificed at 48 hours (top left image). The liver was collected and digested. Neutrophils (CD11b<sup>+</sup>Gr1<sup>+</sup>) were isolated using a gradient centrifugation method, stained and expressed as cells per gram of liver tissue, blood was harvested via cardiac puncture and serum ALT and circulating neutrophil count determined using a coulter counter. A) Circulating neutrophil count is shown B) infiltrating neutrophils per gram of liver tissue are shown C) serum ALT. Each dot in the scatter plots represents a single mouse, the bars represents median values of each group and the Mann Whitney test was used to gauge significance \*P < 0.05, \*\*P < 0.01, \*\*\*P < 0.001.

#### **4.11. Macrophage derived TNF- $\alpha$ recruits' neutrophils to the injured liver**

Macrophages or specifically hepatic Kupffer cells have an important role in paracetamol induced acute liver injury and macrophage depletion has a deleterious effect on the liver after APAP(39,210) overdose. Our data confirmed that hepatic macrophages upregulate podoplanin after toxic liver injury, thus providing a ligand for platelet activation via CLEC-2; additionally we noted that platelets sequester to podoplanin expressing macrophages, and that blocking the CLEC-2-podoplanin axis enhanced this interaction and also increased hepatic platelet sequestration. We have also established that removing either CLEC-2 from platelets or podoplanin (genetically or blocking using an antibody) resulted in enhanced healing from toxic liver injury by enhancing neutrophil recruitment to the injured liver. Our experiments thus far had not however established exactly how removing CLEC-2 from platelets or blocking/removing podoplanin on macrophages enhanced neutrophil recruitment to the injured liver or indeed whether the two were linked.

TNF  $\alpha$  is a cytokine with established roles in liver regeneration (211) and importantly is known to be crucial for CD11b<sup>+</sup>GR1<sup>+</sup> cell recruitment (212–214). We thus analyzed murine serum after liver injury to compare serum TNF  $\alpha$  levels between WT and CLEC-2 deficient mice. At the point of peak damage we noted that there was very little TNF  $\alpha$  in murine serum (fig 4.34), however we argued that if the peak point of injury resolution in the CLEC-2 deficient animals (i.e. 48 hr. after CCl<sub>4</sub> administration) corresponded to peak neutrophil infiltration, the stimulus for this recruitment must

precede hepatic neutrophil infiltration. We thus examined sera from mice at an earlier timepoint (24 hrs. after CCl<sub>4</sub> administration) and found that the CLEC-2 deficient mice had significantly higher levels of serum TNF- $\alpha$  after toxic liver injury compared to their WT counterparts (fig 4.34).

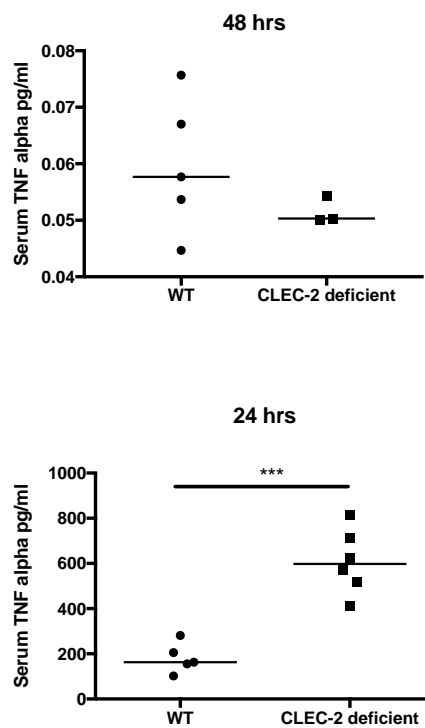


**Figure 4.34 CLEC-2 deficient mice have greater amounts of serum TNF- $\alpha$  at early points after toxic liver injury:**

WT or CLEC-2 deficient mice injected with IP CCl<sub>4</sub> and sacrificed at either 24 or 48 hour. The serum extracted was analyzed using a sandwich ELISA technique. Each dot in the scatter plots represents a single mouse, the bars represents median values of each group and the Mann Whitney test was used to gauge significance \*P < 0.05, \*\*P < 0.01, \*\*\*P < 0.001.

#### **4.11.1. Macrophage TNF $\alpha$ production is enhanced when cells are incubated with CLEC-2 deficient platelets**

There are multiple sources of TNF $\alpha$  in the liver, with macrophages (specifically Kupffer cells) being a particularly potent source during liver injury(205); as abrogating the CLEC-2/ podoplanin axis seemed to enhance systemic TNF $\alpha$  levels, we next sought to establish whether the source of this enhanced TNF $\alpha$  was the altered macrophage-platelet interaction. We thus isolated macrophages from WT murine livers and cultured them in six well plates as before. To mimic inflammatory conditions we treated the isolated macrophage population with 100ng/ml of lipopolysaccharide (LPS). We then measured the amount of TNF $\alpha$  within the macrophage secretome via ELISA. We found as before that compared to macrophages treated with control media alone, macrophages co-cultured with LPS containing media produced more TNF $\alpha$  (fig 4.35).

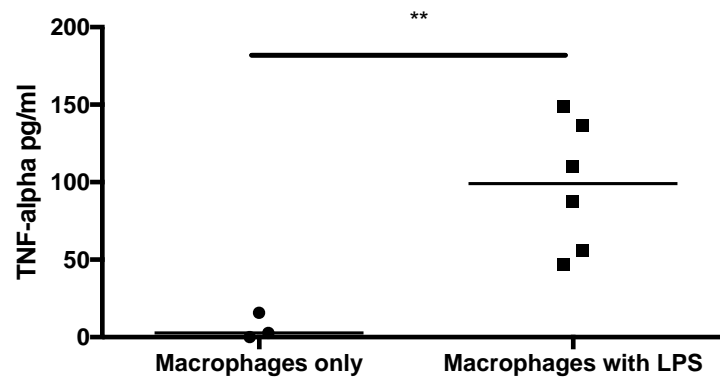


**Figure 4.35 Hepatic macrophages produce TNF- $\alpha$  after stimulation with LPS:**

Non-injured WT mice were sacrificed, their livers were removed and hepatic macrophages isolated. After being stimulated with LPS (or control DMEM alone, the macrophage secretome was collected and analyzed for TNF $\alpha$  levels via a sandwich ELISA. Each dot in the scatter plots represents different wells but macrophages are from a single mouse, the bars represents median values of each group and the Mann Whitney test was used to gauge significance \*P < 0.05, \*\*P < 0.01, \*\*\*P < 0.001.

We next stimulated hepatic macrophages with LPS and co-cultured these with either WT or CLEC-2 deficient platelets and found that the presence of WT platelets suppressed TNF $\alpha$  production by macrophages in response to LPS, but CLEC-2 deficient platelets permitted the macrophages to produce greater amounts of TNF $\alpha$  (fig 4.36)

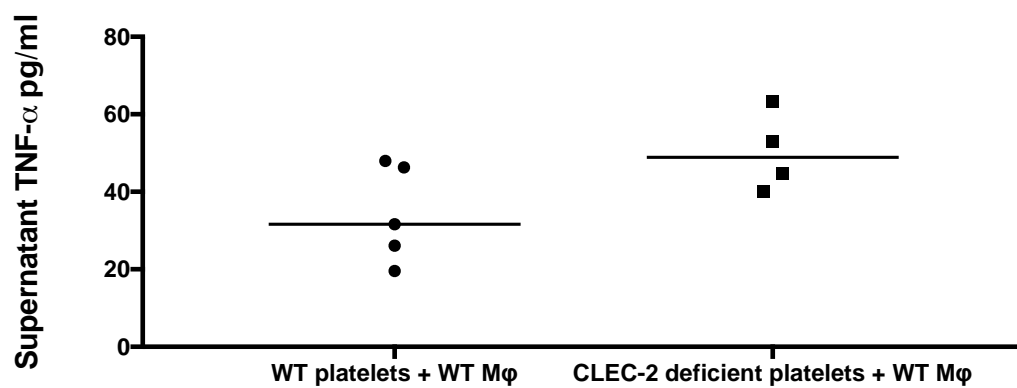


**Figure 4.36 CLEC-2 deficient platelets enhance hepatic macrophage TNF- $\alpha$  production after stimulation with LPS:**

Non-injured WT mice were sacrificed, their livers were removed and hepatic macrophages isolated. After being stimulated with LPS, the macrophages were co-incubated with either WT or CLEC-2 deficient platelets. The macrophage secretome was collected and analyzed for TNF- $\alpha$  levels via a sandwich ELISA. Each dot in the scatter plots represents macrophages from a single mouse, the bars represents median values of each group and the Mann Whitney test was used to gauge significance.

We then used CLEC-2 deficient platelets or podoplanin deficient macrophages and cultured them in LPS containing media. Our results demonstrate that removing CLEC-2 or podoplanin resulted in enhanced TNF $\alpha$  production by macrophages (fig 4.37), compared to CLEC-2 expressing platelet (WT) incubation with podoplanin expressing (WT) macrophages.

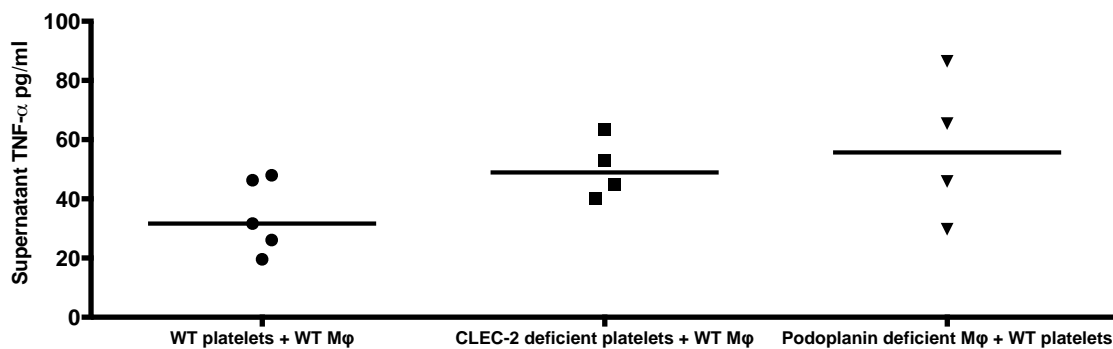


**Figure 4.37 Podoplanin deficient macrophages produce more TNF- $\alpha$  production after stimulation with LPS:**

Non-injured WT mice and podoplanin deficient (*Vav1-iCre<sup>+</sup>pdpn<sup>fl/fl</sup>*) mice were sacrificed, their livers were removed and hepatic macrophages isolated. After being stimulated with LPS, the macrophages were co-incubated with either WT or CLEC-2 deficient platelets. The macrophage secretome was collected and analyzed for TNF- $\alpha$  levels via a sandwich ELISA. Each dot in the scatter plots represents macrophages from a single mouse, the bars represents median values of each group.



#### **4.11.2. Etanercept pre-treatment abrogates neutrophil recruitment in CLEC-2 deficient mice**

We next aimed to confirm whether the enhanced TNF- $\alpha$  production in CLEC-2 deficient mice provided the cue for increased neutrophil recruitment and thus enhanced liver healing. We pretreated CLEC-2 deficient mice with a TNF- $\alpha$  blocking antibody (etanercept) or PBS (as a control), prior to induction of toxic liver injury (see treatment schedule in Fig 4.38). We found that pre-treatment of CLEC-2 deficient mice with etanercept reduced hepatic neutrophil accumulation and restored liver injury to WT levels (fig 4.38).

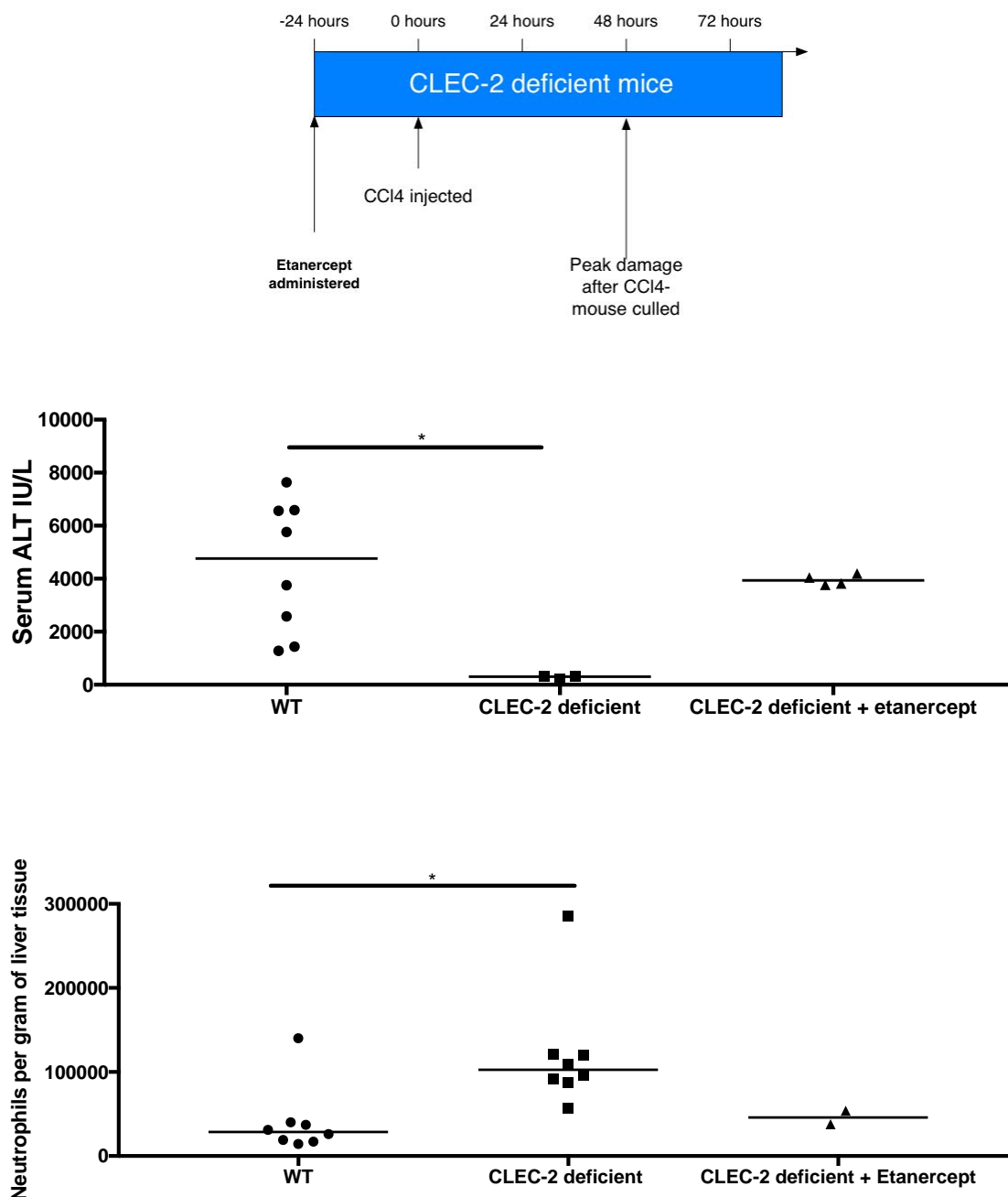


**Figure 4.38 Abrogating TNF- $\alpha$  function by pretreating CLEC-2 deficient mice with etanercept removes the protective effect of CLEC-2 deficiency:**

CLEC-2 deficient mice were pre-treated with either etanercept (10mg/Kg) or PBS as indicated in the timeline. All mice were then administered IP CCl<sub>4</sub> and sacrificed at 48 hours (top image). Pretreating CLEC-2 deficient mice with etanercept reduced hepatic neutrophil infiltration and restored hepatic injury to WT levels (middle and bottom graphs respectively) Each dot in the scatter plots represents a single mouse, the bars represents median values of each group and the Mann Whitney test was used to gauge significance \*P < 0.05, \*\*P < 0.01, \*\*\*P < 0.001.

#### **4.12. Hepatic CYP2E1 expression is unaffected by CLEC-2 or podoplanin deficiency**

Since both APAP and CCl<sub>4</sub> are metabolized by enzymes of the cytochrome P450 system, specifically CYP2E1 we next sought to investigate whether expression of this enzyme was altered in the CLEC-2 or podoplanin deficient mice. This would result in less hepatotoxic metabolites being produced and provide an alternative explanation for our findings. As expected we found that there was no significant difference in induction extent or localization when we examine CYP2E1 expression between WT and CLEC-2 or podoplanin deficient mice (fig 4.39)

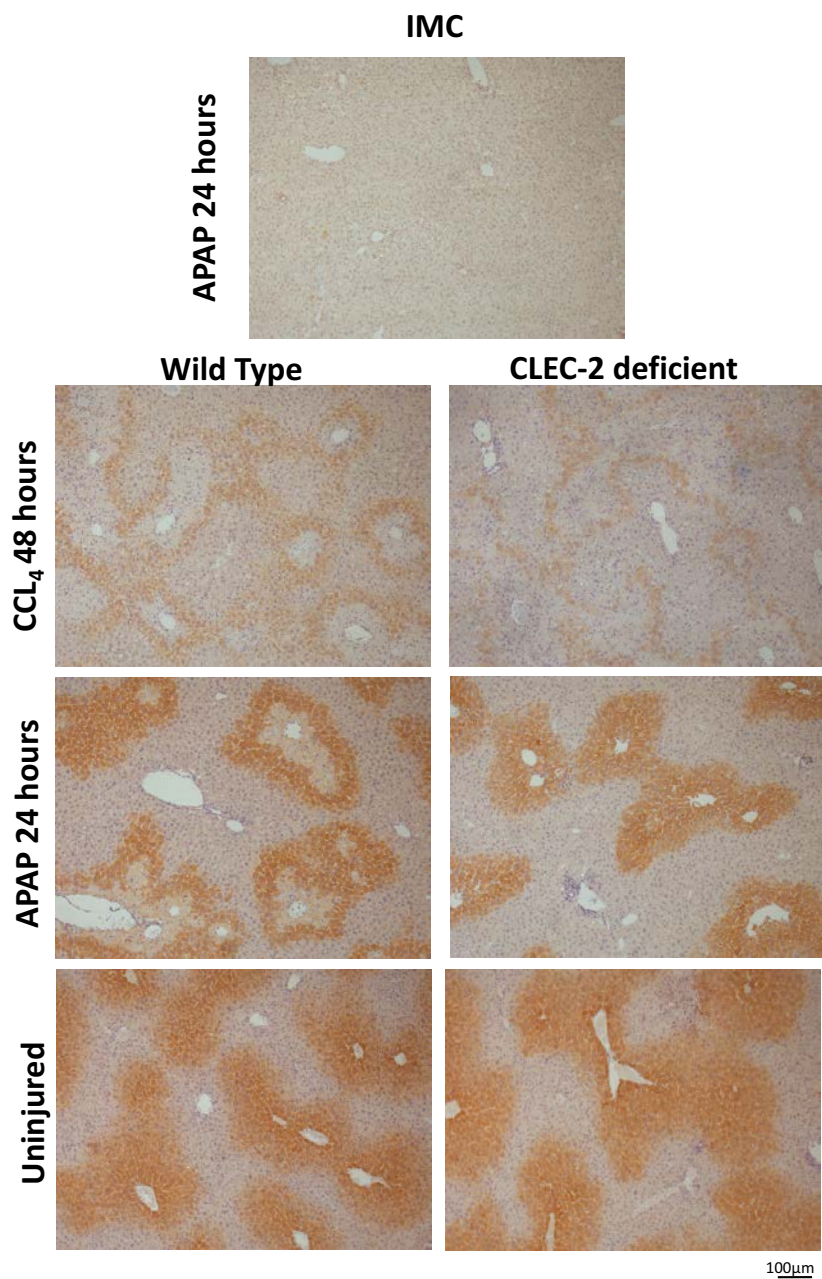


**Figure 4.39 Hepatic CYP2E1 expression is unaffected by CLEC-2 or podoplanin deficiency:**

Uninjured and injured (with APAP or CCl<sub>4</sub>) WT or CLEC-2 deficient mice were sacrificed at peak point of liver injury (48hrs-CCl<sub>4</sub>, 24hrs-APAP), or the corresponding time point for the uninjured control group. Mouse liver tissue was collected and paraffin embedded. The sections were then stained with a CYP2E1 antibody (or isotype matched control) and staining was visualized using DAB substrate (brown). Representatives images from at least 6 mice in each group shown at 10x original magnification.

Mouse genetic variant ( +/- AB pre-treatment)	Paracetamol induced peak liver injury (24 hours)	Carbon tetrachloride induced peak liver injury (48 hours)
WT	ALT <b>high</b> CD11bGR1 <b>low</b>	ALT <b>high</b> CD11bGR1 <b>low</b>
PF4cre <i>CLEC1b</i> <sup>fl/fl</sup>	ALT <b>low</b> CD11bGR1 <b>high</b>	ALT <b>low</b> CD11bGR1 <b>high</b>
Vav-1cre <i>PDPN</i> <sup>fl/fl</sup>	ALT <b>low</b> CD11bGR1 <b>high</b>	ALT <b>low</b> CD11bGR1 <b>high</b>
Podoplanin AB given to WT mice	ALT <b>low</b> CD11bGR1 <b>high</b>	ALT <b>low</b> CD11bGR1 <b>high</b>
Etanercept (antiTNF AB) given to PF4cre <i>CLEC1b</i> <sup>fl/fl</sup>	Data not available	ALT <b>high</b> CD11bGR1 <b>low</b>
Anti-ly6G AB (neutrophil depleting) given to PF4cre <i>CLEC1b</i> <sup>fl/fl</sup> mice	Data no available	ALT <b>high</b> CD11bGR1 <b>low</b>

**Table 4.1 The effect of genetic disruption and antibody treatment on toxic liver injury**

Summary of the effect(s) genetic mutant mice or blocking antibodies have on the development of toxic liver injury as gauged by serum ALT and intrahepatic neutrophil (CD11bGr1) accumulation.

#### 4.13. Discussion

Platelets have important roles in several pathophysiological processes relevant to liver disease (53); however as they often mediate seemingly opposing processes(53) their overall contribution to liver pathology is unclear and is likely to be disease and context dependent(37). We report a completely novel mechanism through which platelets accelerate recovery from acute liver injury in response to APAP and CCl<sub>4</sub> toxicity. After acute toxic injury to the liver (due to either APAP or CCl<sub>4</sub>) podoplanin is upregulated (in both humans and mice) on hepatic macrophages. These macrophages are likely to be derived from a combination of haematogenous and liver resident or Kupffer cells. We confirm that under resting or non-inflammatory conditions there is minimal podoplanin expression by these cells and thus little or no ligand available for CLEC-2 dependent platelet activation. On stimulation (i.e. during acute liver damage), the number of macrophages expressing podoplanin increases within the liver and this macrophage expressed podoplanin then activates platelets via CLEC-2. We demonstrate that abrogating CLEC-2-dependent platelet activation from macrophage expressed podoplanin enhances liver healing after toxic injury by increasing hepatic neutrophil infiltration. This clearly has therapeutic potential in human APAP induced acute liver failure where current therapies have limited efficacy and a challenging window for best benefit. One of the concerns that has been raised in the past when considering anti-platelet therapy in liver disease, is the risk of blocking platelet function in clinical situations where a bleeding diathesis may be present. As CLEC-2 mediated platelet activation is independent of major haemostatic

pathways, and studies confirm that the bleeding risk CLEC-2 blockade confers is minimal(215), this pathway becomes particularly attractive for therapeutic intervention.

#### **4.13.1. Experimental design**

In order to establish the pattern of toxic injury and gauge the sterile inflammatory response in mice I began my experiments with the CCl<sub>4</sub> model. Although arguably not of direct relevance to human liver disease this compound elicits fatty degeneration, fibrosis, hepatocellular death, and carcinogenicity(160) within the liver, these are liver pathological processes with correlates with human liver disease and thus CCl<sub>4</sub> induces a pattern of liver inflammation not dissimilar to human liver diseases including steatohepatitis and drug induced liver injury(216). Another attractive feature of CCl<sub>4</sub> is the solubility of this compound in oil and thus ease of use, lower and more predictable toxicity (compared to APAP) to mice, and finally the reproducibility of the model. I thus used CCl<sub>4</sub> to set up all the initial acute toxic liver injury experiments, and then moved on to paracetamol induced liver damage. Paracetamol due to its lower solubility, and arguably higher and more acute toxicity required greater care in setup and more intensive monitoring after injection. This limited the numbers of animals I was allowed to place on protocol and as a result certain experiments had smaller number of mice than would be required to adequately power studies.

Human paracetamol overdose is mechanistically very similar to what is observed in rodent models. Exposure of primary human hepatocytes to high levels of

paracetamol generates excessive amounts of NAPQI which depletes GSH, drives mitochondrial protein adduct formation and cell death(202) . It should be noted that minor differences between humans and mice have been reported when studying paracetamol induced liver damage including slower but larger amounts of protein adduct formation(202) . However, allowing for these minor differences murine models still provide a very valuable resource for studying acute toxic liver damage.

The podoplanin deficient mice ( $Vav1-iCre^+pdpr^{fl/fl}$ ) were difficult to breed, and thus we only had limited numbers of mice available. Therefore we focused on time points of maximal injury noted from CLEC-2 deficient and WT animals' experiments (fig 4.24). Although we show that in the CLEC-2 deficient mice the initial liver injury after APAP and  $CCl_4$  is comparable between CLEC-2 and WT mice and that there is then enhanced recovery in the CLEC-2 deficient mice, we do not actually show this in the podoplanin deficient or podoplanin antibody injected mice, merely that there is less liver injury compared to WT mice at peak points of liver damage. To demonstrate that the same mechanism was at work in the podoplanin deficient mice, a similar set of experiments comprehensively gauging injury (and healing) at each of the time points after injection would be necessary.

Although we used the same process for isolating macrophages from liver digests as we did for flow cytometric analysis; and we thus confirm that WT mice had little inter-animal variability in terms of number of macrophages, we did not actually count the number of macrophages per well in the vitro studies. To minimize variability I used the one mouse liver and uniformly suspended macrophages prior to plating out in the



6 well plates. To improve accuracy of our experiments, the *in vitro* arm should be repeated with a standardized amount of macrophages per well. This would permit a more accurate way of expressing this data as the amount TNF $\alpha$  produced per a standardized number of cells.

#### **4.13.2. TNF $\alpha$ and macrophages in acute liver injury**

Our data reveals that enhanced liver recovery correlates with increased TNF $\alpha$  levels. Activation of macrophages and the role of TNF $\alpha$  in mediating hepatic regeneration fits with accepted paradigms of liver healing(217–219) . Abrogating TNF $\alpha$  function negatively influences both liver regeneration and outcomes after acute hepatic inflammation in both mice and humans; the failure of anti-TNF $\alpha$  therapy to result in clinical improvement in patients with severe alcoholic hepatitis being particularly notable(11,220). Platelet interaction with macrophages and monocytes has been investigated in ischaemia-reperfusion models(117,186,221) in mice, and the ability of platelets to modulate both monocyte and macrophage function, cytokine profile and even final phenotype have previously been described(139,140); the specific molecular pathways that platelets may use to do this are however less clear. Our investigations suggest that platelets sequester to podoplanin expressing macrophages in the acutely injured liver. To elucidate the role of the CLEC-2/podoplanin pathway in this interaction we isolated hepatic macrophages and used LPS to stimulate expression of podoplanin. We found that LPS stimulated podoplanin expressing macrophages that were co-incubated with CLEC-2 deficient platelets produced larger amounts of TNF $\alpha$  than macrophages co-cultured with WT platelets.

Thus it seems likely that CLEC-2 operates after liver injury to dampen TNF $\alpha$  production. Our *in vivo* investigations substantiate this by revealing that higher serum TNF $\alpha$  levels are found after toxic liver injury in CLEC-2 deficient mice compared to WT mice. Our models demonstrate that the result of enhanced TNF $\alpha$  production after a toxic insult is enhanced hepatic neutrophil infiltration, which then correlates with accelerated liver recovery. Thus CLEC-2 deficiency enhances the TNF $\alpha$  driven inflammatory response. As inflammation is a pleiotropic process that can both heal and worsen organ damage, the physiological role of CLEC-2 in certain situations may actually be protective. However, during toxic liver damage; specifically, APAP and CCl<sub>4</sub> induced liver damage, CLEC-2 mediated platelet activation blocked the development of reparative inflammation which then worsened liver damage. The observation that platelets can promote cytokine release from macrophages is not novel(142) but to our knowledge ours is the first molecular definition of a pathway that links platelet activation with suppression of cytokine responses and liver repair. Ishida et al suggest that TNF $\alpha$  accentuates liver damage during APAP injury(222) and Sato et al report reduced hepatic injury in models of CCl<sub>4</sub> hepatitis using TNF $\alpha$  neutralizing antibodies(205). In contrast to these findings others have noted a reduction in liver healing or hepatocyte proliferation (and thus greater injury) in TNF receptor deficient mice (*TNFR1*<sup>-/-</sup>)(223,224). Our data suggests that TNF $\alpha$  in the context of acute toxic liver injury actually aids liver recovery, but we only have data from the CCl<sub>4</sub> model. Thus it would be necessary to repeat these experiments and

establish the TNF $\alpha$  levels in WT or mice with CLEC-2 abrogation after APAP treatment.

#### **4.13.3. Neutrophil driven liver repair**

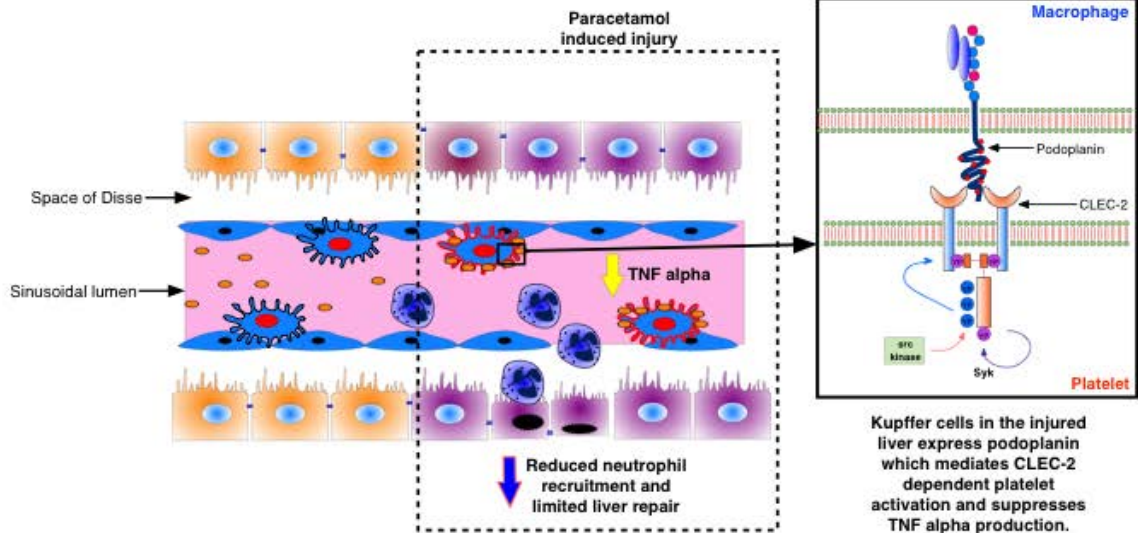
It seems paradoxical that enhancing liver inflammation (specifically increasing hepatic neutrophil infiltration) by blocking the CLEC-2/Podoplanin axis actually aids liver healing, but several studies, including ours confirm the role of restorative neutrophil driven inflammation(216), particularly in the context of sterile injury(50). Neutrophil dysfunction is part of the immune paresis that contributes to poor outcomes after liver inflammation(225); artificially enhancing neutrophil levels using granulocyte-colony stimulating factor (G-CSF) has been shown to improve liver recovery in patients with alcoholic hepatitis(226) and importantly neutrophil activation is critical to injury resolution after APAP overdose (44). TNF- $\alpha$  has well established roles in coordinating neutrophil flux, it thus seems plausible that the enhanced TNF- $\alpha$  production that blocking CLEC-2 mediated platelet activation resulted in drives enhanced neutrophil recruitment to the injured liver which in turn enhanced liver recovery. The molecular and cellular cues that 'switch-on' such neutrophil mediated reparative inflammation are yet to be deciphered. We provide the first evidence that during acute liver injury platelets block the development of such neutrophil mediated 'healing' inflammation; by abolishing CLEC-2 dependent platelet activation we manipulate the inflammatory response after a toxic insult to specifically increase hepatic neutrophil infiltration and enhance liver recovery. We thus provide the first

demonstration to our knowledge of artificially increasing reparative neutrophil recruitment to the acutely damaged liver.

#### **4.13.4. Developmental and egress abnormalities in CLEC-2/Podoplanin deficient mice**

An important point to note is that both CLEC-2 and podoplanin have important roles during lymphatic development, specifically in maintaining blood and lymphatic separation during embryogenesis(170,227), and that CLEC-2 positive dendritic cells use lymphatic- expressed podoplanin to exit the lymph nodes(182). The *PF4CreCLEC1b<sup>fl/fl</sup>* and *Vav1-iCre<sup>+</sup>pdpn<sup>fl/fl</sup>* mice, may have thus had subclinical lymphatic defects which could contribute to neutrophil recruitment or egress in a manner similar to that described for dendritic cells. However, our observations of enhanced neutrophil inflammation and thus repair, when we conducted experiments using a function-blocking podoplanin antibody in adult wild type mice with normal lymphatic development suggested that altered recruitment or retention dynamics linked to lymphatic defects are insignificant.

**a) Preserved CLEC-2 podoplanin axis**



**b) Genetic or antibody mediated disruption of the CLEC-2/podoplanin**

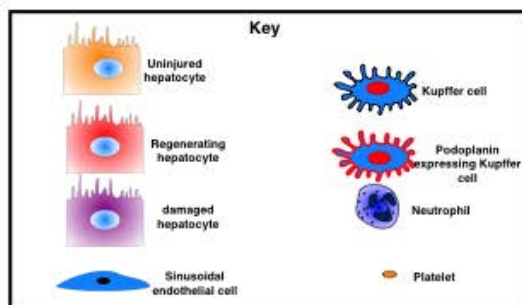
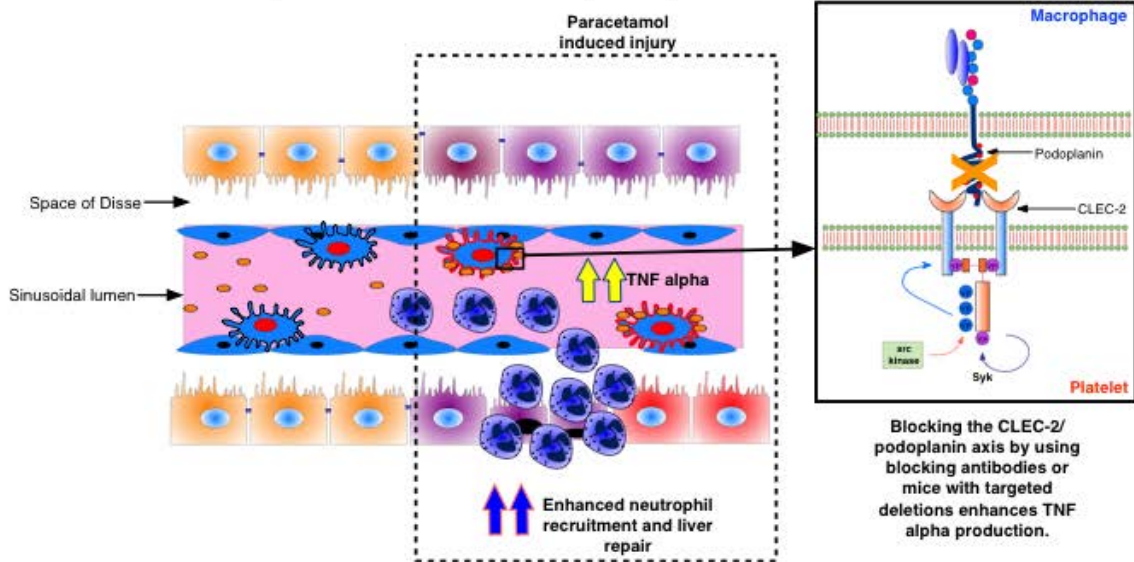


**Figure 4.40 Blocking the CLEC-2 mediated platelet activation enhances TNF- $\alpha$  production to increase neutrophil recruitment and healing in the injured liver**

a) Upon liver injury Kupffer cells express increasing amounts of podoplanin, which then activates platelets via CLEC-2. This interaction dampens the production of Kupffer cell produced TNF- $\alpha$  and results in reduced hepatic neutrophil recruitment and blunted liver recovery. b) Blocking the CLEC-2/podoplanin axis using either mice with targeted deletions for CLEC-2 or podoplanin or using a podoplanin function blocking antibody increases Kupffer cell production of TNF- $\alpha$ . This enhanced TNF- $\alpha$  recruits a larger amount of neutrophils to the damaged liver which then accelerate liver healing.

## 5. The role of platelet CLEC-2 in chronic murine liver injury

Fibrosis is a consequence of chronic activation of the wound healing mechanism within the liver. Iterative bouts of inflammatory activity due to variety of aetiologies including alcoholic and non-alcoholic liver disease, viral hepatitis, auto immune liver disease result in over activation of this reparative pathway eventually causing activation of the hepatic stellate cells(HSCs), which are widely regarded as the key effector cells driving liver fibrosis(228). HSC activation can be divided into two stages: initiation and perpetuation. Initiation, also referred to as the pre inflammatory stage represents the early changes to gene expression and phenotype that occur within HSCs in response to the products of acute hepatic injury including cytokines from KCs, apoptotic bodies(229) and DAMPs(230). This stage in effect primes the HSCs for the next stage, B) Perpetuation-here the HSCs undergo complex behavioural changes including chemotaxis, contractility and proliferation(229). Activated HSCs acquire a myofibroblast like phenotype thus assuming fibrogenic functions and depositing large amounts of extra-cellular matrix (ECM) within the liver. Fibrosis at these early stages remains reversible; removal of the injurious stimuli results in HSC senescence or apoptosis and thus fibrosis reversal (228). Continued activation of this pathway however results in the parenchymal architecture of the liver being progressively replaced by fibrous tissue, the hepatic response to this is the development of regenerative nodules and thus starts cirrhosis which essentially marks the of irreversible end stage liver disease(3).

A critical cell in the control of fibrosis through its ability to modulate HSC plasticity is the macrophage(13). Macrophages contain the potently fibrogenic cytokines TGF- $\beta$  and PDGF, and macrophage conditioned media has been shown to promote HSC activation *in vitro* through the actions of these cytokines (137). Macrophages can also negatively regulate the development of hepatic fibrosis by promoting HSC apoptosis through MMP-9 and TNF $\alpha$  -related apoptosis-inducing ligand (TRAIL) (137) and also dictating extra cellular matrix or scar remodeling during liver fibrosis (by secreting MMP-9 and MMP-13)(231). Depleting macrophages at the time of onset of liver injury or fibrosis blocks the development of fibrosis, however at later time points blocks their ability to aid scar resolution(137). Ramachandran et al have described the principal MMP expressing population of restorative macrophages as the CD11B<sup>hi</sup> F4/80<sup>int</sup>Ly-6C<sup>lo</sup>(45), and demonstrated that depleting this specific population caused a failure in scar remodeling(45). Hepatic macrophages thus both promote and abrogate experimental fibrosis through their downstream actions(40). As our data in the acute models has suggested that platelet activation via macrophage expressed podoplanin is important in the pathogenesis of acute liver damage due to a toxic agent, we sought to explore the relevance of this pathway in chronic liver disease.

Although there are numerous advantages to using animal models to better understand human fibrosis including limiting variables and strategic timing of sampling during fibrosis and resolution phases(232) there are notable limitations. Particularly relevant is the profound aversion rodents have for alcohol, as well as the tenacity their livers have to withstand alcohol induced fibrosis. Differing patterns in



development of fibrosis in mice and humans for example periportal vs pericentral and the lack of murine models to adequately mimic all the different types of human liver disease suggest that caution must be exercised when translating animal data to the human setting(232).

Various animal models of fibrosis are available for experimental use, each with its own advantages and limitations(233). Thus the animal models we used to study hepatic fibrosis are introduced below.

### **5.1. Carbon tetrachloride induced chronic liver injury**

Acute CCl<sub>4</sub> mediated injury is characterized by a transient liver injury and immune cell recruitment allowing a return to hepatic haemostasis. Our experience using carbon tetrachloride to induce hepatic necrosis and then liver healing inflammation after a single injection has been described above (chapter 4). However repetitive CCl<sub>4</sub> injection results in iterative bouts of hepatic damage and over activation of wound healing pathways, which then drive liver fibrosis. Repetitive CCl<sub>4</sub> administration in mice represents a highly tractable and thus reproducible model of liver fibrosis model. The CCl<sub>4</sub> induced liver fibrosis model has the additional benefit of having a resolution phase after cessation of CCl<sub>4</sub> administration, which allows for not only study of development of liver fibrosis but resolution from liver fibrosis as well (232).

The development of liver fibrosis due to CCl<sub>4</sub> can roughly be divided into three phases. The initial phase involves acute toxic injury and a dominantly myeloid cell

driven innate immune response that initially worsens liver damage and then drives a strong regenerative response characterized by hepatocellular (both parenchymal and non-parenchymal) regeneration. The second phase is where the deposition of fibrous tissue is observed, this occurs as early as 3 weeks after bi-weekly IP CCl<sub>4</sub> injections (234). Fibrosis initially appears in pericentral (around the central vein) areas, and then progresses to bridging fibrosis at around 4-6 weeks of treatment(234) followed by nodular regeneration and eventually hepatocellular cancer (235). A notable advantage of the chronic CCl<sub>4</sub> model in mice is the distinct resolution phase one observes once the toxic stimulus is withdrawn, thus several weeks after cessation of CCl<sub>4</sub>, complete regression of fibrosis is observed (234). Such regression or reversal of fibrosis is a component of many human liver diseases including autoimmune hepatitis, biliary obstruction, iron overload, NASH, and viral hepatitis B and C (236–239).

## **5.2. Methionine-choline deficient diet**

NAFLD or non-alcoholic liver disease represents one of the most rapidly rising causes of liver disease in the world and is certainly the commonest cause of abnormal liver enzymes in the United Kingdom(1) . The methionine choline deficient diet is a commonly used model in mice to mimic the development of initially a steatotic liver followed by inflammation or oxidation and thus eventually liver fibrosis(2); this two hit (inflammation within steatotic areas which precedes the development of liver fibrosis) mechanism parallels human NAFLD. Day et al proposed that liver damage in human NAFLD has two distinct driving phases(240).

The first hit is due to a combination of impaired mitochondrial beta oxidation, impaired VLDL synthesis and hepatocyte triglyceride accumulation(234). The second hit is probably due to mitochondrial dysfunction leading to enhanced intrahepatic oxidative stress, which then results in the oxidation of accumulated hepatic fat thus driving a powerful necroinflammatory response(241). The associated chronic inflammatory response is driven and maintained by multiple cytokines including  $TNF\alpha$ , IL-1 and IL-6, which then results in Kupffer cell driven HSC activation and liver fibrosis (241). -

The MCD diet is a commonly used diet to model NASH/NAFLD in rodents. This diet is high in sucrose and fat but lacks methionine and choline which are important for the synthesis of very low density lipoproteins (VLDLs) by the liver and critical in the mitochondrial beta oxidation pathway(235). Thus this diet limits substrate availability for phosphatidylcholine synthesis resulting in the inability of the liver to assemble VLDLs and reduces hepatic triglyceride secretion (242). Mice fed this diet can develop hepatic inflammation as soon as three days after starting the diet, this is followed by pericentral steatosis at around 2 weeks. The timing however of the initial necroinflammatory response is highly variable, and it can take up to 3 weeks. At around 3-4 weeks a pronounced necroinflammatory injury is noted, and this is then followed by progressive fibrosis(241). The MCD diet therefore induces a similar two hit pattern of steatosis followed by inflammatory damage as seen in human NAFLD. Additionally, enhanced levels of ROS driven oxidative stress with concomitant activation of  $TNF\alpha$  signaling seen with this diet have established the MCD diet as

one of the best models for studying non-alcoholic steatohepatitis (234). The major disadvantage of this model is the lack of classical metabolic phenotype that often precedes human fatty liver disease(234). Mice on this diet for instance actually lose weight, have reduced serum cholesterol and triglyceride levels and critically display no insulin resistance(161).

### **5.3. Aims**

We have already established from our studies in chronically damaged and thus fibrotic human livers that a significant upregulation of podoplanin occurs (chapter 3). Investigating CLEC-2-dependent platelet activation and how it may influence macrophage behaviour in the context of hepatic fibrosis has particular relevance when one considers the central role these cells play in modulating HSC behaviour and the fact that our data clearly demonstrates that upon liver injury hepatic macrophages upregulate podoplanin (section 4.5). Thus we wanted to investigate whether the podoplanin-CLEC-2 axis had a role in the development of hepatic fibrosis. Our aims for this section were as follows:

- 1) To establish the pattern of podoplanin expression the chronically injured mouse liver
- 2) To examine whether blocking CLEC-2 dependent platelet activation influenced the development of liver fibrosis in murine models of fibrosis.

## 5.4. Use of the chronic carbon tetrachloride model

The data from acute murine injury models revealed that mice deficient in CLEC-2 or podoplanin exhibited enhanced healing from acute liver injury. Platelet activation due to this axis in the acute setting thus served to perpetuate or worsen liver injury. Furthermore our human data reveals that there was a clear correlation between severity of liver disease as gauged by MELD score (section 3.5.2) and podoplanin expression in humans. We wished to study the role this axis may have in the development of fibrosis and thus used the PF4Cre*CLEC1b*<sup>fl/fl</sup> mouse which has platelets selectively deficient in CLEC-2 and administered bi-weekly CCl<sub>4</sub> injections for 8 weeks to induce liver fibrosis.

### 5.4.1. CLEC-2 deficient and wild type exhibit centrilobular fibrosis after chronic CCl<sub>4</sub> exposure

Both WT and CLEC-2 deficient mice exhibited fibrosis after 7 weeks of intraperitoneal carbon tetrachloride injections. All mice exhibited peri-venular fibrosis with extension to periportal areas (see representative images in fig 5.1). To minimize the acute necro-inflammatory damage a single dose of CCl<sub>4</sub> results in, we only sacrificed the mice 96 hours after the last dose of IP CCl<sub>4</sub> (fig 5.1-time line).

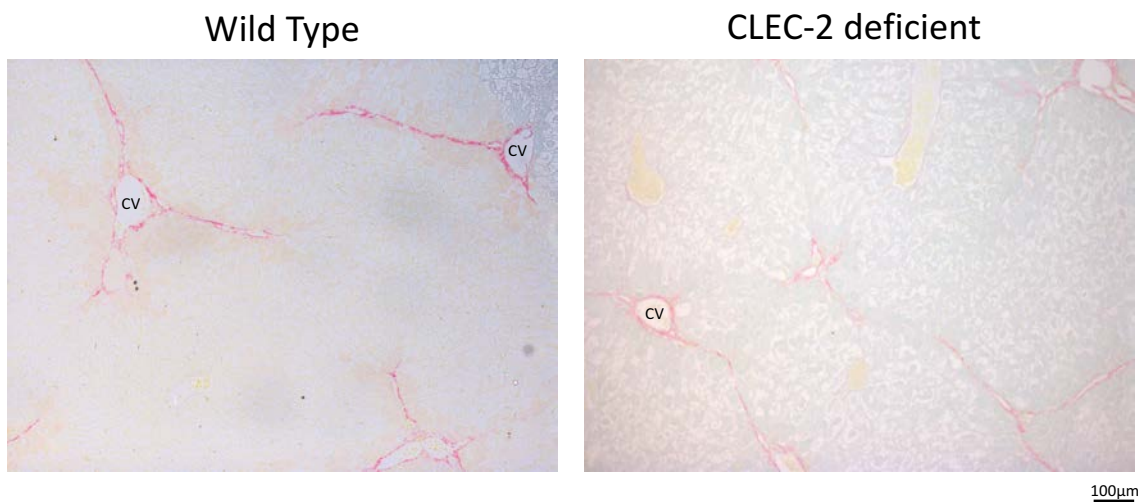
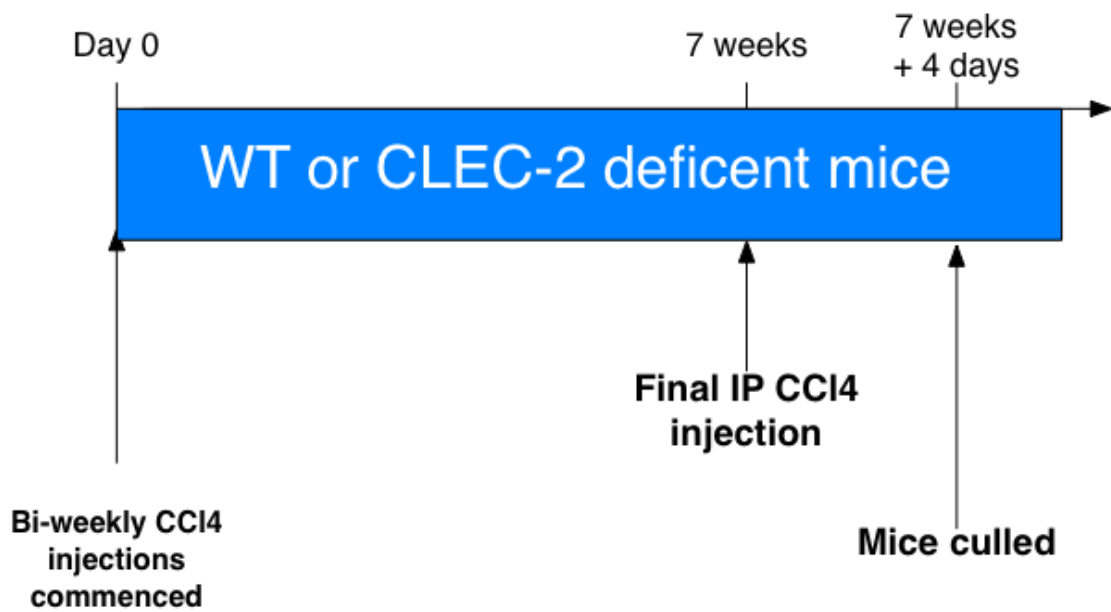


**Figure 5.1 Mice exhibit centrilobular fibrosis after chronic CCl<sub>4</sub> administration:**

WT or CLEC-2 deficient mice were injected twice weekly with CCl<sub>4</sub> injections. Mice were sacrificed at the end of 7 weeks (after a total of 14 injections). The livers were harvested, paraffin embedded and sections stained using picrosirius red. Representative images from at least 5 mice in each group at 10x magnification are shown. CV-central vein.

Initial histological analyses using picosirius red stain seemed to suggest that the CLEC-2 deficient mice exhibited greater amounts of fibrosis than the wild type mice (see representative images in figure 5.2). The fibrosis pattern was however similar in both groups of mice i.e. peri-venular (around central vein) with secondary extension to portal areas.

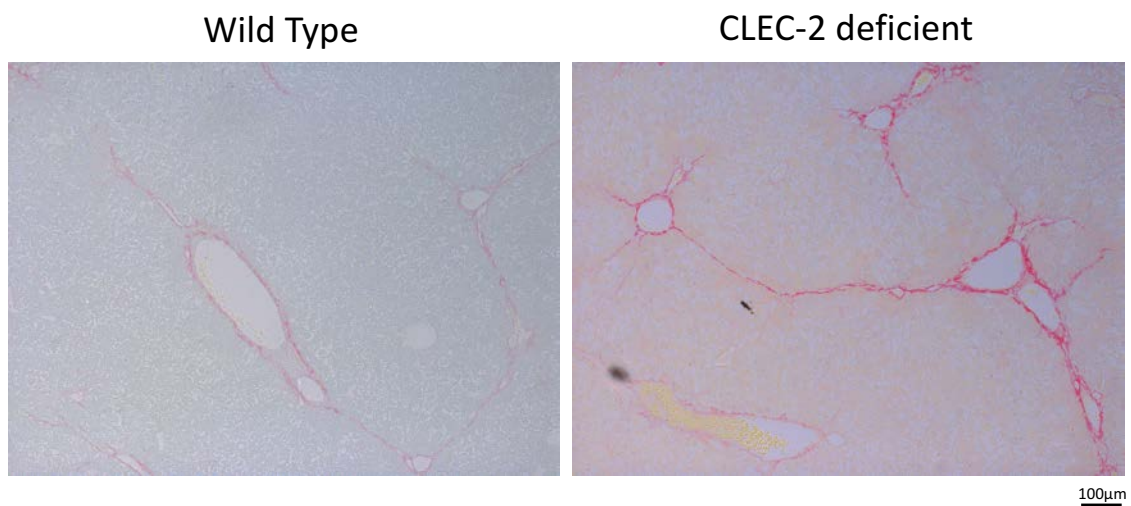


**Figure 5.2 CLEC-2 deficient mice exhibit greater fibrosis after chronic CCl<sub>4</sub> administration:**

WT or CLEC-2 deficient mice were injected twice weekly with CCl<sub>4</sub> injections. Mice were sacrificed at the end of 7 weeks (after a total of 14 injections). The livers were harvested, paraffin embedded and sections stained using picosirius red. Representative images from at least 5 mice in each group at 10x magnification are shown.

To definitively quantify the level of hepatic fibrosis seen, we next undertook a hydroxyproline assay (fig 5.3). This revealed that although the CLEC-2 deficient mice had a slightly higher median (261.85 vs 241.7 $\mu$ g/gm of liver) hydroxyproline content, this was not statistically relevant when compared to WT mice. Reassuringly both WT and CLEC-2 deficient mice that had been administered CCl<sub>4</sub> had a significantly higher content of hepatic hydroxyproline compared to WT control animals that had been administered just mineral oil.

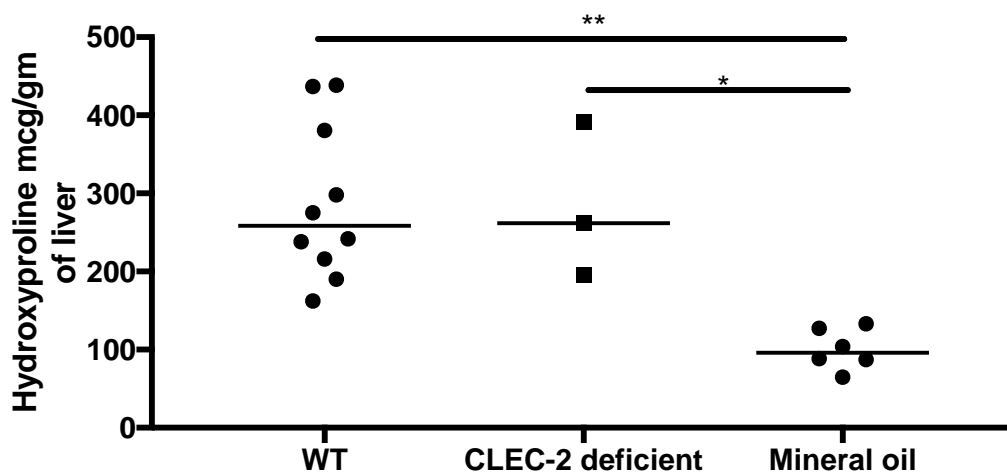


**Figure 5.3 CLEC-2 deficient and WT mice have equivalent levels of fibrosis after chronic CCl<sub>4</sub> administration:**

WT or CLEC-2 deficient mice were injected bi weekly with CCl<sub>4</sub> injections or mineral oil. Mice were sacrificed at the end of 7 weeks (after a total of 14 injections). The livers were harvested, homogenized and treated with trichloroacetic acid to enable protein precipitation. The hydroxyproline concentration of the protein precipitant was then determined by colorimetric analysis using 4-(Dimethylamino)benzaldehyde (DMAB). Groups incorporated between 3 and 10 mice, data from individual mice are shown by a single point and median values are indicated by horizontal bar. Data are amount of hydroxy proline per gram of liver tissue, and test Mann-Whitney indicated significant differences between groups as indicated (\*P < 0.05, \*\*P < 0.01, \*\*\*P < 0.001).



#### 5.4.2. CLEC-2 deficient mice exhibit periportal podoplanin expression after induction of liver fibrosis

We next examined hepatic podoplanin expression after chronic CCl<sub>4</sub> administration. Similar to acute CCl<sub>4</sub> or APAP injury, podoplanin expression was again restricted to portal areas in both WT and CLEC-2 deficient mice after chronic CCl<sub>4</sub> administration.

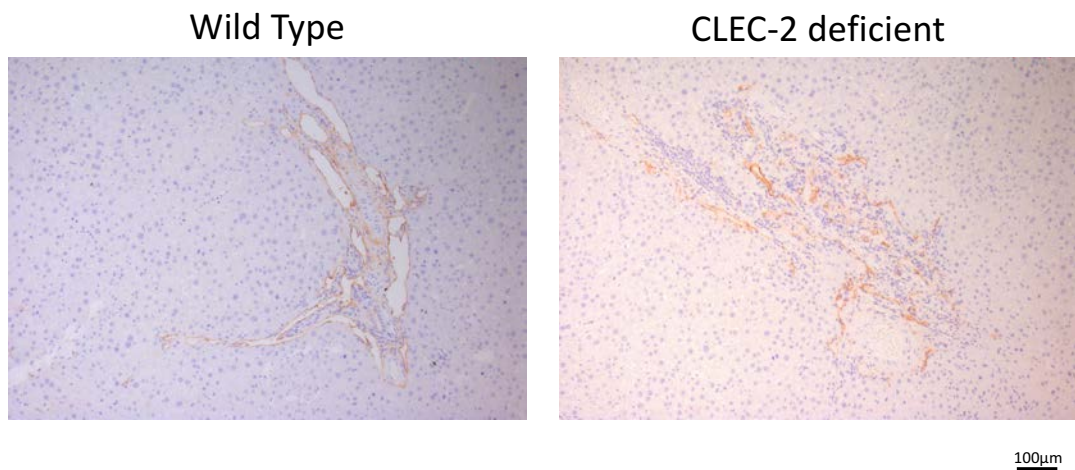


**Figure 5.4 WT and CLEC-2 deficient mice express podoplanin in portal areas after chronic CCl<sub>4</sub> administration:**

WT or CLEC-2 deficient mice were injected with twice weekly CCl<sub>4</sub> injections or mineral oil alone. Mice were sacrificed at the end of 7 weeks (after a total of 14 injections). The livers were harvested and paraffin embedded. Podoplanin was visualized using indirect immunohistochemical staining with DAB substrate(brown) on paraffin-embedded murine liver sections. Representative images from 9 mice are shown at 10X magnification (IMC was negative-not shown)

Analysis of portal areas showed that a large amount of portal podoplanin-expressing cells and vessels were interspersed amongst the fibrotic portal tracts (fig 5.5) when fibrosis was severe enough to include these areas. These cells had a morphological appearance suggesting they were macrophages and the vessels were morphologically consistent with both expanded lymphatics and portal venules. Podoplanin expression seemed greater on cells of the inflammatory infiltrate (macrophages) in the CLEC-2 deficient mice whilst podoplanin expression in WT mice was in contrast upon a combination of lymphatics and veins (figure 5.5).

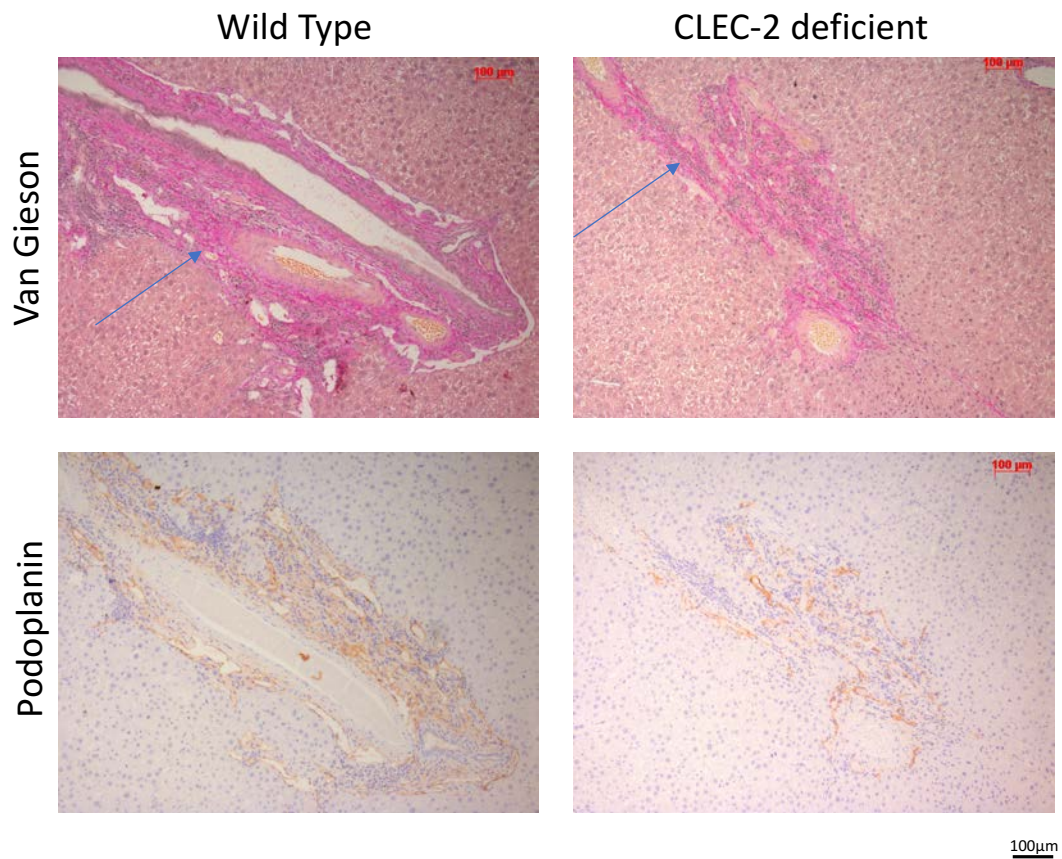


**Figure 5.5 Podoplanin expression increases in fibrotic portal tracts:**

WT or CLEC-2 deficient mice were injected with twice weekly CCl<sub>4</sub> injections or mineral oil alone. Mice were sacrificed at the end of 7 weeks (after a total of 14 injections). The livers were harvested and paraffin embedded. Podoplanin was visualized using indirect immunohistochemical staining with DAB substrate (brown) on paraffin-embedded murine liver sections or the sections were stained for collagen (pink, arrows) using a Van Gieson stain. Representative images of portal tracts are shown at 10X magnification (IMC was negative-not shown). Slides are from sequential sections.

To see whether it was the development of fibrosis that resulted in a 'local' upregulation of podoplanin we also examined centrizonal areas within murine livers where maximal fibrosis was seen in CCl<sub>4</sub> mediated models of fibrosis. Importantly although we noted fibrosis here, podoplanin expression was not seen in centrizonal/peri-venular areas (fig 5.6).

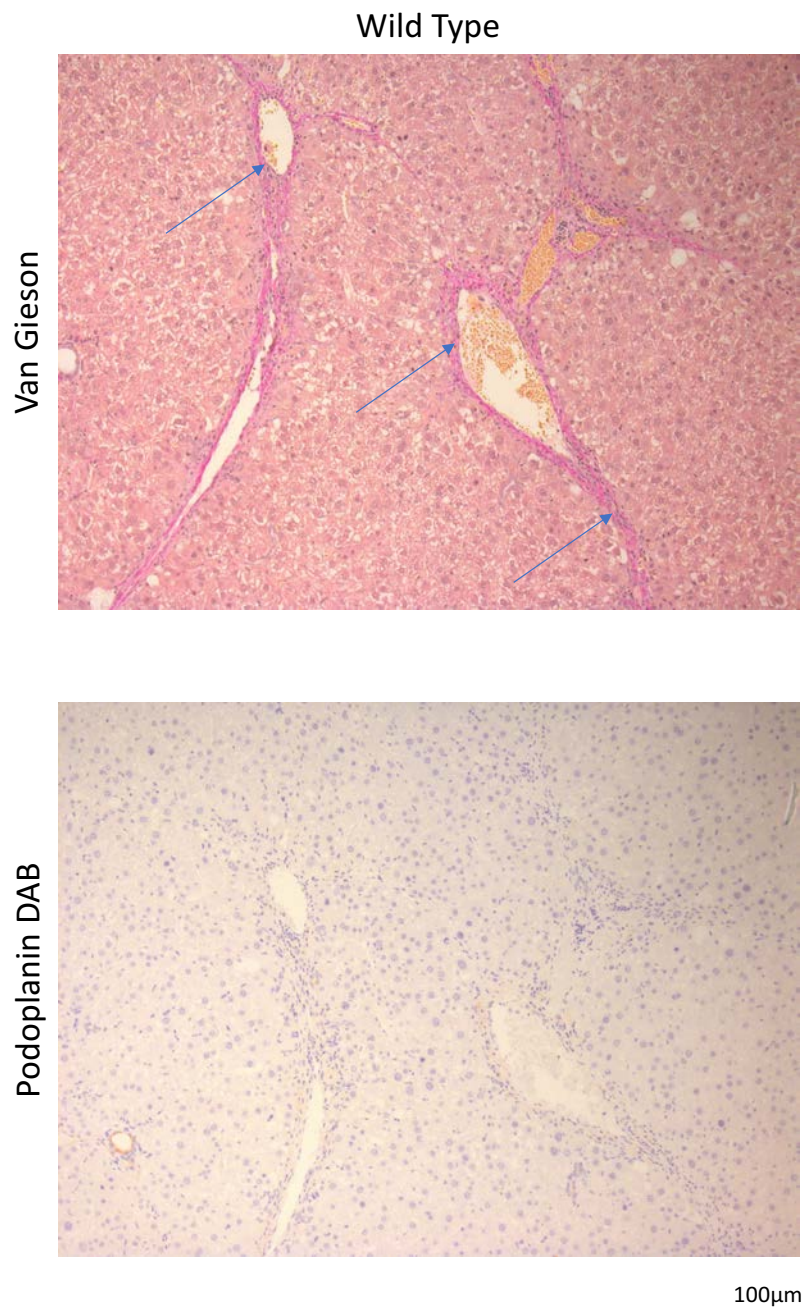


**Figure 5.6 Podoplanin expression does not increase in centrizonal areas after chronic CCl<sub>4</sub> intoxication:**

WT or CLEC-2 deficient mice were injected with twice weekly CCl<sub>4</sub> injections or mineral oil alone. Mice were sacrificed at the end of 7 weeks (after a total of 14 injections). The livers were harvested and paraffin embedded. Podoplanin was visualized using indirect immunohistochemical staining with DAB substrate (brown) on paraffin-embedded murine liver sections or the sections were stained for collagen (pink, arrows) using a Van Gieson stain. Representative images from both WT and CLEC-2 deficient mice are shown at 10X magnification (IMC was negative-not shown). Slides are from sequential sections which thus show the same area.

#### **5.4.3. CLEC-2 deficient mice have altered hepatic inflammation and injury after chronic CCl<sub>4</sub> administration**

We next analyzed the level of injury within the livers of mice after chronic CCl<sub>4</sub> administration and found that similar to our acute experiments the serum ALT was lower in the CLEC-2 deficient group (median serum ALT: WT mice 838IU/L vs CLEC-2 deficient mice 415IU/L) and this correlated with a trend of higher serum TNF  $\alpha$  levels (median serum TNF $\alpha$ : WT mice 10.43pg/ml vs CLEC-2 deficient mice 16.95pg/ml).

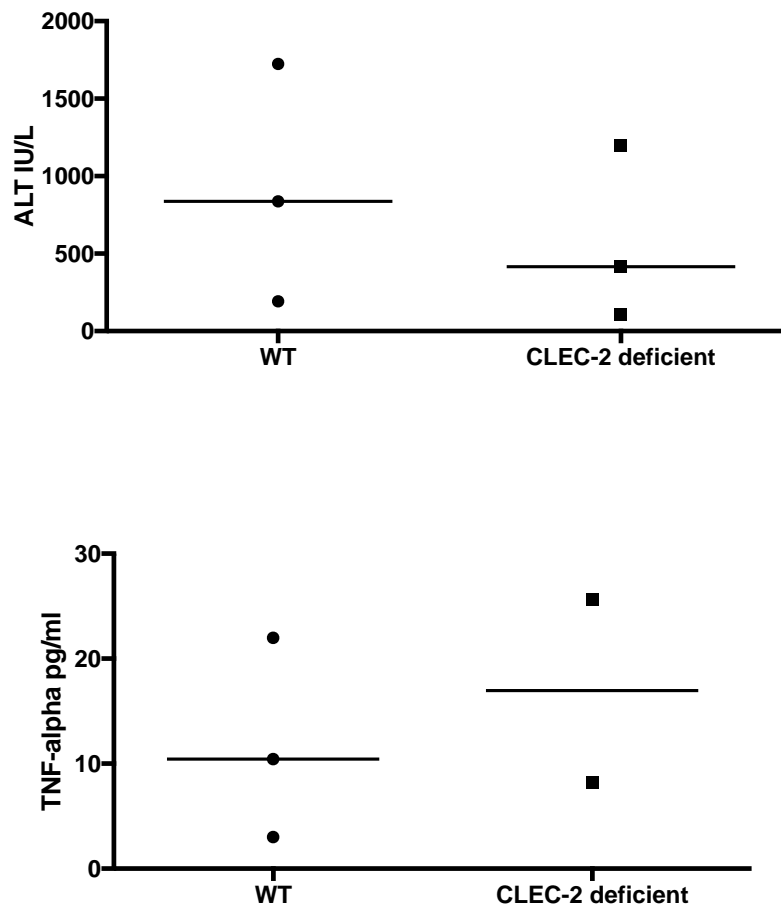


**Figure 5.7 CLEC-2 deficient mice exhibit less necrotic damage after chronic CCl<sub>4</sub> administration:**

WT or CLEC-2 deficient mice were injected with twice weekly CCl<sub>4</sub> injections or mineral oil alone. Mice were sacrificed at the end of 7 weeks (after a total of 14 injections). Groups incorporated 3 mice in each, data from individual mice are shown by a single point and median values are indicated by horizontal bar. Data are serum level of either TNF- $\alpha$  or serum ALT level and the Mann-Whitney test indicated significant differences between groups as indicated.

#### 5.4.4. Cellular infiltration

Next, we used our cytometric approach to see if the higher levels of serum  $\text{TNF}\alpha$  observed in CLEC-2-deficient animals influenced hepatic leukocyte recruitment. We thus digested murine livers and isolated infiltrating leukocytes as described in chapter 2. Importantly we also specifically examined the livers for the presence of pro-fibrotic ( $\text{Cd45}^+\text{Ly6G-Ly6C}^+ \text{Cd11b}^+\text{Cd3}^-$ ), and pro-resolution ( $\text{Cd45}^+\text{Ly6G-Ly6C}^- \text{Cd11b}^+\text{Cd3}^-$ ) (see gating strategy in fig 5.8).



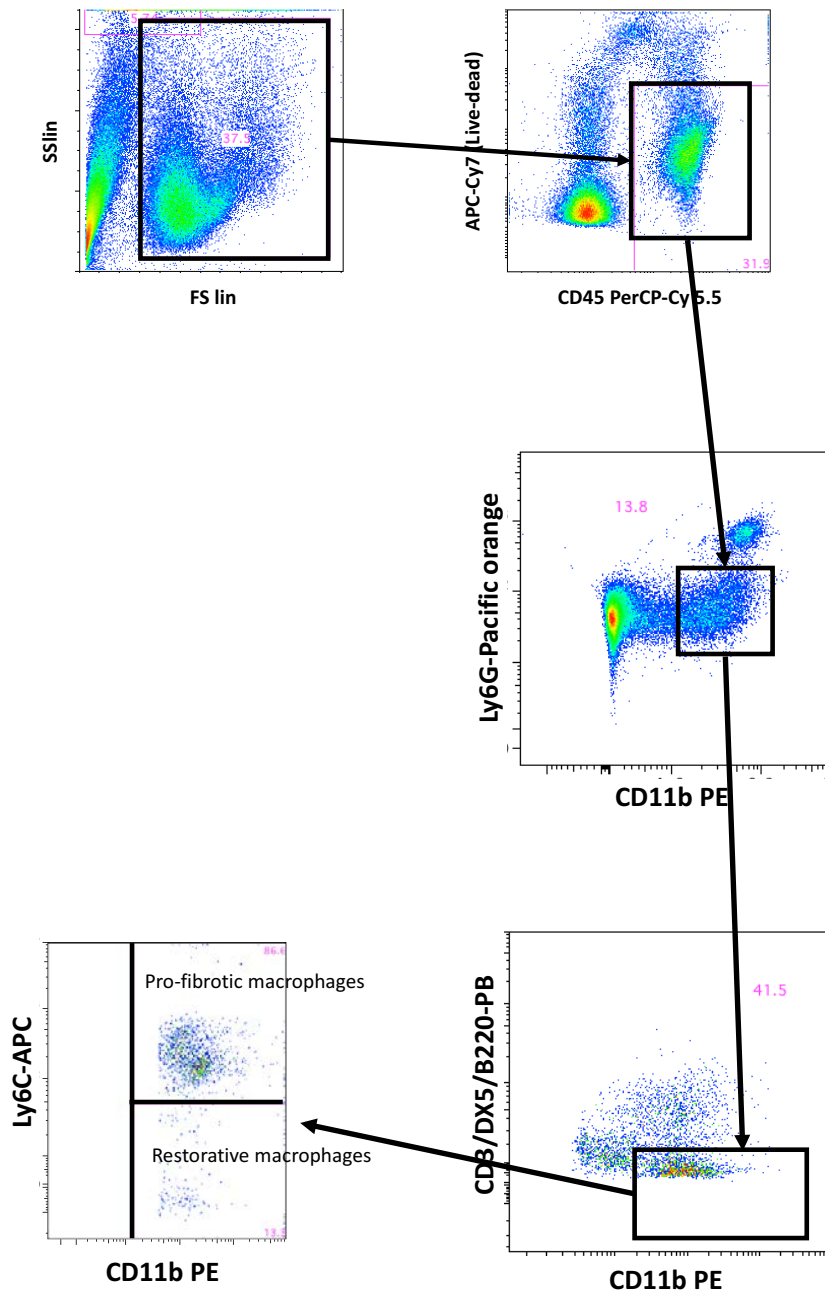


**Figure 5.8 Gating strategy used to define restorative and pro-fibrotic macrophages in our cytometric analysis of liver digests :**

WT or CLEC-2 deficient mice were injected with twice weekly IP CCl<sub>4</sub> injections. Mice were sacrificed at the end of 7 weeks (after a total of 14 injections). Livers were digested and leukocytes isolated using a gradient separation method. Leukocytes were then stained, analyzed using flow cytometric methods and expressed as number of cells per gram of liver tissue. Pro-fibrotic macrophages were defined as live dead viability stain followed by CD45<sup>+</sup>Ly6G<sup>-</sup>Ly6C<sup>+</sup>CD11b<sup>+</sup>CD3<sup>-</sup>. 'Restorative' or anti-fibrotic macrophages were defined as CD45<sup>+</sup>Ly6G<sup>-</sup>Ly6C<sup>-</sup>CD11b<sup>+</sup>CD3<sup>-</sup>.

We found that although the CLEC-2 deficient animals in general had a tendency to have greater numbers of leukocytes after chronic CCl<sub>4</sub> intoxication compared to WT mice. Thus CLEC-2 deficient mice had larger numbers of intra-hepatic neutrophils (median cells per gram of liver tissue: WT mice 7200 cells/gm vs CLEC-2 deficient mice 13269 cells/gm) and CD3<sup>+</sup> T cells (median cells per gram of liver tissue: WT mice 109551 cells/gm vs CLEC-2 deficient mice 154697 cells/gm); owing to the small numbers of animals in each arm none of the differences reached significance.

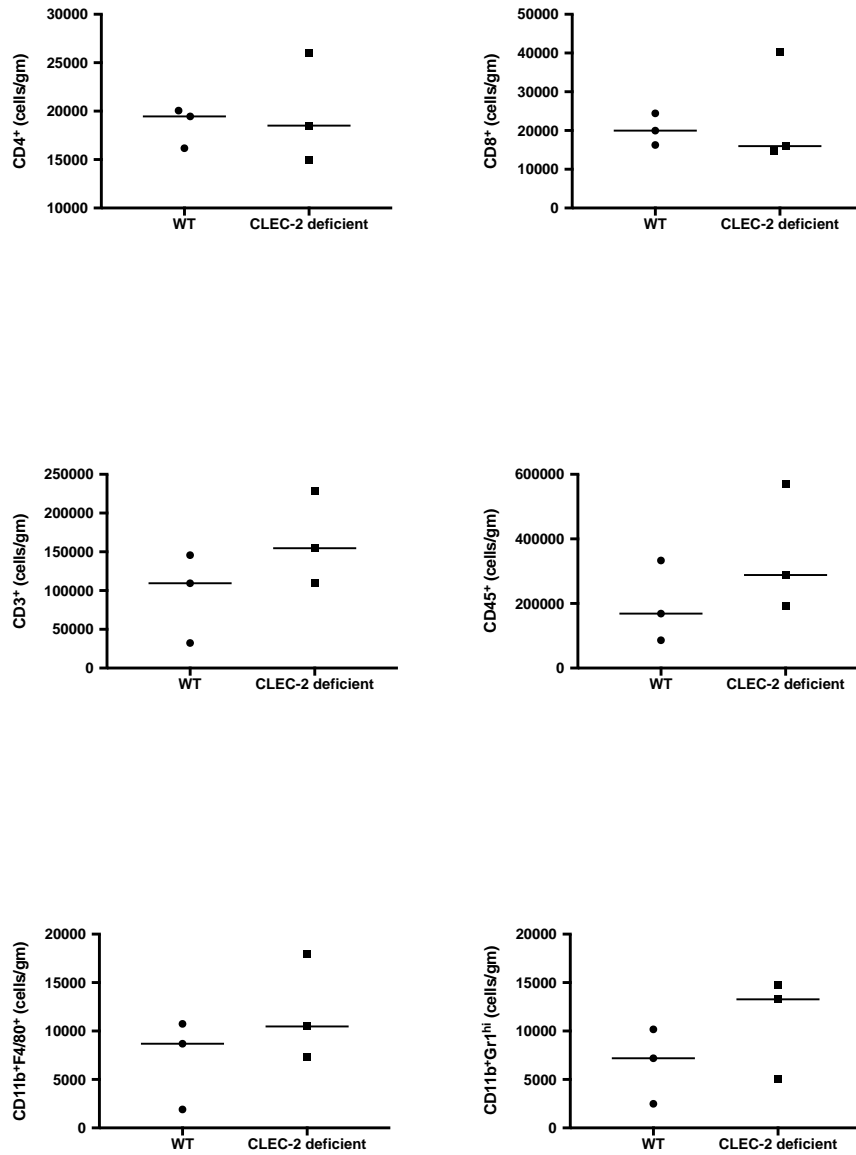


**Figure 5.9 CLEC-2 deficient and WT mice have similar numbers of liver infiltrating leukocytes after chronic CCl<sub>4</sub> administration:**

WT or CLEC-2 deficient mice were injected with twice weekly IP CCl<sub>4</sub> injections. Mice were sacrificed at the end of 7 weeks (after a total of 14 injections). Livers were digested and leukocytes isolated using a gradient separation method. Leukocytes were then stained, analyzed using flow cytometric methods and expressed as number of cells per gram of liver tissue. Cells defined as per previously gating strategies. Groups incorporated 3 mice in each, data from individual mice are shown by a single point and median values are indicated by horizontal bar. Data are cells/ gram of liver tissue.

Interestingly however, comparison of numbers of pro fibrotic and pro-resolution macrophages ( $\text{Cd45}^+\text{Ly6G-Ly6C}^+ \text{Cd11b}^+\text{Cd3-}$ , and  $\text{Cd45}^+\text{Ly6G-Ly6C- Cd11b}^+\text{Cd3-}$  respectively, Figure 5.10) showed that the CLEC-2 deficient animals had lower numbers of both compared to their WT counterparts.

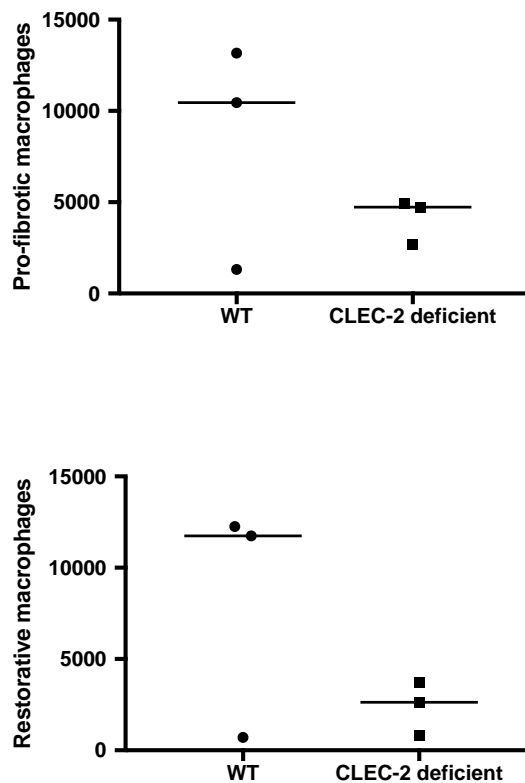


**Figure 5.10 CLEC-2 deficient mice have lower numbers of both restorative and pro-fibrotic macrophages after chronic  $\text{CCl}_4$  administration:**

WT or CLEC-2 deficient mice were injected with twice weekly IP  $\text{CCl}_4$  injections. Mice were sacrificed at the end of 7 weeks (after a total of 14 injections). Livers were digested and leukocytes isolated using a gradient separation method. Leukocytes were then stained, analyzed using flow cytometric methods and expressed as number of cells per gram of liver tissue. Pro-fibrotic macrophages were defined as live dead viability stain followed by  $\text{CD45}^+\text{Ly6G-Ly6C}^+\text{CD11b}^+\text{CD3-}$ . 'Restorative' or anti-fibrotic macrophages were defined as  $\text{CD45}^+\text{Ly6G-Ly6C-CD11b}^+\text{CD3-}$ . Groups incorporated 3 mice in each, data from individual mice are shown by a single point and median values are indicated by horizontal bar. Data are cells/gram of liver tissue.

## 5.5. Regeneration

There appeared to be little observable difference in terms of fibrosis development between CLEC-2 deficient mice and wild type mice after 7 weeks of biweekly CCl<sub>4</sub> administration. We next examined the CLEC-2 deficient mouse (PF4Cre*CLEC1b*<sup>fl/fl</sup>) to see if there was a difference in resolution from fibrosis. Thus after 7 weeks of CCl<sub>4</sub> administration we stopped the bi-weekly CCl<sub>4</sub> dosing to allow the 'resolution from fibrosis' phase to begin (fig 5.11). This phase has been well described in WT mice(45) and typically takes between 3 and 4 weeks after cessation of CCl<sub>4</sub> injections.

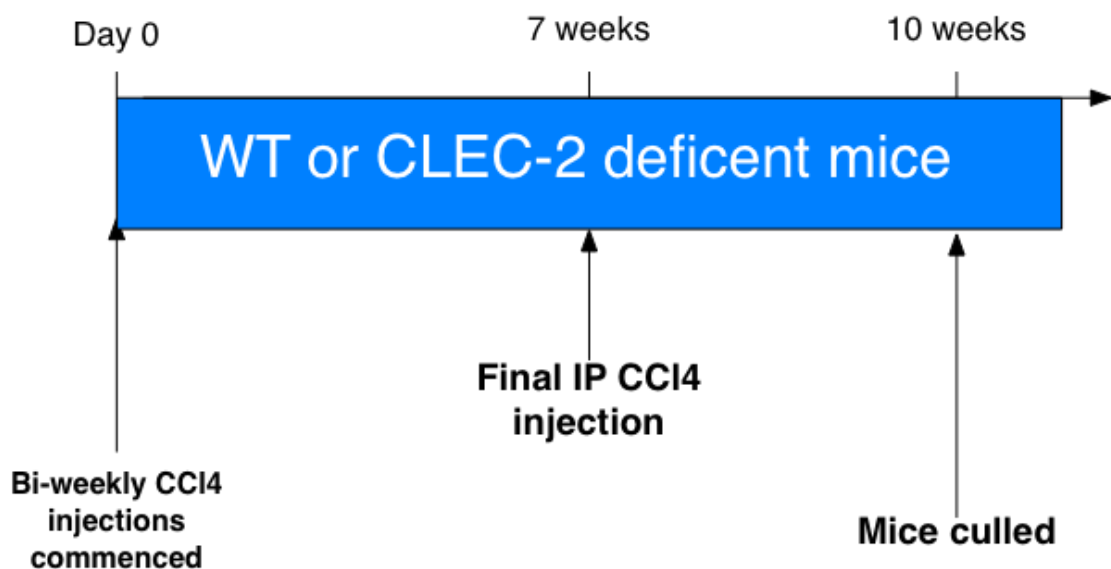
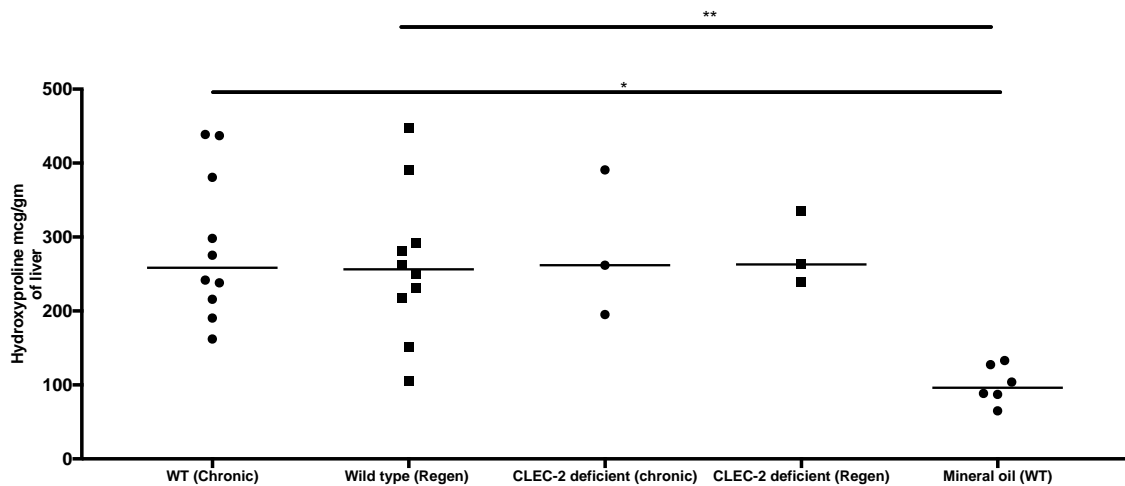


Figure 5.11 Timeline used to allow resolution from chronic CCl<sub>4</sub> administration

### 5.5.1. Minimal resolution from fibrosis is seen after 3 weeks

We stopped the bi-weekly CCl<sub>4</sub> injections at 7 weeks and then culled the mice at 10 weeks (time allowed for resolution from fibrosis was thus 3 weeks). There were 10 mice in the wild type group and 3 in the CLEC-2 deficient group. We noted that the amounts of hepatic fibrosis as quantified by a hydroxy proline assay remained unchanged (compared to the amount seen in mice at the end of 7 weeks of 'active' injecting) in both the CLEC-2 deficient (PF4Cre*CLEC1b*<sup>fl/fl</sup>) mice and WT mice.



**Figure 5.12 CLEC-2 deficient mice and WT do not exhibit resolution of fibrosis three weeks after cessation of IP CCl<sub>4</sub>:**

WT or CLEC-2 deficient mice were injected with twice weekly CCl<sub>4</sub> injections or mineral oil alone for 7 weeks, some mice were taken at this point (chronic). In the group of mice not culled, injections were then stopped. Mice were sacrificed after a further 3 weeks (the mice were not injected during this time-regen group). The livers were harvested, homogenized and treated with trichloroacetic acid to enable protein precipitation. The hydroxyproline concentration of the protein precipitant was then determined by colorimetric analysis using 4-(Dimethylamino)benzaldehyde (DMAB). Groups incorporated between 3 and 10 mice, data from individual mice are shown by a single point and median values are indicated by horizontal bar. Data are amount of hydroxy proline per gram of liver tissue, and test Mann-Whitney indicated significant differences between groups as indicated (\*P < 0.05, \*\*P < 0.01, \*\*\*P < 0.001)

### **5.5.2. CLEC-2 deficient mice have altered patterns of injury and inflammation in the recovery phase**

Although no difference in terms of hydroxyproline was seen between the groups at 3 weeks' post CCl<sub>4</sub> cessation, the CLEC-2 deficient mice had lower serum ALT values and less hepatic necrosis histologically compared to the WT controls at the same timepoint. Again the serum TNF $\alpha$  levels were also higher in the CLEC-2 deficient mice but the magnitude of the differences was marginal (fig 5.13)

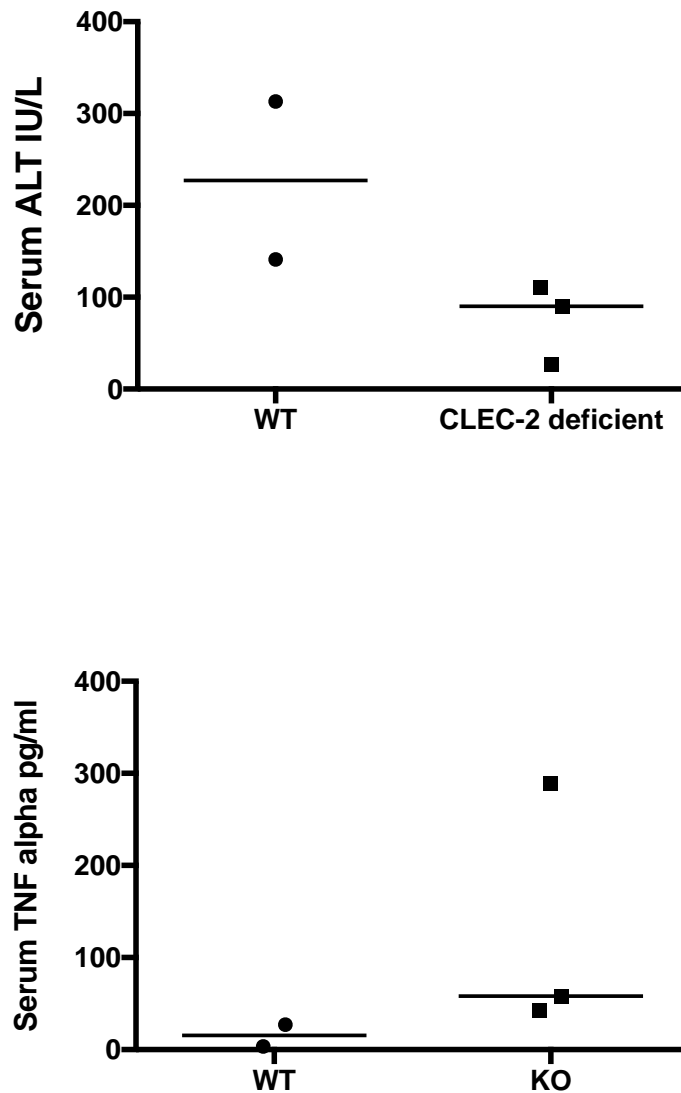


**Figure 5.13 CLEC-2 deficient mice have a lower serum transaminase level but higher TNF- $\alpha$  levels compared to WT mice after chronic CCl<sub>4</sub> administration:**

WT or CLEC-2 deficient mice were injected with twice weekly CCl<sub>4</sub> injections or mineral oil alone for 7 weeks. Injections were then stopped. Mice were sacrificed after a further 3 weeks (the mice were not injected during the final three weeks). Serum was harvested via cardiac puncture and analyzed for TNF- $\alpha$  and serum ALT level. Groups incorporated 3 mice in each, data from individual mice are shown by a single point and median values are indicated by horizontal bar. Data are serum level of either TNF- $\alpha$  or serum ALT level.



### 5.5.3. Cellular infiltration

Overall numbers of intrahepatic leukocytes decreased upon cessation of CCl<sub>4</sub> injections in WT mice (Fig 5.14). In contrast the numbers increased in CLEC-2 deficient mice (fig 5.14). When comparing by leukocyte subtype, again no major differences were seen with similar numbers of lymphoid and myeloid cells seen in both WT and CLEC-2 deficient livers at 10 weeks (fig 5.15). Of note, in contrast to the end of the active injury period, when we compared the numbers of pro-fibrotic and pro-resolution macrophages, during the resolution phase numbers were comparable in WT and KO mice (fig 5.16).

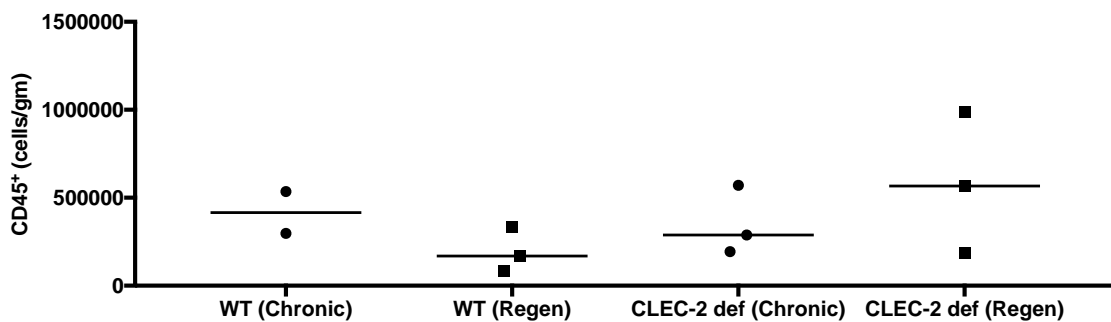


**Figure 5.14 Numbers of intrahepatic leukocytes increase during the fibrosis resolution phase within CLEC-2 deficient mice:**

WT or CLEC-2 deficient mice were injected with twice weekly CCl<sub>4</sub> injections or mineral oil alone for 7 weeks. Injections were then stopped. Mice were sacrificed after a further 3 weeks (the mice were not injected during the final three weeks). Livers were digested and leukocytes isolated using a gradient separation method. Leukocytes were then stained, analyzed using flow cytometric methods and expressed as number of cells per gram of liver tissue. Cells defined as per previously gating strategies. Groups incorporated 3 mice in each, data from individual mice are shown by a single point and median values are indicated by horizontal bar. Data are cells/ gram of liver tissue.

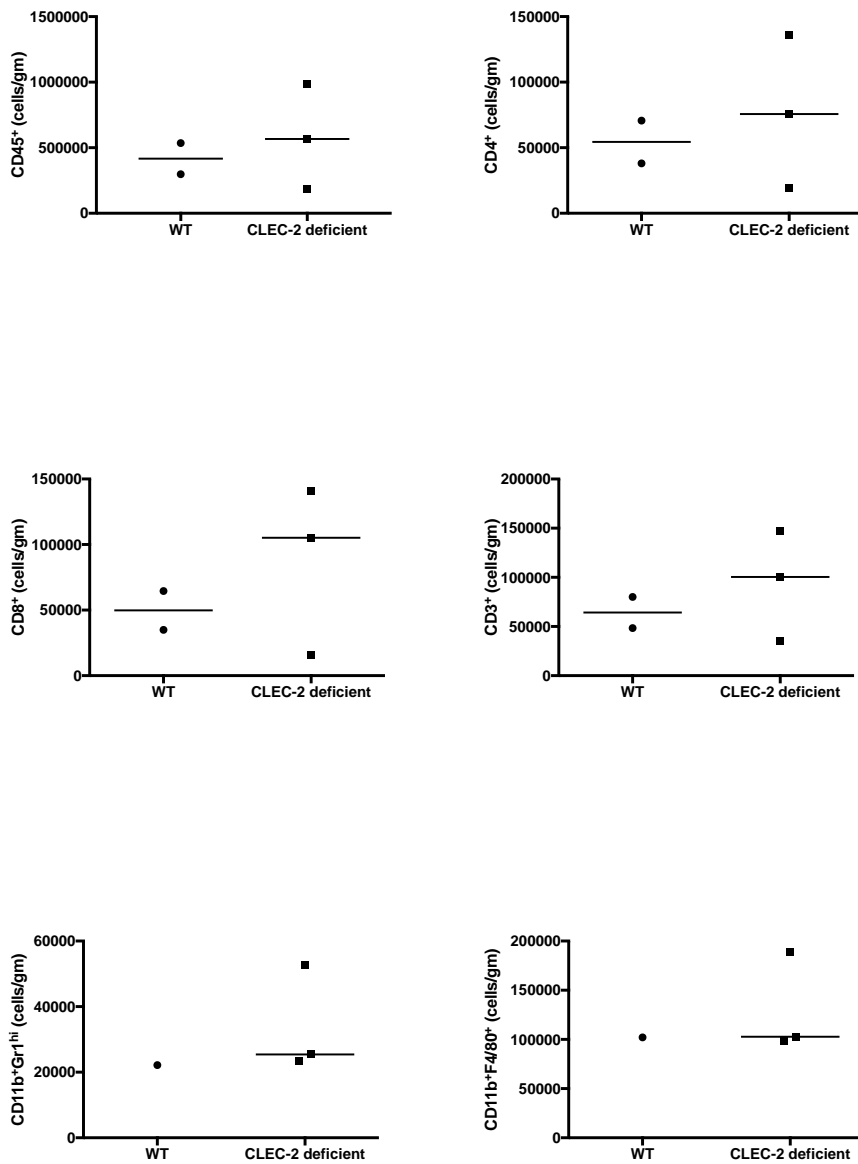


**Figure 5.15 CLEC-2 deficient and WT mice have similar numbers of liver infiltrating leukocytes during the resolution phase after chronic CCl<sub>4</sub> administration:**

WT or CLEC-2 deficient mice were injected with twice weekly CCl<sub>4</sub> injections or mineral oil alone for 7 weeks. Injections were then stopped. Mice were sacrificed after a further 3 weeks (the mice were not injected during the final three weeks). Livers were digested and leukocytes isolated using a gradient separation method. Leukocytes were then stained, analyzed using flow cytometric methods and expressed as number of cells per gram of liver tissue. Cells defined as per previously gating strategies. Groups incorporated 3 mice in each, data from individual mice are shown by a single point and median values are indicated by horizontal bar. Data are cells/ gram of liver tissue.

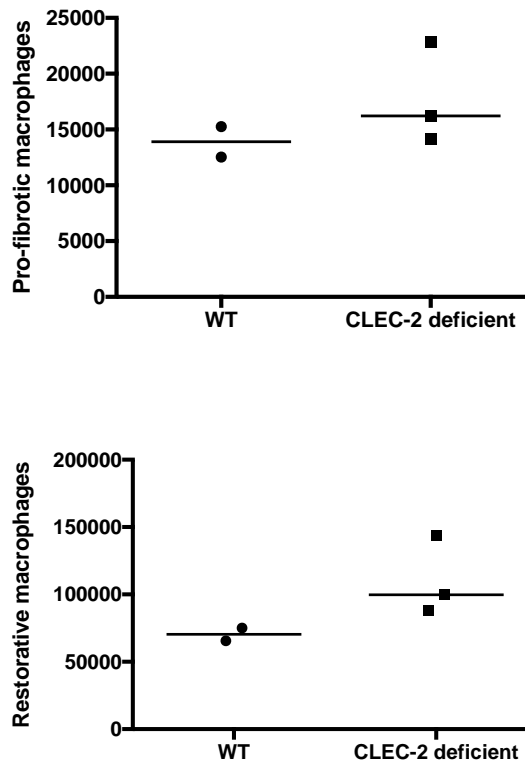
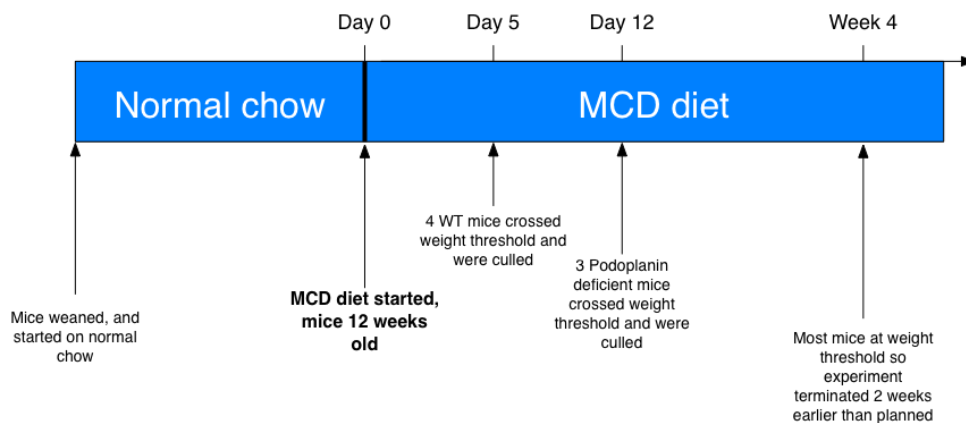


**Figure 5.16 CLEC-2 deficient and WT mice have similar numbers of restorative and pro-fibrotic macrophages during the resolution phase from chronic liver injury:**

WT or CLEC-2 deficient mice were injected with twice weekly CCl<sub>4</sub> injections or mineral oil alone for 7 weeks. Injections were then stopped. Mice were sacrificed after a further 3 weeks (the mice were not injected during the final three weeks). Their livers were digested and leukocytes isolated using a gradient separation method. Leukocytes were then stained, analyzed using flow cytometric methods and expressed as number of cells per gram of liver tissue. Pro-fibrotic macrophages were defined as live dead viability stain followed by CD45<sup>+</sup>Ly6G<sup>-</sup>Ly6C<sup>+</sup>CD11b<sup>+</sup>CD3<sup>-</sup>. 'Restorative' or anti-fibrotic macrophages were defined as CD45<sup>+</sup>Ly6G<sup>-</sup>Ly6C<sup>-</sup>CD11b<sup>+</sup>CD3<sup>-</sup>. Groups incorporated 3 mice in each, data from individual mice are shown by a single point and median values are indicated by horizontal bar. Data are cells/ gram of liver tissue.

## 5.6. Methionine choline deficient (MCD) diet

Platelets have an important role in driving cardiovascular complications of the metabolic syndrome(243) ; the various stages of fatty liver disease represent the hepatic manifestation of the metabolic syndrome(53). We thus wished to examine the role of CLEC-2 mediated platelet activation in driving dietary (MCD) liver damage. As per the stipulations of our animal license we had to cull the mice if they lost 35% of their pre-diet weight. This resulted in a marked reduction in final numbers of particularly wild type mice and podoplanin deficient mice before they developed significant liver damage (fig 5.17). The results below thus reflect the mice numbers that remained. For this experiment we used both podoplanin deficient ( $Vav1-iCre^+pdpn^{fl/fl}$ ) and CLEC-2 deficient ( $PF4CreCLEC1b^{fl/fl}$ ) mice along with wild type mice as controls. The majority of WT mice had to be sacrificed before they developed significant liver injury as they lost weight at a much greater rate than the mutant mice (with CLEC-2 and podoplanin deficient).



Mouse number	Genotype	Day weight threshold reached (35%)	Sufficient liver damage developed as gauged by serum ALT
1	CLEC-2 deficient	4 weeks	Yes
2	CLEC-2 deficient	4 weeks	Yes
3	CLEC-2 deficient	4 weeks	Yes
4	CLEC-2 deficient	4 weeks	Yes
5	CLEC-2 deficient	4 weeks	Yes
6	Podoplanin deficient	Day 12	No
7	Podoplanin deficient	Day 12	No
8	Podoplanin deficient	Day 12	No
9	Podoplanin deficient	4 Weeks	Yes
10	Podoplanin deficient	4 weeks	Yes
11	Wild Type	Day 5	No
12	Wild Type	Day 5	No
13	Wild Type	Day 5	No
14	Wild Type	Day 5	No
15	Wild Type	4 weeks	Yes

**Figure 5.17 Time line depicting when mice reached license threshold weight: Table below gives a breakdown of when mice reached threshold weight and whether any hepatic injury was noted (as gauged by serum ALT)**

### **5.6.1. Podoplanin deficient mice exhibit greater hepatic infiltration by macrophages after 4 weeks MCD diet.**

Cytometric analysis revealed that the numbers of infiltrating leukocytes was different in WT and mutant mice after administration of the MCD diet. We noted that the overall numbers of CD45<sup>+</sup> cells were greatest in the podoplanin deficient mice, although this information is drawn from only two remaining animals. The CLEC-2-deficient mice had less CD45<sup>+</sup> cells per gram of liver tissue compared to the WT and podoplanin-deficient mice, though again these results are from small numbers of animals. However further phenotyping of the infiltrating CD45<sup>+</sup> cells revealed that there were more F4/80<sup>+</sup> macrophages within the livers of the podoplanin-deficient mice compared to both the CLEC-2-deficient and WT mice. When we assessed the murine livers for the numbers of pro-fibrotic and restorative macrophages (defined in section 5.4.4), we noted that the CLEC-2 deficient mice had less restorative or 'fibrosis resolution' macrophages compared to both the WT and podoplanin deficient mice. In contrast, the numbers of profibrotic macrophages were similar between the CLEC-2 and podoplanin deficient mice, with both greater than the WT mouse. In contrast to the pattern of myeloid cell infiltration, the last remaining WT mouse exhibited more CD3<sup>+</sup>, CD4<sup>+</sup> and CD8<sup>+</sup> lymphocyte infiltration compared to either of the mutant strains (fig 5.18).

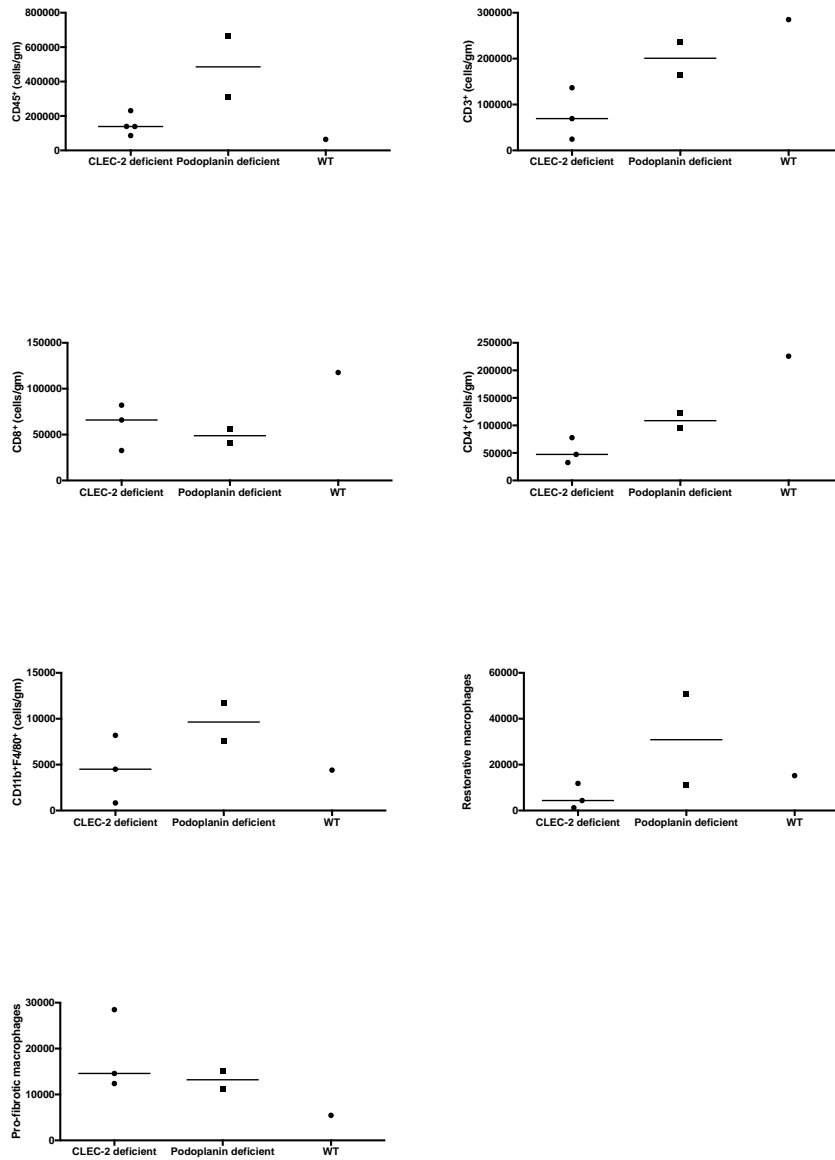


**Figure 5.18 Podoplanin deficient mice exhibit greater macrophage infiltration whilst wild type mice exhibit greater lymphocyte accumulation after 4 weeks of MCD diet:**

12 week old WT, CLEC-2 or podoplanin deficient mice were placed on a methionine choline deficient (MCD) diet. Mice had free access to the diet. The mice were sacrificed after 4 weeks. Livers were digested and leukocytes isolated using a gradient separation method. Leukocytes were then stained, analyzed using flow cytometric methods and expressed as number of cells per gram of liver tissue. Cells defined as per previously gating strategies. Groups incorporated between 1 to 3 mice in each, data from individual mice are shown by a single point and median values are indicated by horizontal bar. Data are cells/ gram of liver tissue.

Although 4 weeks of MCD diet did induce a degree of liver fibrosis in all three groups of mice studied, at this stage no obvious differences were noted between the three groups, the median level for hydroxyproline content per gram of liver was marginally greater in the podoplanin deficient mice. None of the differences were statistically significant.

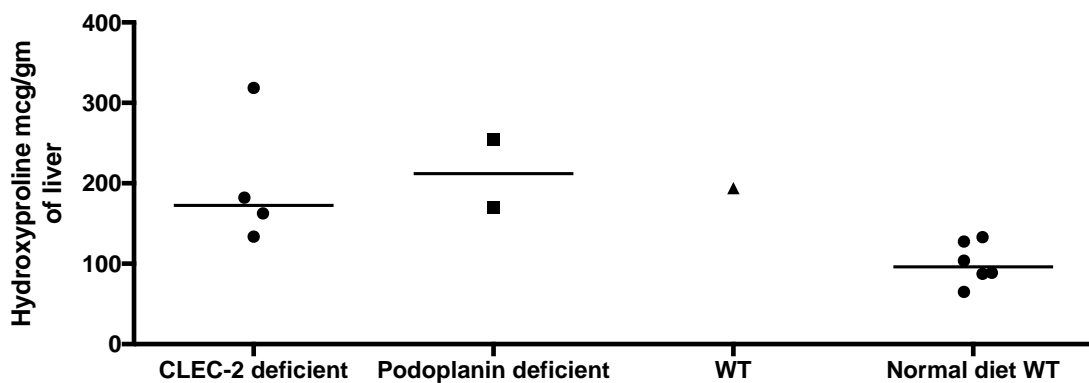


**Figure 5.19 Four weeks of MCD diet induces a small amount of hepatic fibrosis:**

12 week old WT, CLEC-2 or podoplanin deficient mice: were placed on a methionine choline deficient (MCD) diet. Mice had free access to the diet. The mice were sacrificed after 4 weeks. The livers were harvested, homogenized and treated with trichloroacetic acid to enable protein precipitation. The hydroxyproline concentration of the protein precipitant was then determined by colorimetric analysis using 4-(Dimethylamino)benzaldehyde (DMAB). Groups incorporated between 1 and 7 mice, data from individual mice are shown by a single point and median values are indicated by horizontal bar. Data are amount of hydroxy proline per gram of liver tissue.



### 5.6.2. Serum ALT

We noted that the podoplanin deficient mice had a slightly lower ALT compared to WT or CLEC-2 deficient mice (fig 5.20). None of the differences were statistically significant.

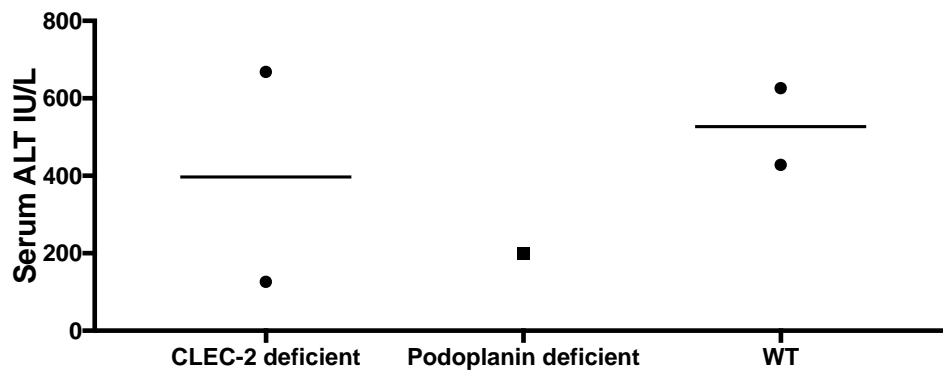


**Figure 1.20 Four weeks of MCD diet causes hepatic necroinflammation:**

12 week old WT, CLEC-2 or podoplanin deficient mice were placed on a methionine choline deficient (MCD) diet. Mice had free access to the diet. The mice were sacrificed after 4 weeks. Serum was harvested via cardiac puncture and analyzed for serum ALT level. Groups incorporated between 1 and 3 mice in each, data from individual mice are shown by a single point and median values are indicated by horizontal bar. Data are serum level of ALT.

## 5.7. Discussion

Most agents used for the induction of fibrosis in mice including CCl<sub>4</sub> are metabolized by the hepatocytes present closest to the central vein (centrizonal). Thus hepatocyte damage thus starts in this area and mice classically develop centrizonal or centrilobular fibrosis. We noted this pattern of in both WT and CLEC-2 deficient mice. If the fibrotic reaction is severe enough, it then extends to the portal areas. This represents an important point of difference with human liver disease, as fibrosis in chronic human liver disease is classically peri-portal. An exception to this is vascular or haemodynamic disorders such a Budd-Chiari syndrome where fibrosis occurs in a centrizonal distribution(233,244). When examining the role of CLEC-2 mediated platelet activation in hepatic fibrosis this fact is particularly relevant as podoplanin (the only known ligand for CLEC-2 mediated platelet activation)is upregulated predominantly in portal areas in both mice and humans. Thus if any difference is seen when blocking the CLEC-2/podoplanin axis it is likely that systemic and paracrine effects of podoplanin mediated platelet activation, including endothelial activation and release of soluble mediators/platelet cytokines play a role.

### 5.7.1. Carbon tetrachloride induced fibrogenesis

Our observations demonstrate that there is a slight increase in the amount of fibrosis observed at the end of the active period of CCl<sub>4</sub> injections in the CLEC-2 deficient mice. This would suggest that CLEC-2 driven platelet activation plays a minimal role (if any at all) in driving hepatic fibrogenesis or resolution from it. However the small

numbers of CLEC-2 deficient animals on the CCl<sub>4</sub> protocol made drawing concrete conclusions challenging.

In agreement with the acute injury experiments (chapter 4) we noted that after both active (where CCl<sub>4</sub> was injected bi-weekly) and passive (where no injections were given for three weeks) phases of CCl<sub>4</sub> mediated fibrotic liver injury a higher serum ALT was noted in WT mice compared to CLEC-2 deficient ones, and this corresponded to higher serum TNF- $\alpha$  levels in the CLEC-2 deficient mice. Studies demonstrate the TNF- $\alpha$  is an important driver of liver fibrosis after bile duct ligation in mice(245), and high levels of TNF- $\alpha$  in both mice and humans with obesity induced NAFLD(246). We did see a trend for increased hydroxyproline and PSR staining in the CLEC-2 deficient mice that had highest TNF $\alpha$  levels, in agreement with a pro-fibrogenic role but the data was not significant. Importantly we are unable to specifically determine the consequences of platelet activation on HSC function. Platelet derived CXCL-4(157), CXCL-7(247) and TGF- $\beta$  (248) are all implicated as cytokines released upon platelet activation with direct effects on the fibrogenic potential of HSCs specifically aiding their conversion into collagen depositing myofibroblasts. It would therefore be expected that reduced platelet activation as a consequence of lack of platelet CLEC-2 would result in less fibrosis. We need further experiments to thus definitively determine the effect of CLEC-2 deficiency on fibrosis. To ascertain whether the CLEC-2-podoplanin pathway is of direct relevance, we will need to assess whether platelets activated by binding to podoplanin on hepatic endothelial cells or macrophage populations produce soluble mediators that can

activate local HSC to enable a phenotype switch to fibrogenic cells. We noted that CLEC-2 deficient mice exhibited reduced pro-fibrotic macrophage recruitment compared to WT mice at the end of the active period of CCl<sub>4</sub> injections; this is conjunction with the lower serum ALT leads us to speculate whether there is perhaps a role for CLEC-2 mediated platelet activation in the recruitment of hepatocyte damaging immune cells.

Another point to note when interpreting this data is that little is known about lymphangiogenesis(188) within the liver during fibrosis; cirrhotic livers seem to have a larger number of lymphatics than non-cirrhotic ones (188). Our data confirms a dramatic upregulation of podoplanin (which is used as a marker of lymphatic vessels) in cirrhotic human livers (chapter 3), we show that not all podoplanin in these damaged livers is exclusively on lymphatic endothelium (figs 3.9, 3,16). We know from embryonic studies that the CLEC-2-podoplanin pathway is critical to blood lymphatic separation and thus lymphatic vessel formation (70,227). CLEC-2 deficient mice may theoretically therefore have an impairment of lymphangiogenesis and as these vessels contain collagen, it may be that our data, which suggests no difference in hydroxyproline content (which measures hepatic collagen) between CLEC-2 deficient and WT mice is affected by potentially differing amounts of lymphangiogenesis in the two arms, specifically potentially less lymphangiogenesis in CLEC-2 deficient animals. We did not assess whether there was a discrepancy in lymphatic vessel formation in the CLEC-2 deficient mice and using an alternative lymphatic marker such as LYVE-1 to quantify lymphangiogenesis in fibrotic mouse

livers will help dissect the contribution (if any) these vessels have to final measured hydroxyproline concentrations.

To minimize the acute necro-inflammatory damage a single dose of CCl<sub>4</sub> results in, we only sacrificed the mice 96 hours after the last dose of IP CCl<sub>4</sub>. Although unlikely this delay in sacrificing mice from the point of the last injection of CCl<sub>4</sub> may have influenced the amount of fibrosis we observed. Overall the small numbers in our study preclude meaningful conclusions to be drawn.

#### **5.7.2. MCD diet**

Owing to the rapid weight loss in mice on the MCD diet we had to cull approximately half of the mice on the MCD diet before we could establish the extent of liver injury developed. Low final numbers precluded meaningful conclusions to again be drawn when examining the role of CLEC-2 mediated platelet activation in MCD diet induced liver injury. It is notable however that more of the WT animals reached threshold, suggesting that in terms of disease development there was some protective effect of the CLEC-2 deficiency. However we did observe that even after 4 weeks of diet mice developed hepatic necroinflammation/injury as gauged by serum ALT. Another point of note is that most mice reached the 35% weight loss point specified by our license and thus had to be culled but remained clinically well, and displayed no other features consistent with distress including postural and motion changes, overgrooming or reduced feeding. Thus increasing the weight loss limit to 40% would allow us to continue mice on the diet for the recommended duration of 6 weeks We consider this particularly feasible as once mice reached 35% weight loss in most

cases their weight stabilized and they maintained this without much more weight lost over the subsequent weeks. Alternately since human fatty liver disease is associated with obesity and insulin resistance which are not recreated in the MCD model we would consider use of alternate models such as the choline-deficient high fat diet(249) to avoid some of the issues we faced with the MCD diet.

Although our experiments were hindered by low mouse numbers and the fact that the mice that were analyzed in the end had only been on the MCD (113) diet for 4 weeks, which may not a sufficient period of time to induce significant liver fibrosis, we feel that further investigation of the role the CLEC-2/podoplanin axis plays in NAFLD is warranted. Additionally some of the serum sent was un-analyzable due to the sample clotting on the analyzer. This was not an issue we encountered with mouse sera obtained from mice that had been on other liver injury protocols. This is likely to have been a technical issue with the actual cardiac puncture procedure as the mice on the diet were a smaller than the other mice we used and thus obtaining blood technically more complicated. This further limited the data available for analysis.

We have established that that Kupffer cells upregulate podoplanin during liver injury and it has been described by various groups how these cells play a crucial role in driving insulin resistance in the metabolic syndrome(250–252). Thus abrogating this pathway in models of NAFLD may potentially yield clinically important data. The fact that soluble CLEC-2 has been shown to manipulate macrophage polarization and improve glucose homeostasis(253) supports this. Future work will involve assessing

metabolic profiles (including serum glucose and lipids) in mice on dietary protocol, and ideally using a diet (such as HFD) that mimics human NAFLD more closely.

## 6. Conclusion and future directions

### 6.1. The macrophage:platelet interaction

Our acute injury model data depends upon macrophage expression of podoplanin to provide the ligand for CLEC-2 dependent platelet activation in the injured liver. To confirm the role of macrophages in these models the next step would be to deplete macrophages thus removing the signal for platelet activation in the injured liver. Studies using mice deficient in the macrophage receptor CCR 2 [a key receptor in macrophage recruitment to the inflamed liver post APAP overdose(33)] reveals delayed healing or recovery from APAP toxicity, but this is in the context of infiltrating macrophages not resident Kupffer cells. Encouragingly studies in rats reveal that gadolinium mediated Kupffer cell depletion reduces the amount of APAP induced liver damage, with the authors speculating that this protective effect may be due to modulation of Kupffer cell activation and not infiltrating cells(33) . However APAP toxicity in rats is generally mild in comparison to mice or humans(254), so two separate experiments depleting both resident and then infiltrating macrophages in mice are necessary to accurately attribute which of the two populations is more important in APAP induced liver damage. KCs renew themselves from resident stem cells and are not replenished by the circulating myeloid monocytic compartment; it is however difficult to distinguish between liver resident macrophages and those derived from the blood. This is partly due to lack of robust conventional cellular phenotype markers to distinguish the two populations (particularly in humans) and partly due to the high cellular plasticity these cells exhibit(38). Future studies



delineating which of the podoplanin expressing macrophages are derived from local precursors and which ones are derived from the bone marrow are necessary.

It is clear that podoplanin is upregulated within the injured liver. Acutely this upregulation is upon hepatic macrophages. In the context of acute toxic liver injury we show this upregulation to provide the necessary ligand for CLEC-2 mediated platelet activation, the end result of this interaction is to dampen overall macrophage dependent TNF- $\alpha$  production and thus the resultant inflammation. The actual mechanism behind this is however less clear. It may be that platelet activation from macrophage podoplanin results in production or secretion of platelet cytokines which then feedback in a paracrine fashion to the stimulating macrophage eliciting TNF- $\alpha$  production. A candidate for such a bioactive mediator is sphingosine-1 phosphate (S1P). Platelet derived S1P (released in a CLEC-2/podoplanin dependent fashion) has already been shown to be important in the maintenance of high endothelial venue integrity during lymphocyte trafficking in lymph nodes(86) . Thus on ligating podoplanin, CLEC-2 driven platelet activation could cause the release of S1P which would then act on macrophages to dampen TNF- $\alpha$  production. Given the abundant potential sources of S1P including the endothelium, plasma, red blood cells, platelets and leukocytes(255), much further study including the development and use of selective cre mice to delineate a specific contribution (if any) of platelet derived S1P to the sterile inflammatory response is necessary. Interestingly, S1P has been shown to already ameliorate immune liver injury by recruiting myeloid derived suppressor

cells(255,256) and blocking S1P signaling enhances recovery from liver fibrosis in mice by enhancing regeneration (257).

Another mechanism which may account for heightened TNF- $\alpha$  production from macrophages when encountering CLEC-2 deficient platelets is the direct effect CLEC-2 may have on macrophages via podoplanin ligation (i.e. without any platelet released soluble bioactive intermediary molecules). Podoplanin itself is linked to the actin cytoskeleton of the cell via the ERM proteins(69). Upregulation of podoplanin expression on macrophages (as we observed *in vitro* and *in vivo*) occurs after an inflammatory stimulus and is known to phosphorylate the ERM proteins and activate the actin cytoskeleton of the cell. Thus ligation of podoplanin by CLEC-2 could conceivably have an effect upon TNF- $\alpha$  containing vesicle trafficking to the surface of the macrophage. Our data suggests that CLEC-2 ligation here would thus serve to dampen TNF- $\alpha$  containing vesicle movement to the surface of the cell. The use of intracellular imaging or the experiments using vesicle traffic inhibitors such as cytochalasin D would be key to confirming the role of this mechanism.

## **6.2. Hepatic inflammation and liver recovery**

Horiguchi et al report enhanced periportal sequestration of leukocytes after CCl<sub>4</sub> administration in mice that had a selective myeloid specific signal transducer and activation of transcription 3 (STAT 3) deficiency (STAT3 Mye<sup>-/-</sup>). They further report reduced hepatic necrosis in these mice albeit with enhanced inflammation(216) . As the histological phenotype (enhanced periportal leukocyte sequestration) is similar to

our findings in acute carbon tetrachloride intoxication, and STAT 3 is known to be an important negative regulator of inflammation it may be that the CLEC-2-podoplanin pathway exerts its effects by activating myeloid STAT-3. Further study in this area is necessary; the effect wild type and CLEC-2 deficient platelets have on STAT3 induction in Kupffer cells will help clarify this. Another point Horiguchi et al mention is the enhanced production of serum interleukin 6 (IL6) in STAT3 Mye<sup>-/-</sup>, our data suggest that it is TNF- $\alpha$  that is enhanced and it may be that the two cytokines work at different points to aid liver recovery(216).

T cells specifically CD4 T cells were noted in larger amounts in the CLEC-2 deficient mice after both APAP and CCl<sub>4</sub> mediated liver injury, notable at peak points of injury (48 hours after CCl<sub>4</sub> injection and at 24 hrs after APAP injection). As not part of the innate immune response per se, the traditional thinking suggests that the role for T cells in the pathogenesis of an acute toxic liver injury is limited thus we chose to focus on the myeloid compartment for our studies. However emerging evidence suggests that there may be a role for T helper cells and CD3<sup>+</sup>CD4<sup>+</sup>CD8<sup>-</sup> cells(33,258) in modulation of the inflammatory response that follows APAP induced liver injury(33). Given that podoplanin has also been described on a subset of T cell (th 17)(167) , further studies examining the role of T cells (by using antibody mediated depletion in the first instance) in mediating the protective effects that a CLEC-2/podoplanin blockade confers during acute toxic liver damage are important.

We have identified some of the key cells and cytokines that result in the enhanced liver healing we noted from a toxic insult. The mechanism of this healing needs to be

elucidated next, it seems likely that neutrophil driven debris clearance accounts for some of our findings including the reduction in serum transaminase levels and restoration in hepatic architecture; the specific aspects of neutrophil function critical to this i.e. respiratory burst, phagocytic capacity etc remains to be established. Slaba et al noted that platelets in fact pave the way into injured livers for neutrophils to enter and drive liver recovery(50); blocking integrin mediated neutrophil activation(259) or using streptococcal protein M5 to inhibit phagocytic clearance(260) will help us to precisely delineate which neutrophil functions are key to driving the liver recovery we observe with CLEC-2 blockade. Additionally recent work in oncology(261) has defined distinct populations of neutrophils with pro and anti-inflammatory functions, it thus becomes imperative in our future studies for us to further phenotype the nature of the neutrophil infiltrate after CLEC-2 blockade in acute liver injury.

### **6.3. Model limitations**

CLEC-2 expression has been described on neutrophils(262) and dendritic cells(182), although we used a PF4cre mouse which would theoretically restrict the CLEC-2 deficiency to cells expressing PF4 i.e. of the megakaryocytic lineage and thus platelets; PF4 expression has been noted in haematopoietic stem cells(263). To ensure the phenotype we observed was due to platelet activation via CLEC-2, further experiments with platelet depletion and flow cytometric phenotyping of liver isolated dendritic cells and neutrophils (from the PF4Cre*CLEC1b<sup>fl/f</sup>* mouse) to ensure CLEC-2 expression is intact on these cells and thus not contributing to our observed phenotype are necessary.

For the experiments where we studied podoplanin blockade or deficiency, we either used a pan-podoplanin blocking antibody or the VAV1 cre mouse. Although the VAV1 cre mouse exhibited reduced injury at key time points after toxic liver injury (after both APAP and CCl<sub>4</sub>), the magnitude of the difference seen was not as impressive as what was observed using the podoplanin blocking antibody; it may be that the antibody was blocking podoplanin on sources other than just haematopoietic cells. Podoplanin is expressed upon lymphatic endothelium(264), and our data [and data from other researchers(189)] confirms that podoplanin is also expressed upon hepatic vascular endothelium. To delineate the contribution (if any) endothelial podoplanin expression has on reduced hepatic injury after toxic insult, we need to use a mouse such as the tie2cre where there is selective deficiency of endothelial podoplanin expression.

Owing to mouse numbers available to us and time restrictions, we were unable to comprehensively define temporal healing patterns in all the models we used. For instance in most of the podoplanin blocking/deficient models of acute toxic injury we focused on the time points of maximal injury, so although we demonstrate reduced injury at these time points (section 4.9) we do not actually demonstrate enhanced recovery which we do with the CLEC-2 deficient mice. Further experiments filling in these gaps, thus confirming a single cogent mechanism are necessary.

Finally alternative methods of blocking platelet activation (including platelet depletion and using anti-platelet therapy such as aspirin and clopidogrel) and blocking

downstream signaling (of CLEC-2) such as syk, would be ideal to compare whether a similar phenotype of enhanced recovery could be achieved.

#### **6.4. Future clinical implications**

In murine models we noted that blocking platelet activation therapeutically using a podoplanin function blocking antibody enhanced liver healing after a toxic liver injury (section 4.9). As we confirm the same axis is present in humans, the ideal next step would be to humanize the antibody for potential use in human fulminant liver failure due to paracetamol overdose. Further preclinical studies analyzing the stoichiometry of podoplanin antibody binding and establishing rates of survival in mice subjected to paracetamol overdose and then treated with the antibody are necessary. Additionally establishing antibody specificity using western blotting or immunoprecipitation assays will be required in the pre-clinical phase. Importantly all of our data was from mice treated with the antibody prior to administration of the toxic insult, in order for the data to be more relevant to the clinical situation the antibody has to be administered after the insult and also be tested in situations of delayed and staggered overdose which are common ways in which human paracetamol overdose presents(265). The cohort of patients we feel would be most suitable for this therapy are patients with acute fulminant liver failure secondary to paracetamol overdose who although meet the Kings college criteria for transplantation are not transplantable (for instance due to extensive comorbidities). Another cohort of patients who could possibly benefit here are patients with acute alcoholic hepatitis, as abrogating TNF- $\alpha$  in these patients has been shown to worsen outcomes(220) .

In chronic liver disease the pattern of podoplanin expression differed to what was noted in acute toxic liver injury as in addition to macrophages we noted that podoplanin was now being expressed on vascular endothelium within the liver; podoplanin expression has not been noted on vascular endothelium previously. This point is particularly poignant as we go on to demonstrate a correlation between the development of portal venous thrombosis and hepatic levels of podoplanin (chapter 3). Thus another potential application for a humanized podoplanin function blocking antibody could be in the treatment of portal venous thrombosis. As portal venous thrombosis can be associated with portal hypertension and thus bleeding oesophageo-gastric varices-an anti-thrombotic therapy that does not increase bleeding risk could potentially be very valuable. Definitively ruling out podoplanin expression in vascular endothelium outside the liver would be critical before any such treatments could be considered.

## Time line for future to take AB to clinical trials

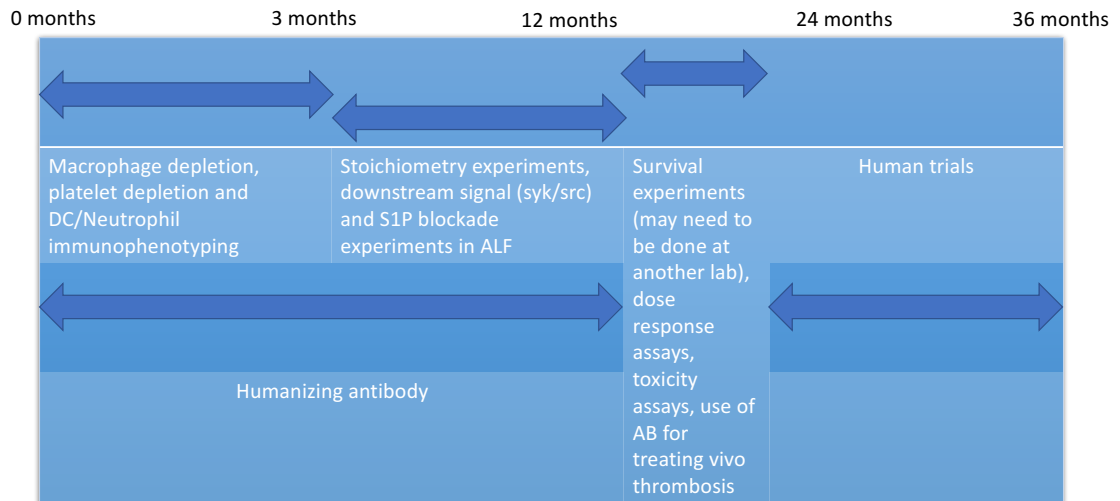


**Figure 2.1 Time line for future experiments**



## 7. Bibliography

1. Williams R, Ashton K, Aspinall R, Bellis MA, Bosanquet J, Cramp ME, et al. Implementation of the lancet standing commission on liver disease in the UK. The Lancet [Internet]. Elsevier; 2015;386(10008):2098–111. Available from: <http://linkinghub.elsevier.com/retrieve/pii/S0140673615006807>
2. Wise J. Deaths from liver disease are four times higher in some parts of England than others. BMJ [Internet]. 2014;349(oct20 19):g6332–g6332. Available from: <http://www.bmj.com/cgi/doi/10.1136/bmj.g6332>
3. D'Amico G, Garcia-Tsao G, Pagliaro L. Natural history and prognostic indicators of survival in cirrhosis: A systematic review of 118 studies. JOURNAL OF HEPATOLOGY [Internet]. 2006;44(1):217–31. Available from: <http://linkinghub.elsevier.com/retrieve/pii/S0168827805006847>
4. Bernal W, Auzinger G, Dhawan A, Wendon J. Acute liver failure. The Lancet [Internet]. Elsevier Ltd; 2010 Jul 17;376(9736):190–201. Available from: [http://dx.doi.org/10.1016/S0140-6736\(10\)60274-7](http://dx.doi.org/10.1016/S0140-6736(10)60274-7)
5. Bernal W, Wendon J. Acute Liver Failure. The New England journal of medicine [Internet]. 2013 Dec 26;369(26):2525–34. Available from: <http://www.nejm.org/doi/abs/10.1056/NEJMra1208937>
6. Bower WA, Johns M, Margolis HS, Williams IT, Bell BP. Population-based surveillance for acute liver failure. The American Journal of Gastroenterology

[Internet]. 2007;102(11):2459–63. Available from:

<http://www.nature.com/doi/10.1111/j.1572-0241.2007.01388.x>

7. Larson AM, Polson J, Fontana RJ, Davern TJ, Lalani E, Hynan LS, et al.

Acetaminophen-induced acute liver failure: Results of a united states multicenter, prospective study. *Hepatology* [Internet]. Department of Internal Medicine, Division of Gastroenterology, University of Washington Medical Center, Seattle, 98195, USA.

[amlarson@u.washington.edu](mailto:amlarson@u.washington.edu); 2005;42(6):1364–72. Available from:

<http://eutils.ncbi.nlm.nih.gov/entrez/eutils/elink.fcgi?dbfrom=pubmed&id=16317692&retmode=ref&cmd=prlinks>

8. Lee WM. Acetaminophen and the u.S. acute liver failure study group: Lowering the risks of hepatic failure. *Hepatology* [Internet]. Division of Digestive and Liver Diseases, University of Texas, Southwestern Medical Center, Dallas, 75390-9151, USA. [William.Lee@utsouthwestern.edu](mailto:William.Lee@utsouthwestern.edu); 2004;40(1):6–9. Available from:

<http://eutils.ncbi.nlm.nih.gov/entrez/eutils/elink.fcgi?dbfrom=pubmed&id=15239078&retmode=ref&cmd=prlinks>

9. Atkuri KR, Mantovani JJ, Herzenberg LA, Herzenberg LA. N-acetylcysteine—a safe antidote for cysteine/glutathione deficiency. *Current Opinion in Pharmacology* [Internet]. 2007;7(4):355–9. Available from:

<http://linkinghub.elsevier.com/retrieve/pii/S1471489207000896>

10. Fagan E, Wannan G. Reducing paracetamol overdoses. *BMJ* [Internet]. BMJ Group; 1996;313(7070):1417–8. Available from:  
<http://www.ncbi.nlm.nih.gov/pmc/articles/PMC2352977/>
11. Thursz M, Morgan TR. Treatment of Severe Alcoholic Hepatitis. *Gastroenterology* [Internet]. Elsevier; 2016 Jun 1;150(8):1823–34. Available from:  
<http://linkinghub.elsevier.com/retrieve/pii/S001650851600295X>
12. Zhou W-C. Pathogenesis of liver cirrhosis. *World Journal of Gastroenterology* [Internet]. 2014;20(23):7312–4. Available from: <http://www.wjgnet.com/1007-9327/full/v20/i23/7312.htm>
13. Holt AP, Salmon M, Buckley CD, Adams DH. Immune Interactions in Hepatic Fibrosis. *Clinics in Liver Disease* [Internet]. 2008 Nov 1;12(4):861–82. Available from:  
<http://linkinghub.elsevier.com/retrieve/pii/S1089326108000731>
14. Galun E, Axelrod JH. The role of cytokines in liver failure and regeneration: Potential new molecular therapies. *Biochimica et biophysica acta* [Internet]. The Goldyne Savad Institute for Gene Therapy, Hadassah Hebrew University Hospital, Ein Kerem, Jerusalem, Israel. [galun@md2.huji.ac.il](mailto:galun@md2.huji.ac.il); 2002;1592(3):345–58. Available from:  
<http://eutils.ncbi.nlm.nih.gov/entrez/eutils/elink.fcgi?dbfrom=pubmed&id=12421677&retmode=ref&cmd=prlinks>
15. Lalor PF, Herbert J, Bicknell R, Adams DH. Hepatic sinusoidal endothelium avidly binds platelets in an integrin-dependent manner, leading to platelet and

endothelial activation and leukocyte recruitment. *AJP: Gastrointestinal and Liver Physiology* [Internet]. 2013 Mar 1;304(5):G469–78. Available from:  
<http://ajpgi.physiology.org/cgi/doi/10.1152/ajpgi.00407.2012>

16. Adams DH, Eksteen B. Aberrant homing of mucosal t cells and extra-intestinal manifestations of inflammatory bowel disease. *Nature Reviews Immunology* [Internet]. Liver Research Laboratories, MRC Centre for Immune Regulation, 5th Floor, Institute for Biomedical Research, Medical School, University of Birmingham, Edgbaston, Birmingham B15 2TT, UK. [d.h.adams@bham.ac.uk](mailto:d.h.adams@bham.ac.uk); 2006;6(3):244–51. Available from:  
<http://eutils.ncbi.nlm.nih.gov/entrez/eutils/elink.fcgi?dbfrom=pubmed&id=16498453&retmode=ref&cmd=prlinks>

17. Kietzmann T. Metabolic zonation of the liver: the oxygen gradient revisited. *Redox Biology* [Internet]. Elsevier B.V.; 2017;11:622–30. Available from:  
<http://dx.doi.org/10.1016/j.redox.2017.01.012>

18. Jaeschke H. Acetaminophen: Dose-Dependent Drug Hepatotoxicity and Acute Liver Failure in Patients. *Digestive Diseases* [Internet]. Department of Pharmacology, Toxicology and Therapeutics, University of Kansas Medical Center, Kansas City, Kans., USA.: Karger Publishers; 2015 Jan 1;33(4):464–71. Available from:  
<http://www.karger.com/?doi=10.1159/000374090>

19. Birchmeier W. Orchestrating wnt signalling for metabolic liver zonation. *Nature Cell Biology* [Internet]. Nature Publishing Group, a division of Macmillan Publishers

Limited. All Rights Reserved.; 2016;18(5):463–5. Available from:

<http://www.nature.com/doi/10.1038/ncb3349>

20. Gao B, Bataller R. Alcoholic liver disease: Pathogenesis and new therapeutic targets. *Gastroenterology* [Internet]. 2011;141(5):1572–85. Available from:

<http://linkinghub.elsevier.com/retrieve/pii/S0016508511012285>

21. You M, Fischer M, Deeg MA, Crabb DW. Ethanol induces fatty acid synthesis pathways by activation of sterol regulatory element-binding protein (sREBP). *Journal of Biological Chemistry* [Internet]. Department of Medicine, Indiana University School of Medicine and Richard Roudebush Veteran's Affairs Medical Center, Indianapolis, Indiana 46202, USA. miyou@iupui.edu; 2002;277(32):29342–7. Available from:

<http://eutils.ncbi.nlm.nih.gov/entrez/eutils/elink.fcgi?dbfrom=pubmed&id=12036955&retmode=ref&cmd=prlinks>

22. Gao B. Hepatoprotective and anti-inflammatory cytokines in alcoholic liver disease. *Journal of Gastroenterology and Hepatology* [Internet]. 2012;27:89–93.

Available from: <http://doi.wiley.com/10.1111/j.1440-1746.2011.07003.x>

23. Paschos P, Paletas K. Non alcoholic fatty liver disease and metabolic syndrome. *Hippokratia* [Internet]. Metabolic Disease Unit, 2nd Internal Medicine Department, Aristotle University of Thessaloniki, Hippokratia Hospital, Thessaloniki, Greece.; 2009 Jan 1;13(1):9–19. Available from:

<http://eutils.ncbi.nlm.nih.gov/entrez/eutils/elink.fcgi?dbfrom=pubmed&id=19240815&retmode=ref&cmd=prlinks>

24. Oseini AM, Sanyal AJ. Therapies in non-alcoholic steatohepatitis (NASH). *Liver International* [Internet]. Division of Gastroenterology, Department of Internal Medicine, Virginia Commonwealth University School of Medicine, Richmond, VA, USA.; 2017 Jan 1;37 Suppl 1:97–103. Available from: <http://eutils.ncbi.nlm.nih.gov/entrez/eutils/elink.fcgi?dbfrom=pubmed&id=28052626&retmode=ref&cmd=prlinks>

25. Dyson JK, Anstee QM, McPherson S. Non-alcoholic fatty liver disease: a practical approach to diagnosis and staging. *Frontline Gastroenterology* [Internet]. 2014 Jun 5;5(3):211–8. Available from: <http://fg.bmj.com/lookup/doi/10.1136/flgastro-2013-100403>

26. Armstrong MJ, Houlihan DD, Bentham L, Shaw JC, Cramb R, Olliff S, et al. Presence and severity of non-alcoholic fatty liver disease in a large prospective primary care cohort. *JOURNAL OF HEPATOLOGY* [Internet]. European Association for the Study of the Liver; 2012 Jan 1;56(1):234–40. Available from: <http://dx.doi.org/10.1016/j.jhep.2011.03.020>

27. Carbone M, Neuberger JM. Autoimmune liver disease, autoimmunity and liver transplantation. *JOURNAL OF HEPATOLOGY* [Internet]. European Association for the Study of the Liver; 2014;60(1):210–23. Available from: <http://dx.doi.org/10.1016/j.jhep.2013.09.020>

28. Moy L, Levine J. Autoimmune hepatitis: A classic autoimmune liver disease. *Current problems in pediatric and adolescent health care* [Internet]. Division of

Pediatric Gastroenterology, New York University School of Medicine, New York, NY.  
Electronic address: jeremiah.levine@nyumc.org.; 2014;44(11):341–6. Available from:  
<http://eutils.ncbi.nlm.nih.gov/entrez/eutils/elink.fcgi?dbfrom=pubmed&id=25466500&retmode=ref&cmd=prlinks>

29. Oo YH, Hubscher SG, Adams DH. Autoimmune hepatitis: New paradigms in the pathogenesis, diagnosis, and management. *Hepatology International* [Internet]. 2010;4(2):475–93. Available from: <http://link.springer.com/10.1007/s12072-010-9183-5>

30. Paumgartner G, Beuers U. Ursodeoxycholic acid in cholestatic liver disease: Mechanisms of action and therapeutic use revisited. *Hepatology* [Internet]. Department of Medicine II, Klinikum Grosshadern, University of Munich, Munich, Germany. [Gustav.Paumgartner@med2.med.uni-muenchen.de](mailto:Gustav.Paumgartner@med2.med.uni-muenchen.de); 2002;36(3):525–31. Available from:  
<http://eutils.ncbi.nlm.nih.gov/entrez/eutils/elink.fcgi?dbfrom=pubmed&id=12198643&retmode=ref&cmd=prlinks>

31. Liaskou E, Wilson DV, Oo YH. Innate Immune Cells in Liver Inflammation. *Mediators of Inflammation* [Internet]. 2012 Jan 1;2012(2):1–21. Available from: <http://www.hindawi.com/journals/mi/2012/949157/>

32. Guidotti LG, Inverso D, Sironi L, Pietro Di Lucia, Fioravanti J, Ganzer L, et al. Immunosurveillance of the Liver by Intravascular Effector CD8<sup>+</sup> T Cells. *Cell*

[Internet]. Elsevier Inc.; 2015 Apr 23;161(3):486–500. Available from:

<http://dx.doi.org/10.1016/j.cell.2015.03.005>

33. Krenkel O, Mossanen JC, Tacke F. Immune mechanisms in acetaminophen-induced acute liver failure. *Hepatobiliary surgery and nutrition* [Internet]. Department of Medicine III, RWTH-University Hospital Aachen, Aachen, Germany.; 2014 Dec 1;3(6):331–43. Available from: <http://hbsn.amegroups.com/article/view/5253/6111>

34. Jaeschke H, Williams CD, Ramachandran A, Bajt ML. Acetaminophen hepatotoxicity and repair: the role of sterile inflammation and innate immunity. *Liver International* [Internet]. 2011 Mar 14;32(1):8–20. Available from:

<http://doi.wiley.com/10.1111/j.1478-3231.2011.02501.x>

35. Wu Z, Han M, Chen T, Yan W, Ning Q. Acute liver failure: mechanisms of immune-mediated liver injury. *Liver International* [Internet]. Blackwell Publishing Ltd; 2010 Apr 8;30(6):782–94. Available from: <http://doi.wiley.com/10.1111/j.1478-3231.2010.02262.x>

36. Bieggs V, Trautwein C. The innate immune response during liver inflammation and metabolic disease. *Trends in Immunology* [Internet]. Elsevier Ltd; 2013 Sep 1;34(9):446–52. Available from: <http://dx.doi.org/10.1016/j.it.2013.04.005>

37. Zimmermann HW, Trautwein C, Tacke F. Functional Role of Monocytes and Macrophages for the Inflammatory Response in Acute Liver Injury. *Frontiers in Physiology* [Internet]. Frontiers; 2012 Oct 19;3. Available from:

<http://journal.frontiersin.org/article/10.3389/fphys.2012.00056/full>



38. Heymann F, Tacke F. Immunology in the liver — from homeostasis to disease. *Nature Reviews Gastroenterology & Hepatology* [Internet]. 2016 Jan 13;13(2):88–110. Available from: <http://www.nature.com/doifinder/10.1038/nrgastro.2015.200>

39. Ju C, Reilly TP, Bourdi M, Radonovich MF, Brady JN, George JW, et al. Protective role of Kupffer cells in acetaminophen-induced hepatic injury in mice. *Chemical research in toxicology* [Internet]. Molecular and Cellular Toxicology Section, Laboratory of Molecular Immunology, National Heart, Lung, and Blood Institute, National Institutes of Health, Department of Health and Human Services, Bethesda, Maryland 20892, USA. Cynthia.Ju@uchsc.edu; 2002 Dec 1;15(12):1504–13. Available from: <http://eutils.ncbi.nlm.nih.gov/entrez/eutils/elink.fcgi?dbfrom=pubmed&id=12482232&retmode=ref&cmd=prlinks>

40. Tacke F, Zimmermann HW. Macrophage heterogeneity in liver injury and fibrosis. *JOURNAL OF HEPATOLOGY* [Internet]. European Association for the Study of the Liver; 2014 Jan 8;60(5):1090–6. Available from: <http://dx.doi.org/10.1016/j.jhep.2013.12.025>

41. Weston CJ, Shepherd EL, Claridge LC, Rantakari P, Curbishley SM, Tomlinson JW, et al. Vascular adhesion protein-1 promotes liver inflammation and drives hepatic fibrosis. *The Journal of clinical investigation* [Internet]. 2014 Dec 22;125(2):501–20. Available from: <http://www.jci.org/articles/view/73722>

42. Galastri S, Zamara E, Milani S, Novo E, Provenzano A, Delogu W, et al. Lack of CC chemokine ligand 2 differentially affects inflammation and fibrosis according to the genetic background in a murine model of steatohepatitis. *Clinical science* (London, England : 1979) [Internet]. Dipartimento di Medicina Interna, University of Florence, Florence, Italy.; 2012 Oct 1;123(7):459–71. Available from: <http://eutils.ncbi.nlm.nih.gov/entrez/eutils/elink.fcgi?dbfrom=pubmed&id=22545719&retmode=ref&cmd=prlinks>
43. Hoshino A, Kawamura YI, Yasuhara M, Toyama-Sorimachi N, Yamamoto K, Matsukawa A, et al. Inhibition of CCL1-CCR8 interaction prevents aggregation of macrophages and development of peritoneal adhesions. *The Journal of Immunology* [Internet]. Department of Medical Ecology and Informatics, International Medical Center of Japan, Tokyo, Japan.; 2007 Apr 1;178(8):5296–304. Available from: <http://eutils.ncbi.nlm.nih.gov/entrez/eutils/elink.fcgi?dbfrom=pubmed&id=17404314&retmode=ref&cmd=prlinks>
44. Aoyama T, Inokuchi S, Brenner DA, Seki E. CX3CL1-CX3CR1 interaction prevents carbon tetrachloride-induced liver inflammation and fibrosis in mice. *Hepatology* [Internet]. Division of Gastroenterology, Department of Medicine, University of California San Diego School of Medicine, La Jolla, CA 92093-0702, USA.; 2010 Oct 1;52(4):1390–400. Available from: <http://eutils.ncbi.nlm.nih.gov/entrez/eutils/elink.fcgi?dbfrom=pubmed&id=20683935&retmode=ref&cmd=prlinks>

45. Ramachandran P, Pellicoro A, Vernon MA, Boulter L, Aucott RL, Ali A, et al. Differential Ly-6C expression identifies the recruited macrophage phenotype, which orchestrates the regression of murine liver fibrosis. *Proceedings of the National Academy of Sciences of the United States of America* [Internet]. University of Edinburgh/Medical Research Council Centre for Inflammation Research, The Queen's Medical Research Institute, Edinburgh EH16 4TJ, United Kingdom.: National Acad Sciences; 2012 Nov 13;109(46):NaN – NaN. Available from: [http://adsabs.harvard.edu/cgi-bin/nph-data\\_query?bibcode=2012PNAS..109E3186R&link\\_type=EJOURNAL](http://adsabs.harvard.edu/cgi-bin/nph-data_query?bibcode=2012PNAS..109E3186R&link_type=EJOURNAL)

46. Holub M, Cheng CW, Mott S, Wintermeyer P, van Rooijen N, Gregory SH. Neutrophils Sequestered in the Liver Suppress the Proinflammatory Response of Kupffer Cells to Systemic Bacterial Infection. *The Journal of Immunology* [Internet]. 2009 Aug 20;183(5):3309–16. Available from: <http://www.jimmunol.org/cgi/doi/10.4049/jimmunol.0803041>

47. Kubes P, Mehal WZ. Sterile inflammation in the liver. *Gastroenterology* [Internet]. Department of Physiology and Pharmacology, University of Calgary, Calgary, Alberta, Canada.: Elsevier; 2012 Nov 1;143(5):1158–72. Available from: <http://linkinghub.elsevier.com/retrieve/pii/S0016508512013649>

48. Kolaczowska E, Kubes P. Neutrophil recruitment and function in health and inflammation. *Nature Reviews Immunology* [Internet]. Nature Publishing Group; 2013 Mar 1;13(3):159–75. Available from: <http://dx.doi.org/10.1038/nri3399>

49. Huang H, Tohme S, Al-Khafaji AB, Tai S, Loughran P, Chen L, et al. Damage-associated molecular pattern-activated neutrophil extracellular trap exacerbates sterile inflammatory liver injury. *Hepatology* [Internet]. Department of Surgery, University of Pittsburgh Medical Center, Pittsburgh, PA.; 2015 Aug 1;62(2):600–14. Available from: <http://doi.wiley.com/10.1002/hep.27841>
50. Slaba I, Wang J, Kolaczowska E, McDonald B, Lee W-Y, Kubes P. Imaging the dynamic platelet-neutrophil response in sterile liver injury and repair in mice. *Hepatology* [Internet]. Department of Physiology and Pharmacology, University of Calgary, Calgary, Alberta, Canada.; 2015 Nov 1;62(5):1593–605. Available from: <http://doi.wiley.com/10.1002/hep.28003>
51. Sitia G. Platelets Promote Liver Immunopathology Contributing to Hepatitis B Virus–Mediated Hepatocarcinogenesis. *Platelets and Cancer* [Internet]. 2014 Jun 1;41(3):402–5. Available from: <http://www.sciencedirect.com/science/article/pii/S0093775414001183>
52. Nurden AT. Platelets, inflammation and tissue regeneration. *Thrombosis and Haemostasis* [Internet]. 2011 Jan 1;105:S13–33. Available from: <http://www.schattauer.de/index.php?id=1214&doi=10.1160/THS10-11-0720>
53. Chauhan A, Adams DH, Watson SP, Lalor PF. Platelets: No longer bystanders in liver disease. *Hepatology* [Internet]. Centre for Liver Research, and NIHR Birmingham Liver Biomedical Research Unit, Institute of Biomedical Research, College of Medical and Dental Sciences, University of Birmingham, Birmingham, B15

2TH, UK.; 2016 Mar 2;64(5):1774–84. Available from:

<http://eutils.ncbi.nlm.nih.gov/entrez/eutils/elink.fcgi?dbfrom=pubmed&id=26934463&retmode=ref&cmd=prlinks>

54. Ripoche J. Blood platelets and inflammation: Their relationship with liver and digestive diseases. *Clinics and Research in Hepatology and Gastroenterology* [Internet]. 2011 May 1;35(5):353–7. Available from:

<http://linkinghub.elsevier.com/retrieve/pii/S221074011100074X>

55. Davì G, Patrono C. Platelet activation and atherothrombosis. *The New England journal of medicine* [Internet]. Center of Excellence on Aging, G. d'Annunzio University Foundation, Chieti, Italy.; 2007;357(24):2482–94. Available from: <http://www.nejm.org/doi/abs/10.1056/NEJMra071014>

56. Nieswandt B, Watson SP. Platelet-collagen interaction: Is GPVI the central receptor? *Blood* [Internet]. Department of Vascular Biology, Rudolf Virchow Center for Experimental Biomedicine Versbacher, Würzburg, Germany. [bernhard.nieswandt@virchow.uni-wuerzburg.de](mailto:bernhard.nieswandt@virchow.uni-wuerzburg.de): American Society of Hematology; 2003;102(2):449–61. Available from:

<http://www.bloodjournal.org/cgi/doi/10.1182/blood-2002-12-3882>

57. Moroi AJ, Watson SP. Impact of the PI3-kinase/Akt pathway on ITAM and hemITAM receptors: Haemostasis, platelet activation and antithrombotic therapy. *Biochemical Pharmacology* [Internet]. Elsevier Inc.; 2015 Apr 1;94(3):186–94. Available from: <http://dx.doi.org/10.1016/j.bcp.2015.02.004>

58. Offermanns S. Activation of Platelet Function Through G Protein-Coupled Receptors. *Circulation Research* [Internet]. 2006 Dec 8;99(12):1293–304. Available from: <http://circres.ahajournals.org/cgi/doi/10.1161/01.RES.0000251742.71301.16>

59. Coughlin SR. Thrombin signalling and protease-activated receptors. *Nature* [Internet]. Cardiovascular Research Institute and Department of Medicine, University of California at San Francisco, 94143-0130, USA. [coughlin@cvrmail.ucsf.edu](mailto:coughlin@cvrmail.ucsf.edu); 2000;407(6801):258–64. Available from: <http://www.nature.com/doi/10.1038/35025229>

60. Lee RH, Bergmeier W. Platelet immunoreceptor tyrosine-based activation motif (ITAM) and hemITAM signaling and vascular integrity in inflammation and development. *Journal of Thrombosis and Haemostasis* [Internet]. 2016 Feb 16;14(4):645–54. Available from: <http://doi.wiley.com/10.1111/jth.13250>

61. Rivera J, Lozano ML, Navarro-Nunez L, Vicente V. Platelet receptors and signaling in the dynamics of thrombus formation. *Haematologica* [Internet]. 2009;94(5):700–11. Available from: <http://www.haematologica.org/cgi/doi/10.3324/haematol.2008.003178>

62. Smyth SS, Woulfe DS, Weitz JI, Gachet C, Conley PB, Goodman SG, et al. G-protein-coupled receptors as signaling targets for antiplatelet therapy. *Arteriosclerosis, Thrombosis, and Vascular Biology* [Internet]. Veterans Affairs Medical Center, Department of Medicine, Physiology, and Pharmacology, University of Kentucky, Lexington, KY, USA. [susansmyth@uky.edu](mailto:susansmyth@uky.edu): Lippincott Williams &

Wilkins; 2009;29(4):449–57. Available from:

<http://atvb.ahajournals.org/cgi/doi/10.1161/ATVBAHA.108.176388>

63. Morrell CN, Aggrey AA, Chapman LM, Modjeski KL. Emerging roles for platelets as immune and inflammatory cells. *Blood* [Internet]. 2014;123(18):2759–67. Available from: <http://www.bloodjournal.org/cgi/doi/10.1182/blood-2013-11-462432>

64. Navarro-Nunez L, Langan SA, Nash GB, Watson SP. The physiological and pathophysiological roles of platelet cLEC-2. *Thrombosis and Haemostasis* [Internet]. 2013;109(6):991–8. Available from:

<http://www.schattauer.de/index.php?id=1214&doi=10.1160/TH13-01-0060>

65. Suzuki-Inoue K, Fuller GLJ, García A, Eble JA, Pöhlmann S, Inoue O, et al. A novel syk-dependent mechanism of platelet activation by the c-type lectin receptor cLEC-2. *Blood* [Internet]. Department of Clinical and Laboratory Medicine, University of Yamanashi, Shimokato Tamaho Nakakoma, Yamanashi 409-3898, Japan.: American Society of Hematology; 2006;107(2):542–9. Available from:

<http://www.bloodjournal.org/cgi/doi/10.1182/blood-2005-05-1994>

66. OZAKI Y, Suzuki-Inoue K, INOUE O. Novel interactions in platelet biology: CLEC-2/podoplanin and laminin/GPVI. *Journal of Thrombosis and Haemostasis* [Internet]. Department of Laboratory Medicine, Faculty of Medicine, University of Yamanashi, Chuo, Yamanashi, Japan. [yozaki@yamanashi.ac.jp](mailto:yozaki@yamanashi.ac.jp); 2009;7 Suppl 1:191–4. Available from:

<http://eutils.ncbi.nlm.nih.gov/entrez/eutils/elink.fcgi?dbfrom=pubmed&id=19630798&retmode=ref&cmd=prlinks>

67. Breiteneder-Geleff S, Matsui K, Soleiman A, Meraner P, Poczewski H, Kalt R, et al. Podoplanin, novel 43-kd membrane protein of glomerular epithelial cells, is down-regulated in puromycin nephrosis. *The American Journal of Pathology* [Internet]. Department of Clinical Pathology, University of Vienna, Austria.: American Society for Investigative Pathology; 1997;151(4):1141–52. Available from: [/pmc/articles/PMC1858024/?report=abstract](http://pmc/articles/PMC1858024/?report=abstract)

68. Ugorski M, Dziegiel P, Suchanski J. Podoplanin - a small glycoprotein with many faces. *American journal of cancer research* [Internet]. Laboratory of Glycobiology and Cell Interactions, Ludwik Hirszfeld Institute of Immunology and Experimental Therapy, Polish Academy of SciencesWroclaw, Poland; Department of Biochemistry, Pharmacology and Toxicology, Faculty of Veterinary Medicine, University of Environmental and Life SciencesWroclaw, Poland.; 2016 Jan 1;6(2):370–86. Available from: <http://eutils.ncbi.nlm.nih.gov/entrez/eutils/elink.fcgi?dbfrom=pubmed&id=27186410&retmode=ref&cmd=prlinks>

69. Astarita JL, Acton SE, Turley SJ. Podoplanin: emerging functions in development, the immune system, and cancer. *Frontiers in immunology* [Internet]. Department of Cancer Immunology and AIDS, Dana Farber Cancer Institute Boston, MA, USA ; Division of Medical Sciences, Harvard Medical School Boston, MA, USA.:



Frontiers; 2012 Jan 1;3:283. Available from:

<http://journal.frontiersin.org/article/10.3389/fimmu.2012.00283/abstract>

70. Finney BA, Schweighoffer E, Navarro-Nunez L, Benezech C, Barone F, Hughes CE, et al. CLEC-2 and Syk in the megakaryocytic/platelet lineage are essential for development. *Blood* [Internet]. 2012 Feb 16;119(7):1747–56. Available from:

<http://www.bloodjournal.org/cgi/doi/10.1182/blood-2011-09-380709>

71. Martin-Villar E, Megias D, Castel S, Yurrita MM, Vilaro S, Quintanilla M. Podoplanin binds eRM proteins to activate rhoA and promote epithelial-mesenchymal transition. *Journal of Cell Science* [Internet]. 2006;119(21):4541–53. Available from:

<http://jcs.biologists.org/cgi/doi/10.1242/jcs.03218>

72. Watson SP, HERBERT MJ, Pollitt AY. GPVI and cLEC-2 in hemostasis and vascular integrity. *Journal of Thrombosis and Haemostasis* [Internet].

2010;8(7):1456–67. Available from: <http://doi.wiley.com/10.1111/j.1538-7836.2010.03875.x>

73. Inoue O, Suzuki-Inoue K, McCarty OJT, Moroi M, Ruggeri ZM, Kunicki TJ, et al. Laminin stimulates spreading of platelets through integrin alpha6beta1-dependent activation of GPVI. *Blood* [Internet]. Department of Clinical and Laboratory Medicine,

Yamanashi Medical University, 1110 Shimokato Tamaho Nakakoma, Yamanashi 409-3898, Japan. [oinoue@yamanashi.ac.jp](mailto:oinoue@yamanashi.ac.jp); 2006;107(4):1405–12. Available from: <http://eutils.ncbi.nlm.nih.gov/entrez/eutils/elink.fcgi?dbfrom=pubmed&id=16219796&retmode=ref&cmd=prlinks>

74. Siljander PRM, Hamaia S, Peachey AR, Slatter DA, Smethurst PA, Ouwehand WH, et al. Integrin activation state determines selectivity for novel recognition sites in fibrillar collagens. *Journal of Biological Chemistry* [Internet]. 2004;279(46):47763–72. Available from: <http://www.jbc.org/cgi/doi/10.1074/jbc.M404685200>

75. Boulaftali Y, Hess PR, Kahn ML, Bergmeier W. Platelet immunoreceptor tyrosine-based activation motif (iTAM) signaling and vascular integrity. *Circulation Research* [Internet]. 2014;114(7):1174–84. Available from: <http://circres.ahajournals.org/lookup/doi/10.1161/CIRCRESAHA.114.301611>

76. Gitz E, Pollitt AY, Gitz-Francois JJ, Alshehri O, Mori J, Montague S, et al. CLEC-2 expression is maintained on activated platelets and on platelet microparticles. *Blood* [Internet]. 2014;124(14):2262–70. Available from: <http://www.bloodjournal.org/cgi/doi/10.1182/blood-2014-05-572818>

77. Manne BK, Badolia R, Dangelmaier C, Eble JA, Ellmeier W, Kahn M, et al. Distinct pathways regulate syk protein activation downstream of immune tyrosine activation motif (iTAM) and hemiTAM receptors in platelets. *The Journal of biological chemistry* [Internet]. From the Department of Physiology, Sol Sherry Thrombosis Research Center, Temple University School of Medicine, Philadelphia, Pennsylvania 19140.: American Society for Biochemistry and Molecular Biology; 2015;290(18):11557–68. Available from: <http://www.jbc.org/lookup/doi/10.1074/jbc.M114.629527>

78. Boulaftali Y, Hess PR, Getz TM, Cholka A, Stolla M, Mackman N, et al. Platelet iTAM signaling is critical for vascular integrity in inflammation. *The Journal of clinical investigation* [Internet]. McAllister Heart Institute, University of North Carolina at Chapel Hill, Chapel Hill, North Carolina, USA.; 2013;123(2):908–16. Available from: <http://eutils.ncbi.nlm.nih.gov/entrez/eutils/elink.fcgi?dbfrom=pubmed&id=23348738&retmode=ref&cmd=prlinks>

79. May F, Hagedorn I, Pleines I, Bender M, Vogtle T, Eble J, et al. CLEC-2 is an essential platelet-activating receptor in hemostasis and thrombosis. *Blood* [Internet]. 2009;114(16):3464–72. Available from: <http://www.bloodjournal.org/cgi/doi/10.1182/blood-2009-05-222273>

80. Hughes CE, Navarro-Nunez L, Finney BA, Mourao-Sa D, Pollitt AY, Watson SP. CLEC-2 is not required for platelet aggregation at arteriolar shear. *Journal of Thrombosis and Haemostasis* [Internet]. 2010;8(10):2328–32. Available from: <http://doi.wiley.com/10.1111/j.1538-7836.2010.04006.x>

81. Suzuki-Inoue K, INOUE O, Ding G, Nishimura S, Hokamura K, Eto K, et al. Essential *in vivo* roles of the c-type lectin receptor cLEC-2: EMBRYONIC/NEONATAL IETHALITY oF cLEC-2-dEFICIENT mICE bY bLOOD/LYMPHATIC mISCONNECTIONS aND iMPAIRED tHROMBUS FORMATION oF cLEC-2-dEFICIENT pLATELETS. *Journal of Biological Chemistry* [Internet]. 2010;285(32):24494–507. Available from: <http://www.jbc.org/cgi/doi/10.1074/jbc.M110.130575>

82. Dütting S, Bender M, Nieswandt B. Platelet GPVI: A target for antithrombotic therapy?! Trends in Pharmacological Sciences [Internet]. Elsevier Ltd; 2012;33(11):583–90. Available from: <http://dx.doi.org/10.1016/j.tips.2012.07.004>

83. Tripodi A, Mannucci PM. MECHANISMS oF dISEASE the coagulopathy of chronic liver disease. Angelo Bianchi Bonomi Hemophilia and Thrombosis Center, Department of Internal Medicine, Università degli Studi di Milano, Milan, Italy. armando.tripodi@unimi.it; 2011;365(2):147–56. Available from: <http://www.nejm.org/doi/abs/10.1056/NEJMra1011170>

84. Kitchens CS, Weiss L. Ultrastructural changes of endothelium associated with thrombocytopenia. Blood [Internet]. 1975;46(4):567–78. Available from: <http://eutils.ncbi.nlm.nih.gov/entrez/eutils/elink.fcgi?dbfrom=pubmed&id=1174690&retmode=ref&cmd=prlinks>

85. Kitchens CS, Pendergast JF. Human thrombocytopenia is associated with structural abnormalities of the endothelium that are ameliorated by glucocorticosteroid administration. Blood [Internet]. 1986;67(1):203–6. Available from: <http://eutils.ncbi.nlm.nih.gov/entrez/eutils/elink.fcgi?dbfrom=pubmed&id=3940548&retmode=ref&cmd=prlinks>

86. Herzog BH, Fu J, Wilson SJ, Hess PR, Sen A, McDaniel JM, et al. Podoplanin maintains high endothelial venule integrity by interacting with platelet CLEC-2. Nature

[Internet]. Nature Publishing Group; 2013 Sep 1;502(7469):1–7. Available from:  
<http://dx.doi.org/10.1038/nature12501>

87. Goerge T, Ho-Tin-Noé B, Carbo C, Benarafa C, Remold-O'Donnell E, Zhao B-Q, et al. Inflammation induces hemorrhage in thrombocytopenia. *Blood* [Internet]. Immune Disease Institute, Harvard Medical School, Boston, MA, USA.: American Society of Hematology; 2008;111(10):4958–64. Available from:  
<http://www.bloodjournal.org/cgi/doi/10.1182/blood-2007-11-123620>

88. Ho-Tin-Noé B, Carbo C, Demers M, Cifuni SM, Goerge T, Wagner DD. Innate immune cells induce hemorrhage in tumors during thrombocytopenia. *The American Journal of Pathology* [Internet]. American Society for Investigative Pathology; 2010;175(4):1699–708. Available from: <http://dx.doi.org/10.2353/ajpath.2009.090460>

89. Ho-Tin-Noé B. Platelets in inflammation: Regulation of leukocyte activities and vascular repair. *Frontiers in immunology*. 2015;678(5):1–8.

90. Kerrigan AM, Navarro-Nunez L, Pyz E, Finney BA, Willment JA, Watson SP, et al. Podoplanin-expressing inflammatory macrophages activate murine platelets via CLEC-2. *Journal of Thrombosis and Haemostasis* [Internet]. 2012 Mar 1;10(3):484–6. Available from:  
<http://eutils.ncbi.nlm.nih.gov/entrez/eutils/elink.fcgi?dbfrom=pubmed&id=22212362&retmode=ref&cmd=prlinks>

91. Abtahian F. Regulation of blood and lymphatic vascular separation by signaling proteins SLP-76 and syk. *Science* [Internet]. 2003;299(5604):247–51. Available from: <http://www.sciencemag.org/cgi/doi/10.1126/science.1079477>
92. Hess PR, Rawnsley DR, Jakus Z, Yang Y, Sweet DT, Fu J, et al. Platelets mediate lymphovenous hemostasis to maintain blood-lymphatic separation throughout life. *The Journal of clinical investigation* [Internet]. 2013 Dec 2;124(1):273–84. Available from: <http://www.jci.org/articles/view/70422>
93. Hovidala-Dilke KM, McHugh KP, Tsakiris DA, Rayburn H, Crowley D, Ullmann-Culleré M, et al.  $\beta$ 3-integrin-deficient mice are a model for glanzmann thrombasthenia showing placental defects and reduced survival. *The Journal of clinical investigation* [Internet]. 1999;103(2):229–38. Available from: <http://www.jci.org/articles/view/5487>
94. Hitchcock JR, Cook CN, Bobat S, Ross EA, Flores-Langarica A, Lowe KL, et al. Inflammation drives thrombosis after *Salmonella* infection via CLEC-2 on platelets. *The Journal of clinical investigation* [Internet]. 2015 Oct 26;125(12):4429–46. Available from: <https://www.jci.org/articles/view/79070>
95. Dixon JT, Gozal E, Roberts AM. Platelet-mediated vascular dysfunction during acute lung injury. *Archives of physiology and biochemistry* [Internet]. Department of Physiology and Biophysics, School of Medicine, University of Louisville, KY 40292, USA.; 2012;118(2):72–82. Available from: <http://www.tandfonline.com/doi/full/10.3109/13813455.2012.665463>

96. Ho-Tin-Noe B, Demers M, Wagner DD. How platelets safeguard vascular integrity. *Journal of Thrombosis and Haemostasis* [Internet]. 2011;9:56–65. Available from: <http://doi.wiley.com/10.1111/j.1538-7836.2011.04317.x>
97. Italiano JE, Richardson JL, Patel-Hett S, Battinelli E, Zaslavsky A, Short S, et al. Angiogenesis is regulated by a novel mechanism: Pro- and antiangiogenic proteins are organized into separate platelet granules and differentially released. *Blood* [Internet]. 2007;111(3):1227–33. Available from: <http://www.bloodjournal.org/cgi/doi/10.1182/blood-2007-09-113837>
98. McNicol A, Israels SJ. Platelet dense granules. *Thrombosis Research* [Internet]. Department of Oral Biology, University of Manitoba, Winnipeg, Canada.: Elsevier; 1999;95(1):1–18. Available from: <http://www.thrombosisresearch.com/article/S0049384899000158/fulltext>
99. Blair P, Flaumenhaft R. Platelet alpha-granules: Basic biology and clinical correlates. *Blood Reviews* [Internet]. Department of Medicine, Division of Hemostasis and Thrombosis, Beth Israel Deaconess Medical Center, Harvard Medical School, Boston, MA 02215, USA.: Elsevier; 2009;23(4):177–89. Available from: <http://linkinghub.elsevier.com/retrieve/pii/S0268960X09000290>
100. Schmaier AH, Smith PM, Colman RW. Platelet c1- inhibitor. a secreted alpha-granule protein. *The Journal of clinical investigation* [Internet]. American Society for Clinical Investigation; 1985;75(1):242–50. Available from: <http://www.jci.org/articles/view/111680>

101. Stokes KY, Granger DN. Platelets: A critical link between inflammation and microvascular dysfunction. *The Journal of Physiology* [Internet]. Department of Molecular & Cellular Physiology, LSU Health Sciences Centre-Shreveport, 1501 Kings Highway Shreveport, LA 71130-3932, USA. [kstoke@lsuhsc.edu](mailto:kstoke@lsuhsc.edu): The Physiological Society; 2012;590(5):1023–34. Available from: <http://www.jphysiol.org/cgi/doi/10.1113/jphysiol.2011.225417>

102. May AE, Seizer P, Gawaz M. Platelets: Inflammatory firebugs of vascular walls. *Arteriosclerosis, Thrombosis, and Vascular Biology* [Internet]. Medizinische Klinik III, Eberhard Karls Universität Tübingen, Otfried-Müller-Strasse 10, D-72076 Tübingen, Germany. [andreas.may@med.uni-tuebingen.de](mailto:andreas.may@med.uni-tuebingen.de): Lippincott Williams & Wilkins; 2008;28(3):NaN – NaN. Available from: <http://atvb.ahajournals.org/cgi/doi/10.1161/ATVBAHA.107.158915>

103. Tsao C-M, Ho S-T, Wu C-C. Coagulation abnormalities in sepsis. *Acta anaesthesiologica Taiwanica* : official journal of the Taiwan Society of Anesthesiologists [Internet]. Department of Pharmacology, National Defense Medical Center, Taipei, Taiwan; Department of Pharmacology, Taipei Medical University, Taipei, Taiwan.; 2014;53(1):16–22. Available from: <http://linkinghub.elsevier.com/retrieve/pii/S1875459714001106>

104. Karpman D, Papadopoulou D, Nilsson K, Sjogren AC, Mikaelsson C, Lethagen S. Platelet activation by shiga toxin and circulatory factors as a pathogenetic mechanism in the hemolytic uremic syndrome. *Blood* [Internet]. Department of Pediatrics, Lund University, Lund, Sweden. [diana.karpman@skane.se](mailto:diana.karpman@skane.se);



2001;97(10):3100–8. Available from:

<http://eutils.ncbi.nlm.nih.gov/entrez/eutils/efetch.fcgi?dbfrom=pubmed&id=11342436&retmode=ref&cmd=prlinks>

105. Karpman D, Manea M, Vaziri-Sani F, Stahl A-L, Kristoffersson A-C. Platelet activation in hemolytic uremic syndrome. *Seminars in thrombosis and hemostasis* [Internet]. Department of Pediatrics, Clinical Sciences Lund, Lund University, Lund, Sweden. [Diana.Karpman@med.lu.se](mailto:Diana.Karpman@med.lu.se); 2006;32(2):128–45. Available from:

<http://www.thieme-connect.de/DOI/DOI?10.1055/s-2006-939769>

106. Tang Y-Q, Yeaman MR, Selsted ME. Antimicrobial peptides from human platelets. *Infection and Immunity* [Internet]. Department of Pathology, College of Medicine, University of California Irvine, 92697, USA.: American Society for Microbiology; 2002;70(12):6524–33. Available from:

<http://iai.asm.org/cgi/doi/10.1128/IAI.70.12.6524-6533.2002>

107. Semple JW, Freedman J. Platelets and innate immunity. *Cellular and Molecular Life Sciences* [Internet]. SP Birkhäuser Verlag Basel; 2009;67(4):499–511. Available from: <http://link.springer.com/10.1007/s00018-009-0205-1>

108. Shiraki R, Inoue N, Kawasaki S, Takei A, Kadotani M, Ohnishi Y, et al. Expression of toll-like receptors on human platelets. *Thrombosis Research* [Internet]. 2004;113(6):379–85. Available from:

<http://linkinghub.elsevier.com/retrieve/pii/S0049384804001847>

109. Aslam R, Speck ER, Kim M, Crow AR, Bang KWA, Nestel FP, et al. Platelet toll-like receptor expression modulates lipopolysaccharide-induced thrombocytopenia and tumor necrosis factor-alpha production *in vivo*. *Blood* [Internet]. Department of Laboratory Medicine and Pathobiology, St Michael's Hospital, 30 Bond St, Toronto, ON, Canada, M5B 1W8.: American Society of Hematology; 2006;107(2):637–41. Available from: <http://www.bloodjournal.org/cgi/doi/10.1182/blood-2005-06-2202>
110. Ma AC, Kubes P. Platelets, neutrophils, and neutrophil extracellular traps (nETs) in sepsis. *Journal of Thrombosis and Haemostasis* [Internet]. Blackwell Publishing Ltd; 2008;6(3):415–20. Available from: <http://onlinelibrary.wiley.com/doi/10.1111/j.1538-7836.2007.02865.x/full>
111. Hundelshausen P von, Schmitt MMN. Platelets and their chemokines in atherosclerosis-clinical applications. *Frontiers in Physiology* [Internet]. Institute for Cardiovascular Prevention, Ludwig-Maximilians-University of Munich Munich, Germany.; 2014;5(212):294. Available from: <http://journal.frontiersin.org/article/10.3389/fphys.2014.00294/abstract>
112. Elzey BD, Tian J, Jensen RJ, Swanson AK, Lees JR, Lentz SR, et al. Platelet-mediated modulation of adaptive immunity. a communication link between innate and adaptive immune compartments. *Immunity* [Internet]. The University of Iowa, Department of Urology, Iowa City, IA 52242, USA.: Elsevier; 2003;19(1):9–19. Available from: <http://linkinghub.elsevier.com/retrieve/pii/S1074761303001778>

113. Sitia G, Iannacone M, Guidotti LG. Anti-platelet therapy in the prevention of hepatitis B virus-associated hepatocellular carcinoma. *JOURNAL OF HEPATOLOGY* [Internet]. Division of Immunology, Transplantation and Infectious Diseases, San Raffaele Scientific Institute, Milan 20132, Italy.; 2013 Nov 1;59(5):1135–8. Available from: <http://linkinghub.elsevier.com/retrieve/pii/S0168827813003735>
114. Guidotti LG, Iannacone M. Effector cD8 t cell trafficking within the liver. *Molecular Immunology* [Internet]. 2013;55(1):94–9. Available from: <http://linkinghub.elsevier.com/retrieve/pii/S0161589012004464>
115. Iannacone M, Sitia G, Narvaiza I, Ruggeri ZM, Guidotti LG. Antiplatelet drug therapy moderates immune-mediated liver disease and inhibits viral clearance in mice infected with a replication-deficient adenovirus. *Clinical and Vaccine Immunology* [Internet]. Department of Molecular and Experimental Medicine, Scripps Research Institute, 10550 North Torrey Pines Rd., La Jolla, CA 92037, USA.: American Society for Microbiology; 2007;14(11):1532–5. Available from: <http://cdli.asm.org/cgi/doi/10.1128/CVI.00298-07>
116. Iannacone M, Sitia G, Isogawa M, Marchese P, Castro MG, Lowenstein PR, et al. Platelets mediate cytotoxic T lymphocyte–induced liver damage. *Nature Medicine* [Internet]. 2005 Oct 30;11(11):1167–9. Available from: <http://www.nature.com/doi/10.1038/nm1317>
117. Tamura T, Kondo T, Pak S, Nakano Y, Murata S, Fukunaga K, et al. Interaction between Kupffer cells and platelets in the early period of hepatic ischemia-

reperfusion injury--an *in vivo* study. The Journal of surgical research [Internet].

Department of Surgery, Doctoral Program in Clinical Science, Graduate School of Comprehensive Human Sciences, University of Tsukuba, Tsukuba, Japan.; 2012

Nov 1;178(1):443–51. Available from:

<http://linkinghub.elsevier.com/retrieve/pii/S0022480411020130>

118. Nakano Y, Kondo T, Matsuo R, Hashimoto I, Kawasaki T, Kohno K, et al.

Platelet dynamics in the early phase of postischemic liver *in vivo*. 2008;149(2):192–8.

Available from: <http://linkinghub.elsevier.com/retrieve/pii/S0022480407005598>

119. Ogawa K. Influence of kupffer cells and platelets on ischemia-reperfusion injury

in mild steatotic liver. World Journal of Gastroenterology [Internet]. 2013;19(9):1396.

Available from: <http://www.wjgnet.com/1007-9327/full/v19/i9/1396.htm>

120. Pittman K, Kubes P. Damage-associated molecular patterns control neutrophil

recruitment. Journal of Innate Immunity [Internet]. 2013;5(4):315–23. Available from:

<http://www.karger.com?doi=10.1159/000347132>

121. Laschke MW, Dold S, Menger MD, Jeppsson B, Thorlacius H. Platelet-

dependent accumulation of leukocytes in sinusoids mediates hepatocellular damage in bile duct ligation-induced cholestasis. British Journal of Pharmacology [Internet].

Blackwell Publishing Ltd; 2008 Jan 1;153(1):148–56. Available from:

<http://doi.wiley.com/10.1038/sj.bjp.0707578>

122. Laschke MW, Dold S, Menger MD, Jeppsson B, Thorlacius H. The Rho-kinase

inhibitor Y-27632 inhibits cholestasis-induced platelet interactions in the hepatic

microcirculation. *Microvascular Research* [Internet]. Elsevier Inc.; 2009 Jun 1;78(1):95–9. Available from: <http://dx.doi.org/10.1016/j.mvr.2009.04.003>

123. Sullivan BP, Wang R, Tawfik O, Luyendyk JP. Protective and Damaging Effects of Platelets in Acute Cholestatic Liver Injury Revealed by Depletion and Inhibition Strategies. *Toxicological Sciences* [Internet]. Department of Pharmacology, Toxicology, and Therapeutics, The University of Kansas Medical Center, Kansas City, Kansas 66160, USA.: Oxford University Press; 2010 Apr 15;115(1):286–94. Available from: <http://www.toxsci.oxfordjournals.org/cgi/doi/10.1093/toxsci/kfq042>

124. Joshi N, Kopec AK, O'Brien KM, Towery KL, Cline-Fedewa H, Williams KJ, et al. Coagulation-driven platelet activation reduces cholestatic liver injury and fibrosis in mice. Department of Pharmacology and Toxicology, Michigan State University, East Lansing, MI, USA; Center for Integrative Toxicology, Michigan State University, East Lansing, MI, USA.; 2015 Jan 1;13(1):57–71. Available from: <http://doi.wiley.com/10.1111/jth.12770>

125. Watanabe M, Murata S, Hashimoto I, Nakano Y, Ikeda O, Aoyagi Y, et al. Platelets contribute to the reduction of liver fibrosis in mice. *Journal of Gastroenterology and Hepatology* [Internet]. Blackwell Publishing Asia; 2009 Jan 1;24(1):78–89. Available from: <http://doi.wiley.com/10.1111/j.1440-1746.2008.05497.x>

126. Meyer J, Lejmi E, Fontana P, Morel P, Gonelle-Gispert C, Bühler L. A focus on the role of platelets in liver regeneration: Do platelet-endothelial cell interactions

initiate the regenerative process? JOURNAL OF HEPATOLOGY [Internet]. European Association for the Study of the Liver; 2015;63(5):1263–71. Available from: <http://dx.doi.org/10.1016/j.jhep.2015.07.002>

127. Wong J, Johnston B, Lee SS, Bullard DC, Smith CW, Beaudet AL, et al. A minimal role for selectins in the recruitment of leukocytes into the inflamed liver microvasculature. The Journal of clinical investigation [Internet]. 1997;99(11):2782–90. Available from: <http://www.jci.org/articles/view/119468>

128. Lang PA, Contaldo C, Georgiev P, El-Badry AM, Recher M, Kurrer M, et al. Aggravation of viral hepatitis by platelet-derived serotonin. Nature Medicine [Internet]. 2008 May 30;14(7):756–61. Available from: <http://www.nature.com/doi/10.1038/nm1780>

129. Lesurtel M, Graf R, Aleil B, Walther DJ, Tian Y, Jochum W, et al. Platelet-derived serotonin mediates liver regeneration. Science [Internet]. Department of Visceral and Transplantation Surgery, University Hospital of Zurich, Switzerland.: American Association for the Advancement of Science; 2006 Apr 7;312(5770):104–7. Available from: <http://www.sciencemag.org/cgi/doi/10.1126/science.1123842>

130. Croner RS, Hoerer E, Kulu Y, Hackert T, Gebhard M-M, Herfarth C, et al. Hepatic platelet and leukocyte adherence during endotoxemia. Critical Care [Internet]. Department of Surgery, University of Erlangen-Nuernberg, Germany. Roland.Croner@chir.imed.uni-erlangen.de: BioMed Central Ltd; 2006 Jan 9;10(1):R15. Available from: <http://ccforum.com/content/10/1/R15>

131. Khandoga A, Hanschen M, Kessler JS, Krombach F. CD4<sup>+</sup> T cells contribute to postischemic liver injury in mice by interacting with sinusoidal endothelium and platelets. *Hepatology* [Internet]. Wiley Subscription Services, Inc., A Wiley Company; 2006 Jan 1;43(2):306–15. Available from: <http://doi.wiley.com/10.1002/hep.21017>

132. Badrnya S, Schrottmaier WC, Kral JB, Yaiw K-C, Volf I, Schabbauer G, et al. Platelets mediate oxidized low-density lipoprotein-induced monocyte extravasation and foam cell formation. *Arteriosclerosis, Thrombosis, and Vascular Biology* [Internet]. From the Institute of Physiology, Center for Physiology and Pharmacology, Medical University of Vienna, Vienna, Austria (S.B., W.C.S., J.B.K., I.V., G.S., A.A.); and Department of Medicine, Solna, Center for Molecular Medicine, Karolinska Institute, Stockholm, Sweden (K.-C.Y., C.S.-N., A.A.); 2014 Mar 1;34(3):571–80. Available from: <http://atvb.ahajournals.org/cgi/doi/10.1161/ATVBAHA.113.302919>

133. Hundelshausen P von, Schmitt MMN. Platelets and their chemokines in atherosclerosis—clinical applications. *Frontiers in Physiology* [Internet]. Frontiers Media S.A.; 2014 Jan 1;5:294. Available from: <http://www.ncbi.nlm.nih.gov/pmc/articles/PMC4126210/>

134. Lievens D, Zerneck A, Seijkens T, Soehnlein O, Beckers L, Munnix ICA, et al. Platelet CD40L mediates thrombotic and inflammatory processes in atherosclerosis. *Blood* [Internet]. Washington, DC: American Society of Hematology; 2010 Nov 18;116(20):4317–27. Available from: <http://www.ncbi.nlm.nih.gov/pmc/articles/PMC2993630/>

135. Mantovani A, Garlanda C. Platelet-macrophage partnership in innate immunity and inflammation. Nature Publishing Group [Internet]. Nature Publishing Group; 2013 Aug 1;14(8):768–70. Available from: <http://dx.doi.org/10.1038/ni.2666>

136. Jaeschke H. Neutrophil-mediated tissue injury in alcoholic hepatitis. Alcohol [Internet]. Department of Pharmacology and Toxicology, University of Arkansas for Medical Sciences, 4301 West Markham Street, Mailslot 638, Little Rock, AR 72205-7199, USA. JaeschkeHarmutW@uams.edu; 2002 Apr 30;27(1):23–7. Available from: <http://eutils.ncbi.nlm.nih.gov/entrez/eutils/elink.fcgi?dbfrom=pubmed&id=12062633&retmode=ref&cmd=prlinks>

137. Pellicoro A, Ramachandran P, Iredale JP. Reversibility of liver fibrosis. Fibrogenesis & Tissue Repair [Internet]. BioMed Central Ltd; 2012 Jun 6;5:S26. Available from: <http://www.fibrogenesis.com/content/5/S1/S26>

138. Ramaiah SK, Jaeschke H. Role of neutrophils in the pathogenesis of acute inflammatory liver injury. Toxicologic Pathology [Internet]. Department of Pathobiology, College of Veterinary Medicine & Biomedical Sciences, Texas University, College Station, TX 77843-4467, USA. sramaiah@cvm.tamu.edu: SAGE Publications; 2007 Oct 1;35(6):757–66. Available from: <http://tpx.sagepub.com/cgi/doi/10.1080/01926230701584163>

139. Gleissner CA, Shaked I, Little KM, Ley K. CXC Chemokine Ligand 4 Induces a Unique Transcriptome in Monocyte-Derived Macrophages. The Journal of



Immunology [Internet]. 2010 Apr 21;184(9):4810–8. Available from:

<http://www.jimmunol.org/cgi/doi/10.4049/jimmunol.0901368>

140. Vasina EM, Cauwenberghs S, Feijge MAH, Heemskerk JWM, Weber C, Koenen RR. Microparticles from apoptotic platelets promote resident macrophage differentiation. *Cell Death and Disease* [Internet]. Nature Publishing Group; 2011 Sep 17;2(9):NaN – NaN. Available from: <http://dx.doi.org/10.1038/cddis.2011.94>

141. Xia CQ. Effect of CXC chemokine platelet factor 4 on differentiation and function of monocyte-derived dendritic cells. *International Immunology* [Internet]. 2003 Aug 1;15(8):1007–15. Available from:

<http://www.intimm.oupjournals.org/cgi/doi/10.1093/intimm/dxg100>

142. Scull CM, Hays WD, Fischer TH. Macrophage pro-inflammatory cytokine secretion is enhanced following interaction with autologous platelets. *Journal of inflammation (London, England)* [Internet]. Francis Owen Blood Research Lab, Department of Pathology and Laboratory Medicine, University of North Carolina at Chapel Hill, 125 University Lake Rd, Chapel Hill, NC 27516, USA.

cms2232@columbia.edu.: BioMed Central Ltd; 2010 Jan 1;7(1):53. Available from: <http://www.journal-inflammation.com/content/7/1/53>

143. Borges E, Tietz W, Steegmaier M, Moll T, Hallmann R, Hamann A, et al. P-selectin glycoprotein ligand-1 (pSGL-1) on t helper 1 but not on t helper 2 cells binds to p-selectin and supports migration into inflamed skin. *The Journal of experimental medicine* [Internet]. Institut für Zellbiologie, ZMBE, Universität Münster, Germany.;

1997;185(3):573–8. Available from:

<http://eutils.ncbi.nlm.nih.gov/entrez/eutils/elink.fcgi?dbfrom=pubmed&id=9053457&retmode=ref&cmd=prlinks>

144. Ozhan H, Aydin M, Yazici M, Yazgan O, Basar C, Gungor A, et al. Mean platelet volume in patients with non-alcoholic fatty liver disease. *Platelets* [Internet]. 2010 Jan 1;21(1):29–32. Available from:

<http://informahealthcare.com/doi/abs/10.3109/09537100903391023>

145. Alkhoury N, Kistangari G, Campbell C, Lopez R, Zein NN, Feldstein AE. Mean platelet volume as a marker of increased cardiovascular risk in patients with nonalcoholic steatohepatitis. *Hepatology* [Internet]. 2011 Dec 21;55(1):331–331. Available from: <http://doi.wiley.com/10.1002/hep.24721>

146. Fujita K, Nozaki Y, Wada K, Yoneda M, Endo H, Takahashi H, et al. Effectiveness of antiplatelet drugs against experimental non-alcoholic fatty liver disease. *Gut* [Internet]. 2008 Oct 21;57(11):1583–91. Available from: <http://gut.bmj.com/cgi/doi/10.1136/gut.2007.144550>

147. Shen H, Shahzad G, Jawairia M, Bostick RM, Mustacchia P. Association between aspirin use and the prevalence of nonalcoholic fatty liver disease: a cross-sectional study from the Third National Health and Nutrition Examination Survey. *Alimentary Pharmacology & Therapeutics* [Internet]. 2014 Sep 1;40(9):1066–73. Available from: <http://doi.wiley.com/10.1111/apt.12944>

148. Kodama T, Takehara T, Hikita H, Shimizu S, Li W, Miyagi T, et al.

Thrombocytopenia exacerbates cholestasis-induced liver fibrosis in mice.

Department of Gastroenterology and Hepatology, Osaka University Graduate School of Medicine, Suita, Osaka, Japan.; 2010 Jun 1;138(7):2487–98. Available from:

<http://linkinghub.elsevier.com/retrieve/pii/S0016508510003276>

149. Myronovych A, Murata S, Chiba M, Matsuo R, Ikeda O, Watanabe M, et al.

Role of platelets on liver regeneration after 90% hepatectomy in mice. JOURNAL OF HEPATOLOGY [Internet]. Elsevier; 2008 Sep 1;49(3):363–72. Available from:

<http://linkinghub.elsevier.com/retrieve/pii/S0168827808003498>

150. Tomikawa M, Hashizume M, Highashi H, Ohta M, Sugimachi K. The role of the spleen, platelets, and plasma hepatocyte growth factor activity on hepatic regeneration in rats. Journal of the American College of Surgeons [Internet].

Department of Surgery II, Faculty of Medicine, Kyushu University, Fukuoka, Japan.; 1996 Jan 1;182(1):12–6. Available from:

<http://eutils.ncbi.nlm.nih.gov/entrez/eutils/elink.fcgi?dbfrom=pubmed&id=8542083&retmode=ref&cmd=prlinks>

151. Murata S, Hashimoto I, Nakano Y, Myronovych A, Watanabe M, Ohkohchi N.

Single administration of thrombopoietin prevents progression of liver fibrosis and promotes liver regeneration after partial hepatectomy in cirrhotic rats. Annals of surgery [Internet]. Department of Surgery, Graduate School of Comprehensive

Human Sciences, University of Tsukuba, Ibaraki, Japan.; 2008 Nov 1;248(5):821–8.

Available from:

<http://content.wkhealth.com/linkback/openurl?sid=WKPTLP:landingpage&an=00000658-200811000-00018>

152. Takahashi K, Murata S, Ohkohchi N. Novel therapy for liver regeneration by increasing the number of platelets. *Surgery Today* [Internet]. Springer Japan; 2012 Nov 21;43(10):1081–7. Available from: <http://link.springer.com/10.1007/s00595-012-0418-z>

153. Nowatari T, Murata S, Nakayama K, Sano N, Maruyama T, Nozaki R, et al. Sphingosine 1-phosphate has anti-apoptotic effect on liver sinusoidal endothelial cells and proliferative effect on hepatocytes in a paracrine manner in human. *Hepatology research : the official journal of the Japan Society of Hepatology* [Internet]. Department of Surgery, Division of Gastroenterological and Hepatobiliary Surgery and Organ Transplantation, University of Tsukuba, Tsukuba, Ibaraki, Japan.; 2015 Nov 4;45(11):1136–45. Available from: <http://doi.wiley.com/10.1111/hepr.12446>

154. Kawasaki T, Murata S, Takahashi K, Nozaki R, Ohshiro Y, Ikeda N, et al. Activation of human liver sinusoidal endothelial cell by human platelets induces hepatocyte proliferation. *JOURNAL OF HEPATOLOGY* [Internet]. Department of Surgery, Graduate School of Comprehensive Human Sciences, University of Tsukuba, Tsukuba, Japan.: European Association for the Study of the Liver; 2010 Oct 1;53(4):648–54. Available from: <http://dx.doi.org/10.1016/j.jhep.2010.04.021>

155. DeLeve LD. Liver sinusoidal endothelial cells and liver regeneration. The Journal of clinical investigation [Internet]. American Society for Clinical Investigation; 2013 May 1;123(5):1861–6. Available from: <http://www.jci.org/articles/view/66025>

156. Bachem MG, Melchior R, Gressner AM. The role of thrombocytes in liver fibrogenesis: effects of platelet lysate and thrombocyte-derived growth factors on the mitogenic activity and glycosaminoglycan synthesis of cultured rat liver fat storing cells. Journal of clinical chemistry and clinical biochemistry Zeitschrift fur klinische Chemie und klinische Biochemie [Internet]. Abteilung fur Klinische Chemie, Philipps Universitat Marburg, Federal Republic of Germany.; 1989 Sep 1;27(9):555–65.

Available from:

<http://eutils.ncbi.nlm.nih.gov/entrez/eutils/elink.fcgi?dbfrom=pubmed&id=2607320&retmode=ref&cmd=prlinks>

157. Zaldivar MM, Pauels K, Hundelshausen P von, Berres M-L, Schmitz P, Bornemann J, et al. CXC chemokine ligand 4 (Cxcl4) is a platelet-derived mediator of experimental liver fibrosis. Hepatology [Internet]. Wiley Subscription Services, Inc., A Wiley Company; 2009 Nov 13;51(4):1345–53. Available from:

<http://doi.wiley.com/10.1002/hep.23435>

158. Poujol-Robert A, Boëlle P-Y, Conti F, Durand F, Duvoux C, Wendum D, et al. Aspirin may reduce liver fibrosis progression: Evidence from a multicenter retrospective study of recurrent hepatitis C after liver transplantation. Clinics and Research in Hepatology and Gastroenterology [Internet]. Elsevier Masson SAS; 2014 Oct 1;38(5):570–6. Available from: <http://dx.doi.org/10.1016/j.clinre.2014.07.004>

159. Aiolfi R, Sitia G. Chronic hepatitis B: role of anti-platelet therapy in inflammation control. *Cellular and Molecular Immunology* [Internet]. 2015 Jan 12;12(3):264–8. Available from: <http://www.nature.com/doi/10.1038/cmi.2014.124>
160. Karlmark KR, Weiskirchen R, Zimmermann HW, Gassler N, Ginhoux F, Weber C, et al. Hepatic recruitment of the inflammatory Gr1<sup>+</sup> monocyte subset upon liver injury promotes hepatic fibrosis. *Hepatology* [Internet]. Wiley Subscription Services, Inc., A Wiley Company; 2009 Mar 16;50(1):261–74. Available from: <http://doi.wiley.com/10.1002/hep.22950>
161. Rinella ME, Elias MS, Smolak RR, Fu T, Borensztajn J, Green RM. Mechanisms of hepatic steatosis in mice fed a lipogenic methionine choline-deficient diet. *Journal of lipid research* [Internet]. 2008 Jan 30;49(5):1068–76. Available from: <http://www.jlr.org/cgi/doi/10.1194/jlr.M800042-JLR200>
162. Daley JM, Thomay AA, Connolly MD, Reichner JS, Albina JE. Use of ly6G-specific monoclonal antibody to deplete neutrophils in mice. *Journal of Leukocyte Biology* [Internet]. 2007;83(1):64–70. Available from: <http://www.jleukbio.org/cgi/doi/10.1189/jlb.0407247>
163. Moses K, Klein JC, nn LM, Klingberg A, Gunzer M, Brandau S. Survival of residual neutrophils and accelerated myelopoiesis limit the efficacy of antibody-mediated depletion of ly-6G<sup>+</sup> cells in tumor-bearing mice. *Journal of Leukocyte Biology* [Internet]. 2016;1–13. Available from: <http://www.jleukbio.org/cgi/doi/10.1189/jlb.1HI0715-289R>

164. Li P, Li J, Li M, Gong J, He K. An efficient method to isolate and culture mouse Kupffer cells. *Immunology Letters* [Internet]. Elsevier B.V.; 2014 Feb 22;158(1):52–6. Available from: <http://dx.doi.org/10.1016/j.imlet.2013.12.002>

165. Suzuki-Inoue K, Osada M, OZAKI Y. Physiologic and pathophysiologic roles of interaction between C-type lectin-like receptor 2 and podoplanin: partners from in utero to adulthood. *Journal of Thrombosis and Haemostasis* [Internet]. Department of Clinical and Laboratory Medicine, Faculty of Medicine, University of Yamanashi, Chuo, Yamanashi, Japan.; 2017 Feb 1;15(2):219–29. Available from: <http://eutils.ncbi.nlm.nih.gov/entrez/eutils/elink.fcgi?dbfrom=pubmed&id=27960039&retmode=ref&cmd=prlinks>

166. Schacht V, Ramirez MI, Hong YK, Hirakawa S, Feng D, Harvey N, et al. T1 $\alpha$ /podoplanin deficiency disrupts normal lymphatic vasculature formation and causes lymphedema. *The EMBO Journal* [Internet]. Cutaneous Biology Research Center, Massachusetts General Hospital and Harvard Medical School, Charlestown, MA 02129, USA.: EMBO Press; 2003 Jul 15;22(14):3546–56. Available from: <http://emboj.embopress.org/cgi/doi/10.1093/emboj/cdg342>

167. Peters A, Pitcher LA, Sullivan JM, Mitsdoerffer M, Acton SE, Franz B, et al. Th17 Cells Induce Ectopic Lymphoid Follicles in Central Nervous System Tissue Inflammation. *Immunity* [Internet]. 2011 Dec 1;35(6):986–96. Available from: <http://linkinghub.elsevier.com/retrieve/pii/S1074761311005036>

168. Douglas YL, Mahtab EAF, Jongbloed MRM, Uhrin P, Zaujec J, Binder BR, et al. Pulmonary vein, dorsal atrial wall and atrial septum abnormalities in podoplanin knockout mice with disturbed posterior heart field contribution. *Pediatric research* [Internet]. Department of Cardio-thoracic Surgery, University Medical Center Groningen, Groningen 9700 RB, The Netherlands.; 2009;65(1):27–32. Available from:

<http://eutils.ncbi.nlm.nih.gov/entrez/eutils/elink.fcgi?dbfrom=pubmed&id=18784615&retmode=ref&cmd=prlinks>

169. Jakus Z, Gleghorn JP, Enis DR, Sen A, Chia S, Liu X, et al. Lymphatic function is required prenatally for lung inflation at birth. *The Journal of experimental medicine* [Internet]. 2014;211(5):815–26. Available from:

<http://www.jem.org/lookup/doi/10.1084/jem.20132308>

170. Bertozzi CC, Schmaier AA, Mericko P, Hess PR, Zou Z, Chen M, et al. Platelets regulate lymphatic vascular development through CLEC-2-SLP-76 signaling. *Blood* [Internet]. 2010 Jul 29;116(4):661–70. Available from:

<http://www.bloodjournal.org/cgi/doi/10.1182/blood-2010-02-270876>

171. Ramirez MI, Millien G, Hinds A, Cao Y, Seldin DC, Williams MC. T1alpha, a lung type I cell differentiation gene, is required for normal lung cell proliferation and alveolus formation at birth. *Developmental biology* [Internet]. Pulmonary Center, Boston University School of Medicine, Boston, MA 02118, USA.

[mramirez@lung.bumc.bu.edu](mailto:mramirez@lung.bumc.bu.edu); 2003;256(1):61–72. Available from:



<http://eutils.ncbi.nlm.nih.gov/entrez/eutils/elink.fcgi?dbfrom=pubmed&id=12654292&retmode=ref&cmd=prlinks>

172. Lowe KL, Finney BA, Deppermann C, Hagerling R, Gazit SL, Frampton J, et al. Podoplanin and cLEC-2 drive cerebrovascular patterning and integrity during development. *Blood* [Internet]. Centre for Cardiovascular Sciences, Institute for Biomedical Research, College of Medical and Dental Sciences, University of Birmingham, Birmingham, United Kingdom; 2015;125(24):3769–77. Available from: <http://eutils.ncbi.nlm.nih.gov/entrez/eutils/elink.fcgi?dbfrom=pubmed&id=25908104&retmode=ref&cmd=prlinks>

173. Asai J, Hirakawa S, Sakabe J, Kishida T, Wada M, Nakamura N, et al. Platelets regulate the migration of keratinocytes via podoplanin/CLEC-2 signaling during cutaneous wound healing in mice. *The American Journal of Pathology* [Internet]. Department of Dermatology, Kyoto Prefectural University of Medicine, Kyoto, Japan.; 2016;186(1):101–8. Available from: <http://eutils.ncbi.nlm.nih.gov/entrez/eutils/elink.fcgi?dbfrom=pubmed&id=26597882&retmode=ref&cmd=prlinks>

174. Menter DG, Tucker SC, Kopetz S, Sood AK, Crissman JD, Honn KV. Platelets and cancer: A casual or causal relationship: Revisited. *Cancer metastasis reviews* [Internet]. Gastrointestinal Medical Oncology, The University of Texas MD Anderson Cancer Center, Houston, TX, 77054, USA.; 2014;33(1):231–69. Available from: <http://eutils.ncbi.nlm.nih.gov/entrez/eutils/elink.fcgi?dbfrom=pubmed&id=24696047&retmode=ref&cmd=prlinks>

175. Rodrigo JP, García-Carracedo D, González MV, Mancebo G, Fresno MF, García-Pedrero J. Podoplanin expression in the development and progression of laryngeal squamous cell carcinomas. *Molecular cancer* [Internet]. Department of Otolaryngology-Head and Neck Surgery, Hospital Universitario Central de Asturias, Instituto Universitario de Oncología del Principado de Asturias, Universidad de Oviedo, Asturias, Spain. [juanpablo.rodrigo@sespa.princast.es](mailto:juanpablo.rodrigo@sespa.princast.es): BioMed Central; 2010;9(1):48. Available from: <http://molecular-cancer.biomedcentral.com/articles/10.1186/1476-4598-9-48>

176. Arpin M, Chirivino D, Naba A, Zwaenepoel I. Emerging role for eRM proteins in cell adhesion and migration. *Cell Adhesion & Migration* [Internet]. 2014;5(2):199–206. Available from: <http://www.tandfonline.com/doi/abs/10.4161/cam.5.2.15081>

177. Schoppmann SF, Berghoff A, Dinhof C, Jakesz R, Gnant M, Dubsy P, et al. Podoplanin-expressing cancer-associated fibroblasts are associated with poor prognosis in invasive breast cancer. *Breast Cancer Research and Treatment* [Internet]. 2012;134(1):237–44. Available from: <http://link.springer.com/10.1007/s10549-012-1984-x>

178. Li Y-Y, Zhou C-X, Gao Y. Podoplanin promotes the invasion of oral squamous cell carcinoma in coordination with mT1-mMP and rho gTPases. *American journal of cancer research* [Internet]. Department of Oral Pathology, Peking University School and Hospital of Stomatology Beijing, PR China.; 2015;5(2):514–29. Available from: <http://eutils.ncbi.nlm.nih.gov/entrez/eutils/elink.fcgi?dbfrom=pubmed&id=25973294&retmode=ref&cmd=prlinks>

179. Ito T, Ishii G, Nagai K, Nagano T, Kojika M, Murata Y, et al. Low podoplanin expression of tumor cells predicts poor prognosis in pathological stage iB squamous cell carcinoma of the lung, tissue microarray analysis of 136 patients using 24 antibodies. *Lung cancer (Amsterdam, Netherlands)* [Internet]. Pathology Division, Research Center for Innovative Oncology, National Cancer Center Hospital East, 6-5-1, Kashiwanoha, Kashiwa, Chiba, Japan.; 2009;63(3):418–24. Available from: <http://eutils.ncbi.nlm.nih.gov/entrez/eutils/elink.fcgi?dbfrom=pubmed&id=18657337&retmode=ref&cmd=prlinks>
180. Longatto-Filho A, Pinheiro C, Pereira SMM, Etlinger D, Moreira MAR, Jubé LF, et al. Lymphatic vessel density and epithelial d2-40 immunoreactivity in pre-invasive and invasive lesions of the uterine cervix. *Gynecologic oncology* [Internet]. Life and Health Sciences Research Institute, School of Health Sciences, University of Minho, Braga, Portugal. [longatto@ecsaude.uminho.pt](mailto:longatto@ecsaude.uminho.pt); 2007;107(1):45–51. Available from: <http://dx.doi.org/10.1016/j.ygyno.2007.05.029>
181. Kato Y, Fujita N, Kunita A, Sato S, Kaneko M, Osawa M, et al. Molecular identification of Aggrus/T1alpha as a platelet aggregation-inducing factor expressed in colorectal tumors. *Journal of Biological Chemistry* [Internet]. Institute of Molecular and Cellular Biosciences, The University of Tokyo, Bunkyo-ku, Tokyo 113-0032, Japan.; 2003 Dec 1;278(51):51599–605. Available from: <http://eutils.ncbi.nlm.nih.gov/entrez/eutils/elink.fcgi?dbfrom=pubmed&id=14522983&retmode=ref&cmd=prlinks>

182. Acton SE, Farrugia AJ, Astarita JL, Mourão-Sá D, Jenkins RP, Nye E, et al. Dendritic cells control fibroblastic reticular network tension and lymph node expansion. *Nature* [Internet]. Nature Publishing Group; 2014 Oct 15;514(7523):498–502. Available from: <http://dx.doi.org/10.1038/nature13814>
183. Eckert C, Kim YO, Julich H, Heier E-C, Klein N, Krause E, et al. Podoplanin discriminates distinct stromal cell populations and a novel progenitor subset in the liver. *AJP: Gastrointestinal and Liver Physiology* [Internet]. 2015 Nov 12;NaN – NaN. Available from: <http://ajpgi.physiology.org/lookup/doi/10.1152/ajpgi.00344.2015>
184. Kamath PS, Kim WR. The model for end-stage liver disease (mELD). *Hepatology* [Internet]. Advanced Liver Disease Study Group, Miles and Shirley Fiterman Center for Digestive Diseases, Mayo Clinic College of Medicine, Rochester, MN 55905, USA. [Kamath.Patrick@mayo.edu](mailto:Kamath.Patrick@mayo.edu); 2007;45(3):797–805. Available from: <http://eutils.ncbi.nlm.nih.gov/entrez/eutils/elink.fcgi?dbfrom=pubmed&id=17326206&retmode=ref&cmd=prlinks>
185. Wong CHY, Jenne CN, Petri B, Chrobok NL, Kubes P. Nucleation of platelets with blood-borne pathogens on Kupffer cells precedes other innate immunity and contributes to bacterial clearance. *Nature Immunology* [Internet]. 2013 Jun 16;14(8):785–92. Available from: <http://www.nature.com/doifinder/10.1038/ni.2631>
186. Ogawa K, Kondo T, Tamura T, Matsumura H, Fukunaga K, Murata S, et al. Interaction of Kupffer Cells and Platelets Determines the Severity of Ischemia-Reperfusion Injury in Steatosis. *The Tohoku Journal of Experimental Medicine*

[Internet]. 2014 Jan 1;232(2):105–13. Available from:

<http://jlc.jst.go.jp/DN/JST.JSTAGE/tjem/232.105?lang=en&from=CrossRef&type=abstract>

187. Chung C, Iwakiri Y. The lymphatic vascular system in liver diseases: its role in ascites formation. *Clinical and Molecular Hepatology* [Internet]. 2013 Jan 1;19(2):99. Available from: <http://e-cmh.org/journal/view.php?doi=10.3350/cmh.2013.19.2.99>

188. Tanaka M, Iwakiri Y. The Hepatic Lymphatic Vascular System: Structure, Function, Markers, and Lymphangiogenesis. *Cellular and Molecular Gastroenterology and Hepatology* [Internet]. Elsevier Inc; 2016 Nov 1;2(6):733–49. Available from: <http://dx.doi.org/10.1016/j.jcmgh.2016.09.002>

189. Patten DA, Wilson GK, Bailey D, Shaw RK, Jalkanen S, Salmi M, et al. Human liver sinusoidal endothelial cells promote intracellular crawling of lymphocytes during recruitment: A new step in migration. *Hepatology* [Internet]. National Institute for Health Research Birmingham Liver Biomedical Research Unit and Centre for Liver Research, Medical School, University of Birmingham, Birmingham, United Kingdom.; 2017 Jan 1;65(1):294–309. Available from: <http://doi.wiley.com/10.1002/hep.28879>

190. Ponziani FR. What we should know about portal vein thrombosis in cirrhotic patients: A changing perspective. *World Journal of Gastroenterology* [Internet]. 2012 Jan 1;18(36):5014–7. Available from: <http://www.wjgnet.com/1007-9327/full/v18/i36/5014.htm>

191. Gouw ASH, Clouston AD, Theise ND. Ductular reactions in human liver: Diversity at the interface. *Hepatology* [Internet]. Wiley Subscription Services, Inc., A Wiley Company; 2011 Oct 13;54(5):1853–63. Available from: <http://doi.wiley.com/10.1002/hep.24613>

192. Kono H, Fujii H, Suzuki-Inoue K, INOUE O, Furuya S, Hirayama K, et al. The platelet-activating receptor C-type lectin receptor-2 plays an essential role in liver regeneration after partial hepatectomy in mice. *Journal of Thrombosis and Haemostasis* [Internet]. Department of Clinical and Laboratory Medicine, Faculty of Medicine, University of Yamanashi, Yamanashi, Japan.; 2017 May 1;15(5):998–1008. Available from: <http://eutils.ncbi.nlm.nih.gov/entrez/eutils/elink.fcgi?dbfrom=pubmed&id=28294559&retmode=ref&cmd=prlinks>

193. Kwon H-J, Won Y-S, Park O, Feng D, Gao B. Opposing effects of prednisolone treatment on T/NKT cell- and hepatotoxin-mediated hepatitis in mice. *Hepatology* [Internet]. 2014 Jan 21;59(3):1094–106. Available from: <http://doi.wiley.com/10.1002/hep.26748>

194. Sankiewicz A, Guszcz T, Mena-Hortelano R, Zukowski K, Gorodkiewicz E. Podoplanin serum and urine concentration in transitional bladder cancer. *Cancer biomarkers : section A of Disease markers* [Internet]. Department of Electrochemistry, Institute of Chemistry, University of Bialystok, Bialystok, Poland.; 2016 Jan 1;16(3):343–50. Available from:

<http://eutils.ncbi.nlm.nih.gov/entrez/eutils/elink.fcgi?dbfrom=pubmed&id=26835590&retmode=ref&cmd=prlinks>

195. Wong FW, Chan WY, Lee SS. Resistance to carbon tetrachloride-induced hepatotoxicity in mice which lack CYP2E1 expression. *Toxicology and Applied Pharmacology* [Internet]. 1998 Nov 1;153(1):1–10. Available from: <http://linkinghub.elsevier.com/retrieve/pii/S0041008X98985477>

196. Basu S. Carbon tetrachloride-induced lipid peroxidation: eicosanoid formation and their regulation by antioxidant nutrients. *Toxicology* [Internet]. 2003 Jul 15;189(1):113–27. Available from: <http://linkinghub.elsevier.com/retrieve/pii/S0300483X03001574>

197. Weber LWD, Boll M, Stampfl A. Hepatotoxicity and mechanism of action of haloalkanes: carbon tetrachloride as a toxicological model. *Critical reviews in toxicology* [Internet]. Institute of Toxicology, GSF-National Research Center for Environment and Health, Munich, P.O. Box 1129, D-85758 Neuherberg (FRG). [ldweber@yahoo.com](mailto:ldweber@yahoo.com); 2003 Jan 1;33(2):105–36. Available from: <http://www.tandfonline.com/doi/full/10.1080/713611034>

198. Recknagel RO, Glende EA, Dolak JA, Waller RL. Mechanisms of carbon tetrachloride toxicity. 1989 Jan 1;43(1):139–54. Available from: <http://eutils.ncbi.nlm.nih.gov/entrez/eutils/elink.fcgi?dbfrom=pubmed&id=2675128&retmode=ref&cmd=prlinks>

199. Mossanen J, Tacke F. Acetaminophen-induced acute liver injury in mice. *Laboratory Animals* [Internet]. 2015 Apr 2;49(1):30–6. Available from: <http://lan.sagepub.com/lookup/doi/10.1177/0023677215570992>

200. Jaeschke H. Acetaminophen hepatotoxicity and sterile inflammation: The mechanism of protection of Chlorogenic acid. *Chemico-Biological Interactions* [Internet]. Elsevier Ltd; 2016 Jan 5;243:148–9. Available from: <http://dx.doi.org/10.1016/j.cbi.2015.08.025>

201. McGill MR, Sharpe MR, Williams CD, Taha M, Curry SC, Jaeschke H. The mechanism underlying acetaminophen-induced hepatotoxicity in humans and mice involves mitochondrial damage and nuclear DNA fragmentation. *The Journal of clinical investigation* [Internet]. 2012 Apr 2;122(4):1574–83. Available from: <http://www.jci.org/articles/view/59755>

202. Jaeschke H, Xie Y, McGill MR. Acetaminophen-induced Liver Injury: from Animal Models to Humans. *Journal of Clinical and Translational Hepatology* [Internet]. 2014 Sep 15;2(3):153–61. Available from: [http://www.jcthn.net.com/index.php?option=com\\_content&view=article&id=165&Itemid=852](http://www.jcthn.net.com/index.php?option=com_content&view=article&id=165&Itemid=852)

203. Sanz-Garcia C, Ferrer-Mayorga G, González-Rodríguez Á, Valverde ÁM, Martín-Duce A, Velasco-Martín JP, et al. Sterile Inflammation in Acetaminophen-induced Liver Injury Is Mediated by Cot/tpl2. *The Journal of biological chemistry* [Internet]. 9650 Rockville Pike, Bethesda, MD 20814, U.S.A.: American Society for



Biochemistry and Molecular Biology; 2013 May 24;288(21):15342–51. Available from: <http://www.ncbi.nlm.nih.gov/pmc/articles/PMC3663553/>

204. Woolbright BL, Jaeschke H. Sterile inflammation in acute liver injury: myth or mystery? *Expert Review of Gastroenterology & Hepatology* [Internet]. 2015 Jun 24;9(8):1027–9. Available from: <http://www.tandfonline.com/doi/full/10.1586/17474124.2015.1060855>

205. Sato A, Nakashima H, Nakashima M, Ikarashi M, Nishiyama K, Kinoshita M, et al. Involvement of the TNF and FasL Produced by CD11b Kupffer Cells/Macrophages in CCl<sub>4</sub>-Induced Acute Hepatic Injury. *PLoS ONE* [Internet]. 2014 Mar 25;9(3):e92515. Available from: <http://dx.plos.org/10.1371/journal.pone.0092515>

206. Xu R, Huang H, Zhang Z, Wang F-S. The role of neutrophils in the development of liver diseases. *Cellular and Molecular Immunology* [Internet]. Nature Publishing Group; 2014 Jan 1;11(3):224–31. Available from: <http://dx.doi.org/10.1038/cmi.2014.2>

207. Jaeschke H. Mechanisms of Liver Injury. II. Mechanisms of neutrophil-induced liver cell injury during hepatic ischemia-reperfusion and other acute inflammatory conditions. *AJP: Gastrointestinal and Liver Physiology* [Internet]. 2006 Jun 1;290(6):G1083–8. Available from: <http://ajpgi.physiology.org/cgi/doi/10.1152/ajpgi.00568.2005>

208. Marra F, Tacke F. Roles for chemokines in liver disease. *Gastroenterology* [Internet]. Department of Medicine III, RWTH University Hospital Aachen, Aachen,

Germany. Electronic address: frank.tacke@gmx.net.; 2014 Sep 1;147(3):577–94.

Available from:

<http://eutils.ncbi.nlm.nih.gov/entrez/eutils/elink.fcgi?dbfrom=pubmed&id=25066692&retmode=ref&cmd=prlinks>

209. Georgiades P, Ogilvy S, Duval H, Licence DR, Charnock-Jones DS, Smith SK, et al. VavCre transgenic mice: A tool for mutagenesis in hematopoietic and endothelial lineages. *Genesis* (New York, NY : 2000) [Internet]. Department of Pathology, University of Cambridge, Tennis Court Road, Cambridge, UK.; 2002;34(4):251–6. Available from:

<http://eutils.ncbi.nlm.nih.gov/entrez/eutils/elink.fcgi?dbfrom=pubmed&id=12434335&retmode=ref&cmd=prlinks>

210. Holt MP, Cheng L, Ju C. Identification and characterization of infiltrating macrophages in acetaminophen-induced liver injury. *Journal of Leukocyte Biology* [Internet]. The Society for Leukocyte Biology; 2008;84(6):1410–21. Available from: <http://www.ncbi.nlm.nih.gov/pmc/articles/PMC2614594/>

211. Akerman P, Cote P, Yang SQ, McClain C, Nelson S, Bagby GJ, et al. Antibodies to tumor necrosis factor-alpha inhibit liver regeneration after partial hepatectomy. *The American journal of physiology* [Internet]. Department of Medicine, Johns Hopkins University School of Medicine, Baltimore, Maryland 21205.; 1992;263(4 Pt 1):NaN – NaN. Available from:

<http://eutils.ncbi.nlm.nih.gov/entrez/eutils/elink.fcgi?dbfrom=pubmed&id=1415718&retmode=ref&cmd=prlinks>

212. Zhao X, Rong L, Zhao X, Li X, Liu X, Deng J, et al. TNF signaling drives myeloid-derived suppressor cell accumulation. *The Journal of clinical investigation* [Internet]. 2012;122(11):4094–104. Available from: <http://www.jci.org/articles/view/64115>

213. Lauterbach M, O'Donnell P, Asano K, Mayadas TN. Role of tNF priming and adhesion molecules in neutrophil recruitment to intravascular immune complexes. *Journal of Leukocyte Biology* [Internet]. Center for Excellence in Vascular Biology, Department of Pathology, Brigham and Women's Hospital and Harvard Medical School, Boston, MA 02115, USA.; 2008;83(6):1423–30. Available from: <http://eutils.ncbi.nlm.nih.gov/entrez/eutils/elink.fcgi?dbfrom=pubmed&id=18372339&retmode=ref&cmd=prlinks>

214. Gabrilovich DI, Nagaraj S. Myeloid-derived suppressor cells as regulators of the immune system. *Nature Reviews Immunology* [Internet]. 2009;9(3):162–74. Available from: <http://www.nature.com/doifinder/10.1038/nri2506>

215. Bergmeier W, Stefanini L. Platelet iTAM signaling. *Current opinion in hematology* [Internet]. University of North Carolina, Chapel Hill, North Carolina 27599-7035, USA. [bergmeie@email.unc.edu](mailto:bergmeie@email.unc.edu); 2013;20(5):445–50. Available from: <http://eutils.ncbi.nlm.nih.gov/entrez/eutils/elink.fcgi?dbfrom=pubmed&id=23921514&retmode=ref&cmd=prlinks>

216. Horiguchi N, Lafdil F, Miller AM, Park O, Wang H, Rajesh M, et al. Dissociation between liver inflammation and hepatocellular damage induced by carbon

tetrachloride in myeloid cell-specific signal transducer and activator of transcription 3 gene knockout mice. *Hepatology* [Internet]. 2010 Jan 28;51(5):1724–34. Available from: <http://doi.wiley.com/10.1002/hep.23532>

217. Shiratori Y, Hongo S, Hikiba Y, Ohmura K, Nagura T, Okano K, et al. Role of macrophages in regeneration of liver. *Digestive diseases and sciences* [Internet]. Department of Internal Medicine (II), Faculty of Medicine, University of Tokyo, Japan.; 1996 Oct 1;41(10):1939–46. Available from: <http://eutils.ncbi.nlm.nih.gov/entrez/eutils/elink.fcgi?dbfrom=pubmed&id=8888704&retmode=ref&cmd=prlinks>

218. Amemiya H, Kono H, Fujii H. Liver regeneration is impaired in macrophage colony stimulating factor deficient mice after partial hepatectomy: the role of M-CSF-induced macrophages. *The Journal of surgical research* [Internet]. First Department of Surgery, University of Yamanashi, Yamanashi, Japan.; 2011 Jan 1;165(1):59–67. Available from: <http://eutils.ncbi.nlm.nih.gov/entrez/eutils/elink.fcgi?dbfrom=pubmed&id=20031174&retmode=ref&cmd=prlinks>

219. Nishiyama K, Nakashima H, Ikarashi M, Kinoshita M, Nakashima M, Aosasa S, et al. Mouse CD11b<sup>+</sup>Kupffer Cells Recruited from Bone Marrow Accelerate Liver Regeneration after Partial Hepatectomy. *PLoS ONE* [Internet]. 2015 Sep 2;10(9):NaN – NaN. Available from: <http://dx.plos.org/10.1371/journal.pone.0136774>

220. Blendis L, Dotan I. Anti-TNF therapy for severe acute alcoholic hepatitis: What went wrong? *Gastroenterology* [Internet]. 2004 Nov 1;127(5):1637–9. Available from: <http://linkinghub.elsevier.com/retrieve/pii/S0016508504017603>

221. BS RK, PhD LHT-PM. Kupffer cell and platelet interactions in hepatic ischemia reperfusion. Elsevier Inc.; 2013 May 15;181(2):219–21. Available from: <http://dx.doi.org/10.1016/j.jss.2012.02.043>

222. Ishida Y. The pathogenic roles of tumor necrosis factor receptor p55 in acetaminophen-induced liver injury in mice. *Journal of Leukocyte Biology* [Internet]. 2003 Oct 2;75(1):59–67. Available from: <http://www.jleukbio.org/cgi/doi/10.1189/jlb.0403152>

223. Chiu H. Role of tumor necrosis factor receptor 1 (p55) in hepatocyte proliferation during acetaminophen-induced toxicity in mice. *Toxicology and Applied Pharmacology* [Internet]. 2003 Oct 30;1–10. Available from: <http://linkinghub.elsevier.com/retrieve/pii/S0041008X03003697>

224. Gardner C. Exaggerated hepatotoxicity of acetaminophen in mice lacking tumor necrosis factor receptor-1 Potential role of inflammatory mediators. *Toxicology and Applied Pharmacology* [Internet]. 2003 Oct 15;192(2):119–30. Available from: <http://linkinghub.elsevier.com/retrieve/pii/S0041008X03002734>

225. Dhanda AD. Immune dysfunction in acute alcoholic hepatitis. *World Journal of Gastroenterology* [Internet]. 2015 Jan 1;21(42):11904–11. Available from: <http://www.wjgnet.com/1007-9327/full/v21/i42/11904.htm>

226. Moreau MD R, Rautou MPP-E. Editorial: G-CSF Therapy for Severe Alcoholic Hepatitis: Targeting Liver Regeneration or Neutrophil Function? *The American Journal of Gastroenterology* [Internet]. American College of Gastroenterology; 2014 Sep 1;109(9):1424–6. Available from:

<http://www.nature.com/doi/10.1038/ajg.2014.250>

227. Uhrin P, Zaujec J, Breuss JM, Olcaydu D, Chrenek P, Stockinger H, et al. Novel function for blood platelets and podoplanin in developmental separation of blood and lymphatic circulation. *Blood* [Internet]. 2010 May 13;115(19):3997–4005. Available from: <http://www.bloodjournal.org/cgi/doi/10.1182/blood-2009-04-216069>

228. Yin C, Evason KJ, Asahina K, Stainier DYR. Hepatic stellate cells in liver development, regeneration, and cancer. *The Journal of clinical investigation* [Internet]. 2013;123(5):1902–10. Available from:

<http://www.jci.org/articles/view/66369>

229. Lee UE, Friedman SL. Mechanisms of hepatic fibrogenesis. *Best Practice & Research Clinical Gastroenterology* [Internet]. Division of Liver Diseases, Mount Sinai School of Medicine, 1425 Madison Ave, Room 11-76, New York, NY 10029, USA. [Ursula.Lang@mssm.edu](mailto:Ursula.Lang@mssm.edu); Elsevier; 2011;25(2):195–206. Available from:

<http://linkinghub.elsevier.com/retrieve/pii/S152169181100031X>

230. Szabo G, Csak T. Inflammasomes in liver diseases. *JOURNAL OF HEPATOLOGY* [Internet]. European Association for the Study of the Liver; 2012;57(3):642–54. Available from: <http://dx.doi.org/10.1016/j.jhep.2012.03.035>

231. Giannandrea M, Parks WC. Diverse functions of matrix metalloproteinases during fibrosis. *Disease Models & Mechanisms* [Internet]. 2014;7(2):193–203. Available from: <http://dmm.biologists.org/cgi/doi/10.1242/dmm.012062>

232. Starkel P, Leclercq IA. *Best Practice Research Clinical Gastroenterology* [Internet]. Elsevier Ltd; 2011;25(2):319–33. Available from: <http://dx.doi.org/10.1016/j.bpg.2011.02.004>

233. Iredale JP. Models of liver fibrosis: Exploring the dynamic nature of inflammation and repair in a solid organ. *The Journal of clinical investigation* [Internet]. 2007;117(3):539–48. Available from: <http://www.jci.org/cgi/doi/10.1172/JCI30542>

234. Liedtke C, Luedde T, Sauerbruch T, Scholten D, Streetz K, Tacke F, et al. Experimental liver fibrosis research: Update on animal models, legal issues and translational aspects. *Fibrogenesis & Tissue Repair* [Internet]. BioMed Central; 2013;6(1):19. Available from: <http://fibrogenesis.biomedcentral.com/articles/10.1186/1755-1536-6-19>

235. Martínez AK, Maroni L, Marzioni M, Ahmed ST, Milad M, Ray D, et al. Mouse models of liver fibrosis mimic human liver fibrosis of different etiologies. *Current Pathobiology Reports* [Internet]. 2014;2(4):143–53. Available from: <http://link.springer.com/10.1007/s40139-014-0050-2>

236. Friedman SL, Bansal MB. Reversal of hepatic fibrosis – fact or fantasy? *Hepatology* [Internet]. Division of Liver Diseases, Department of Medicine, Mount

Sinai School of Medicine, New York, NY 10029, USA. Scott.Friedman@mssm.edu;

2006;43(2 Suppl 1):NaN – NaN. Available from:

<http://eutils.ncbi.nlm.nih.gov/entrez/eutils/elink.fcgi?dbfrom=pubmed&id=16447275&retmode=ref&cmd=prlinks>

237. Poynard T, Bedossa P, Opolon P. Natural history of liver fibrosis progression in patients with chronic hepatitis c. the oBSVIRC, mETAVIR, cLINIVIR, and dOSVIRC groups. *The Lancet* [Internet]. Service d'Hepato Gastroenterologie, URA CNRS 1484, Groupe Hospitalier Pitie Salpetriere, Paris, France.; 1997;349(9055):825–32.

Available from:

<http://eutils.ncbi.nlm.nih.gov/entrez/eutils/elink.fcgi?dbfrom=pubmed&id=9121257&retmode=ref&cmd=prlinks>

238. Ismail M, Pinzani M. Reversal of hepatic fibrosis: Pathophysiological basis of antifibrotic therapies. *Hepatic Medicine: Evidence and Research* [Internet]. 2011;69.

Available from: <http://www.dovepress.com/reversal-of-hepatic-fibrosis-pathophysiological-basis-of-antifibrotic-peer-reviewed-article-HMER>

239. Dufour J-F. Reversibility of hepatic fibrosis in autoimmune hepatitis. *Annals of Internal Medicine* [Internet]. 1997;127(11):981–5. Available from:

<http://annals.org/article.aspx?doi=10.7326/0003-4819-127-11-199712010-00006>

240. Day CP, James OF. Steatohepatitis: a tale of two 'hits'? *Gastroenterology* [Internet]. 1998 Apr 1;114(4):842–5. Available from:



<http://eutils.ncbi.nlm.nih.gov/entrez/eutils/elink.fcgi?dbfrom=pubmed&id=9547102&retmode=ref&cmd=prlinks>

241. Fung G. Animal models of non-alcoholic fatty liver disease: From genetics to nutrition [Internet]. 2013 p. 1–14. Available from:  
<https://www.google.co.uk/url?sa=t&rct=j&q=&esrc=s&source=web&cd=10&ved=0CIMBEBYwCQ&url=https%3A%2F%2Fwww.iconceptpress.com%2Fdownload%2Fpaper%2F12052304373271.pdf&ei=8OCJU8zTGMSAOPqCgdgl&usg=AFQjCNEvq9nZTjFuC8COQNNA0qXqdJt3pw&bvm=bv.67720277,d.ZWU>

242. Lee GS, Yan JS, Ng RK, Kakar S, Maher JJ. Polyunsaturated fat in the methionine-choline-deficient diet influences hepatic inflammation but not hepatocellular injury. *Journal of lipid research* [Internet]. Liver Center, University of California, San Francisco, San Francisco, CA 94110, USA.: American Society for Biochemistry and Molecular Biology; 2007;48(8):1885–96. Available from:  
<http://www.jlr.org/cgi/doi/10.1194/jlr.M700181-JLR200>

243. Santilli F, Vazzana N, Liani R, Guagnano MT, Davi G. Platelet activation in obesity and metabolic syndrome. *Obesity reviews : an official journal of the International Association for the Study of Obesity* [Internet]. Internal Medicine and Center of Excellence on Aging, G. D'Annunzio University of Chieti, Chieti, Italy.; 2012;13(1):27–42. Available from:  
<http://eutils.ncbi.nlm.nih.gov/entrez/eutils/elink.fcgi?dbfrom=pubmed&id=21917110&retmode=ref&cmd=prlinks>

244. Jang JH, Kang KJ, Kim YH, Kang YN, Lee IS. Reevaluation of experimental model of hepatic fibrosis induced by hepatotoxic drugs: An easy, applicable, and reproducible model. TPS [Internet]. Department of Surgery, School of Medicine and Institute for Medical Science, Keimyung University, Daegu, Korea.: Elsevier; 2008;40(8):2700–3. Available from:  
<http://linkinghub.elsevier.com/retrieve/pii/S0041134508008646>

245. Osawa Y, Hoshi M, Yasuda I, Saibara T, Moriwaki H, Kozawa O. Tumor necrosis factor- $\alpha$  promotes cholestasis-induced liver fibrosis in the mouse through tissue inhibitor of metalloproteinase-1 production in hepatic stellate cells. PLoS ONE [Internet]. Public Library of Science; 2013;8(6):e65251. Available from:  
<http://dx.plos.org/10.1371/journal.pone.0065251>

246. Copaci I, Micu L, Voiculescu M. The role of cytokines in non-alcoholic steatohepatitis. a review. Journal of gastrointestinal and liver diseases: JGLD [Internet]. Center of Internal Medicine, Fundeni Clinical Institute, Bucharest, Romania.; 2006;15(4):363–73. Available from:  
<http://eutils.ncbi.nlm.nih.gov/entrez/eutils/elink.fcgi?dbfrom=pubmed&id=17205149&retmode=ref&cmd=prlinks>

247. Berres ML, Lettow I, Fischer P, Heinrichs D, Trautwein C, Wasmuth HE. The platelet-derived chemokine cXCL7 stimulates pro-angiogenic properties of hepatic stellate cells via cXCR1 activation. JOURNAL OF HEPATOLOGY [Internet]. European Association for the Study of the Liver; 2012;56:S147. Available from:  
[http://dx.doi.org/10.1016/S0168-8278\(12\)60375-4](http://dx.doi.org/10.1016/S0168-8278(12)60375-4)

248. Mann DA, Marra F. Fibrogenic signalling in hepatic stellate cells. *JOURNAL OF HEPATOLOGY* [Internet]. European Association for the Study of the Liver; 2010;52(6):949–50. Available from: <http://dx.doi.org/10.1016/j.jhep.2010.02.005>

249. Hill-Baskin AE, Markiewski MM, Buchner DA, Shao H, DeSantis D, Hsiao G, et al. Diet-induced hepatocellular carcinoma in genetically predisposed mice. *Human molecular genetics* [Internet]. Department of Genetics, Case Western Reserve University School of Medicine, Cleveland, OH 44106, USA.; 2009;18(16):2975–88. Available from: <http://eutils.ncbi.nlm.nih.gov/entrez/eutils/elink.fcgi?dbfrom=pubmed&id=19454484&retmode=ref&cmd=prlinks>

250. Lanthier N, Molendi-Coste O, Horsmans Y, Rooijen N van, Cani PD, Leclercq IA. Kupffer cell activation is a causal factor for hepatic insulin resistance. *AJP: Gastrointestinal and Liver Physiology* [Internet]. 2009;298(1):G107–16. Available from: <http://ajpgi.physiology.org/cgi/doi/10.1152/ajpgi.00391.2009>

251. Tencerova M, Aouadi M, Vangala P, Nicoloso SM, Yawe JC, Cohen JL, et al. Activated kupffer cells inhibit insulin sensitivity in obese mice. *FASEB journal : official publication of the Federation of American Societies for Experimental Biology* [Internet]. \\*Program in Molecular Medicine, Department of Surgery, and Department of Pediatrics, University of Massachusetts Medical School, Worcester, Massachusetts, USA myriam.aouadi@ki.se michael.czech@umassmed.edu.; 2015;29(7):2959–69. Available from:

<http://eutils.ncbi.nlm.nih.gov/entrez/eutils/elink.fcgi?dbfrom=pubmed&id=25805830&retmode=ref&cmd=prlinks>

252. Odegaard JI, Ricardo-Gonzalez RR, Goforth MH, Morel CR, Subramanian V, Mukundan L, et al. Macrophage-specific pPAR $\gamma$  controls alternative activation and improves insulin resistance. *Nature* [Internet]. Division of Endocrinology, Metabolism and Gerontology, Department of Medicine, Stanford University School of Medicine, Stanford, California 94305-5103, USA.; 2007;447(7148):1116–20. Available from: <http://eutils.ncbi.nlm.nih.gov/entrez/eutils/elink.fcgi?dbfrom=pubmed&id=17515919&retmode=ref&cmd=prlinks>

253. Wu X, Zhang J, Ge H, Gupte J, Baribault H, Lee KJ, et al. Soluble cLEC2 extracellular domain improves glucose and lipid homeostasis by regulating liver kupffer cell polarization. *EBIOM* [Internet]. Elsevier B.V.; 2015;2(3):214–24. Available from: <http://dx.doi.org/10.1016/j.ebiom.2015.02.013>

254. McGill MR, Williams CD, Xie Y, Ramachandran A, Jaeschke H. Acetaminophen-induced liver injury in rats and mice: Comparison of protein adducts, mitochondrial dysfunction, and oxidative stress in the mechanism of toxicity. *Toxicology and Applied Pharmacology* [Internet]. 2012 Nov 1;264(3):387–94. Available from: <http://linkinghub.elsevier.com/retrieve/pii/S0041008X12003572>

255. Książek M, Chacińska M, Chabowski A, Baranowski M. Sources, metabolism, and regulation of circulating sphingosine-1-phosphate. *Journal of lipid research* [Internet]. Department of Physiology, Medical University of Białystok, Białystok,

Poland.: American Society for Biochemistry and Molecular Biology; 2015 Jul 1;56(7):1271–81. Available from: <http://www.jlr.org/lookup/doi/10.1194/jlr.R059543>

256. Liu G, Bi Y, Wang R, Yang H, Zhang Y, Wang X, et al. Targeting s1P1 receptor protects against murine immunological hepatic injury through myeloid-derived suppressor cells. *Journal of immunology (Baltimore, Md : 1950)* [Internet]. Key Laboratory of Medical Molecular Virology of Ministries of Education and Health, Department of Immunology, School of Basic Medical Sciences, Fudan University, Shanghai 200032, China; American Association of Immunologists; 2014;192(7):3068–79. Available from: <http://www.jimmunol.org/cgi/doi/10.4049/jimmunol.1301193>

257. Ikeda H, Watanabe N, Ishii I, Shimosawa T, Kume Y, Tomiya T, et al. Sphingosine 1-phosphate regulates regeneration and fibrosis after liver injury via sphingosine 1-phosphate receptor 2. *The Journal of Lipid Research* [Internet]. 2008;50(3):556–64. Available from: <http://www.jlr.org/cgi/doi/10.1194/jlr.M800496-JLR200>

258. Getachew Y, Cusimano FA, James LP, Thiele DL. The role of intrahepatic CD3<sup>+</sup>/CD4<sup>-</sup>/CD8<sup>-</sup> double negative T (DN T) cells in enhanced acetaminophen toxicity. *Toxicology and Applied Pharmacology* [Internet]. Division of Digestive and Liver Diseases, Department of Internal Medicine, University of Texas Southwestern Medical Center, 5323 Harry Hines Blvd., Dallas, TX 75390-9151, USA.; 2014 Oct 1;280(2):264–71. Available from:

<http://eutils.ncbi.nlm.nih.gov/entrez/eutils/elink.fcgi?dbfrom=pubmed&id=25168425&retmode=ref&cmd=prlinks>

259. Yago T, Petrich BG, Zhang N, Liu Z, Shao B, Ginsberg MH, et al. Blocking neutrophil integrin activation prevents ischemia–reperfusion injury. *The Journal of experimental medicine* [Internet]. 2015;212(8):1267–81. Available from: <http://www.jem.org/lookup/doi/10.1084/jem.20142358>

260. Weineisen M, Sjobring U, Fallman M, Andersson T. Streptococcal m5 protein prevents neutrophil phagocytosis by interfering with cD11b/CD18 receptor-mediated association and signaling. *The Journal of Immunology* [Internet]. Experimental Pathology, Lund University, Malmo University Hospital, Malmo, Sweden. maria.weineisen@mig.lu.se; 2004;172(6):3798–807. Available from: <http://eutils.ncbi.nlm.nih.gov/entrez/eutils/elink.fcgi?dbfrom=pubmed&id=15004185&retmode=ref&cmd=prlinks>

261. Sagiv JY, Michaeli J, Assi S, Mishalian I, Kisos H, Levy L, et al. Phenotypic diversity and plasticity in circulating neutrophil subpopulations in cancer. *Cell Reports* [Internet]. Elsevier; 2015;10(4):562–73. Available from: <http://linkinghub.elsevier.com/retrieve/pii/S2211124714010924>

262. Kerrigan AM, Dennehy KM, Mourao-Sa D, Faro-Trindade I, Willment JA, Taylor PR, et al. CLEC-2 Is a Phagocytic Activation Receptor Expressed on Murine Peripheral Blood Neutrophils. *The Journal of Immunology* [Internet]. 2009 Apr

1;182(7):4150–7. Available from:

<http://www.jimmunol.org/cgi/doi/10.4049/jimmunol.0802808>

263. Calaminus SDJ, Guitart A, Sinclair A, Schachtner H, Watson SP, Holyoake TL, et al. Lineage Tracing of Pf4-Cre Marks Hematopoietic Stem Cells and Their Progeny. PLoS ONE [Internet]. 2012 Dec 27;7(12):NaN – NaN. Available from: <http://dx.plos.org/10.1371/journal.pone.0051361>

264. Yokomori H, Oda M, Kaneko F, Kawachi S, Tanabe M, Yoshimura K, et al. Lymphatic marker podoplanin/D2-40 in human advanced cirrhotic liver- Re-evaluations of microlymphatic abnormalities. BMC Gastroenterology [Internet]. 2010 Nov 8;10(1):239–10. Available from: <http://bmcgastroenterol.biomedcentral.com/articles/10.1186/1471-230X-10-131>

265. Craig DGN, Bates CM, Davidson JS, Martin KG, Hayes PC, Simpson KJ. Staggered overdose pattern and delay to hospital presentation are associated with adverse outcomes following paracetamol-induced hepatotoxicity. British Journal of Clinical Pharmacology [Internet]. 2012 Jan 6;73(2):285–94. Available from: <http://doi.wiley.com/10.1111/j.1365-2125.2011.04067.x>



























